ABSTRACT

Title of Dissertation: VEHICLE BRIDGE INTERACTION ANALYSIS ON CONCRETE AND STEEL CURVED BRIDGES

Yunchao Ye, Ph.D. of Civil Engineering, 2019

Dissertation Directed By: Professor Chung C. Fu, Ph.D., P.E.

Civil and Environmental Engineering

This study investigation is intended to research the dynamic reactions of horizontally curved bridge under heavy vehicle load. Most of the main factors that affect the bridge dynamic response due to moving vehicles are considered.

First, an improved grid model is developed for the analysis of curved bridges based on the shear-flexibility grillage analyzing method, in which the effects of warping stiffness and moment of inertia are both considered. Based on commercial software ANSYS Mechanical APDL, 3D beam element, mass element and spring-damper element are integrated together in building a 3D vehicle and bridge system. A simplified numeric method is developed for solving the interaction problem, considering the effect of

random road roughness and its velocity term. This system is tested on two case study bridges, Manchuria concrete bridge and Veteran's Memorial steel bridge.

Second, with the model and numerical method presented, a series of parametric studies are conducted to study during the curved bridge dynamic interaction. In the study, the effects of curvature of radius, bridge surface roughness, bridge span configuration, traffic lane eccentricities and speed are investigated and analyzed. The dynamic response and dynamic impact factors are calculated and compared. The analysis results provide good references for the stipulation of impact factor formulae in the later studies.

Third, based on the investigation of determining factors of curve bridge dynamic interaction, the expression for upper-bound envelop for impact factors of maximum deflection is given in different surface conditions and highway speed limits as a function of bridge fundamental frequency or bridge central angle. A study is conducted on comparing this empirical equation and serval other major design codes, comments and suggestion are made based on the discoveries.

VEHICLE BRIDGE INTERACTION ANALYSIS ON CONCRETE AND STEEL CURVED BRIDGES

by

Yunchao Ye

Dissertation submitted to the Faculty of the Graduate School of the
University of Maryland, College Park, in partial fulfillment
of the requirements for the degree of
Doctor of Philosophy
2019

Advisory Committee:
Professor Chung. C. Fu Advisor, Chair
Professor M. Sherif Aggour
Professor Amde M. Amde
Professor Brian M. Phillips
Professor Sung Lee

Acknowledgements

I would like to take this opportunity to thank my advisor, Dr. Chung C. Fu, for his kind guidance during my studies. His advice was very crucial for the success of this work. I have truly enjoyed my time working for him,

I also thank my committee members: Dr. Aggour, Dr. Amde, Dr. Phillip and Dr. Lee for their valuable time reading my work and providing their insight and comments.

Financial support provided by Dr. Fu and the Bridge Engineering Software and Technology (BEST) Center is gratefully acknowledged.

Finally, I would like to thank all my family members and my friends from BEST Center for their patience and support throughout the course of this research.

Table of Contents

List of Figures

List of Tables

1. Introduction

1.1 Research Motivation

On February 21, 2011, the Shangyu bridge curve overpass in Zhejiang, China, collapsed when three heavy trucks passed through the bridge. This accident led to four trucks tumbling under the bridge and three people injured. This bridge failed after only six years in service. According to the statistics, there were three other curved bridges collapsed due to vehicle bridge interaction in the past decade.

Due to the advantages in economic, reliability and aesthetic, single-column pier bridges such as Shangyu Bridge, are frequently adopted worldwide. Forensic evidence from Shangyu Overpass Bridge after collapse suggested that the bridge failure was initiated by extremely eccentric overload and the low overturning limits of single-column pier bridges. In the United States, multi-column pier bridges are more common in bridge design and construction. But the traffic-induced impact (vehicle bridge interaction) still poses a threat for curved bridges such as ramp and highway approach. It becomes especially important to be able to accurately understand bridge structure when under extensive heavy vehicle load.

Figure 1-1 Shangyu curved bridge accident

1.2 Background

The interaction between bridge and the traffic moving across the bridge is a nonlinear dynamic coupled problem that represents a special discipline within the broad area of structural dynamics. In theory, the bridge and moving vehicle are usually simulated as two independent elastic structures. These two subsystems interact with each other through the contact forces that induced at the contact points between bridge surface and vehicle wheels. Such problem should be considered as nonlinear and time-dependent due to the constant moving contact points and contact forces. The way these two subsystems interact with each other is primarily determined by their inherent frequencies

and the driving frequencies. Such interaction between the two subsystems is usually called vehicle-bridge interaction (VBI).

Curved girder bridges are widely used in highway viaducts and approach bridges of larger mainline bridges due to the need to reduce traffic congestion and constraints of limited right of way. However, comparing to normal straight highway bridge, they are more vulnerable to heavy truck traffic due to the geometric property of the structure. Heavy truck traffic can have a considerable dynamic effect on the curved highway bridges. This dynamic effect could result in deterioration of bridges and increasing the maintenance cost.

For curved girder bridge, in addition to those force characteristics of the straight girder bridge, there are other effects that engineers need to consider.

1. Horizontal force. When a car is driving on a curved bridge, horizontal centrifugal force is generated on the bridge deck. Since there is still a certain vertical height difference between the centrifugal force point and the shear center of the section, therefore the additional torque is generated. Concrete shrinkage, pre-stress, creep and temperature can also cause the deformation of the girder. These effects produce not only vertical horizontal force on the bridge, but also forces on the horizontal direction. The lateral force generated by the external load on the bridge will increase the cross-section torque of the girder and the bending moment of the piers, and make the girder produce lateral displacement and plane rotation.

2. Bending and torsion of the beam coupling. Under the action of external load, the curved girder bridge will generate bending moment and torque at the same time, and influence each other so that the girder is in a state of bending-torsion coupling. The main tensile stress of the girder is often much larger than that of the corresponding straight girder bridge. Due to the strong torque, the curved bridge produces torsional deformation, and the vertical deflection outside the curve is larger than that of the straight bridge with the same span length. Due to the coupling between bending and torsion, warping may also occur at the beam ends.

3. The inner and outer girders are not evenly loaded. Due to the presence of large torque, the curved bridge usually results in an overloaded outer section and a light-loaded inner section. Since the reaction forces of the inner and outer sections often vary greatly, the reaction of the inner fulcrum may even become negative when the live load is eccentric. If the support cannot bear the tension, separation of the girder(s) from the support could occurs and cause damage to the bridge bearing(s).

In the current bridge code, the dynamic effect of vehicle load and vehicle-bridge interaction adopts mostly for straight bridges, curved bridge dynamic effect is not sufficiently considered. Knowledge of dynamic vehicle load effect on structure can be beneficial for determination of bridge condition evaluation and achieve successful infrastructure system preservation.

1.3 Research objective

Although considerable deal of research has been done on the coupling vibration of bridge, most of the previous researches focused on the research of the straight girder bridge. Few studies have been done on the impact effect of curved bridges. Engineers do not have full understanding of the influencing factors of vehicle bridge coupled vibration of curved bridges, and further research is needed. Besides, the current impact factor for traffic load on highway does not reflect the influence from the grade of bridge surface roughness. However, surface roughness is proven by majority of researchers to have a great impact on the vehicle dynamic load. Whether the bridge dynamic response can be covered by a unified impact factor calculation formula, and whether the existing impact factor formula can be directly applied to the curved bridge, such problems have no answers yet. More theoretical studies are needed in order to provide a practical empirical formula to improve the design theory of curved bridges and maintenance and retrofit methods for existing curved bridges.

The specific objective of this research is to study the curved bridge dynamic response under vehicle-bridge interaction. First, by using commercial program ANSYS, several multi-beam models of an existing bridges were built based on shear force flexible grillage method. The warping stiffness and moment of inertia are both considered in this model. A spatial vehicle model with 24 degrees of freedoms (DOFs) with three-dimensional beam element, mass element and spring-damper elements is adopted in the model. Taking effect of random surface roughness, the separation iteration algorithm is

used to the coupled vibration of the two subsystems. Second, using the model proposed above, this research analyzes the influence of vehicle speed, surface roughness, radius of curvature, lane eccentricity, stiffness and damping of tires and bridge structure, in order to fully understand the influence factors of dynamic response of curved bridges. Also, the influence of multi-lane loading, vehicle number and vehicle spacing on the impact factor is studied.

2. Literature review

2.1 Vehicle model

By treating the vehicle as a moving force or pulsating load and neglecting the vehicle inertia effect, Timoshenko (1922) published considerable different approximate solutions for the moving load over simple beam structure dynamic interaction problem (Figure 2.1). Hu Ding et al. (2013) investigated the dynamic interaction problem with a beam supported by nonlinear viscoelastic foundations. With this beam model, essential dynamic characteristics of bridge under moving traffic can be observed with a reasonable degree of accuracy. However, this method ignores the interaction between the bridges and moving vehicle, therefore the moving load method is only available for cases where the mass of the traffic is relatively small to the bridge. Since the moving force/load model is the simplest model that can be applied to the interaction problem, this method has been frequently adopted by researchers when dealing with the vehicle-bridge interaction problem. Arshad Mehmood (2014) developed a method combines finite element method and Newmark time integration method in vibration analysis. Using computer code written in Matlab, the dynamic response of the structures and critical load velocities can be found with high accuracy.

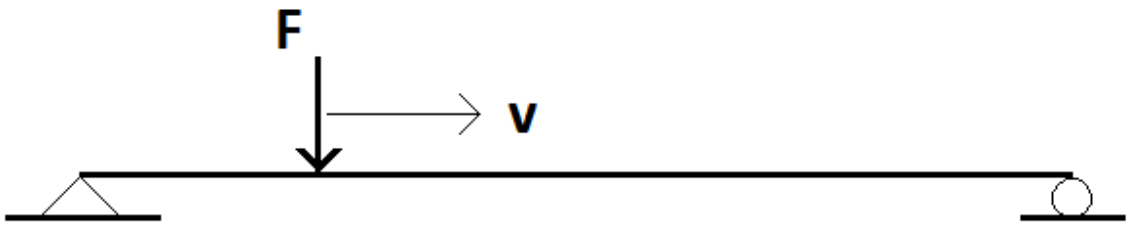

Figure 2-1 Moving load model

When the inertia of the vehicle should be taken into consideration, the moving mass model (Figure 2.2) is the simplest model that can be adopted. The inertial effects of bridge and the moving vehicle were studied as early as in 1929 by Jeffcott by the method of successive approximations. The investigations along this line were later carried out by many researchers. Ting (1974) and Sadiku (1987) developed the algorithms for moving mass problem using Green's function. Ichikawa and Miyakawa (2000) combine eigen-function expansion or modal analysis method and the direct integration method to obtain a simple solution for moving mass vibration analysis. Eftekhar Azam et al. (2012) transformed the partial differential equations of the system into the Ordinary Differential Equations and obtained a reasonable accuracy. One of the major drawbacks of the moving mass solution is that it fails to introduce the behavior of the bouncing action of the vehicle and the bridge. This so-called bouncing effect is usually considered to be significant when poor surface condition is presented.

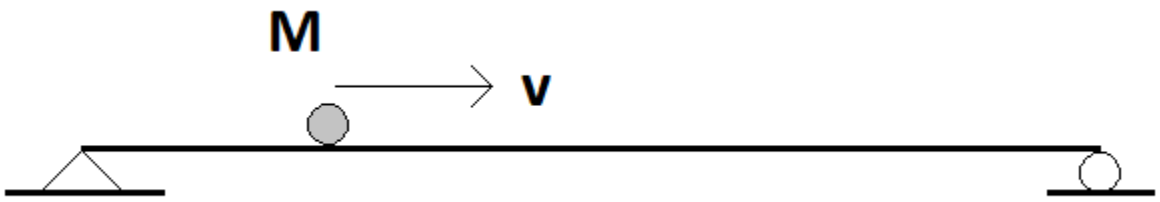

Figure 2-2 Moving mass model

By considering the elastic and damping effects of the suspension system, the vehicle model can be further enhanced. One simplest model, in this case, is the sprung mass model which is a moving mass supported by a spring unit (Figure 2.3). Since early 60s, researchers such as Biggs (1964) presented a semi-analytical solution to the simple beam sprung mass interaction problem. Pesterev (2001) studied the behavior of an elastic continuum when under multiple moving oscillations using the series expansion technique. Later on, he discovered that for a simply support beam under oscillator load and moving mass problem, there is little difference in area of the beam displacements, but the difference of the beam stresses is quite noticeable. Also, it was shown that for spring with small stiffness, the moving oscillator problem is equivalent to the moving load problem.

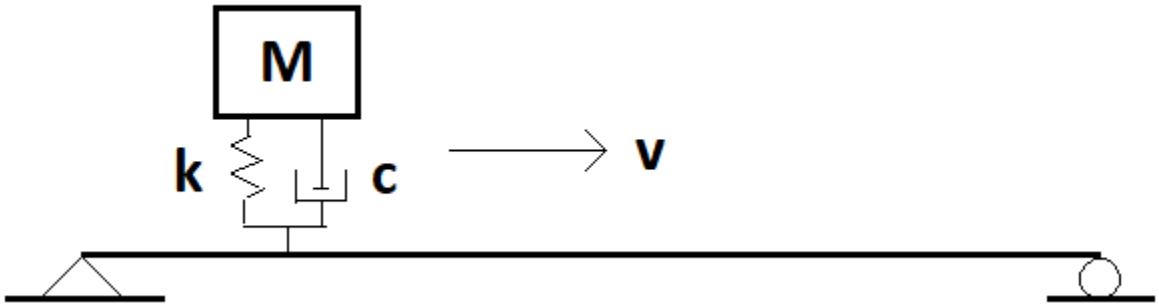

Figure 2-3 Sprung mass model

With the emergence of the high performance computers and computation software, it becomes feasible to have a more realistic modeling of the dynamic properties of a moving vehicle. The multiple-axle truck can be represented as a number of discrete masses each support by a set of spring and dashpot (Figure 2.4). Yang (1999) created a vehicle model as two sets of the spring dashpot unit supporting a rigid beam as vehicle body, each set of spring support is modeled on top of a mass unit representing wheel. To better represent the various dynamic properties of heavy trucks, vehicle models with multiple degrees of freedom have been devised and used by Chu (1986), Wang (1991) and Zhang (2001). Zhang introduced a classic 11 degrees-of-freedom model for the three axle tractor-trailer HS20-44 truck, the truck is modeled as a nonlinear vehicle model with five sprung masses. Such model is widely modified and applied in other researchers' study. Mario Fafard (1996) proposed a sophisticated tractor and semi-trailer combination model with 18 DOFs to describe its movement, the vertical displacement, pitching and transverse rotations are accounted and assume to remain small throughout the analysis. Although the use of a more sophisticated vehicle model can make the simulation more

realistic, it does cause certain computation problems, where divergence and slow convergence may occur in the process of iteration.

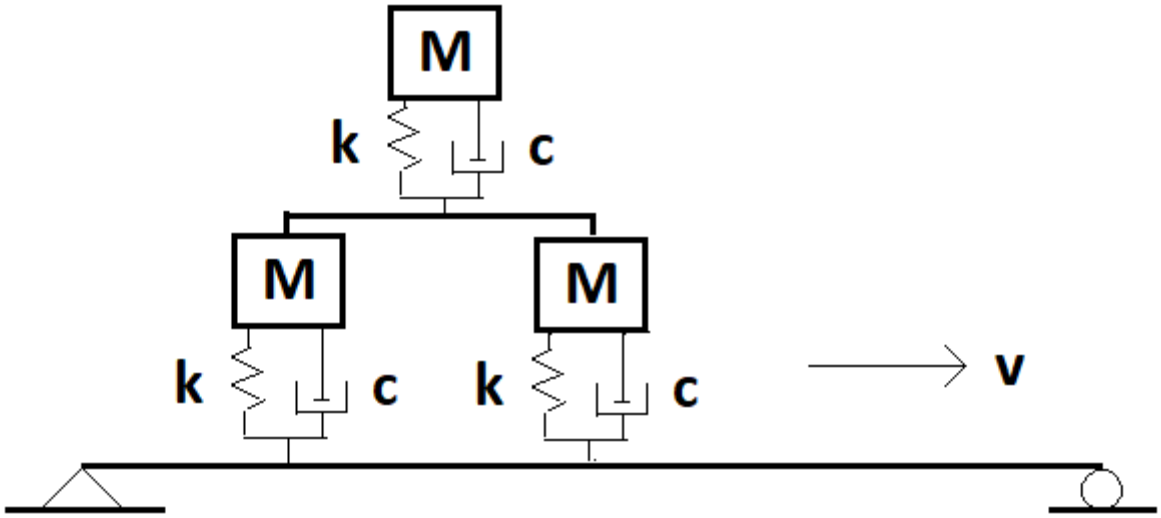

Figure 2-4 Multiple-axle truck model

2.2 Bridge model

Beam model with simply-supported at both ends is the most well known structure that has ever been adopted in the study of vehicle-bridge interactions. Usually, this model is considered having no restriction on the type of structures involved in the vehicle-interaction problems, since the structure can always be represented by finite elements of various forms. This beam model has been adopt in past vehicle bridge interaction researches on various types of bridges, such studies include multi-span bridge (Wu, Dai

1987; Marchesiello et al,. 1999), multi-girder bridge (Huang, Nowak, 1991), continuous beams bridges (Yang, 1995) and curved girder bridges (Chang,1997; Yang, 2001).

One major concern in the simulation of the bridge response under vehicle load is the influence of road surface roughness (Figure 2.5). It has been reported that road surface or pavement roughness can significantly affect the impact response of bridges (Paultre, 1992).The surface profile depends primarily on the quality of the construction of road pavement and the maintenance level after bridges enter service. In most cases, this three-dimensional surface roughness is often approximated by random two-dimensional profile. Gupta (1980) used a sine function to represent road surface roughness. The roughness profile can be created using stationary Gaussian random process and specific power spectral density functions to describe the randomness property of the bridge deck. Similar methods were widely adopted by researchers in this area (Huang and Nowak, 1991; Chang and Lee, 1994). The power spectral density functions developed by Dodds and Robson (1973) has been modified and used by Wang and Huang (1992) in their analyses. Marcondes and Burgess (1991) generated three different categories of the pavement by using the data collected from field measurement.

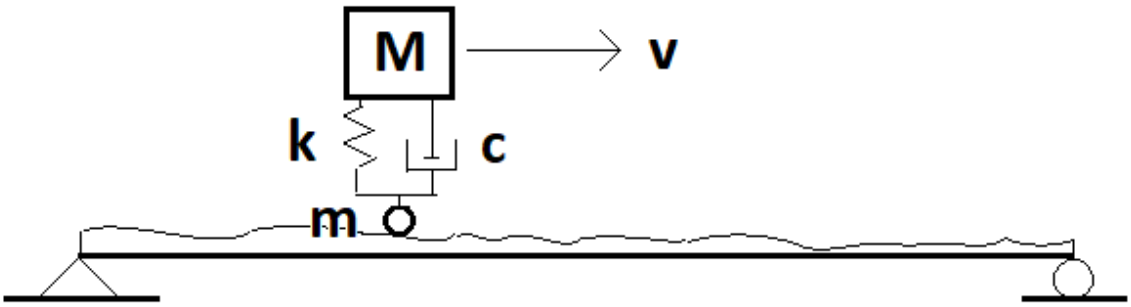

Figure 2-5 vehicle bridge interaction with surface roughness model

2.3 Influence of horizontal curvature

The majority of early vehicle –induced vibration studies were focus on straight beams scenarios. The horizontal moving load can be regarded as the centrifugal forces created by the interaction force between curved bridge lane and moving vehicle. This horizontal centrifugal force is usually constantly changing, contrary to the vertical moving loads, which always stay at the same direction and received less impact from vehicle traveling status such as speed. Pioneer researchers such as Tan and Shore (1968) conducted research on vertical or out-of-plane vibration of curved girder interaction. However, the in plane vibration of centrifugal focus acting on a curved girder was rarely studied.

2.4 Method of Solution

Two sets of equations of motion can be written in a vehicle-bridge interaction system, one for the bridge and the other for the vehicle. The two sets of equations are

considered coupled due to the contact (interaction) forces existing at the contact points which also physically connecting these two subsystems (vehicle system and bridge system). The system matrices are time-dependent due to moving contact points, therefore the matrices must be updated and factorized at each time step. To solve these equations, one method (Huang and Nowak, 1991) is assuming a set of initial values of displacements of these subsystems' contact points to start the analysis, the initial interaction forces from vehicle can be solved as the model starting status. Next, the more precise values of contact points displacements can be calculated by updating the bridge integration equation with the contact forces from last step. This method can generate both vehicles and bridge responses at any instant simultaneously. However, for studies involving bridge cases that require more realistic and complex environment, such as high volume traffic, different driving pattern and multiple surface conditions, the convergence rate of such iteration could be low. To increase the convergence rate and calculation efficient, later research develop a condensation method for model elements. Such condensation procedure is widely accepted and considered as one of more efficient approaches for solving the vehicle-bridge interaction problem. Yang and Lin (1995) used the dynamic condensation method to eliminate the degrees of freedom associated with each vehicle on the element level. Other methods that have been employed in solving the equations of motion in the vehicle-bridge interaction problem include:

1. Direct integration methods (Newmark method 1959) and fourth-order Runge-Kutta method (Chu, 1986);

2. Modal superposition method (Blejwas, 1979) along with various integration schemes;
3. Fourier transformation method (Green and Cebon, 1994; Chang and Lee, 1994).

A more versatile approach was developed by Yang and Wu (2001), in this method the vehicle equations are discretized in time domain. For each time step, Yang considered the vehicle contact forces as a set of external loads and transformed as nodal loads matrix to apply to bridge subsystem. In such way, the coupled subsystems' behavior such as bridge displacements, vehicle status for next time step can be solved. For the curved bridge vehicle interaction where vertical and horizontal contract forces are both involved, this procedure has been demonstrated to be quite flexible.

2.5 Damping influence

Damping refers to the consumption of energy in the process of structural vibration, which is the fundamental parameter of structural dynamic analysis. The damping performance has an important influence on the dynamic response of the structure. Currently, most researchers have studied the influence of damping on the seismic response of the building structure and bridge structure. The influence in the vehicle-bridge interaction problem is less studied. The previous researchers focused on the following two issues: (1) the selection method of damping value and damping parameter; (2) the influence of damping value on the seismic response. The existing research results

show that damping can effectively dissipate the seismic energy and reduce the seismic response of the structure. Y.F Song and S.H He (2001) analyzed the impact coefficient of the bridge by taking the damping ratio as 0.02 and 0.05 respectively and pointed out that the damping ratio has a great influence on the impact coefficient of the bridge, especially at high speeds and lousy pavement conditions. Research from M. Maijka (2008) shows that vehicle speed, axle system frequency, mass-span ratio, and bridge structure damping have a significant influence on the dynamic response of the bridge, while the influence of vehicle damping on the bridge response is almost negligible.

2.6 Impact factor

In practice, the dynamic response of a bridge is usually considered ideally by introducing an impact factor during the calculation, the actual interaction force is taken as the static load multiplied by this impact factor. This impact factor is defined as the ratio of the maximum bridge dynamic response to the maximum bridge static response under certain load situation and then minus one. One typical definition for the impact factor I is:

$$I = \frac{R_d(x) - R_s(x)}{R_s(x)} \qquad (2.1)$$

where $R_d(x)$ and $R_s(x)$ represent the maximum dynamic and static responses of the bridge at the cross section x of the bridge.

It is well known that serval variables could affect the impact factor of a bridge under the excitation of moving vehicle, such as vehicle dynamic properties, vehicle speed and pavement roughness. The bridge code, American Association of State Highway and Transportation Officials (AASHTO) Standard Specification (2014 edition), used to relate the impact factor to the bridge span length L, the impact factor I is defined as the increment of the static response of the vehicle load and can be determined by the formula:

$$I = \frac{50}{L+125} \leq 0.3 \qquad (2.2)$$

However, in the AASHTO LRFD Bridge Design Specifications (2017), dynamic load allowance is not a function of span length, and its value depends only on the component and the limit state. AASHTO currently assigns values to dynamic load allowance as following:

Table 2-1 Dynamic load allowance in AASHTO LRFD Bridge Design Specification

Limit State	Dynamic Load
Deck Joints: All Limit States	75%
All Other Components: Fatigue and Fracture Limit State	15%
All Other Components: All Other Limit States	33%

In codes from other countries, such as Canada and Australia, the dynamic behavior is considered related to the fundamental frequency of the bridge. Canadian Ontario

Bridge Design Code (OHBDC-1983) introduced dynamic load allowance in the vehicle bridge interaction, the allowance is specified as a function of the natural frequency of vibration of the bridge. However, later field study indicates the field measurements have a considerable scatter of values.

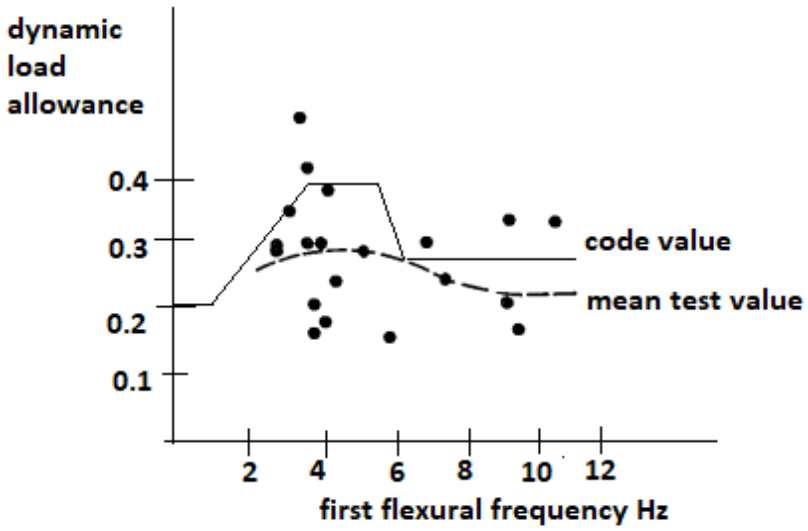

Figure 2-6 Dynamic load allowance in OHBDC

For curved bridge impact factor, Koichi (1985) field test on 21 curved bridges and came up with equation for impact factor I:

$$1 + I = \frac{R_s}{R_p}\frac{5}{L} \leq 1.4 \qquad (2.3)$$

where R_s is the radius of curvature at the shear center of the curved bridge (m), R_p is the radius of curvature of the point of loading (m), L is the span of curved bridge. His research also pointed out that impact factors generated by irregular loads are generally smaller than those of continuously loads, and the outer girders tend to have larger impact factors than those of inner girders.

3. Research Outline

Chapter 1 Introduction

The chapter illustrates the background, motivations, objectives and limitations of the research.

Chapter 2 Literature Review

The chapter reviews the previous research work on vehicle bridge interaction analysis, modeling method. The review lays the foundations and start point of the research.

Chapter 3 Vehicle bridge interaction model

The chapter describes the basic theory of the vehicle and bridge structure model that is going to be used in the research.

Chapter 4 Vehicle bridge interaction analysis using simple beam model, grillage model and multi-beam grillage model

Two selected bridges, concrete and steel curved bridges, were modeled using triple-beam model.

Chapter 5 Vehicle bridge interaction analysis using three-dimensional solid FEM model

Model the selected bridge using three-dimensional solid FEM model for comparison.

Chapter 6 and 7 Parametric Study

A parameter study is performed in order to quantify the effects of different parameters on vehicle bridge dynamic interaction, including curvature radius, span configurations, bridge pavement condition, lane location, vehicle properties and traveling speed.

Chapter 8 Calculation of impact factor based on empirical functions

A simplified empirical function is summarized from previous parametric data. The function is also compared to current method of determining impact factor. Comments and suggestions are made.

4. Theory of Vehicle-Bridge Analysis

4.1 Dynamic Analysis Model and Dynamic Characteristic Parameter

Analysis of Curved Girder Bridge

For curved bridges, the principal axis of cross section of the girder beam and the applied load are generally not in the same plane, which will cause vibration in three dimensions. Therefore spatial beam element with six degrees of freedom for each node is required to model the structure.

The x-axis is the axial direction of the unit, and the y-axis and z-axis are the main axes of inertia of the section respectively. The displacements of the i and j nodes of the unit are denoted as

$$\{\delta_i\} = \left[u_i\ v_i\ w_i\ \theta_{xi}\ \theta_{yi}\ \theta_{zi}\right]^T$$

$$\{\delta_j\} = \left[u_j\ v_j\ w_j\ \theta_{xj}\ \theta_{yj}\ \theta_{zj}\right]^T \qquad (4.1)$$

The element displacement matrix as

$$\{\delta^e\} = \left[u_i\ v_i\ w_i\ \theta_{xi}\ \theta_{yi}\ \theta_{zi}\ u_j\ v_j\ w_j\ \theta_{xj}\ \theta_{yj}\ \theta_{zj}\right]^T \qquad (4.2)$$

For a common curved girder in bridge engineering, the displacement and deformation of the bridge can be described by four basic displacements: longitudinal

displacement in beam axis u(x, t), the x-y plane lateral displacement v(x, t), the x-z plane vertical displacement w(x, t) and rotation angle θ(x, t). In addition to the nodal displacement {f} during the movement, there are speed matrix $\{f'\}$ and acceleration matrix$\{f''\}$. Assuming the material density as ρ and damping coefficient as μ, there are damping force - $\mu\{f'\}$ and inertia force - $\rho\{f''\}$. The element displacement matrix can then be expressed as:

$$\{f\} = [u(x,t)\ v(x,t)\ w(x,t)\ \theta_x(x,t)]^T = [N(x)\{\delta^e\}] \qquad (4.3)$$

Where the [N(x)] is the element shape function

$$[N(x)] = \begin{bmatrix} N_{iu} & 0 & 0 & 0 & 0 & 0 & N_{ju} & 0 & 0 & 0 & 0 & 0 \\ 0 & N_{iv} & 0 & 0 & 0 & N_{i\theta z} & 0 & N_{jv} & 0 & 0 & 0 & N_{j\theta z} \\ 0 & 0 & N_{iw} & 0 & N_{i\theta y} & 0 & 0 & 0 & N_{jw} & 0 & N_{j\theta y} & 0 \\ 0 & 0 & 0 & N_{i\theta x} & 0 & 0 & 0 & 0 & 0 & N_{j\theta x} & 0 & 0 \end{bmatrix}$$

Where,

$$N_{iu} = N_{iu}(x) = 1 - \frac{x}{l}, N_{ju} = N_{ju}(x) = \frac{x}{l}$$

$$N_{i\theta x} = N_{i\theta x}(x) = 1 - \frac{x}{l}, N_{j\theta x} = N_{j\theta x}(x) = \frac{x}{l}$$

$$N_{iv} = N_{iv}(x) = 1 - 3(\frac{x}{l})^2 + 2(\frac{x}{l})^3, N_{jv} = N_{jv}(x) = 3(\frac{x}{l})^2 - 2(\frac{x}{l})^3$$

$$N_{iw} = N_{iw}(x) = 1 - 3(\frac{x}{l})^2 + 2(\frac{x}{l})^3, N_{jw} = N_{jw}(x) = 3(\frac{x}{l})^2 - 2(\frac{x}{l})^3$$

$$N_{i\theta y} = N_{i\theta y}(x) = 1 - 2l(\frac{x}{l})^2 + l(\frac{x}{l})^3, N_{j\theta y} = N_{j\theta y}(x) = -l(\frac{x}{l})^2 + l(\frac{x}{l})^3$$

$$N_{i\theta z} = N_{i\theta z}(x) = 1 - 2l(\frac{x}{l})^2 + l(\frac{x}{l})^3, N_{j\theta z} = N_{j\theta z}(x) = -l(\frac{x}{l})^2 + l(\frac{x}{l})^3$$

The speed and acceleration matrix can then be expressed as,

$$\{f'\} = [u'(x,t)\ v'(x,t)\ w'(x,t)\ \theta'(x,t)]^T = [N(x)]\{\delta'^e\} \qquad (4.4)$$

$$\{f''\} = [u''(x,t)\ v''(x,t)\ w''(x,t)\ \theta''(x,t)]^T = [N(x)]\{\delta''^e\} \qquad (4.5)$$

For element nodal load can be expressed as,

$$\{F\}_\mu^e = -\int [N(x)]^T\ \mu\{\mathrm{f}'\}\mathrm{dV}$$

$$\{F\}_\rho^e = -\int [N(x)]^T\ \rho\{\mathrm{f}''\}\ \mathrm{dV} \qquad (4.6)$$

Which can also be expressed as,

$$\{F\}_\mu^e = -\int [N(x)]^T\ \mu\{N(x)\}\{\delta'^e\}\mathrm{dV} = -[c^e]\{\delta'^e\}$$

$$\{F\}_\rho^e = -\int [N(x)]^T\ \rho\{N(x)\}\{\delta''^e\}\mathrm{dV} = -[m^e]\{\delta''^e\} \qquad (4.7)$$

Where

$$[c^e] = \int [N(x)]^T\ \mu\{N(x)\}\mathrm{dV}$$

$$[m^e] = \int [N(x)]^T\ \rho\{N(x)\}\mathrm{dV}$$

Assuming that the unit force is been applied nodal load $\{P^e\}$, the element equilibrium equation can be written as

$$[m^e]\{\delta''^e\} + [c^e]\{\delta'^e\} + [k^e]\{\delta^e\} = \{P^e\} \quad (4.8)$$

And the global equilibrium equation

$$[M]\{\delta''\} + [C]\{\delta'\} + [K]\{\delta\} = [P] \quad (4.9)$$

Without any damping effect, an undamped free vibration equation of the structure can be obtained

$$[M]\{\delta''\} + [K]\{\delta\} = [0] \quad (4.10)$$

Assume this free vibration is simple harmonic vibration

$$[\delta(t)] = [\varphi]\sin(\omega t + \theta)$$

$$\{[K] - \omega^2[M]\}[\varphi] = [0]$$

According to the Cramer's rule, to obtain a nontrivial solution to a homogeneous linear system of equations, the coefficient determinant mush equal to zero. In this case, it is

$$\{[K] - \omega^2[M]\} = [0] \quad (4.11)$$

This equation is called the frequency equations of the system. For an equation of a N-degree-of-freedom system will have N roots of the equation representing the frequencies of the N possible modes of the system. These N frequencies arranged in the order from small to large will constitute the spectrum of the system. The smallest frequency is the fundamental frequency of the structure and the fundamental mode

corresponding to the first vibration mode. Such eigenvalue problems are usually solved by matrix iterative method, this research use Block Lanczos method.

4.2 Multi-axis vehicle model description

4.2.1 Vehicle model coordinate systems

In order to describe the dynamics of vehicles moving on curved bridges, three sets of coordinate systems are introduced, the fixed ground coordinate system, the vehicle coordinate system and the wheel coordinate system.

Fixed ground coordinate system

To describe the steering attitude and trajectory of the vehicle, Cartesian coordinate system fixed on the ground (X, Y, Z) is selected as the reference frame. For convenience, the origin of the fixed ground coordinate system is set at the center of the curvature and the driving trajectory of the vehicle is described as a cylindrical-coordinate system.

Vehicle coordinate system

The vehicle coordinate system (x, y, z) is a coordinate system that is fixed on the vehicle with the vehicle mass center (MC) as the origin and moves with the vehicle. The vehicle motion parameters according to the right-handed Cartesian coordinate define the coordinate system as follows.

x – Forward, travelling direction of the vehicle

y – Pointing to the left side of the vehicle travelling direction

z – Pointing vertically upward from vehicle

θ_x – The roll angle around the axis x

θ_y – The pitch angle around the axis y

θ_z – The yaw angle around the axis z.

Wheel coordinate system

The wheel coordinate system (x_i, y_i, z_i) is a coordinate system that is fixed on the wheel and moves with the wheel based on the axle center TC. The system is used to describe the dynamic interaction force between the vehicle and the bridge and it is defined by the right-handed Cartesian coordinated system as follows.

x_i – Forward, on the longitudinal plane of symmetry of the wheel

y_i – Point to the left along the axle in the wheel rolling direction

z_i – Point upward in the vertical direction from the wheel

δ_L – The attack angle of the steering wheel around the axis, called the Ackermann steering angle, which is used to describe the kinematic effect of a vehicle's steady-state steering.

4.2.2 Simplified vehicle model (3-axle)

In this study, the typical 3-axle vehicle is simplified into a vibration system connected by mass, spring and damper. The body is modeled as a rigid body, and the

suspension system and tire are modeled jointly by a spring and a viscous damper with energy dissipation capability. The mass of the suspension system and tire is simulated by the ideal mass elements. The model considers the vertical and horizontal vibrations of the vehicle and the rotational vibration around the three axes. The simplified model of the vehicle is shown in the figure below. The model contains a total of 12 generalized degrees of freedom. Among them, four generalized coordinates of $y_m, z_m, \theta_{xm}, \theta_{ym}$ are selected to describe the lateral vibration, vertical vibration, roll around the x axis and pitch vibration around the y axis. Coordinates z_1, z'_1, y_1 from front suspension are selected to describe the vertical vibration, lateral vibration, five generalized coordinates from rear suspension $z_2, z'_2, z_3, z'_3, y_1, y_2$ are used to describe its vertical vibration, Lateral vibration, rolling, and pitching vibration, respectively.

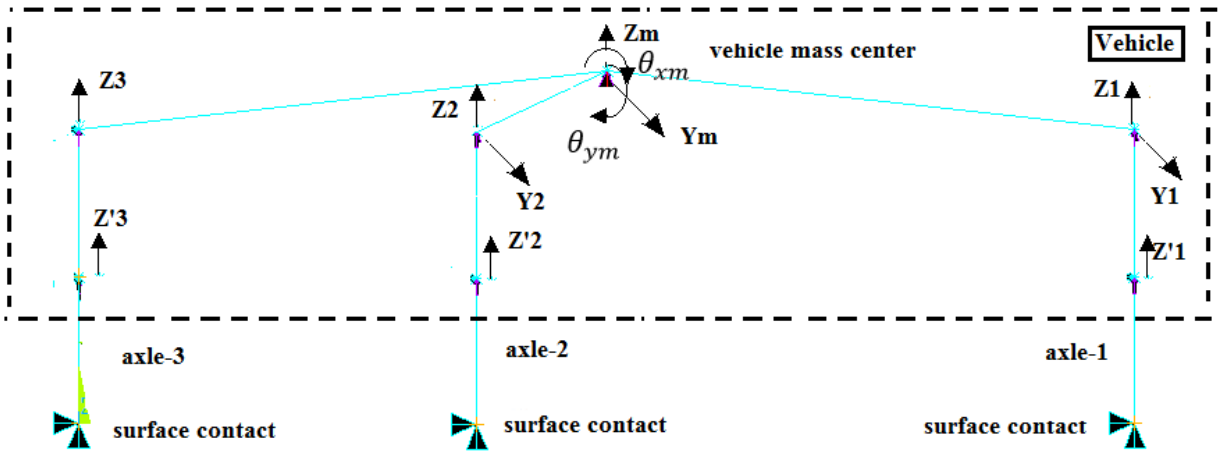

Figure 4-1 3-axle truck model and degrees of freedom

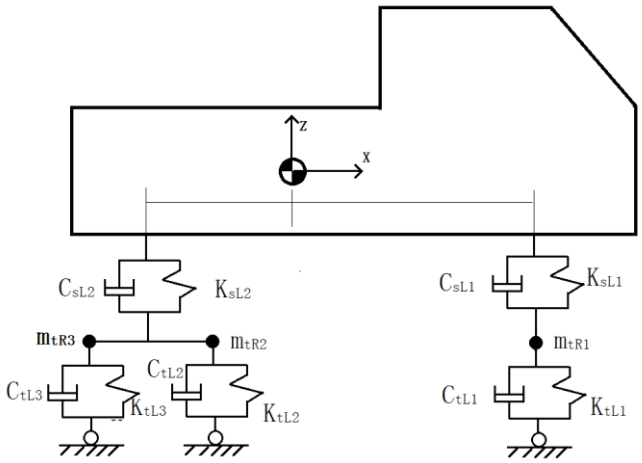

Figure 4-2 3-axle truck model and degrees of freedom

4.2.3 Simplified vehicle model (3D, 3-axle)

In this study, an improved 3D vehicle model which is based on the typical 2D model, is introduced in the later analysis. Vehicle is considered as two connected 'half truck' models. Additional pseudo beam is also modeled in the bridge model to support the 3D vehicle model and distribute the interaction forces. By applying the elevation differentials of the support beam, the influence of the curved bridge horizontal elevation in the vehicle bridge interaction can be studied.

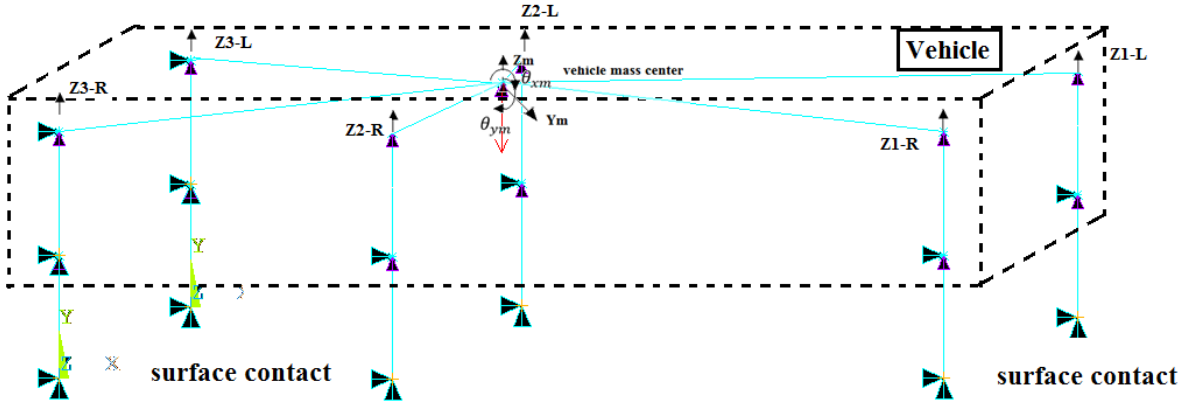

Figure 4-3 3D truck model

4.3 Random surface roughness

It is assumed that the roughness of the pavement is a Gaussian random process with power spectrum to represent the statistical characteristics of the pavement. In this study, analysis chooses method developed by Eui-Seung Hwang and Wewak (1990),

$$S_r(\Omega) = \begin{cases} \alpha\Omega_k^{-\beta} & \Omega_L < \Omega_K < \Omega_U \\ 0 & otherwise \end{cases} \qquad (4.12)$$

Where

β – Frequency factor, 0.2

α – Surface roughness ratios

Ω – Spatial frequency, the inverse of the wavelength, indicating the number of occurrences of a harmonic in each meter.

Ω_L Ω_U – Lower and upper limits of the spatial frequency

After applying inverse fast Fourier transform to above formula, the vertical distribution function of the vertical irregular shape of the bridge deck can be obtained.

$$r(s) = \sum_{K=1}^{N} \alpha_K \, COS(2\pi\Omega_k \, s + \phi_k) \qquad (4.13)$$

Where

α_K – Amplitude

ϕ_k- Random phase angle, random numbers between [0, 2π];

s - Longitudinal coordinates of the bridge.

4.4 Vehicle-Bridge coupling analysis

4.4.1 Basic assumptions

In current study, the models used for vehicle bridge interaction analysis follow these assumptions.

1. When a vehicle travels along the curved bridge, the instantaneous center of rotation coincides with the center of curvature of the circular curve, and the deflection angle of the inner steering wheel is greater than the deflection angle of the outer steering wheel.

2. The vehicle lateral slip angle of the center of mass does not change with time and the vehicle makes a steady circular motion on the circumference. Also, the attack angle of the vehicle front wheel remains constant.

3. This study ignores the elastic deformation of the vehicle body, the suspension and axle. The vehicle body, suspension and axle are treated as rigid bodies where they are connected by springs and dampers. Dampers are assumed to have linear viscous damping property.

4. The body, the suspension and each pair of rigid bodies of the wheelset make small displacement vibration at the balance position, and does not consider the influence of the change of the vehicle center of gravity height on the centrifugal force and the centrifugal moment caused by the slight vibration generated by the vehicle body under the unevenness of the bridge deck.

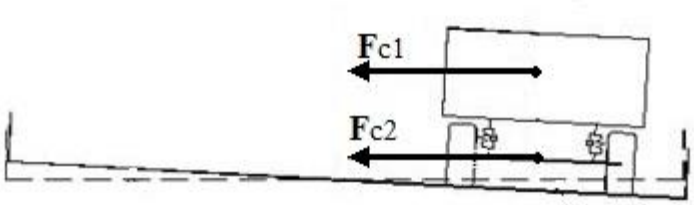

Figure 4-4 Centrifugal forces on the moving vehicle

5. The vehicle model is symmetrical along the longitudinal direction; the model ignores the vibration along the longitudinal axis. The rear wheels are travelling on the ruts of the front wheels.

4.4.2 Motion equations of vehicle

Based on the commercial finite element analysis software ANSYS, the spring-damping element, mass element and the rigid rod space rod element are used to simulate the components of the vehicle. The vehicle model is discretely modeled according to the finite element method. The vibration equation of the vehicle can be expressed as.

$$m_v z'' + c_v z' + k_v z = f_v \qquad (4.14)$$

Where m_v, c_v, k_v and f_v represent vehicle mass matrix, damping matrix, stiffness matrix and outside external excitation vector, respectively.

4.4.3 Motion equations of bridge

The bridge model is discretized by the finite element method, and the equation of motion of bridge is,

$$[M_b]\{\delta''\} + [C_b]\{\delta'\} + [K_b]\{\delta\} = [P_b] \qquad (4.15)$$

Where $[M_b], [C_b], [K_b]$ represent global mass matrix, global damping matrix and global stiffness matrix of the bridge structure, respectively. $[P_b]$ is the external load vector, which is resulting from the vehicle bridge interaction. To simplify the global damping matrix, the $[C_b]$ is usually taken as

$$[C_b] = \alpha[M_b] + \beta[K_b] \qquad (4.16)$$

The factors α and β can be obtained by,

$$\alpha = (2\omega_1\ \omega_2\ (\xi_1\omega_2 - \xi_2\omega_1))/(\omega_2^2 - \omega_1^2)$$

$$\beta = \frac{2(\xi_2\omega_2 - \xi_1\omega_1)}{\omega_2^2 - \omega_1^2} \qquad (4.17)$$

Where ω_1, ω_2 are free vibration frequencies of two selected mode shapes, and ξ_1 , ξ_2 are their respective damping ratios.

4.4.4 Solution of vehicle bridge dynamic interaction force

The forces acting on the bridge by a vehicle traveling on a curved girder bridge include the following two factors. First, vertical and lateral wheel loads due to centrifugal

forces, and second, dynamic loads caused by vehicle self-weight and bridge deck roughness excitation.

4.4.5 Centrifugal force effect

When a vehicle travelling in a uniform circular motion, centrifugal force $m_v v^2/\rho$ and moment $m_v v^2 h/\rho$ will apply to the mass center of the vehicle. During the circular motion, the mass center will have a lateral displacement $h\ sinx$ (hx). The total moment can be expressed as.

$$M = \frac{m_v v^2 h}{\rho} + m_v g h x \qquad (4.18)$$

Assume the distances between vehicle mass center to the front and rear suspension centers to be l_V, l_H. The centrifugal forces for front and rear suspensions would be $m_v v^2 l_v/(\rho l)$ and $m_v v^2 l_H/(\rho l)$.

Assume the rolling angular stiffness for front and rear axles are C_V, C_H. The total moment can also be expressed as.

$$M = (C_V + C_H)x \qquad (4.19)$$

The rolling angle can then be expressed as.

$$x = \frac{m_v\left(\frac{v^2}{\rho}\right)h}{C_V + C_H - m_v g h} \qquad (4.20)$$

And the spring moment for both axles.

$$M_{FV} = C_V x = \frac{C_v m_v gh}{C_V + C_H - m_v gh} \frac{v^2}{\rho g}$$

$$M_{FH} = C_H x = \frac{C_H m_v gh}{C_V + C_H - m_v gh} \frac{v^2}{\rho g} \quad (4.21)$$

The load differential of front and rear axle is.

$$\Delta F_{z1} s_1 = M_{FV} + \frac{m_v v^2 l_H p_V}{\rho l} + m_1 v^2 h_v / \rho$$

$$\Delta F_{zH} s_H = M_{FH} + \frac{m_v v^2 l_V p_H}{\rho l} + m_2 v^2 h_H / \rho \quad (4.22)$$

Where the rear axle $\Delta F_{zH} = \Delta F_{z2} + \Delta F_{z3} = 2\Delta F_{z2} = 2\Delta F_{z3}$, p_H, p_v are the horizontal and vertical distances of the suspension center to road surface, h_H, h_v are the horizontal and vertical distances of axle mass center to road surface.

By combining the equations above, the differences between dynamic and static wheel loads are.

$$\Delta F_{z1} = m_v v^2 / \rho \left(\frac{C_V}{C_V + C_H - m_v gh} \frac{h}{s_1} + \frac{l_H}{l} \frac{p_V}{s_1} + \frac{m_1}{m_v} \frac{h_v}{s_1} \right)$$

$$\Delta F_{z2} = \Delta F_{z3} = m_v v^2 / \rho \left(\frac{C_H}{C_V + C_H - m_v gh} \frac{h}{s_2} + \frac{l_V}{l} \frac{p_H}{s_2} + \frac{m_2}{m_v} \frac{h_H}{s_1} \right) \quad (4.23)$$

4.4.6 Bridge deck roughness effect

Assuming that the wheels and the deck are always in contact with each other when the vehicle runs through the bridge, the wheel and bridge contact points can be used

to generate the dynamic load of the bridge. The dynamic loading between wheels and bridge can be written as.

$$F_{dij} = c_{tij}\left[z'_{sij} - \zeta'_{tij}(s,t) - r'(s_{ij})\right] + k_{tij}\left[z_{sij} - \zeta_{tij}(s,t) - r(s_{ij})\right] \quad (4.24)$$

Where

i = L, R represents left or right side of vehicle

j = 1,2,3 represents the axle number

$\zeta_{tij}(s,t)$ represents the bridge displacement at given time and location

$r(s_{ij})$ represents the roughness at given location

The external excitation due to surface roughness can then be expressed as.

$$f_{vij} = c_{tij}\left[\frac{\partial \zeta_{tij}(s,t)}{\partial t} + v\frac{\partial r(s)}{\partial s}\right] + k_{tij}\left[\zeta_{tij}(s,t) + r(s)\right] \quad (4.25)$$

5. Vehicle bridge interaction analysis and preliminary result

5.1 Case study bridge models

To study the vehicle-bridge dynamic analysis, two typical curved bridges, Manchuria concrete bridge in China and Veteran's Memorial steel bridge in Florida, United States, were selected to be modeled in ANSYS. Three different models, a simple beam model, a grid model and a three-dimensional solid element model, were built and analyzed.

5.1.1 Manchuria Interchange Bridge

Manchuria Interchange is a cross-over bridge on the HaiMan Highway, built in 2007 with a bridge deck width of 12m, carriageway of 11m and a 6% cross-slope. The superstructure adopts prestressed concrete continuous curved box girder with a curve radius of 280m. The main girder is a single-box double-chamber section with a beam height of 1.90m. The whole structure is a consolidation of pier and beam rigid frame system. The lower structure is a ribbed platform, the foundation of the pier is a rock-fill pile foundation, and the abutment adopts a basin rubber bearing as shown in Figure 5.1.

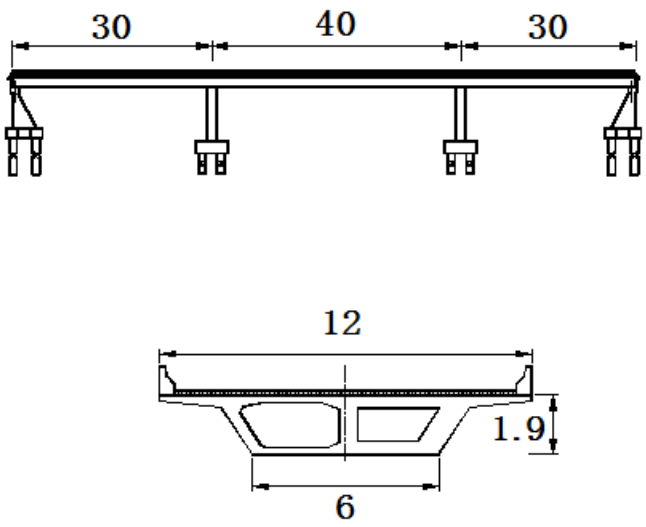

Figure 5-1 Manchuria bridge layout and cross section

Table 5-1 Section properties of bridge model

Section property	Girder	Pier
Cross-section area A(m^2)	7.998~16.022	2.400
Vertical bending inertia I_y (m^4)	4.047~5.808	0.288
Horizontal bending inertia I_z (m^4)	86.720~114.700	0.800
Free torsional inertia I_d (m^4)	9.627~14.681	0.721
Fixed torsional inertia I_ω (m^4)	12.178~17.488	0.022

According to the design drawings of the actual bridge, considering the influence of the crash barriers on the dynamic characteristics of the structure, the simplified beam-type and triple-beam grid dynamic analysis models were respectively established. The

properties of concrete in the model are as follows: Young's modulus$E_c = 34.5GPa$, Poisson's ratio $v = 0.20$, mass density $\rho = 2500kg/m^3$.

The three-beam dynamic analysis model reasonably distributes the mass and stiffness of the deck system to the middle and two side beams according to a certain equivalent method. Based on this, the mass distribution and cross-section characteristics of each main beam in the model are determined. To represent the actual bridge, section properties of the main girders in the triple-girder model are calculated by the formulas in Table 5.2. The stiffness of the horizontal beam is related to the spacing b_1 of the girder. The horizontal beam is modeled by a massless element. The piers are fixed at the bottom where both ends of the main beam only constrained the vertical displacement.

Table 5-2 Section property of triple-beam model

	Section properties
Equivalent mass distribution	$M_1 = M - I_m/b^2$ $M_2 = I_m/2b^2$
Equivalent horizontal stiffness	$A_1 = A - (I_y + I_z)/\beta b^2$ $A_2 = (I_y + I_z)/2\beta b^2$ $I_{z1} = I_z - 2A_2 b^2$ $I_{z2} = 0$
Equivalent vertical stiffness and fixed torsional stiffness	$I_{y1} = I_y - I_\omega/b^2$ $I_{y2} = I_\omega/2b^2$
Equivalent free torsional stiffness	$I_{d1} = I_d, I_{d2} = 0$

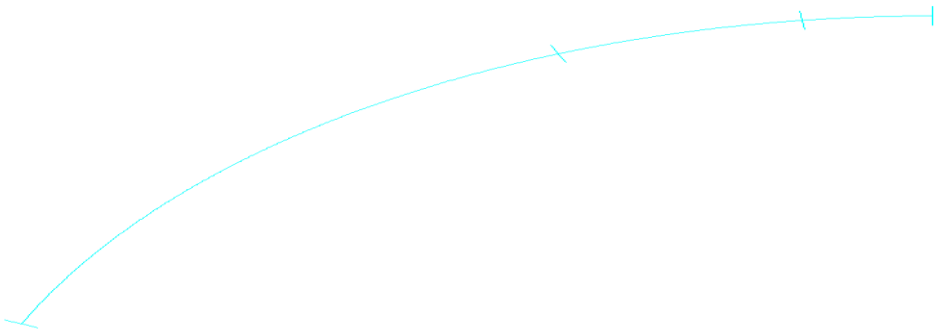

Figure 5-2 Dynamic Analysis models of the Curved Bridge- Simple beam model

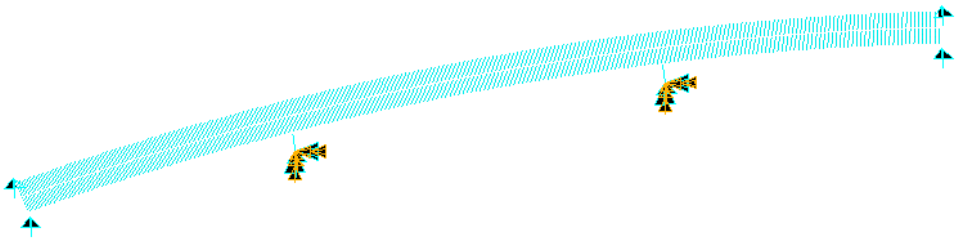

Figure 5-3 Dynamic Analysis models of the Curved Bridge- Triple-beam model

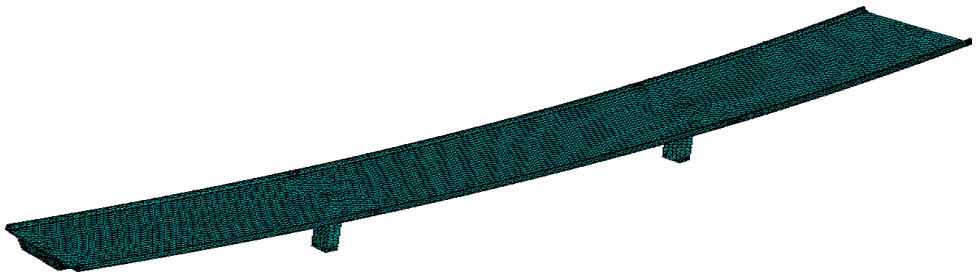

Figure 5-4 Dynamic Analysis models of the Curved Bridge- Solid finite element model

Based on the bridge design and assumptions in Chapter 4, three types of model, simple beam model, triple-beam model and finite element model, were built (Figure 5.2 to Figure 5.4). All three models have equivalent section properties. In the study, the triple-beam model is focused.

For triple-beam model, three typical HS20 truck models (two 2D models and one 3D model) were built with spring-damper-mass elements as shown in Figure 5.5 to Figure 5.7.

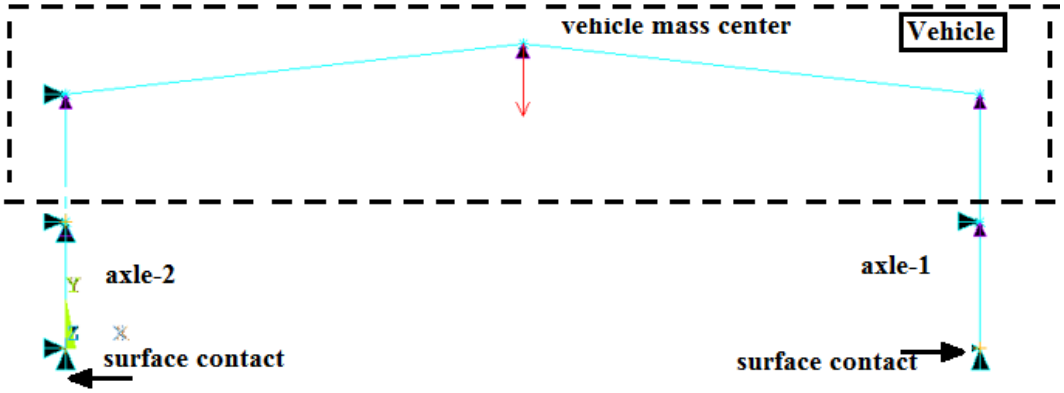

Figure 5-5 Typical 2-axle truck models used in the vehicle-bridge

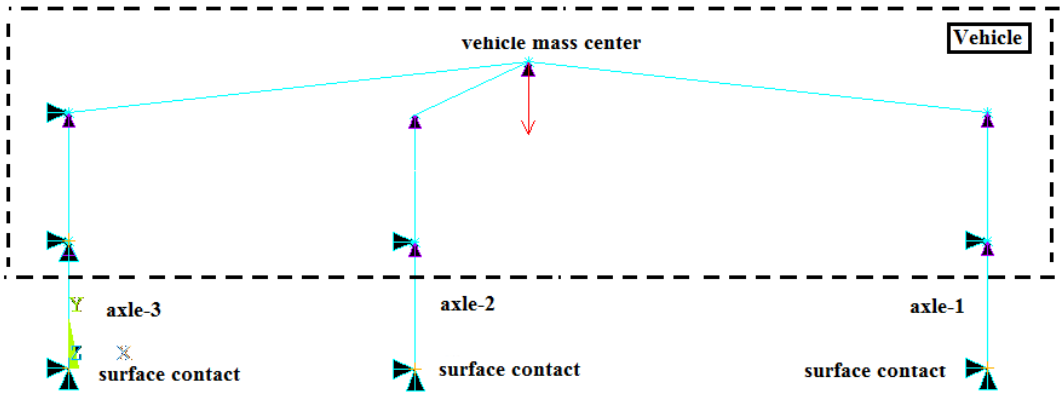

Figure 5-6 Typical 3-axle truck models used in the vehicle-bridge

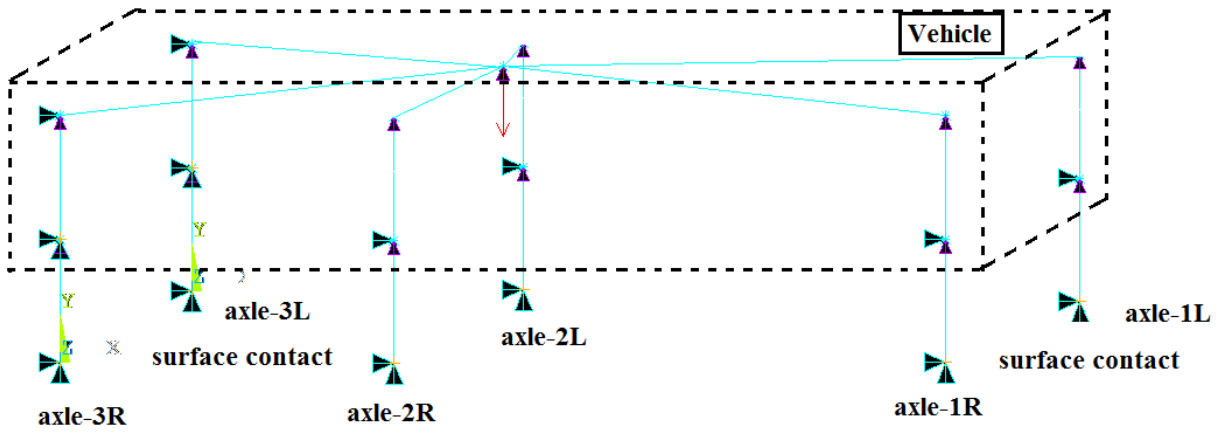

Figure 5-7 Typical 3D 3-axle truck models used in the vehicle-bridge analysis

For 3D vehicle model, additional pesudo beam is created in the bridge model to support the vehicle. By adjusting the bridge horizontal elevation, the influnence of elevation in the curved bridge vehicle interaction is studied.

To study the influence of bridge surface roughness during vehicle-bridge interaction. Using Matlab Three sets of roughness profiles representing different bridge deck conditions are randomly generated and applied during the dynamic analysis. Good surface condition ($a = 0.18 \times 10^{-6} m^3/circle$), normal surface condition ($a = 2.5 \times 10^{-6} m^3/circle$), poor surface condition ($a = 10 \times 10^{-6} m^3/circle$) are shown in Figure 5.4a, b, and c, respectively. Additional profile of perfect surface condition (smooth surface) is also modeled for comparison purpose.

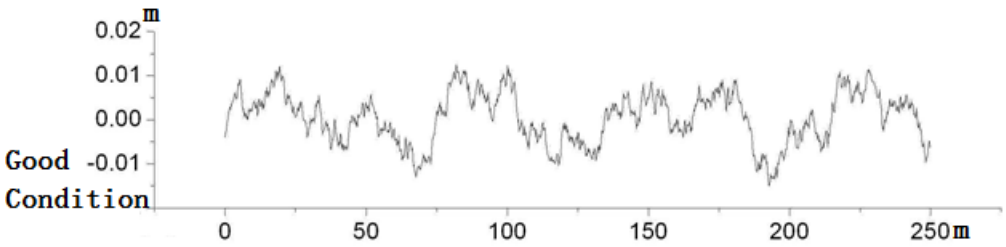

Figure 5-8 Roughness profiles of different types of deck (Good surface condition)

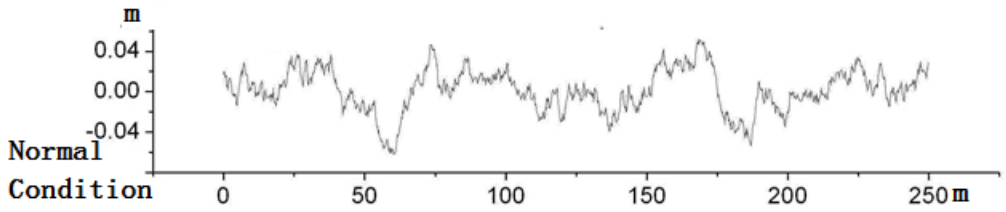

Figure 5-9 Roughness profiles of different types of deck (Normal surface condition)

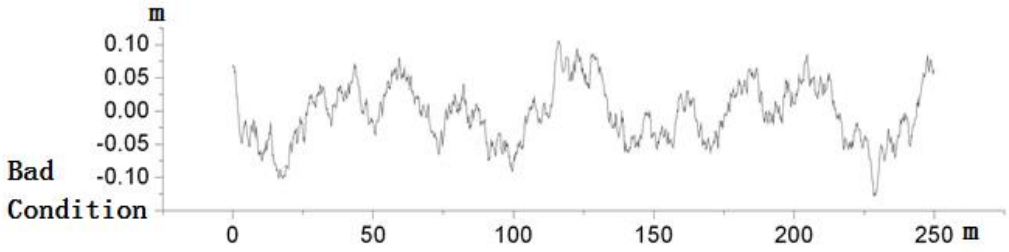

Figure 5-10 Roughness profiles of different types of deck (Bad surface condition)

To reduce the effect of extreme values in the randomly generated surface conditions, each class of roughness profile is respresented by three sets of surface condition profiles using the same variables in the generating process. The mean values of model reactions are selected in the study.

To study the influence of eccentric traffic during the dynamic interaction, three types of eccentric conditions (e=-3.1m, e=0m, e=+3.1m) were also considered to simulate the situation where trucks traveling in different lanes.

5.1.2 Veteran's Memorial Bridge

As a second example, Veteran's Memorial Bridge is a curved steel box girder bridge carrying US-319 in Tallahassee, Florida. The same bridge is tested and analized before by Huang(2002). It consists of two sections of three-span continuous girders; one section is straight and the other is curved. The end spans of the curved box girder bridge are 50.54m long and the middle span is 75.80m long. The cross section is composed of two built-up steel-box girders and composite with the deck. Top flange thickness varies from 2.22 to 6.99 cm and the bottom flange thickness varies from 1.27 to 3.18 cm. The deck is 20.32 cm thick and 13.31 m wide from outside to outside. Internal cross frames are spaced at 3.08 m, except for the end spacing, which is 2.71 m. There is no external bracing between box girders, except at sections over the supports (Figure 5.5).

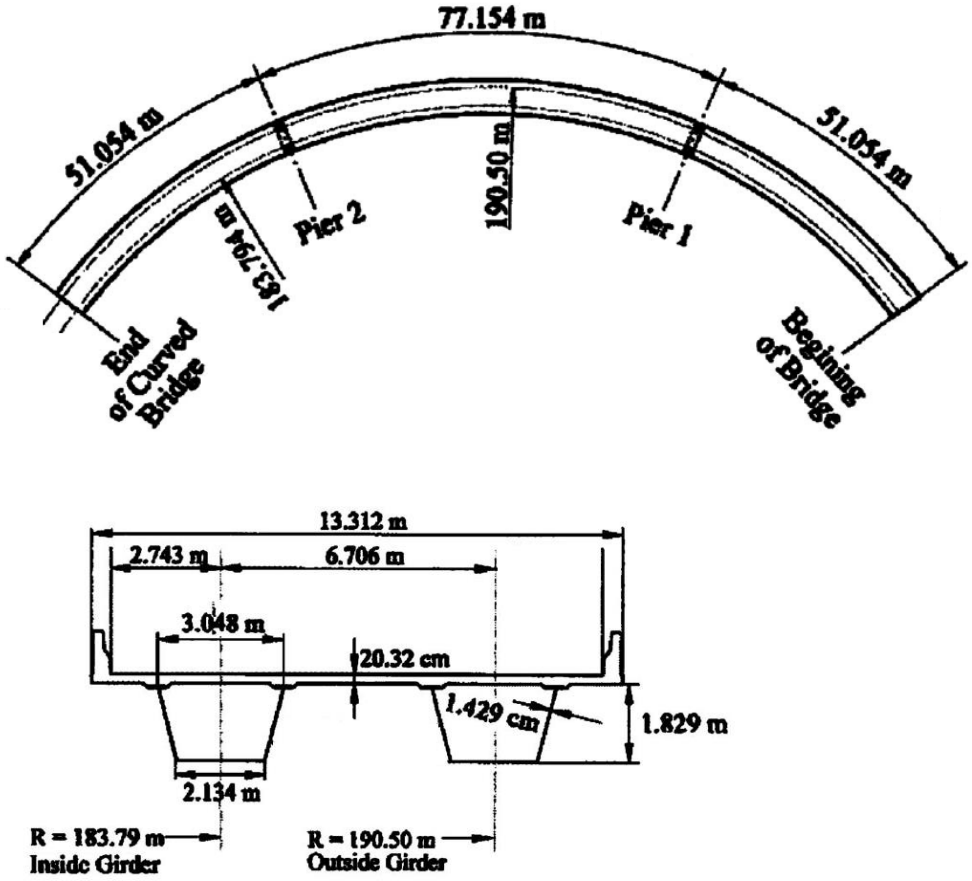

Figure 5-11 Veteran's bridge layout and cross section

Table 5-3 Section properties of bridge model

Section property	Girder	Pier
Cross-section area A(m^2)	5.4876	2.400
Vertical bending inertia I_y (m^4)	3.699	0.288
Horizontal bending inertia I_z (m^4)	77.2807	0.800
Free torsional inertia I_d (m^4)	3.7185	0.721

Similar to the Manchuria bridge, a triple-beam model was constructed with typical 2-axle and 3-axle truck moving across the bridge with three different types of deck surface conditions.

5.2 Preliminary case study results

5.2.1 Manchuria Concrete Curved Bridge

Figures 5.12 to Figure 5.19 shows the displacement and moment responses of the bridge when vehicle travel across the bridge with different speeds. It can be noticed that in good surface condition, the maximum bridge response and moment response remain relatively the same, regardless of the vehicle travelling speed. However, as the traveling speed increased, the response curves became unstable

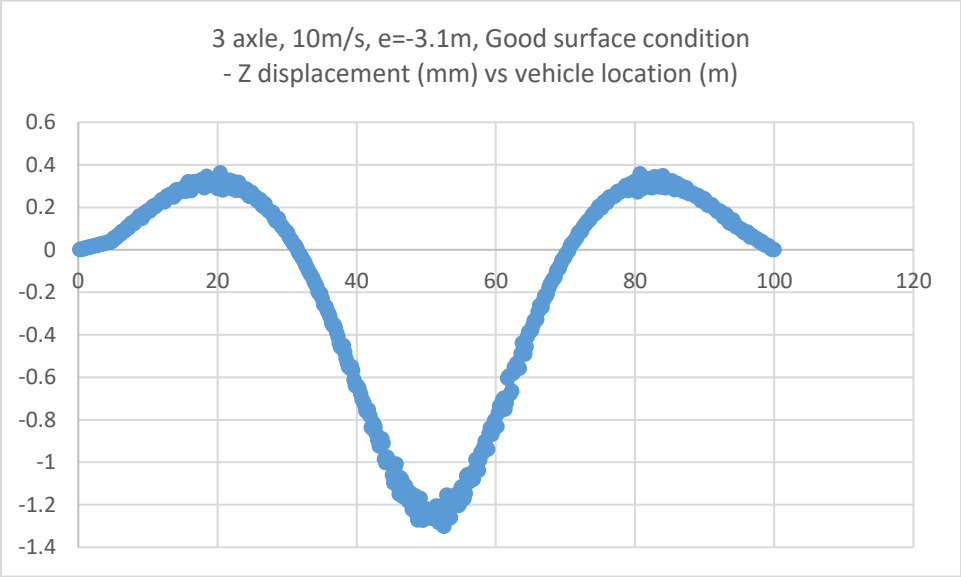

Figure 5-12 Flange deflection of mid span (vehicle speed v=10m/s)

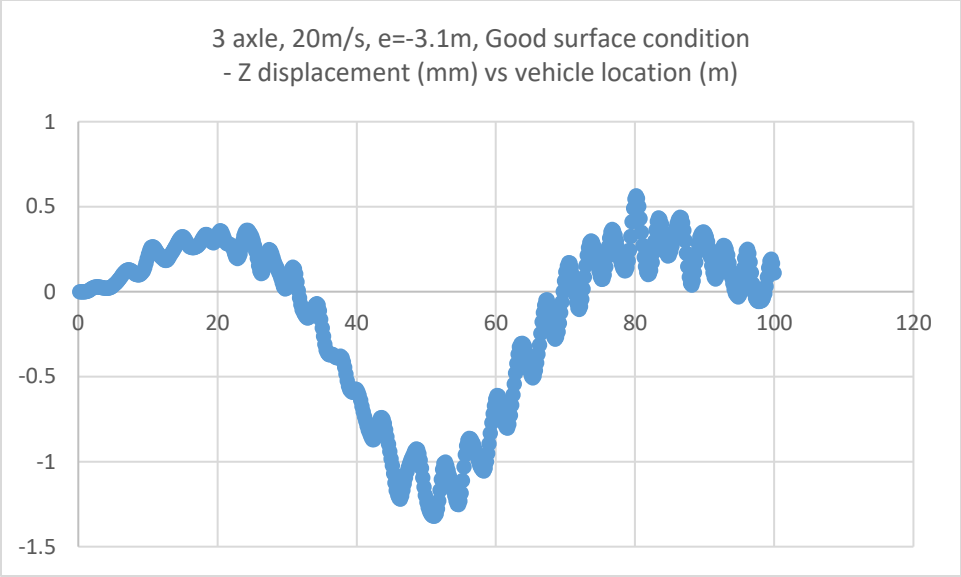

Figure 5-13 Flange deflection of mid span (vehicle speed v=20m/s)

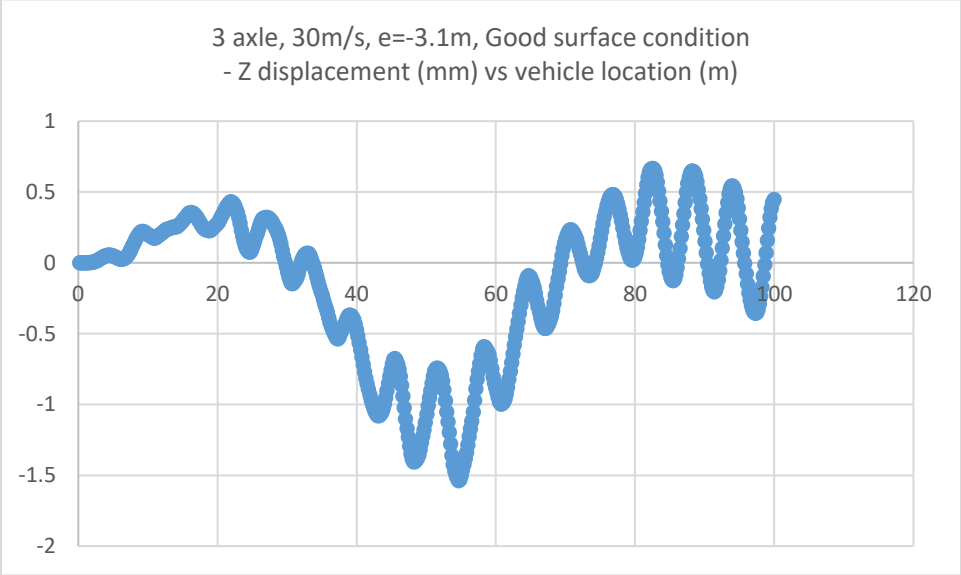

Figure 5-14 Flange deflection of mid span (vehicle speed v=30m/s)

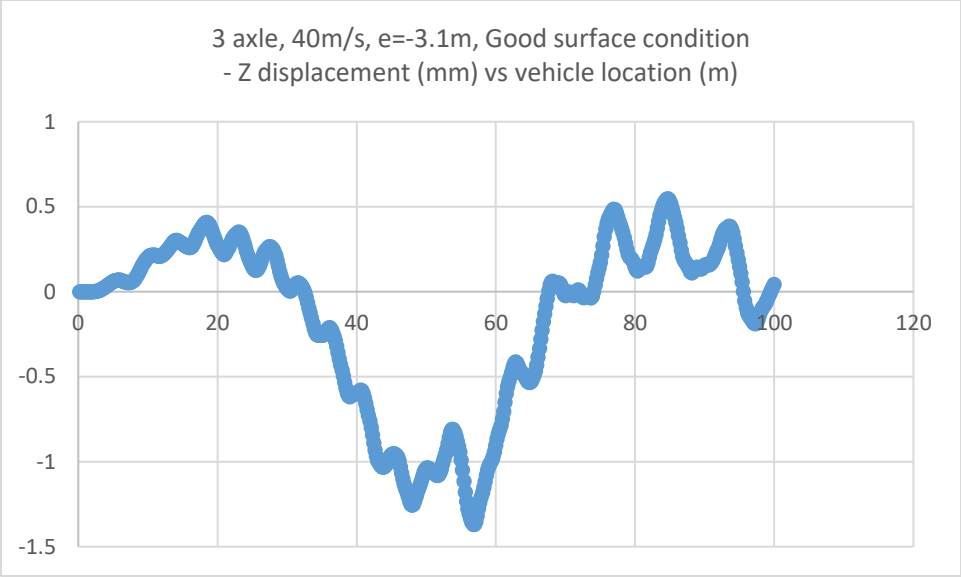

Figure 5-15 Flange deflection of mid span (vehicle speed v=40m/s)

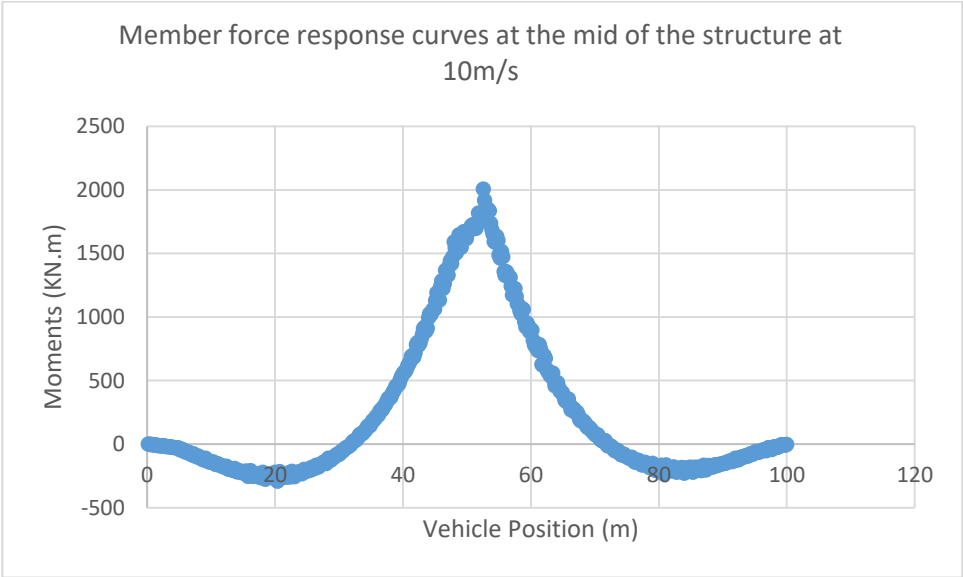

Figure 5-16 Moment force response of mid span at v=10m/s

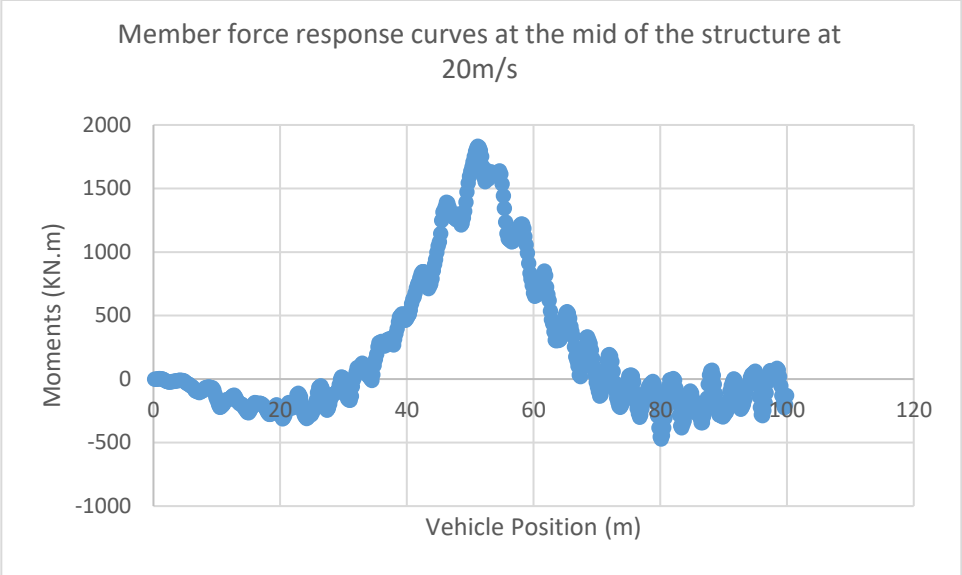

Figure 5-17 Moment force response of mid span at v=20m/s

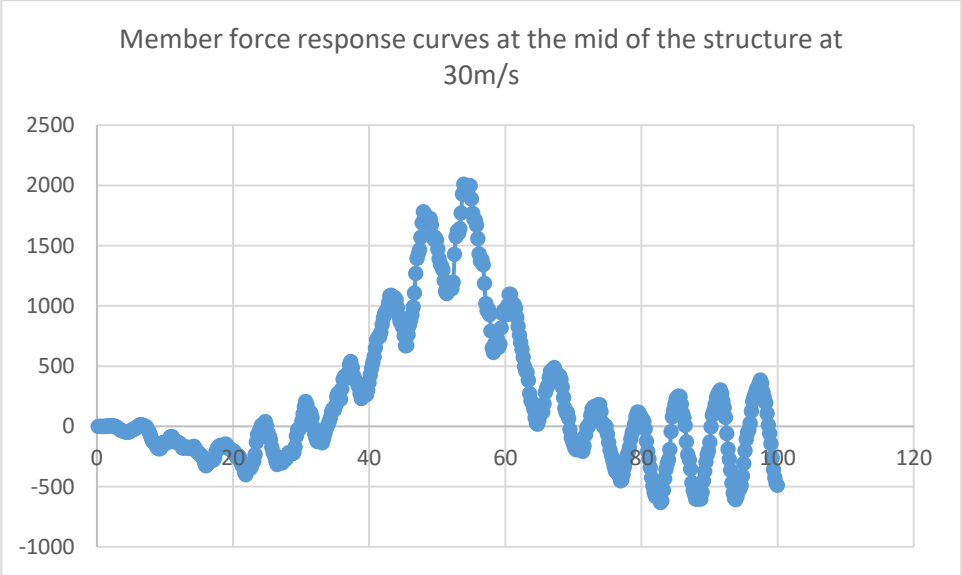

Figure 5-18 Moment force response of mid span at v=30m/s

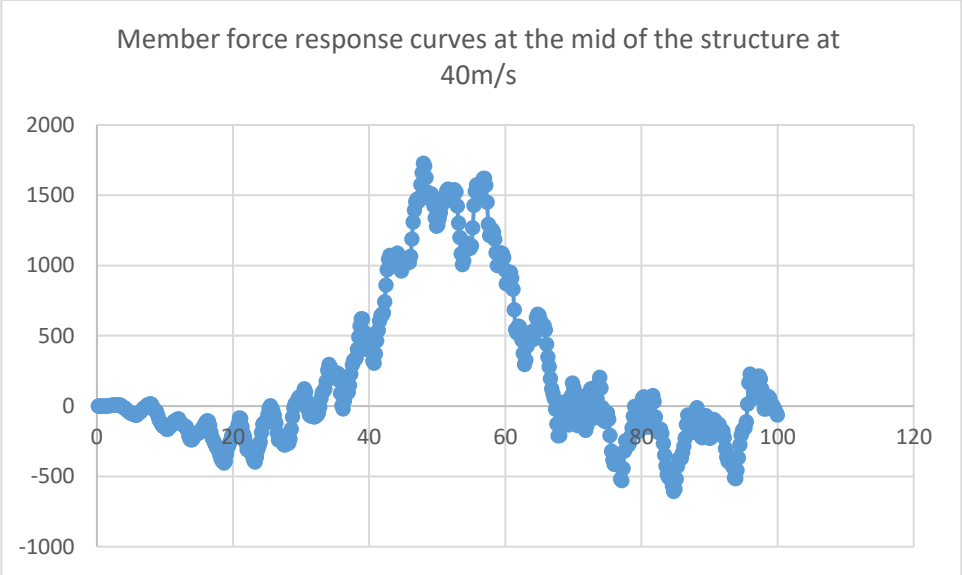

Figure 5-19 Moment force response of mid span at v=40m/s

Figure 5.20 summarizes all amplification factors from the case study including mid-span displacement, shear, moment, end-span displacement, shear and moment. As shown in the figure, as the vehicle traveling speed increase, all the dynamic amplication factors also increased slightly.

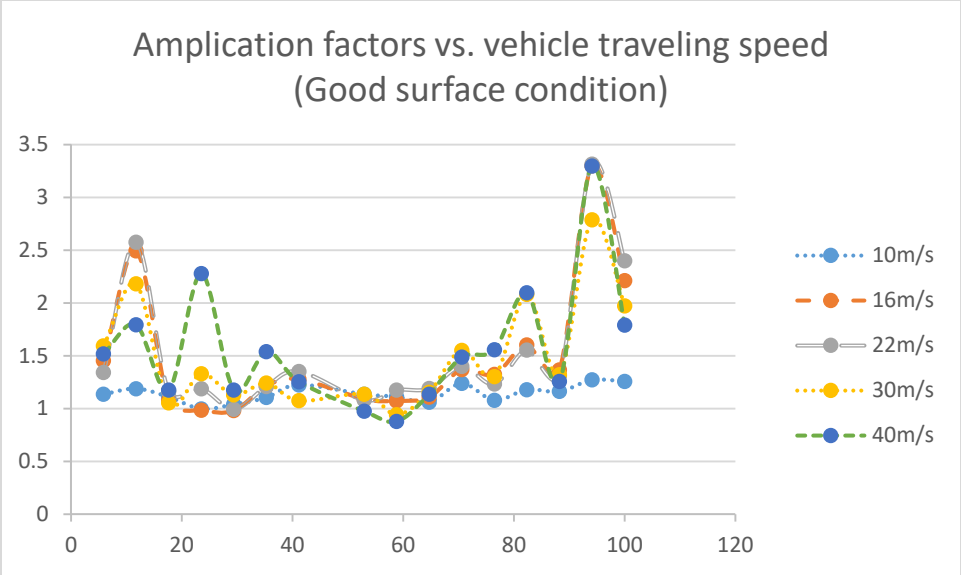

Figure 5-20 Amplication factors of different traveling speeds.

Figure 5.21 to 5.25 shows bridge dynamic reaction when a 3-axle truck traveling at outside good surface condition lane with the speed of 20m/s. By comparing displacement charts from different surface condition, the influence of surface condition to bridge dynamic response can be observed. Additional comparison is made between no surface roughness (smooth surface) and 'good condition' surface. Noticed that as the surface condition deteriorate, the impact of the truck on the bridge becomes larger, the vibration of the structure is aggravated, and the amplitude of the dynamic response also gradually increases.

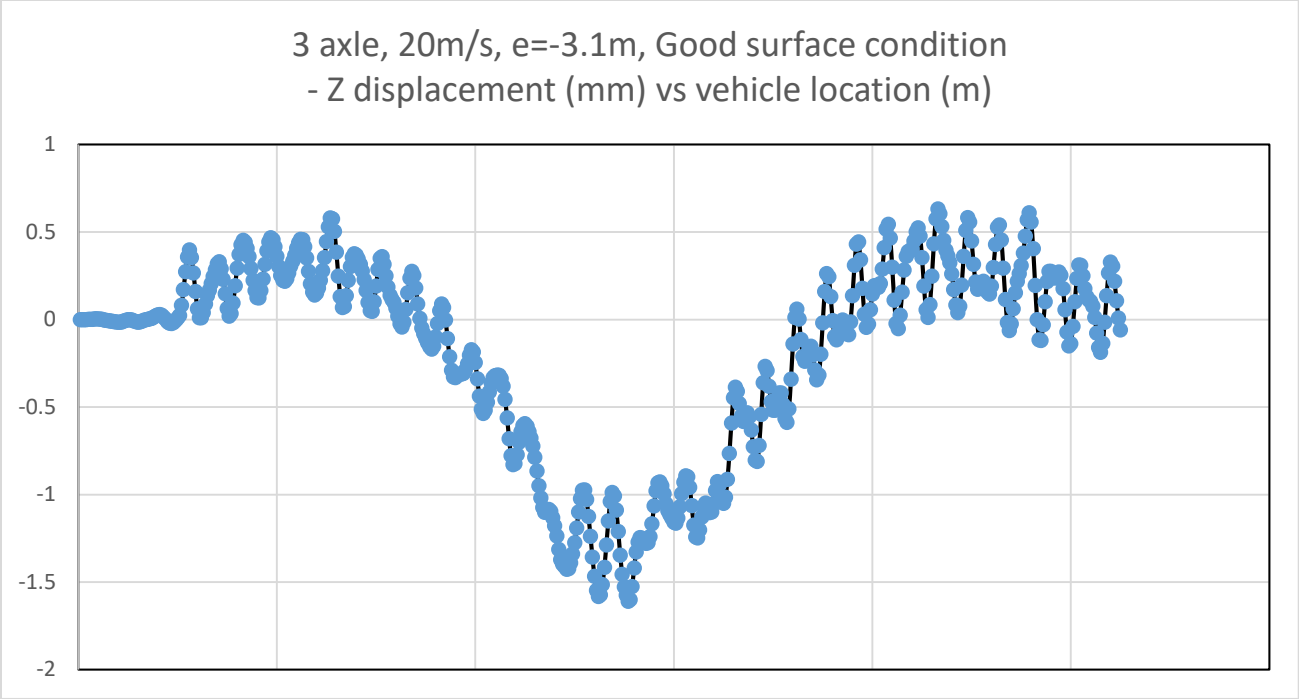

Figure 5-21 Bridge girder deflection response of a 3-axle truck passing through the bridge.

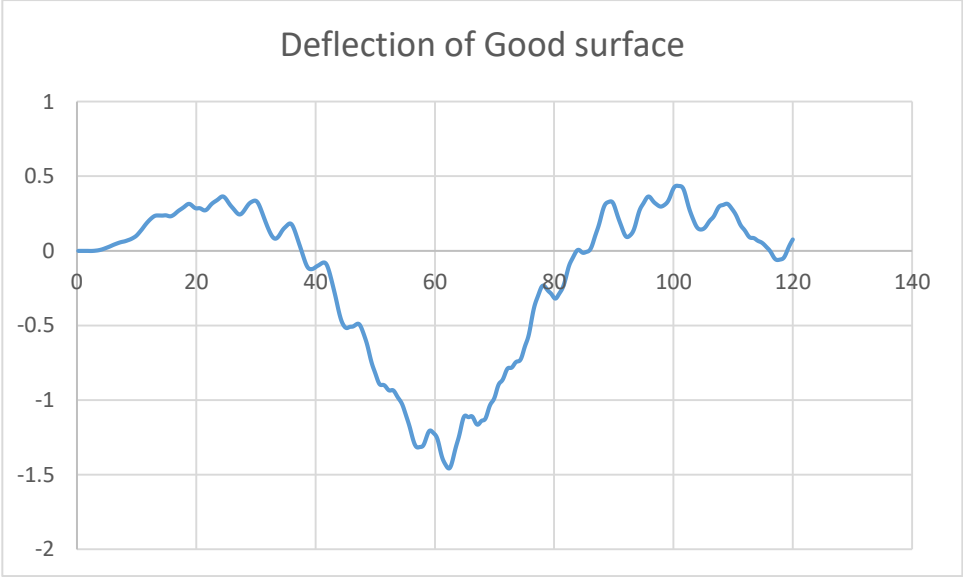

Figure 5-22 Bridge deflection response vs Good surface condition

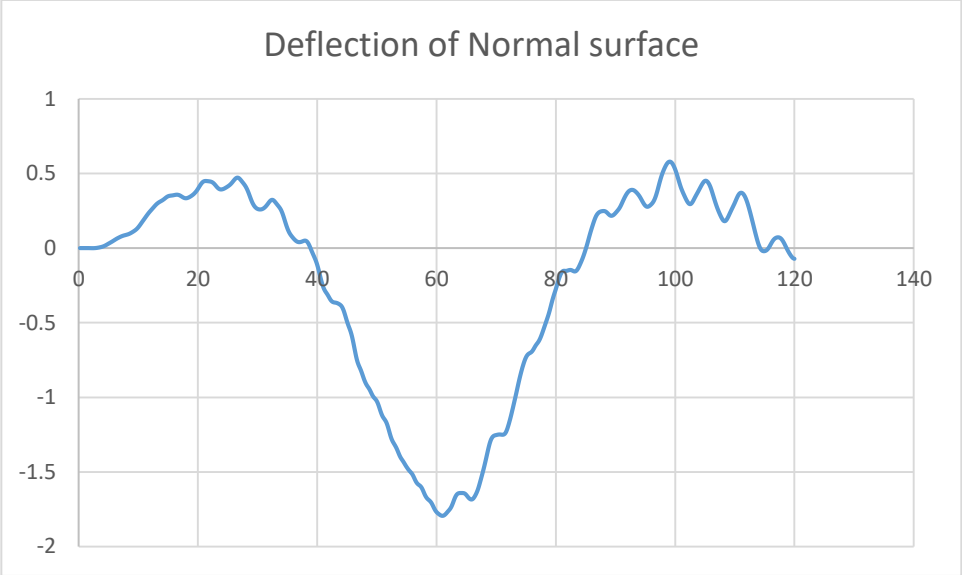

Figure 5-23 Bridge deflection response vs Normal surface condition

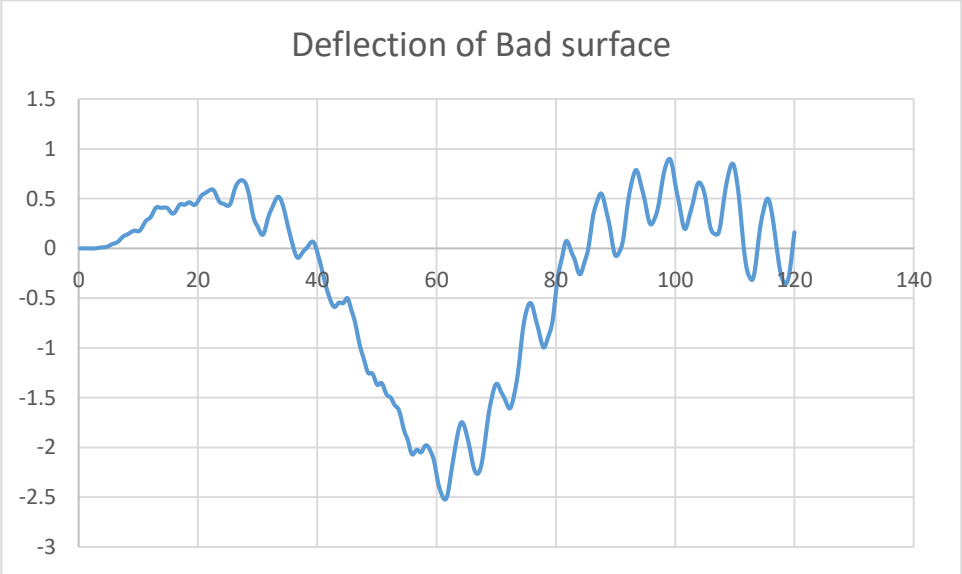

Figure 5-24 Bridge deflection response vs Bad surface condition

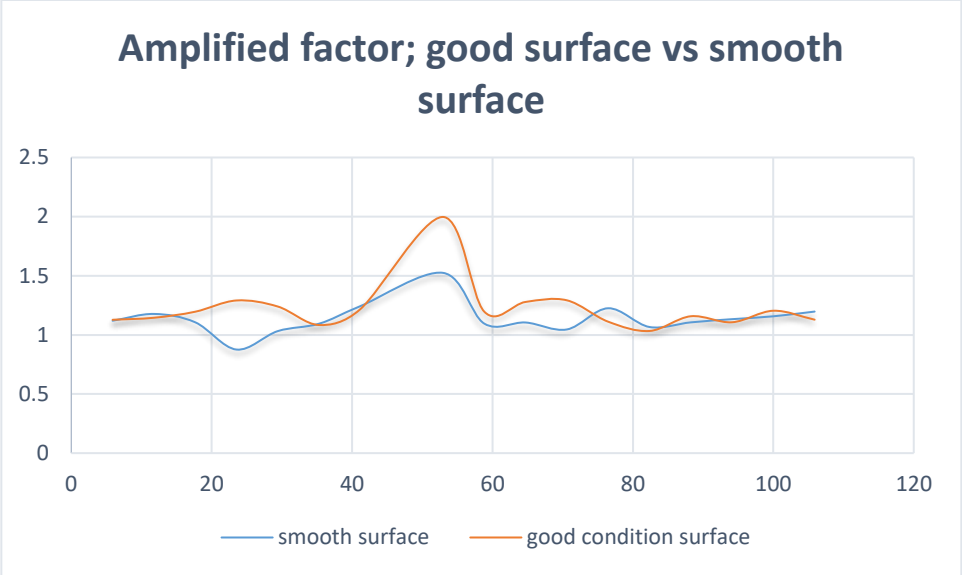

Figure 5-25 Amplified factor vs different surface conditions

Figure 5.26 and 5.27 show the effect of deck roughness on the maximum absolute displacement and dynamic amplification factor at the girder. It can be observed that when the surface condition is 'Good', vehicle impact factor remains relative small regardless of its travelling speed. With the deck condition deteriorates, the impact factor, as well as the maximum absolute displacement starts to increase. The maximum impact factors increase from 1.3 (Good condition) to 1.7 (Normal condition), while the maximum deflection increase from 2.15mm (Good condition) to 2.7mm (Normal condition), roughly 26% increment.

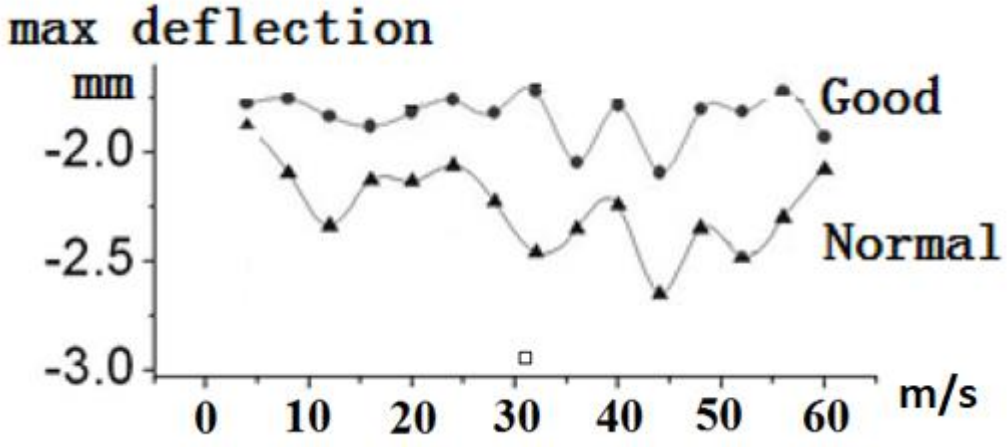

Figure 5-26 Maximum deflections under different vehicle traveling speed and road condition

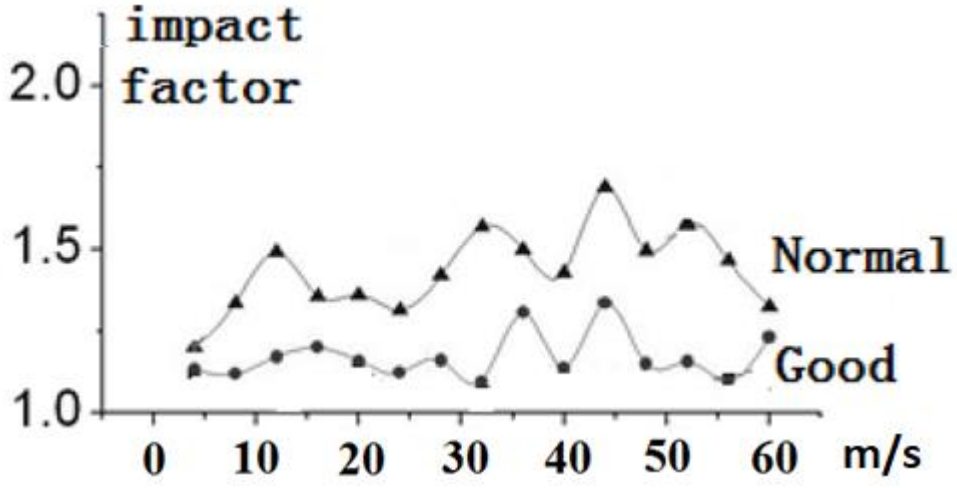

Figure 5-27 Impact factor of bridge under different vehicle traveling speed and road condition

Additional hypothetical straight bridge with the same Manchuria bridge properties is modeled to observe the influence of curved bridge layout in the bridge vehicle interaction. The detailed comparion are shown in Figure 5.28 to 5.30. Though the figures show little differences in z-displacement and member force responses between these two bridges, the impact factor comparison shows that the curved bridge has a noticable increasment comparing to the straight one. It is reasonable to draw the conclusion that the curved bridge layout have increased the vehicle bridge interaction.

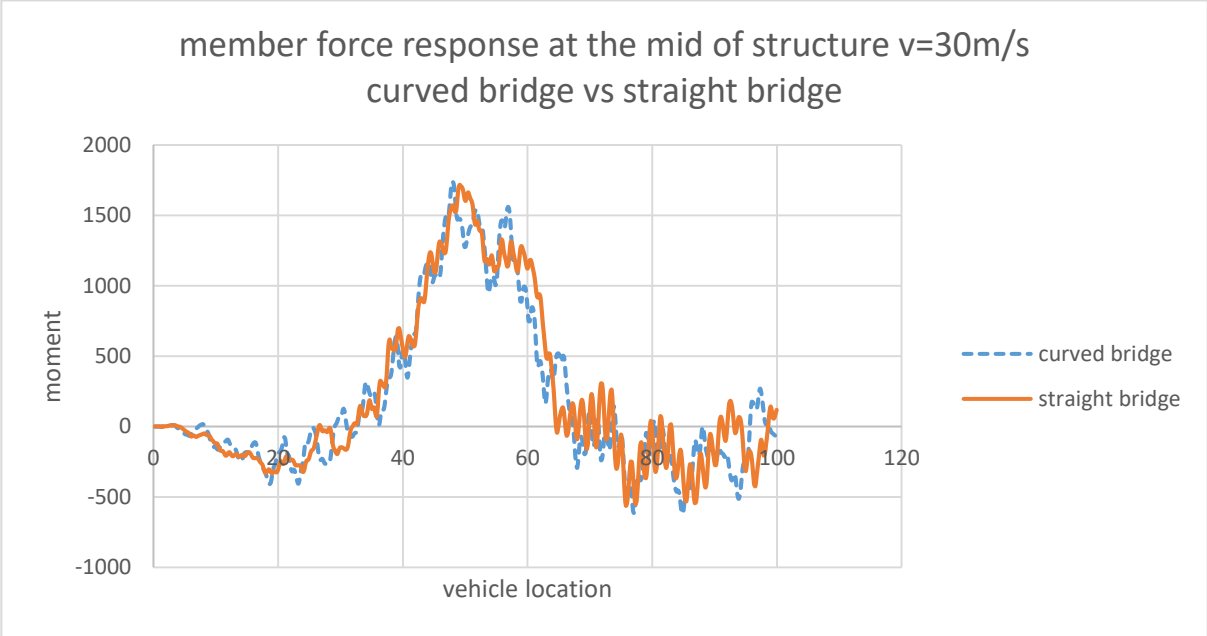

Figure 5-28 Moment response comparison between curved Manchuria Bridge and hypothetical straight Manchuria Bridge.

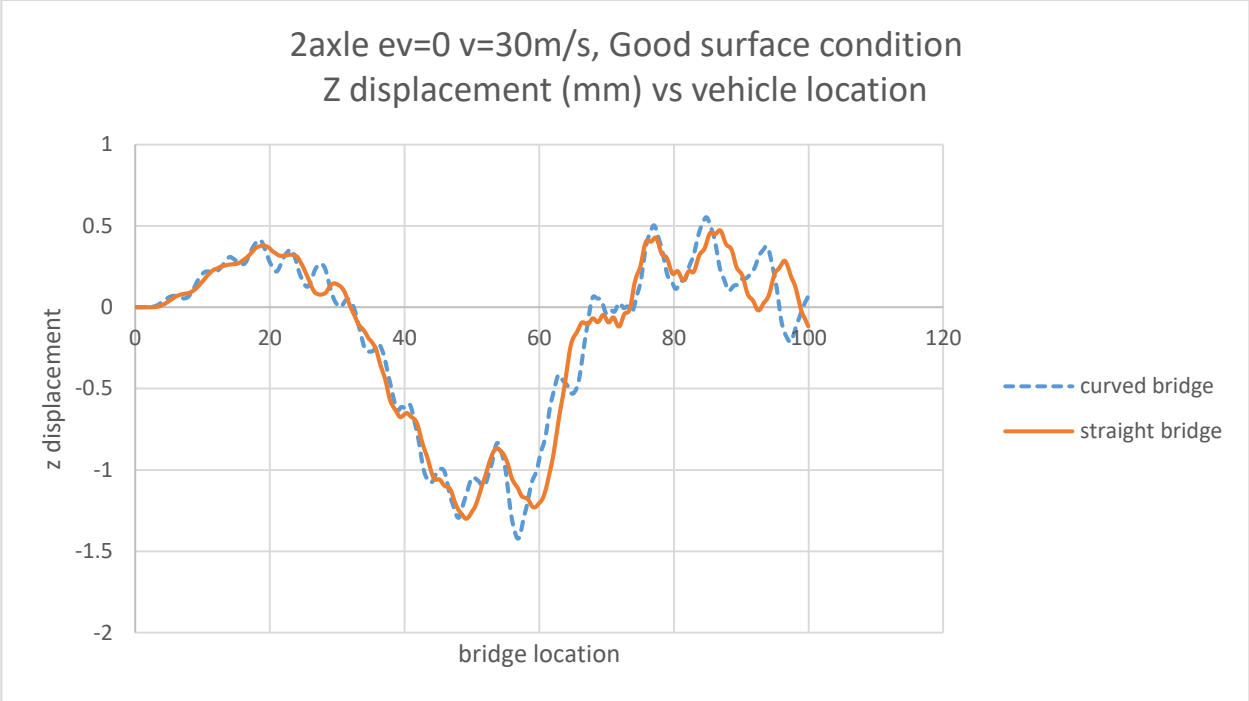

Figure 5-29 Z-displacements comparison between curved Manchuria Bridge and hypothetical straight Manchuria Bridge.

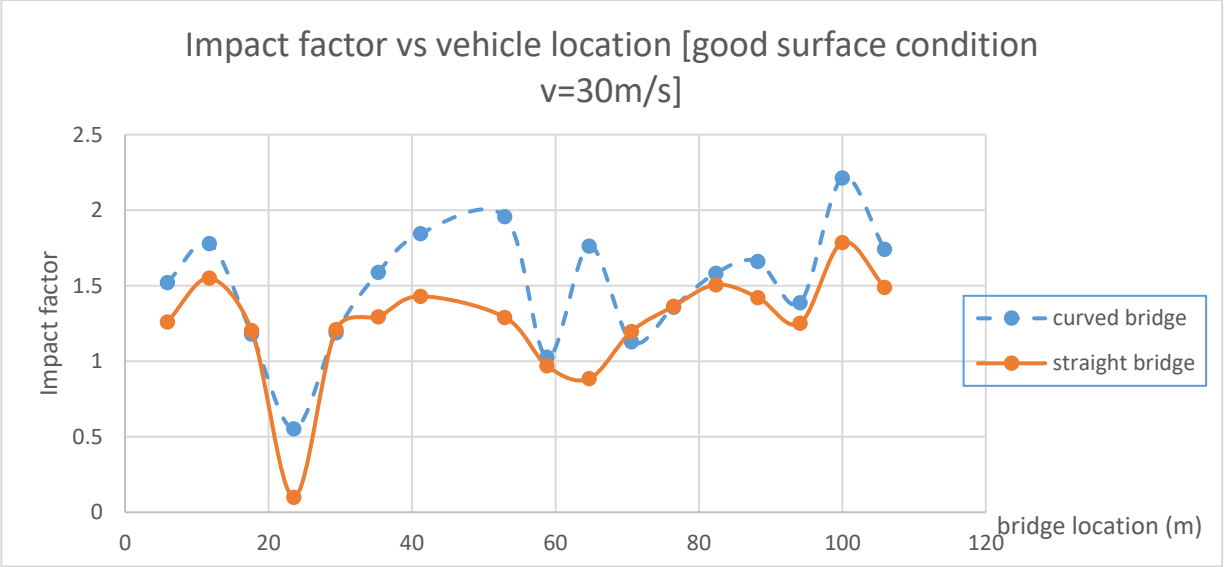

Figure 5-30 Impact factor comparison between curved Manchuria Bridge and hypothetical straight Manchuria Bridge.

5.2.2 Veteran's Memorial Steel Curved Bridge

Figures 5.31 to 5.36 show the displacement and moment responses of the bridge when vehicle travel through the bridge with different speeds. Compared to the Manchuria concrete bridge, the bridge response is much higher. This is most likely due to the bridge layout and materials. Also, as the vehicle speed increased, the maximum response of the bridge slightly increased.

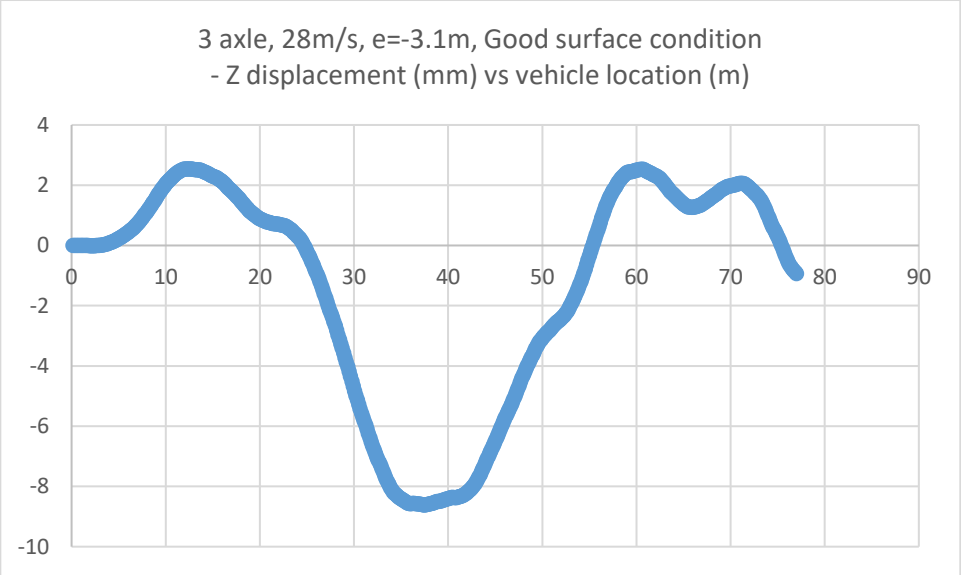

Figure 5-31 Girder deflection of mid span (vehicle speed v=28m/s)

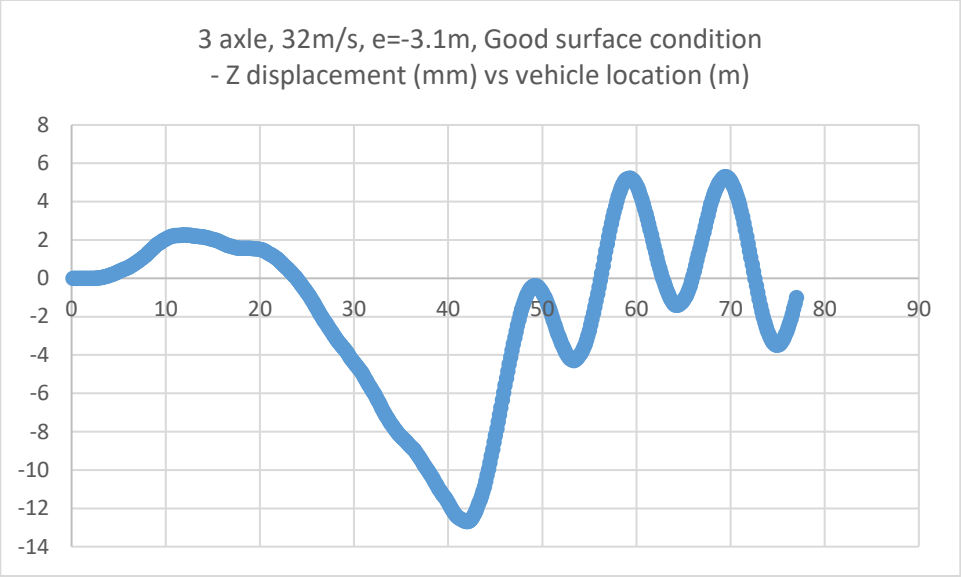

Figure 5-32 Girder deflection of mid span (vehicle speed v=32m/s)

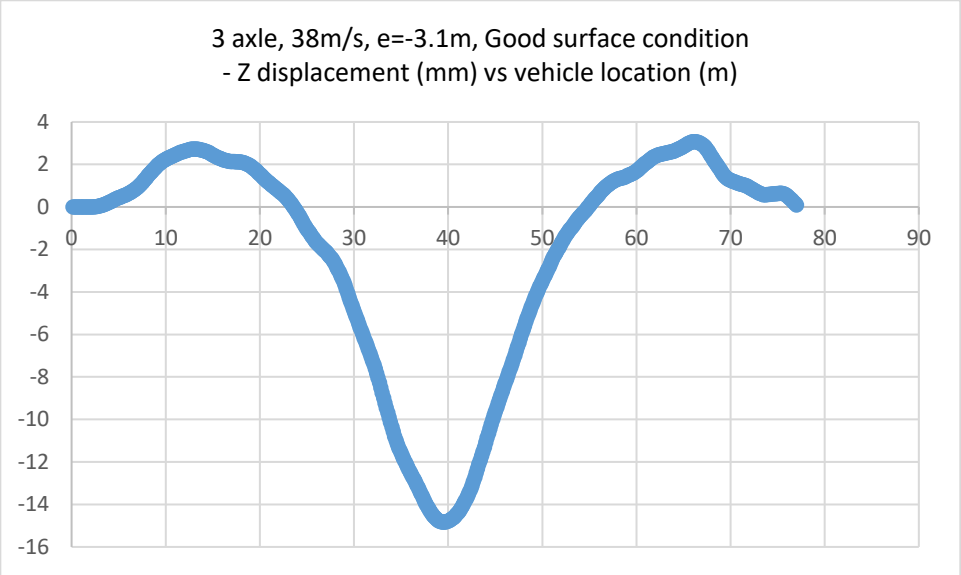

Figure 5-33 Girder deflection of mid span (vehicle speed v=38m/s)

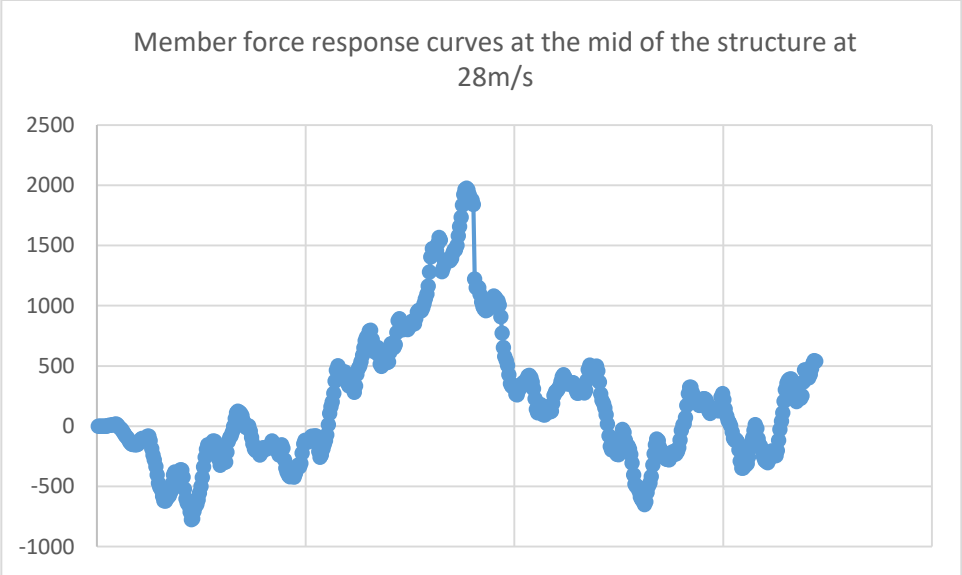

Figure 5-34 Moment force response of mid span (vehicle speed v=28m/s)

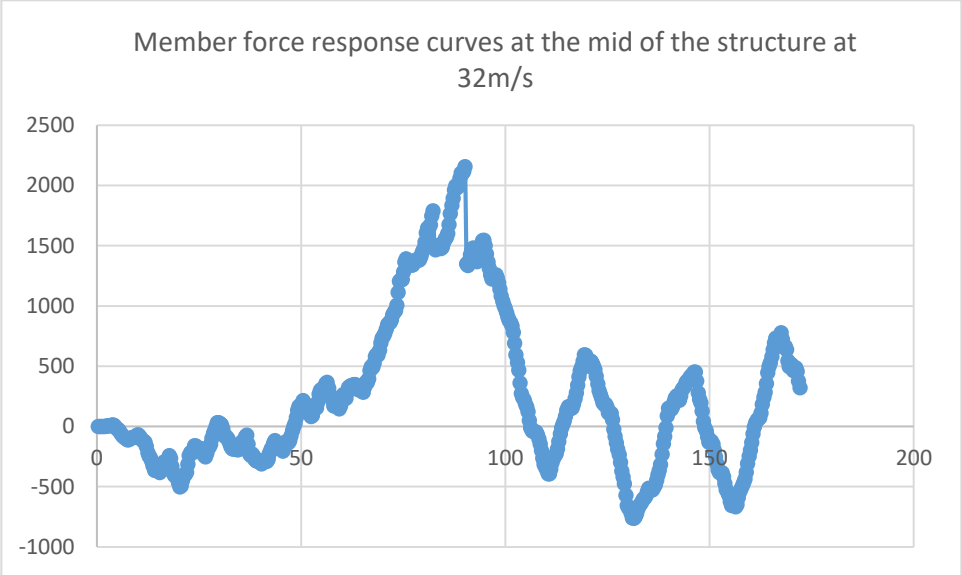

Figure 5-35 Moment force response of mid span (vehicle speed v=32m/s)

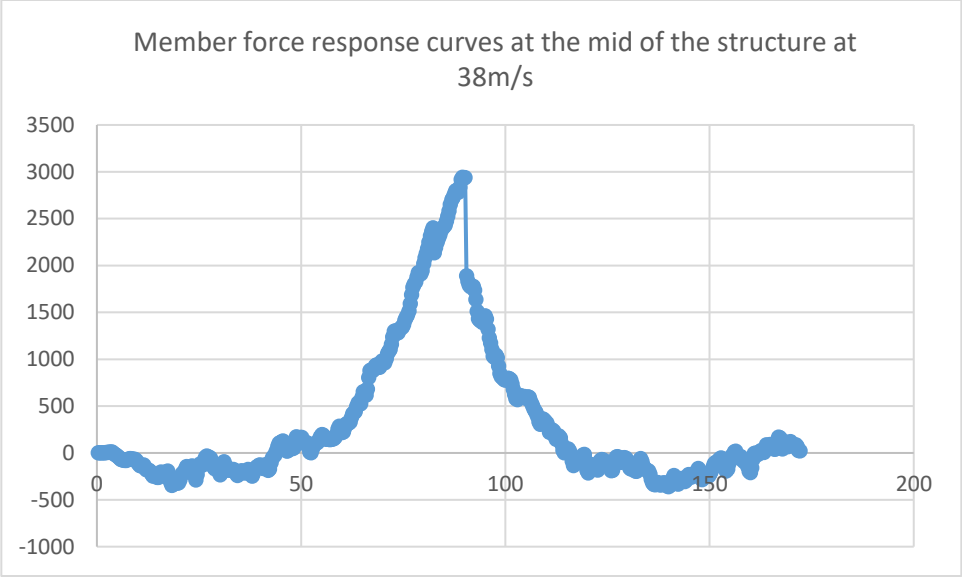

Figure 5-36 Moment force response of mid span (vehicle speed v=38m/s)

Additional hypothetical straight bridge with the same Veteran's Memorial Bridge properties is modeled to observe the influence of curved bridge layout in the bridge vehicle interaction. The detailed comparion are shown in Figure 5.37 to 5.39. The impact factor comparison shows that though most sections of the bridges have the similar reaction, some sections of the bridge have higher impact factors in curved bridge layout.

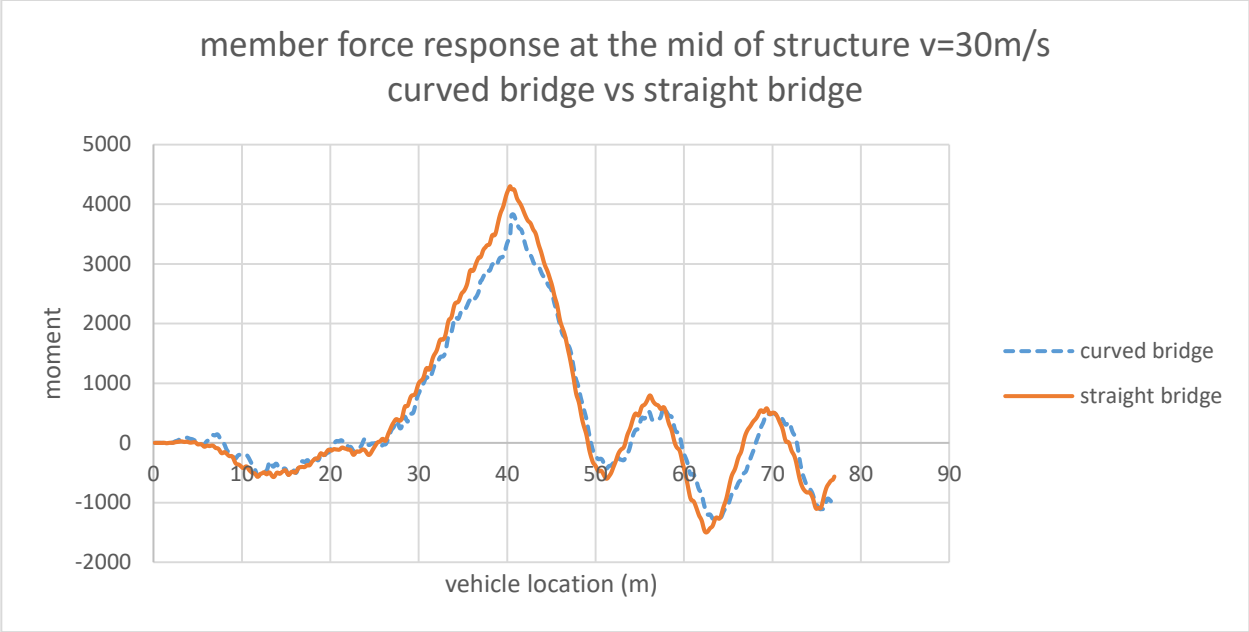

Figure 5-37 Moment response comparison between curved Veteran's Memorial Bridge and hypothetical straight Veteran's Memorial Bridge.

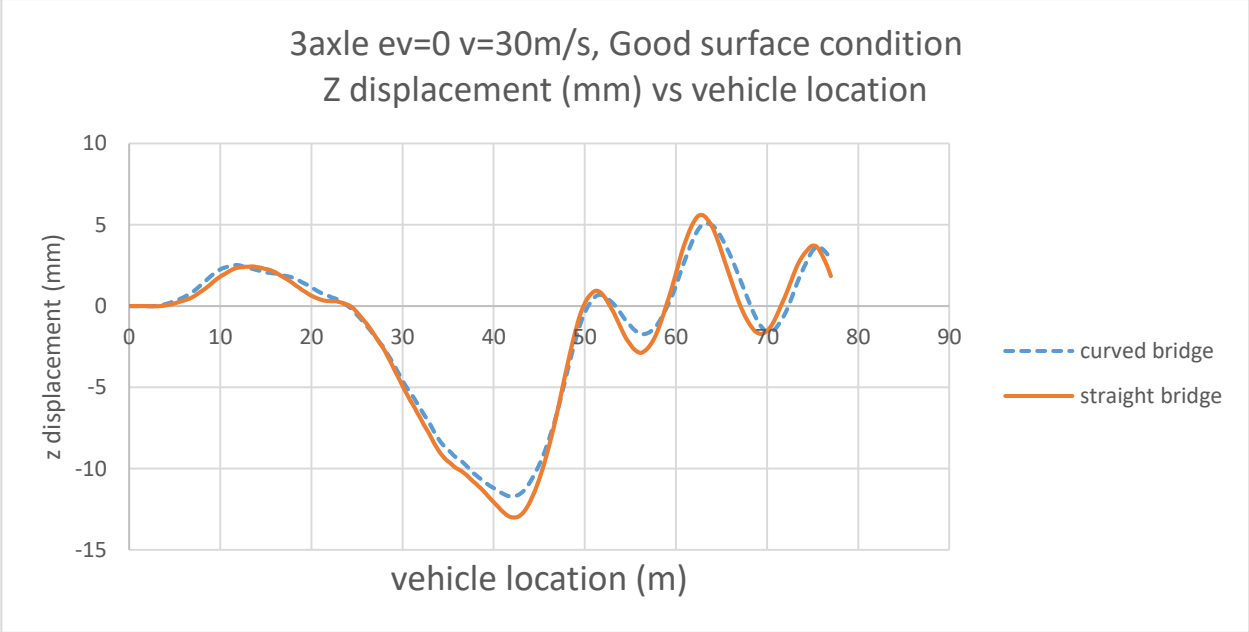

Figure 5-38 Z-displacements comparison between curved Veteran's Memorial Bridge and hypothetical straight Veteran's Memorial Bridge.

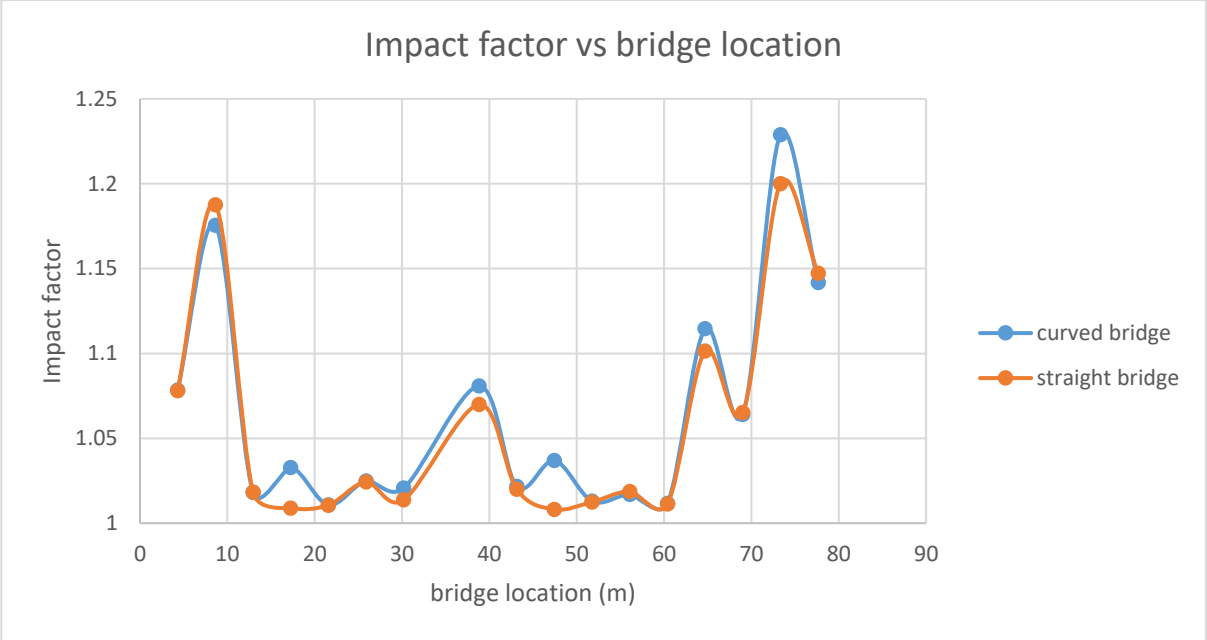

Figure 5-39 Impact factor comparison between curved Veteran's Memorial Bridge and hypothetical straight Veteran's Memorial Bridge.

5.3 Preliminary case study summary

Comparison is made for the case study Manchuria concrete bridge and Memorial steel bridge. By examining their bridge responses, it can be observed that the dynamic interaction of a curved bridge could be greatly influence by various factors. As the vehicle travelling speeds increase and surface conditions deteriorate, the bridge impact factors increase considerably. Such behavior agrees with most previous researches regarding vehicle bridge interaction. The hypothetical straight bridge models of both cases show that the curvature also plays an important part in such dynamic interaction, the curved models generally have a higher dynamic response than the straight versions. A

detail parametric study is required to understanding how each factor contribute in the vehicle bridge interaction problem.

6. Parametric Study

6.1 Introduction

The vehicle bridge interaction has discussed in two different bridges from previous chapter. The object of this chapter is to expand the previous obtained results to a wider range of curved bridges in order to evaluate the interaction behavior comprehensively.

Different parameters can affect the behavior of curved bridges under dynamic traffic loads. Among these parameters are curvature radius, span configurations, bridge pavement condition, lane location, vehicle properties and traveling speed. A parameter study is performed in order to quantify the effects of above parameters on vehicle bridge dynamic interaction.

6.2 Analysis Cases

This parameter study focuses on following span variables in the vehicle bridge interaction system.

Three spans – 50m, 75m, 50m long.

Three spans – 35m, 50m, 35m long.

Three spans – 70m, 95m, 70m long.

Two spans – 95m each span.

Two spans – 75m each span.

Two spans – 50m each span.

Each of the above bridges was configured as curved bridge with radii of 50m, 75m, 100m, 150m, 190m, 250m, 300m and one additional straight bridge case for comparison, resulting in 48 bridge configurations. These bridge cross sections need to be designed first according to the AASHTO LRFD code and design standard using DESCUS-II@ for box girder bridges.

Four sets of surface pavement conditions were integrated in the above bridge models, perfect, good, normal and bad conditions. The roughness ratio of these surface conditions are a=0, $0.24\times10^{-6}\leq a\leq1.0\times10^{-6}$, $1.0\times10^{-6}\leq a\leq4.0\times10^{-6}$ and $4.0\times10^{-6}\leq a\leq16.0\times10^{-6}$, respectively. Figures 6.1 to 6.3 show the different roughness profiles used in this parametric study.

Three sets of lane configuration were integrated in the bridge models, vehicle travel in center lane e=0m, vehicle travel in inner lane e=-3.0m and vehicle travel in outer lane e=+3.0m. Each lane has a test vehicle travelling from 20m/s to 70m/s through the bridge.

Combining the surface conditions and lane configurations, there are 576 model configurations in this study.

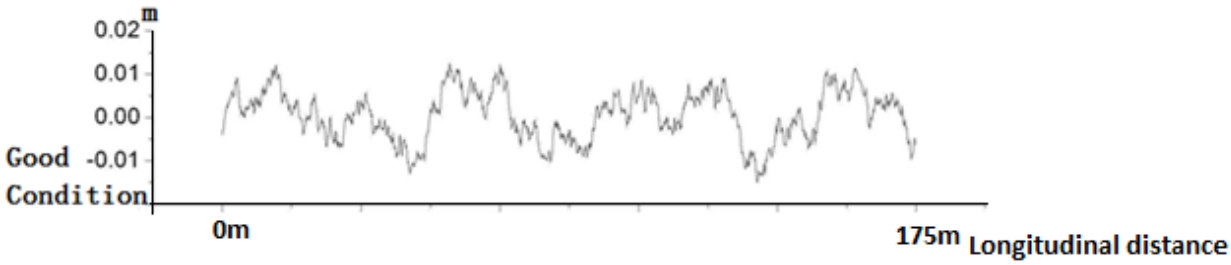

Figure 6-1 Good surface condition applied in parametric study

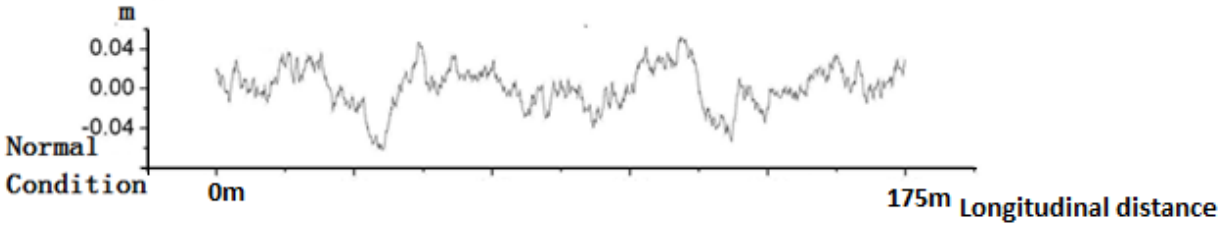

Figure 6-2 Normal surface condition applied in parametric study

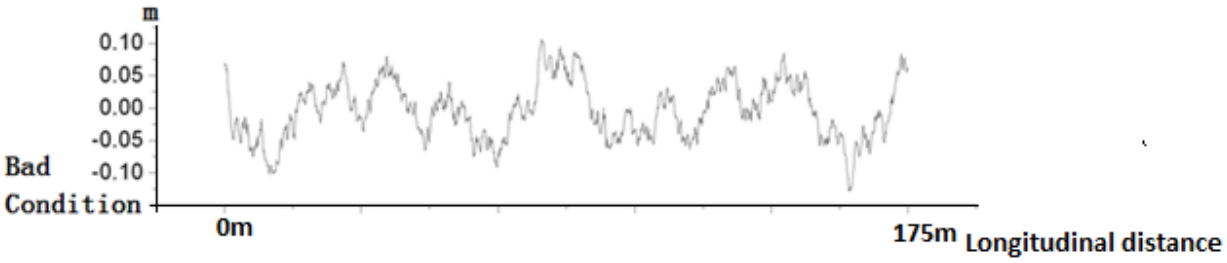

Figure 6-3 Bad surface condition applied in parametric study

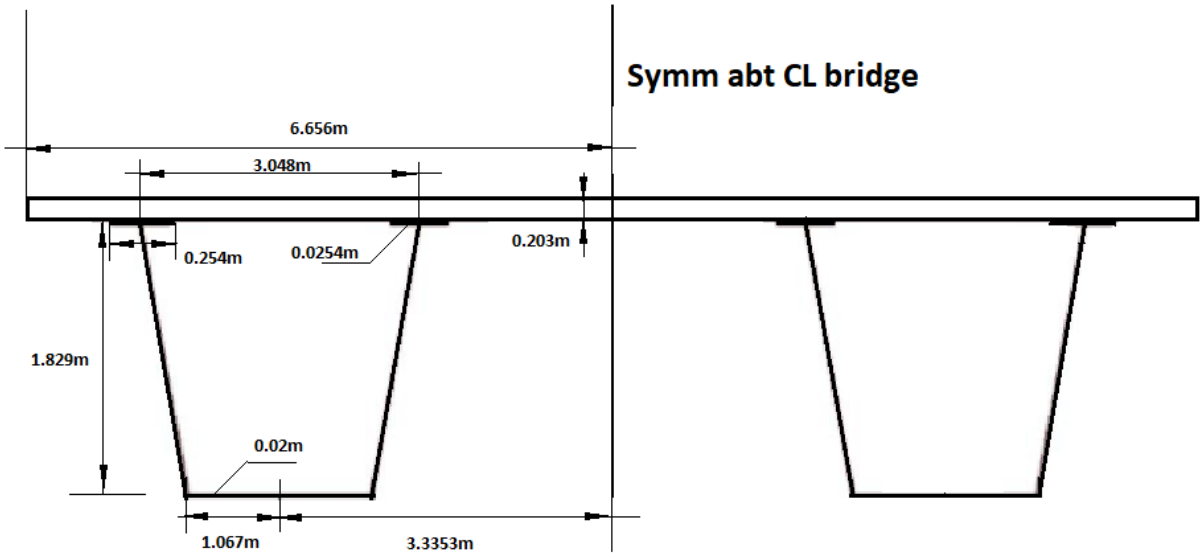

Figure 6-4 Typical steel box girder cross section (Case 1 L=175m).

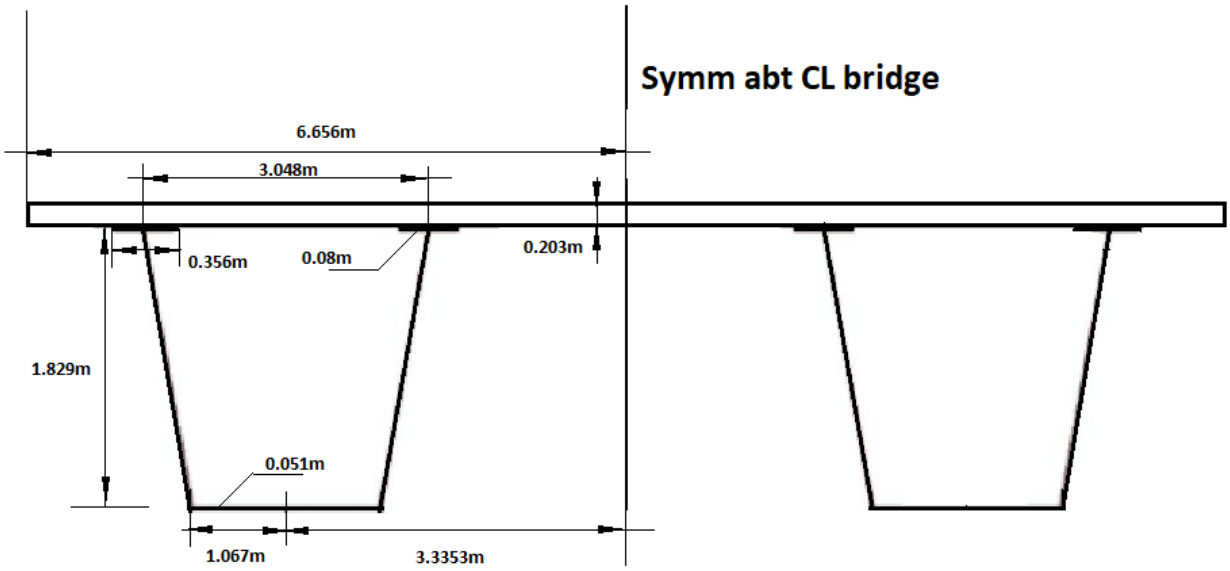

Figure 6-5 Typical steel box girder cross section near pier location (Case 1 L=175m)

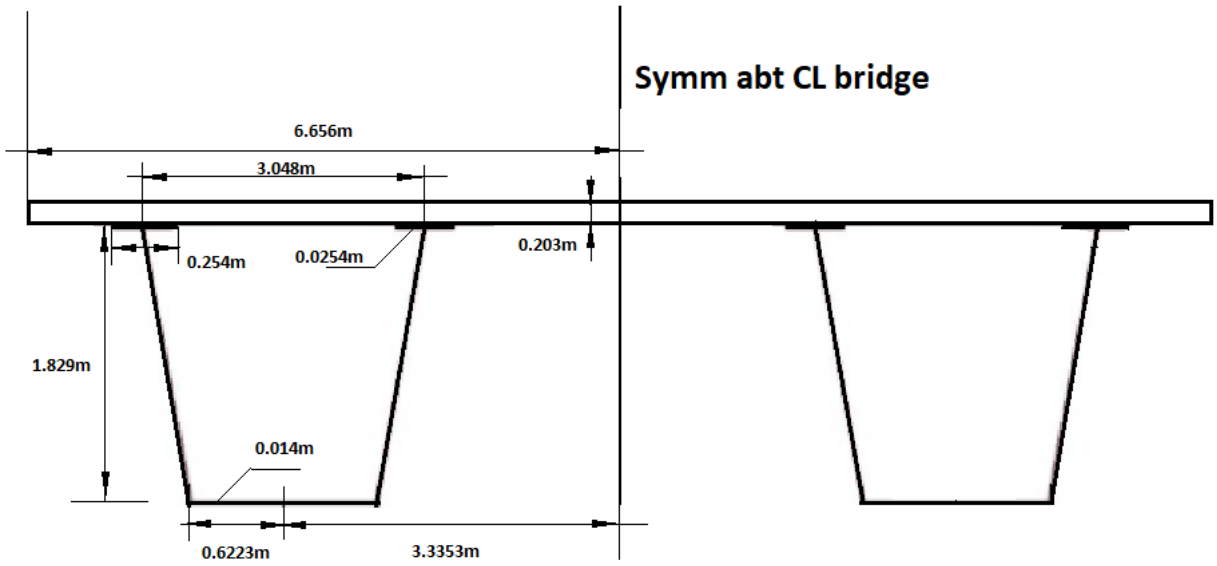

Figure 6-6 Typical steel box girder cross section (Case 2 L=120m)

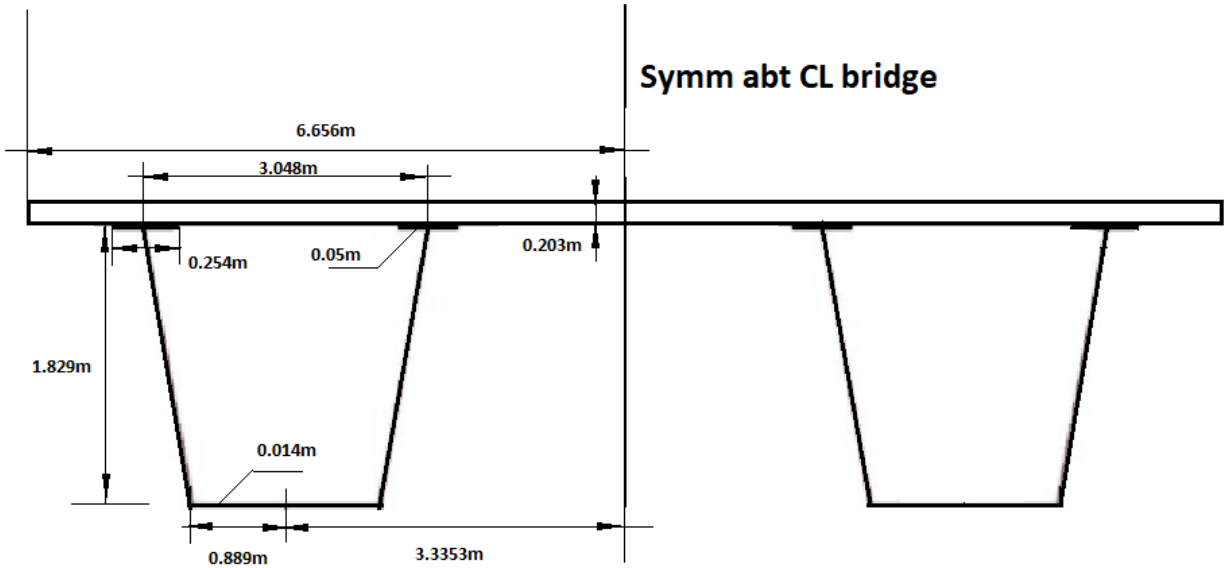

Figure 6-7 Typical steel box girder cross section near pier location (Case 2 L=120m)

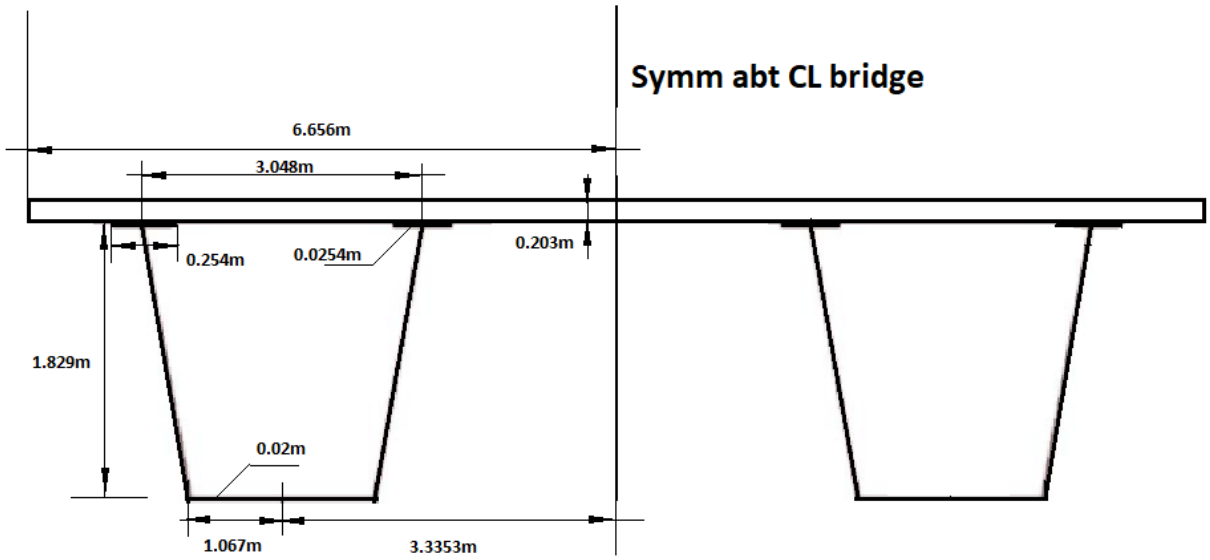

Figure 6-8 Typical steel box girder cross section (Case 3 L=235m)

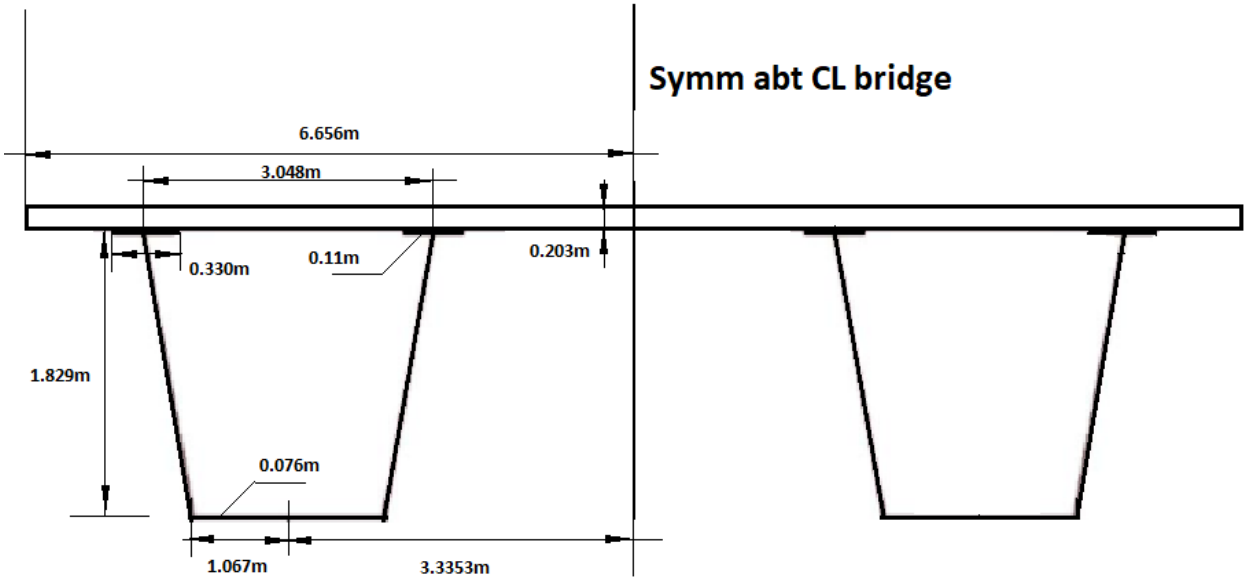

Figure 6-9 Typical steel box girder cross section near pier location (Case 3 L=235m)

Table 6-1 Typical section properties for different span length bridge models.

	50-75-50m	35-50-35m	70-95-70m
Area (m^2)	4.6154	4.3211	4.6177
J(m^4)	3.3739	2.426	3.377
I_{22}(m^4)	2.7859	1.9251	2.7902
I_{33}(m^4)	66.2009	62.3644	66.2285

Table 6-2 Typical near pier section properties for different span length bridge models.

	50-75-50m	35-50-35m	70-95-70m
Area (m^2)	6.5756	5.0042	7.6057
J(m^4)	4.33	3.2682	4.4172
I_{22}(m^4)	5.5217	3.2436	6.9937
I_{33}(m^4)	92.7649	70.8285	104.3963

Each model utilizes two different frame sections depending on the span length as shown in figure 6.10. Figures 6.4 to 6.9 show the cross section details for different models, Tables 6.1 and 6.2 list the section property used in the analysis models for different span length. Each cross section was designed for two different locations along the bridge. Section A is defined as the section that is away from bridge piers, section B is defined as the section that near the bridge piers. Table 6.3 and 6.4 list the data used for creating 3-span and 2-span bridges models.

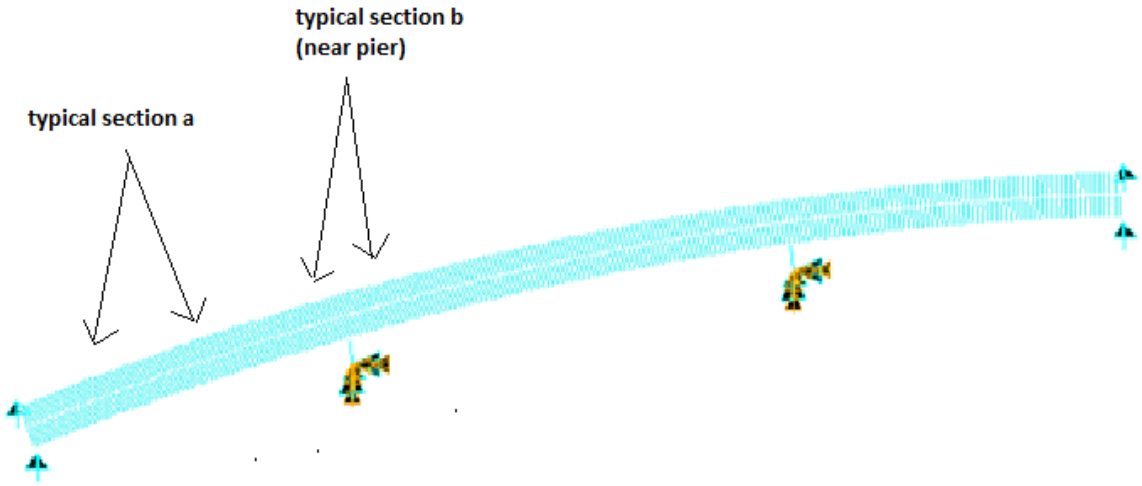

Figure 6-10 Typical curved bridge layout

Table 6-3 3-span bridge models

3-span Bridge models (m)			
Main span length	**Bridge configuration**	**total span length**	**Radius**
75	50-75-50	175	50 75 100 150 190 250 300 Straight
50	35-50-35	120	50 75 100 150 190 250 300 Straight
75	70-95-70	235	50 75 100 150 190 250 300 Straight

Table 6-4 2-span bridge models

2-span Bridge models (m)			
Main span length	**Bridge configuration**	**total span length**	**Radius**
75	75-75	150	50 75 100 150 190 250 300 Straight
50	50-50	100	50 75 100 150 190 250 300 Straight
95	95-95	190	50 75 100 150 190 250 300 Straight

7. Results of Parametric Study

7.1 Introduction

This chapter summarizes the results of a parametric study of the effect of various parameters of curved bridge vehicle interaction. Parameters investigated in the study were span length, curvature radius, surface condition and vehicle traveling location and speed. The bridge displacement amplification factor of each span center point is the primary focus in the study in order to characterize the dynamic interaction behavior.

7.2 Analysis Results

The analysis investigates the interaction behavior of curved bridges with span lengths increased from 125m to 235m. For 3-span bridges, they were designed that the outer spans are a percentage of roughly 70% of the main span length. For 2-span bridges, both spans were designed with the same span lengths.

7.2.1 For 3 span configurations

As mentioned before, the parametric analysis is performed for different configurations of bridge with previous designed bridge sections. The first group is for 3-span bridge models with the total span ranging from 120m to 235m and layout curvature radii ranging from 50m to 300m. Figures 7.1 through 7.18 illustrate the mid-span center point reactions profiles (displacement, shear force and moment) from the 3-span bridge configuration for different bridge curvature radii. In this comparison, the bridge surface conditions are set to normal, vehicle traveling through the inner side of girder (e=-3m) with a speed of 20m/s. Also, the static bridge response is compared in these figures to show the influence from dynamic interaction. Figures 7.19 to 7.27 illustrate the mid-span center point reactions profile for three different total span length. To isolate the influence of traffic speed, figure 7.28 to 7.33 are generated to illustrate the mid-span center point reactions for same bridge under different vehicle travelling speeds. Figures 7.34 to 7.48 show the bridge mid-span center point reactions of different span type and different surface conditions, ranging from "Perfect surface (a=0m^3/circle)", "Good surface (a=0.62×10^{-6} m^3/circle)", "Normal surface (a=2.5×10^{-6} m^3/circle)" and "Bad surface (a=10×10^{-6} m^3/circle)".

7.2.2 Curvature comparison study

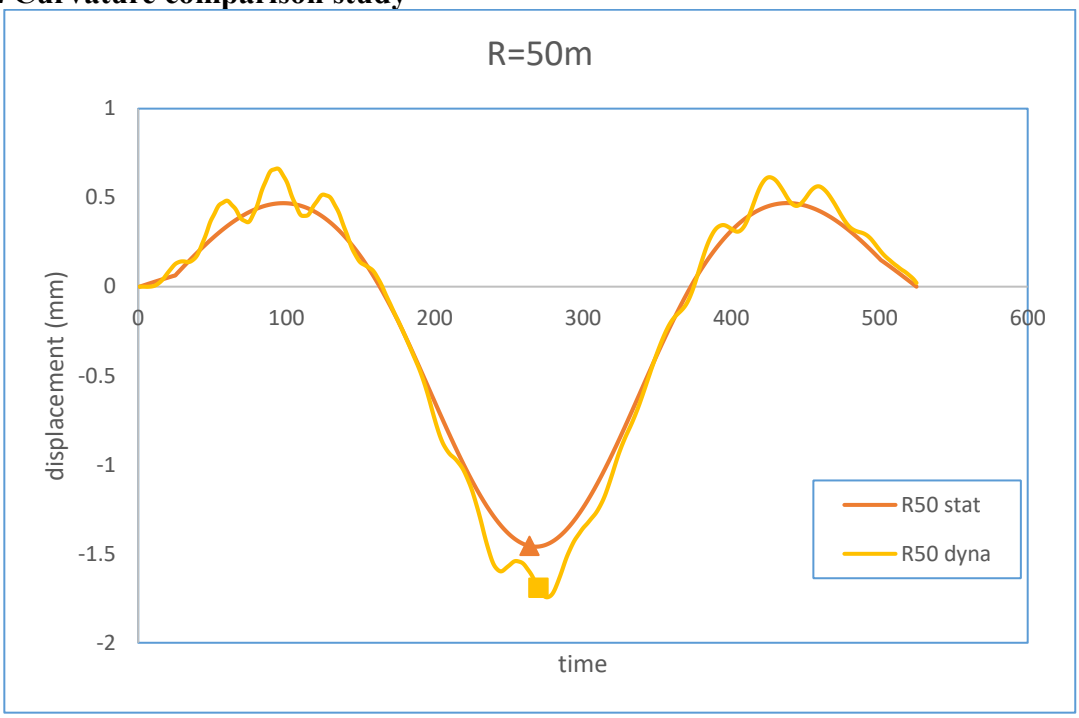

Figure 7-1 Mid-span displacement for 3-span bridge model R=50m

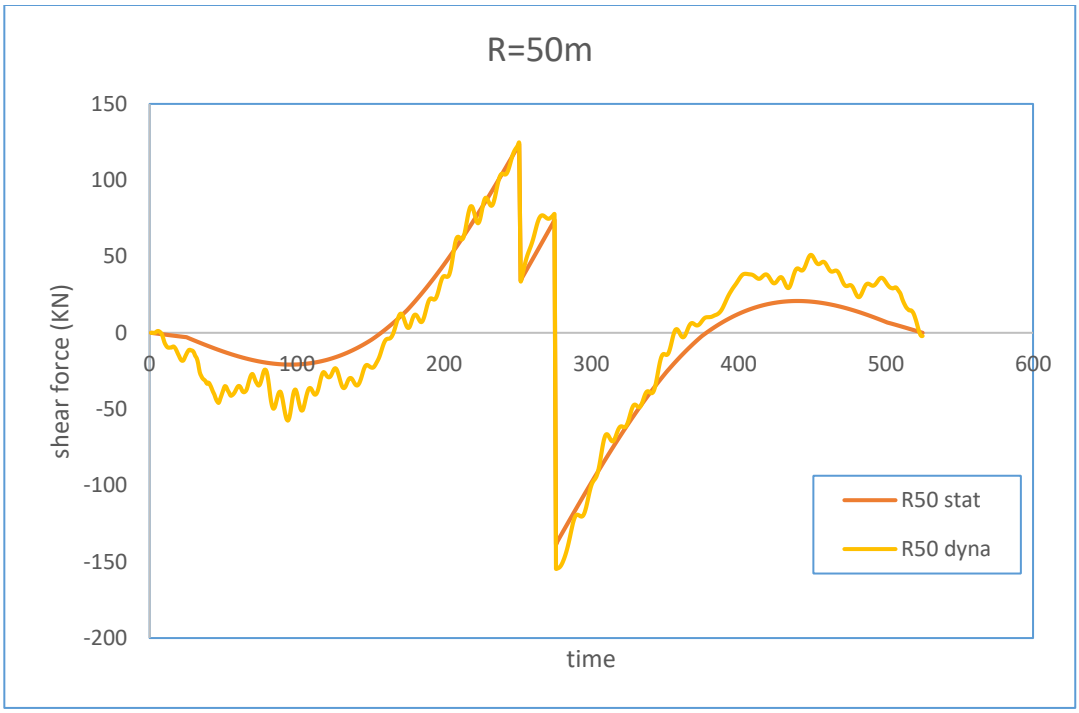

Figure 7-2 Mid-span shear force for 3-span bridge model R=50m

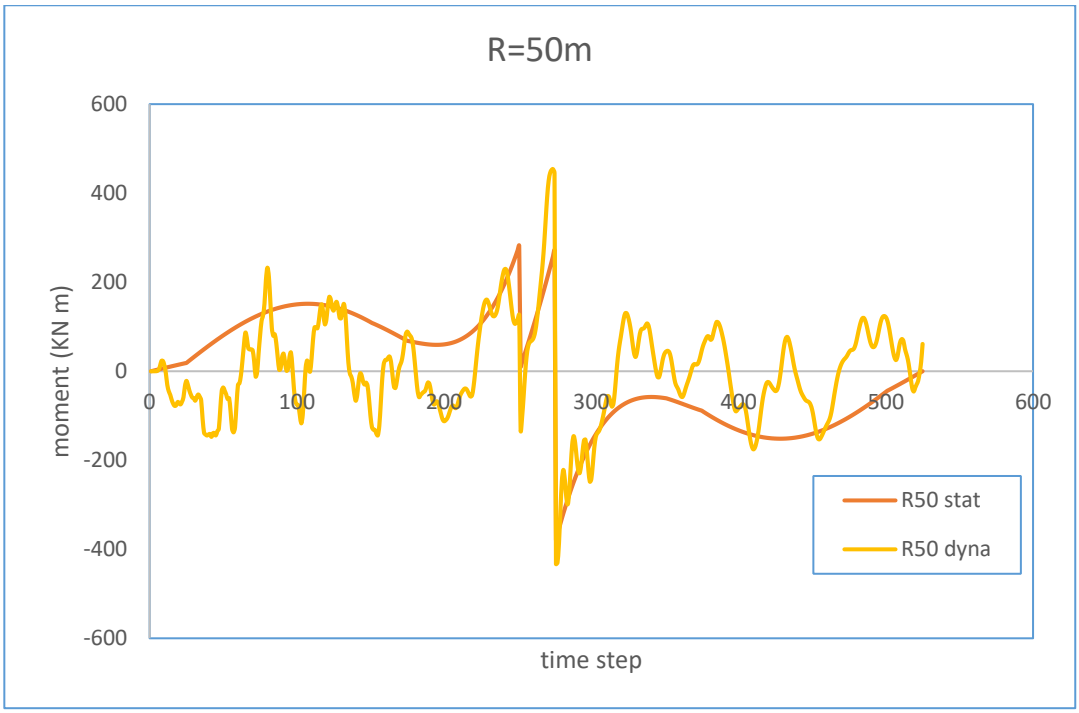

Figure 7-3 Mid-span moment for 3-span bridge model R=50m

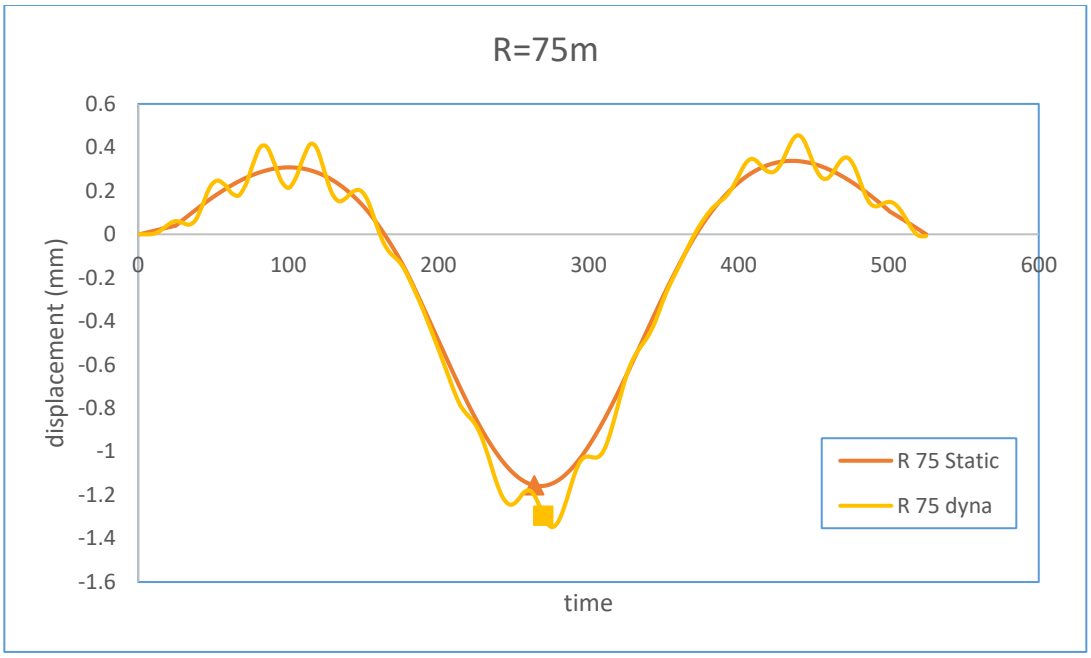

Figure 7-4 Mid-span displacement for 3-span bridge model R=75m

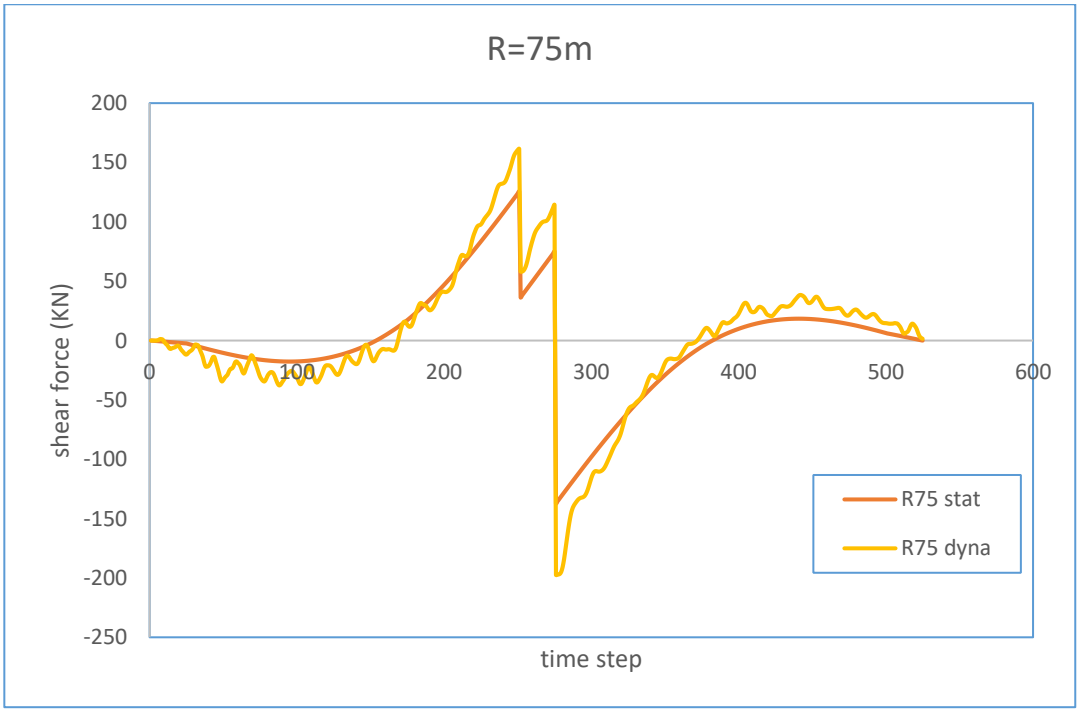

Figure 7-5 Mid-span shear force for 3-span bridge model R=75m

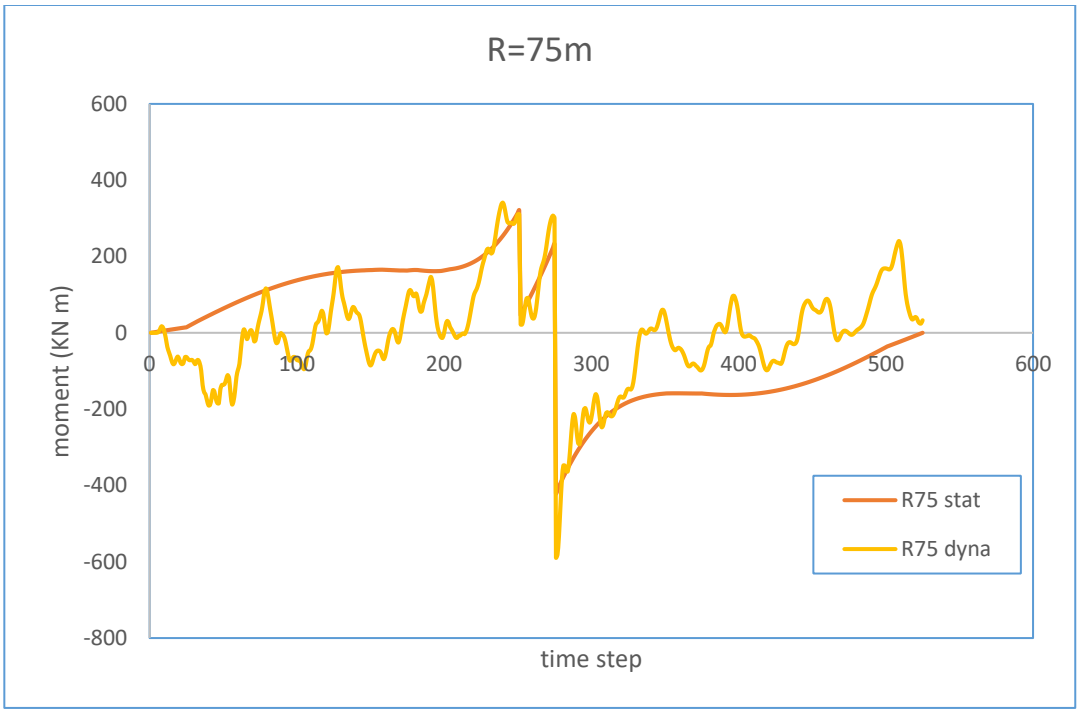

Figure 7-6 Mid-span moment for 3-span bridge model R=75m

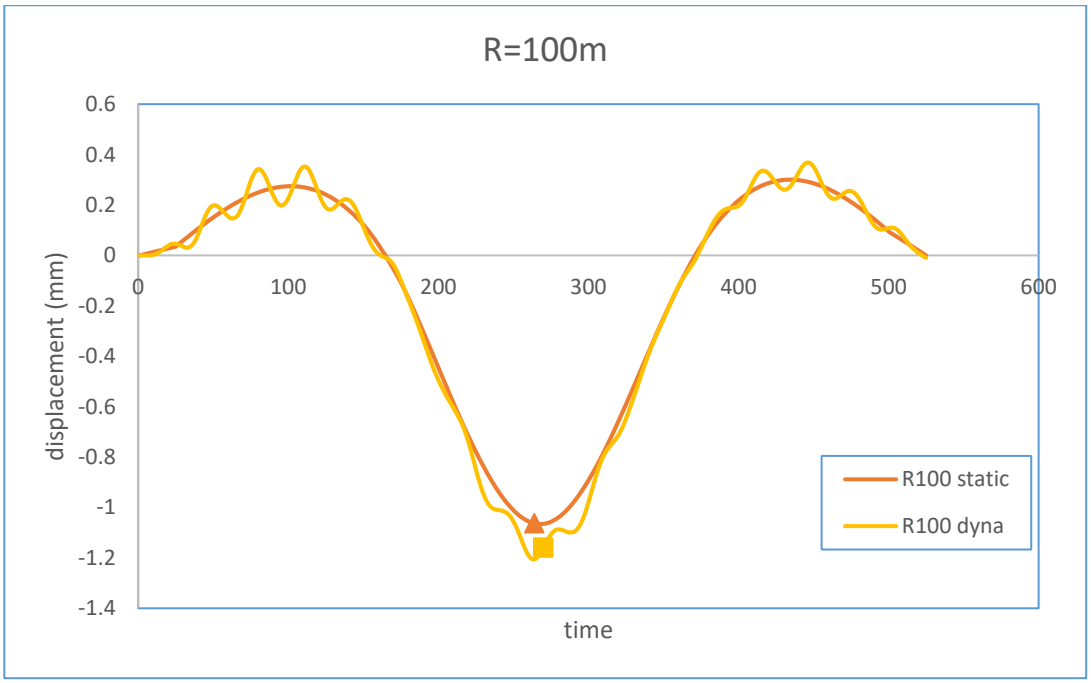

Figure 7-7 Mid-span displacement for 3-span bridge model R=100m

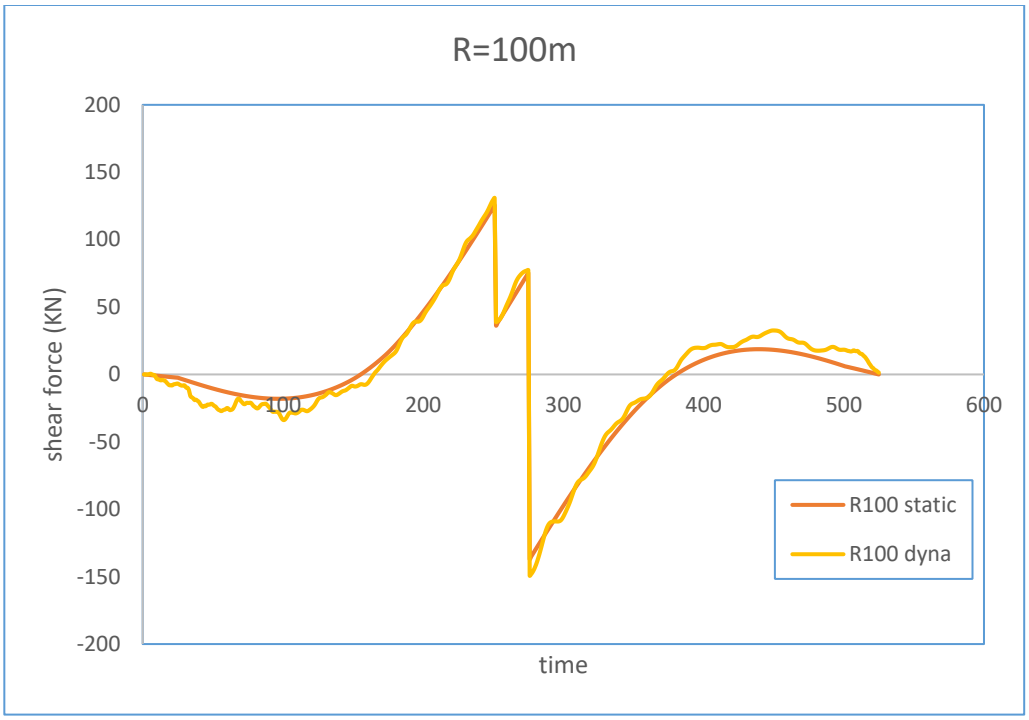

Figure 7-8 Mid-span shear force for 3-span bridge model R=100m

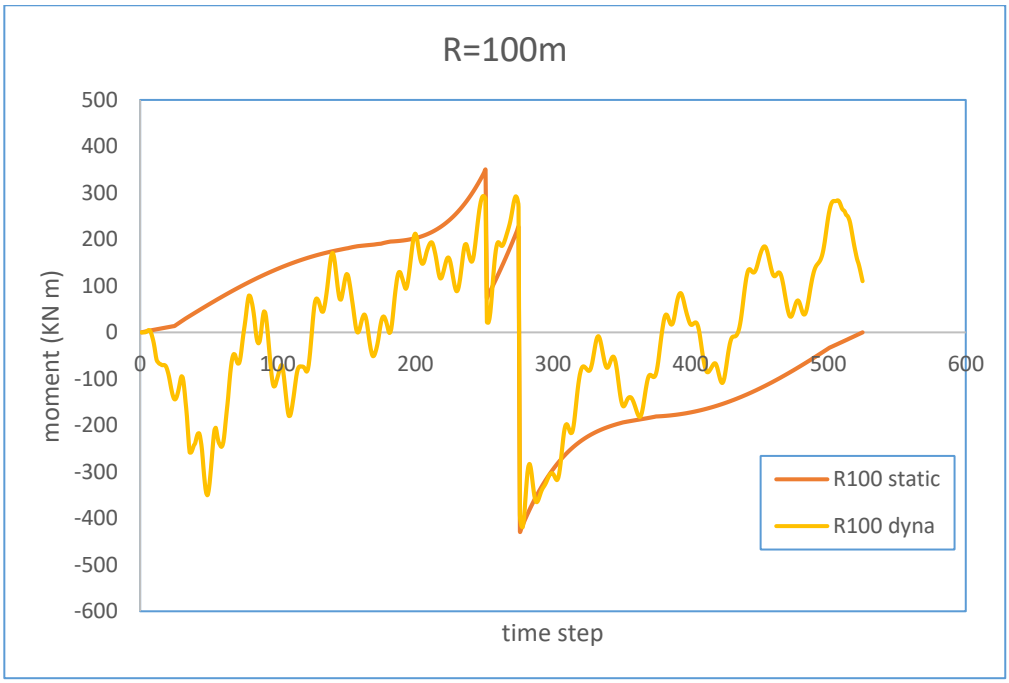

Figure 7-9 Mid-span shear force for 3-span bridge model R=100m

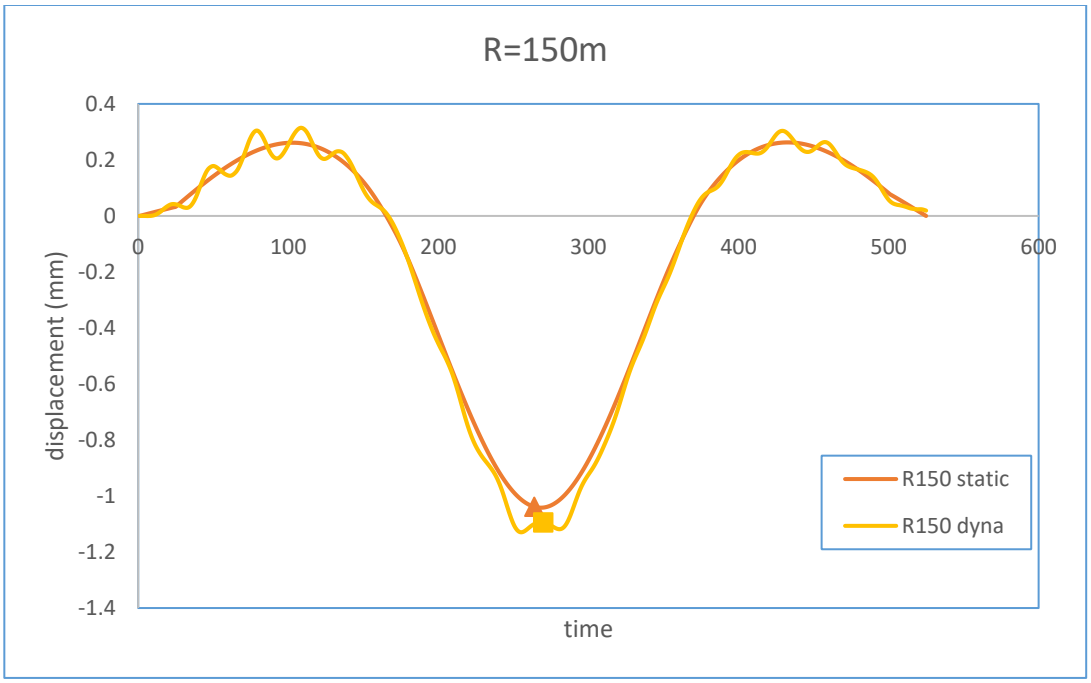

Figure 7-10 Mid-span displacement for 3-span bridge model R=150m

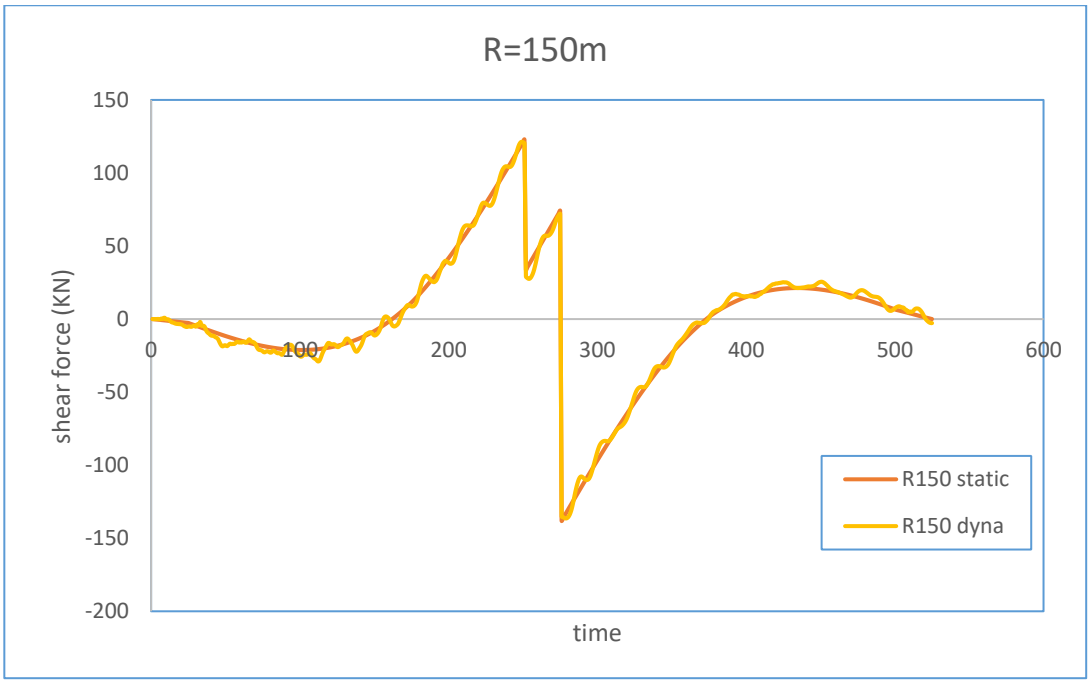

Figure 7-11 Mid-span shear force for 3-span bridge model R=150m

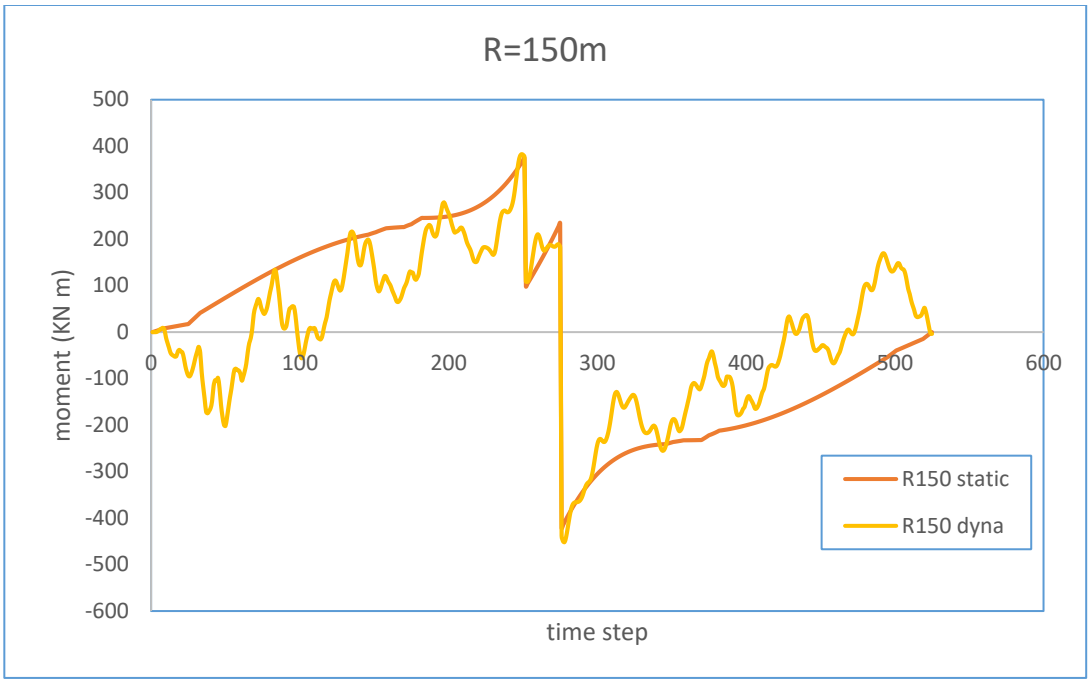

Figure 7-12 Mid-span shear force for 3-span bridge model R=150m

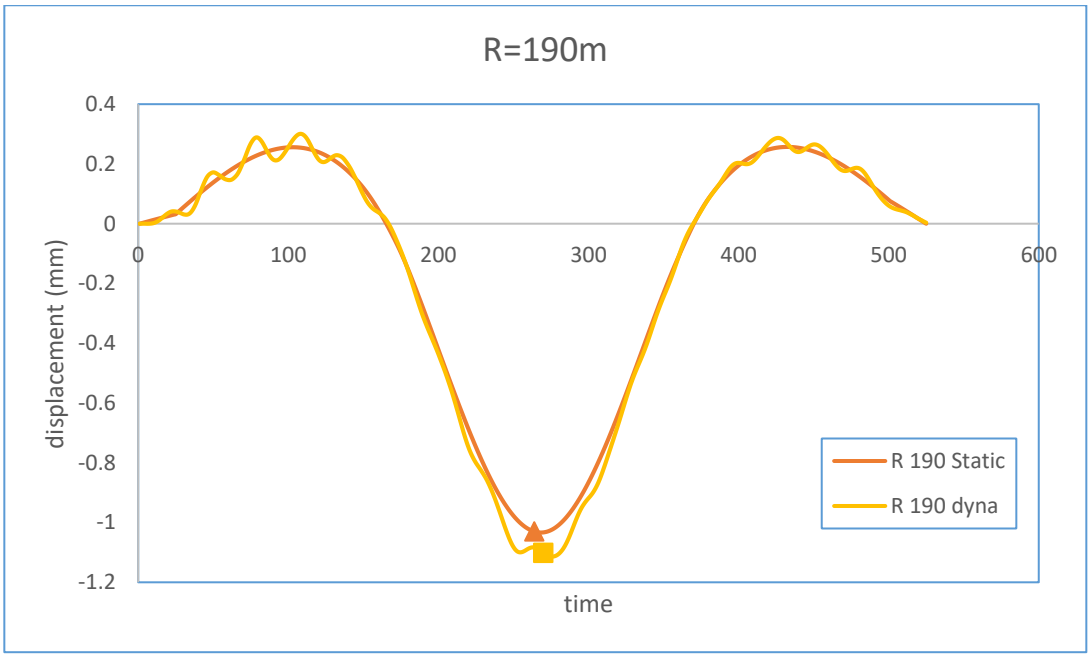

Figure 7-13 Mid-span displacement for 3-span bridge model R=190m

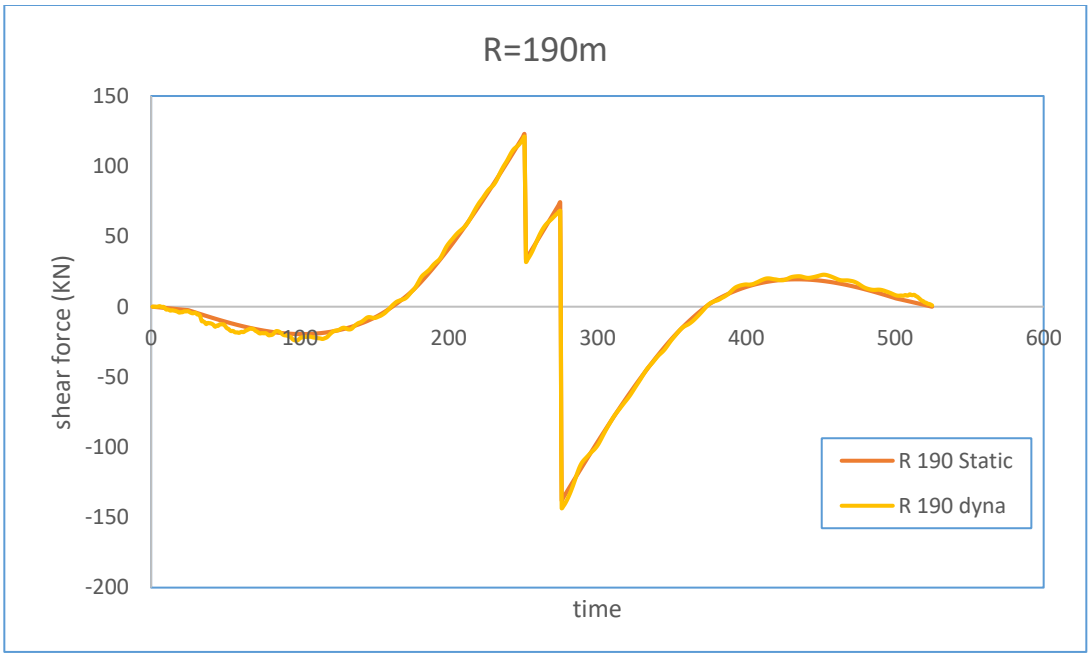

Figure 7-14 Mid-span shear force for 3-span bridge model R=190m

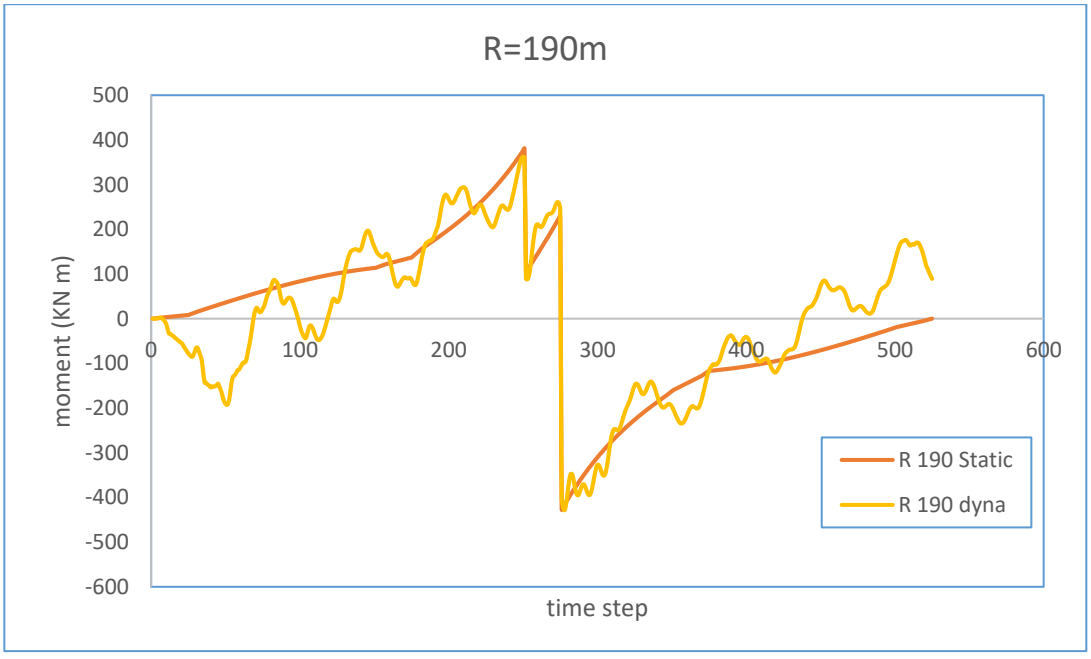

Figure 7-15 Mid-span shear force for 3-span bridge model R=190m

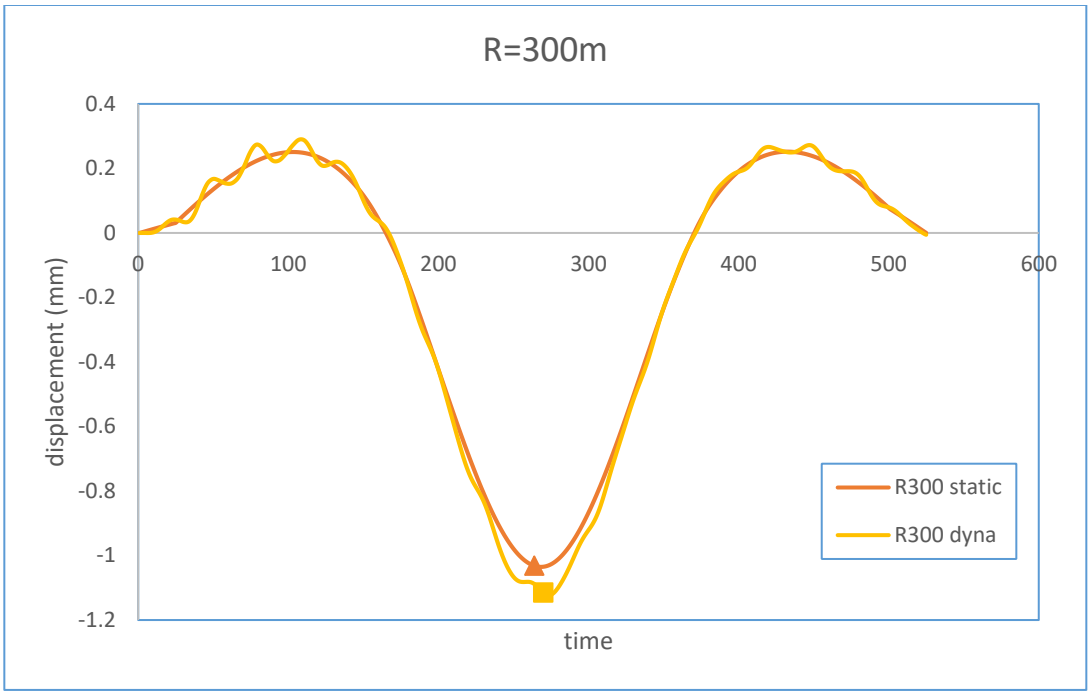

Figure 7-16 Mid-span displacement for 3-span bridge model R=300m

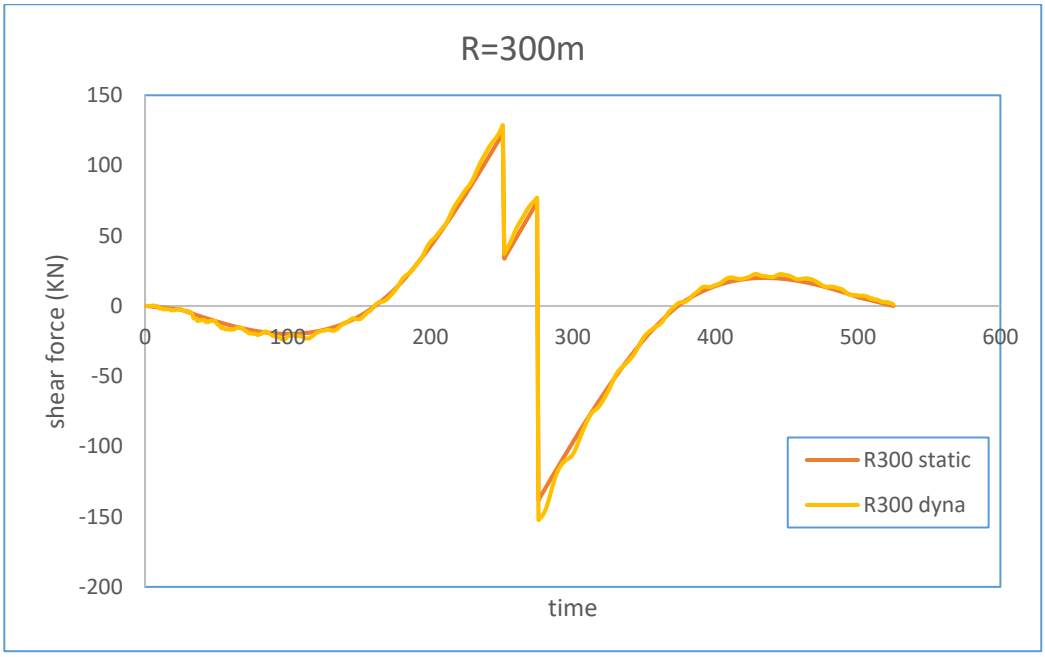

Figure 7-17 Mid-span shear force for 3-span bridge model R=300m

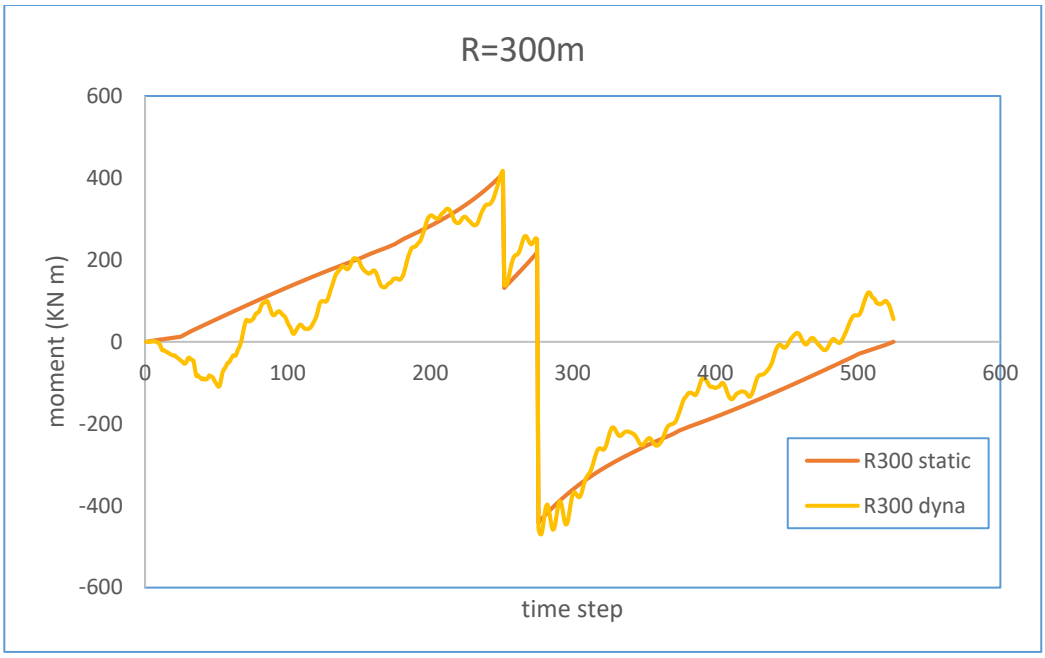

Figure 7-18 Mid-span shear force for 3-span bridge model R=300m

7.2.3 Span lengths comparison study

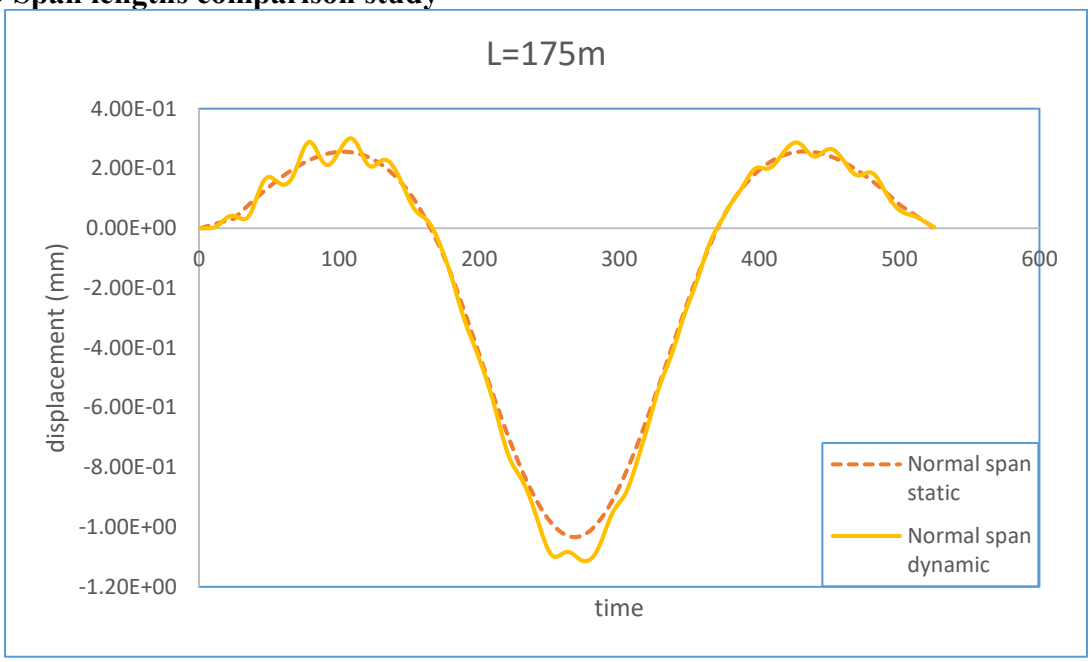

Figure 7-19 Mid-span displacement for 3-span bridge model L=175m

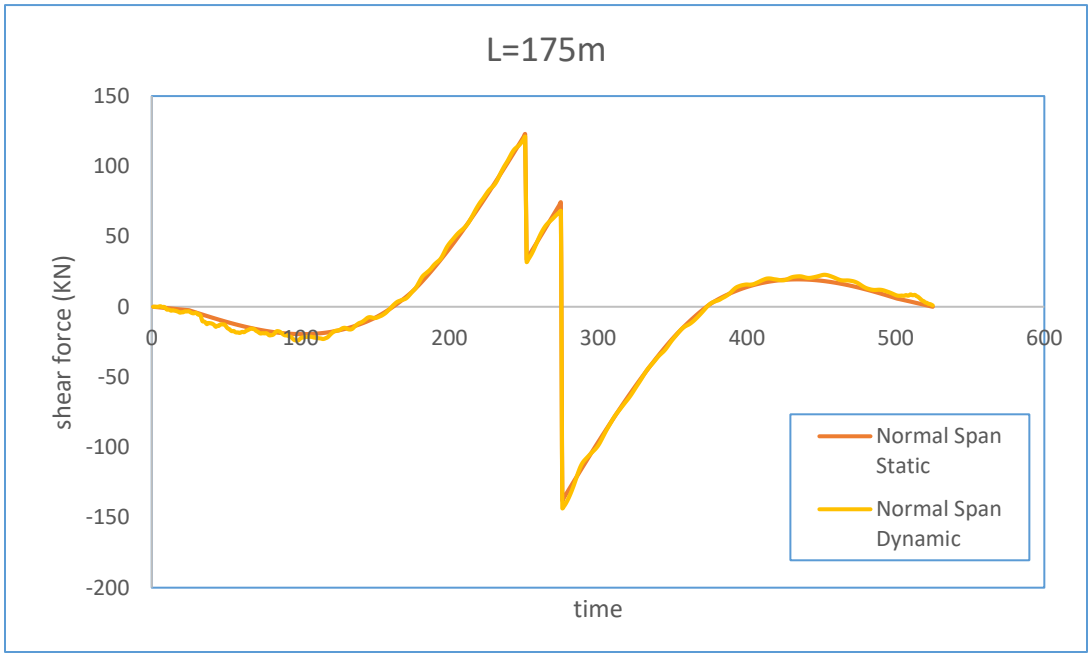

Figure 7-20 Mid-span shear force for 3-span bridge model L=175m

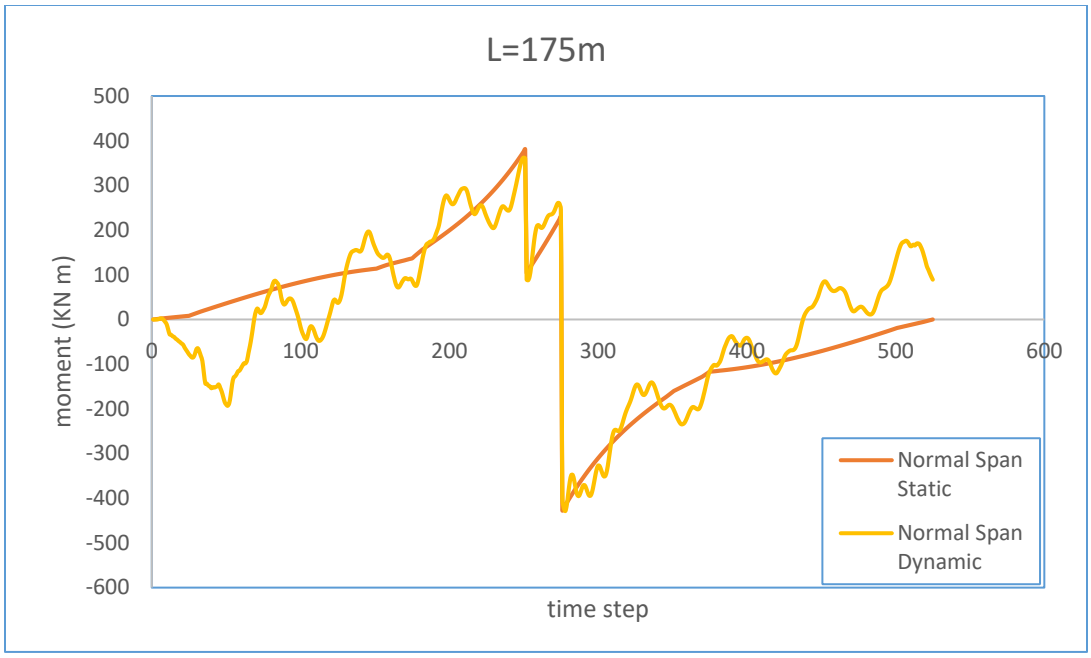

Figure 7-21 Mid-span shear force for 3-span bridge model L=175m

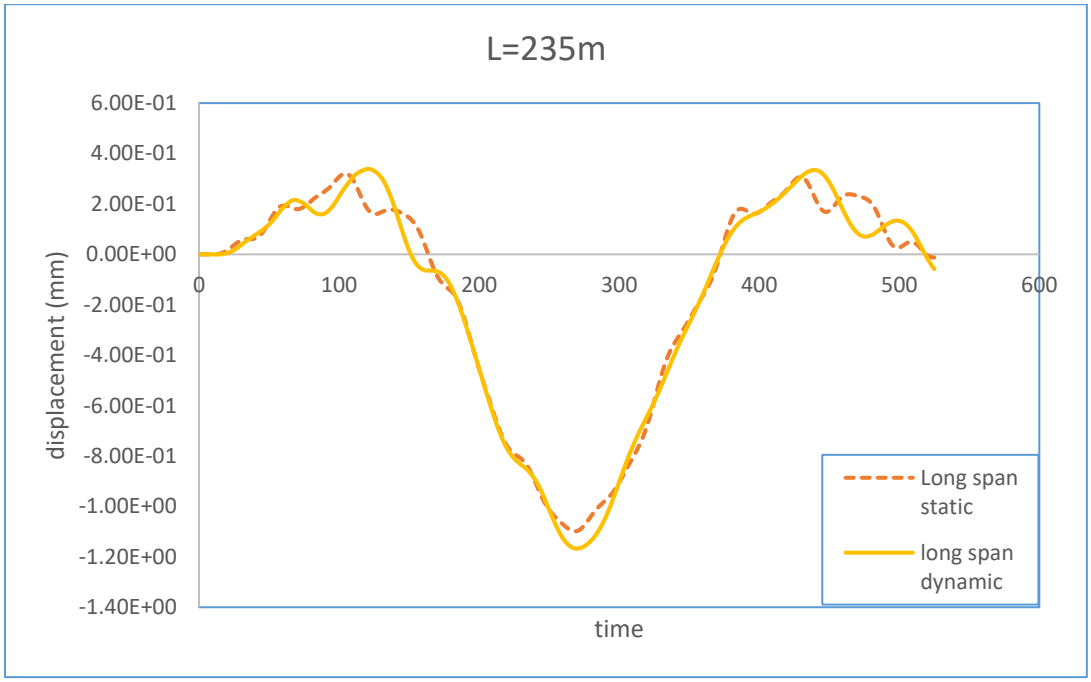

Figure 7-22 Mid-span displacement for 3-span bridge model L=235m

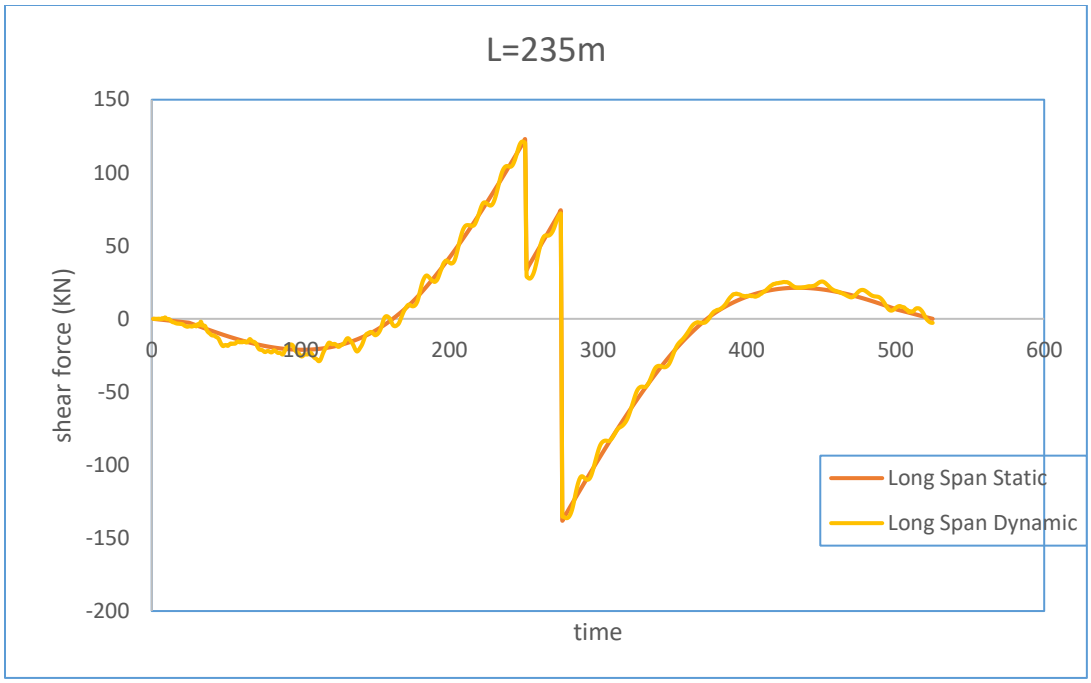

Figure 7-23 Mid-span shear force for 3-span bridge model L=235m

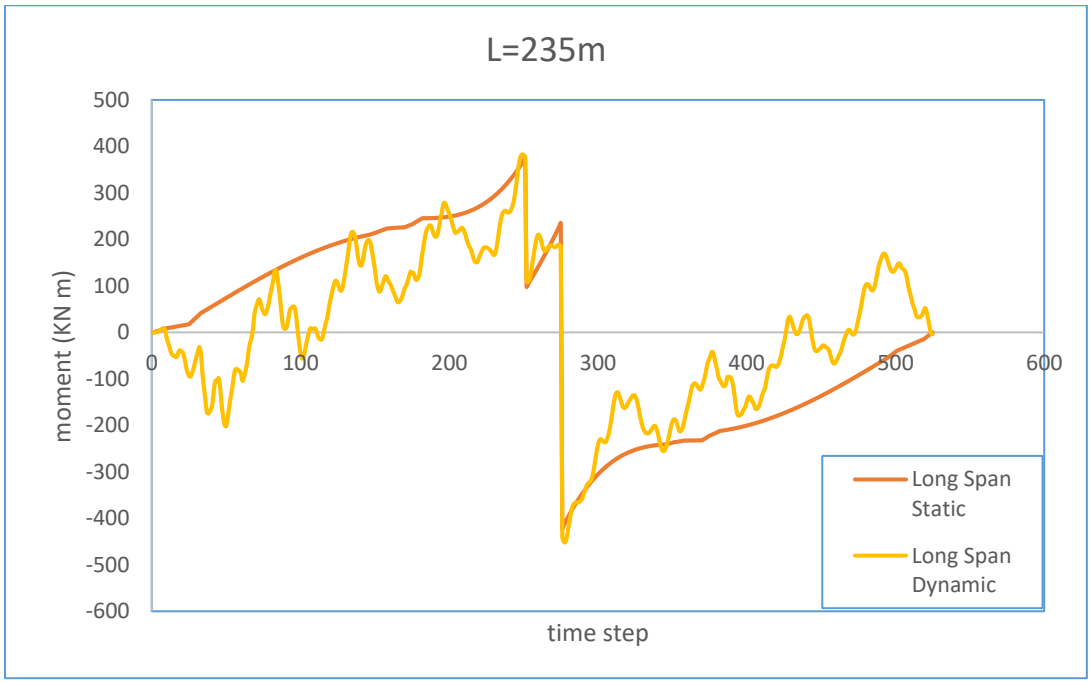

Figure 7-24 Mid-span shear force for 3-span bridge model L=235m

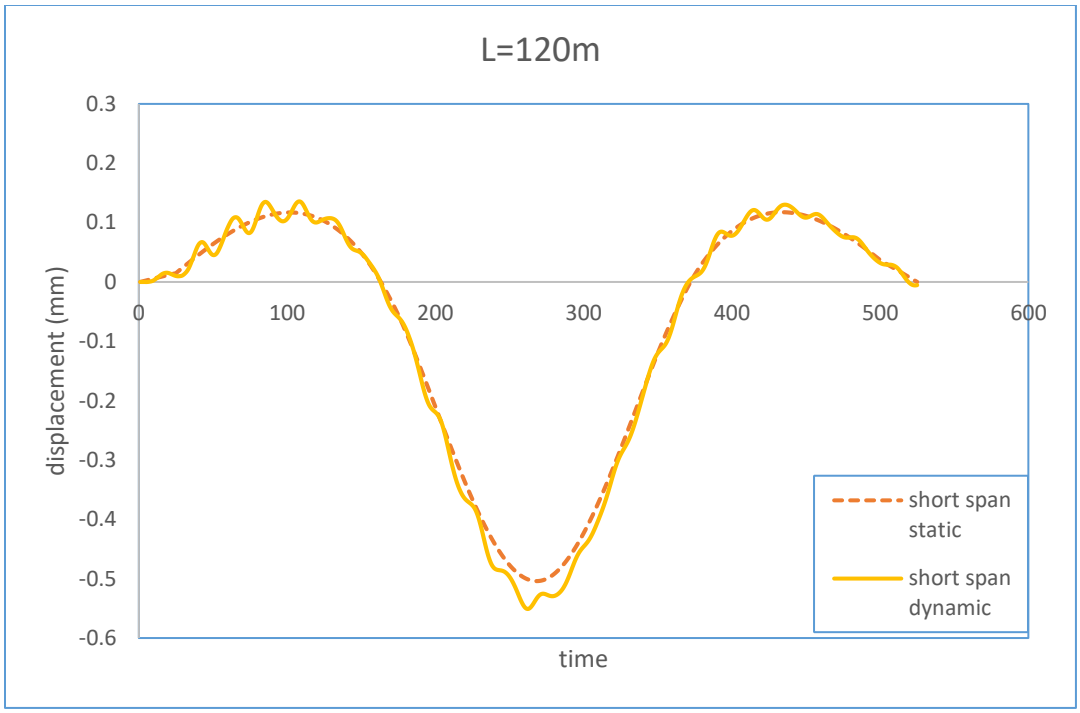

Figure 7-25 Mid-span displacement for 3-span bridge model L=120m

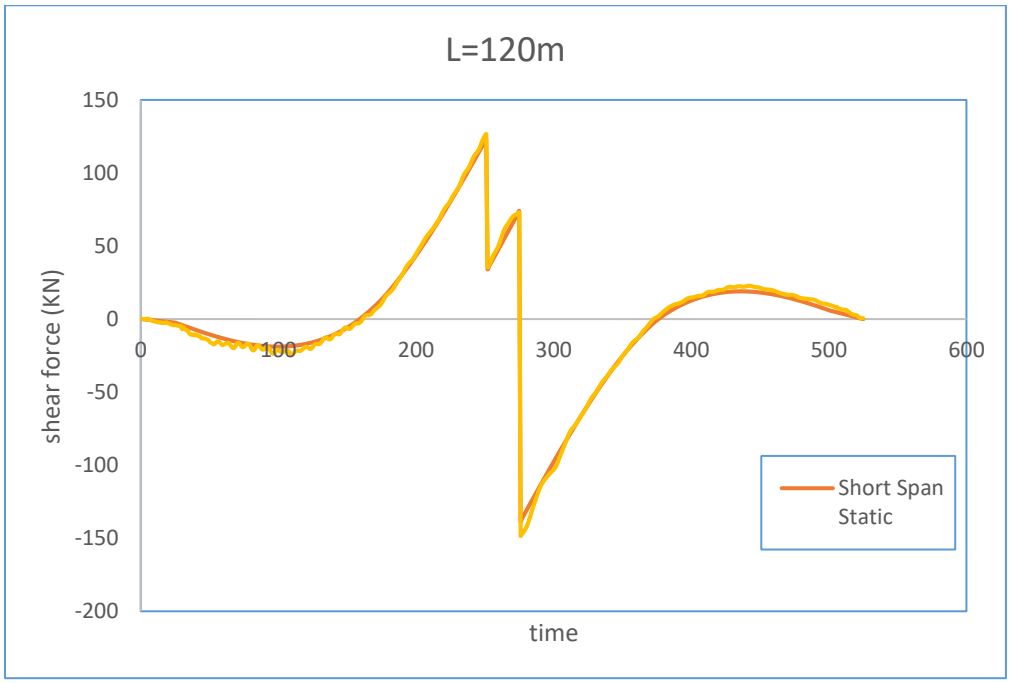

Figure 7-26 Mid-span shear force for 3-span bridge model L=120m

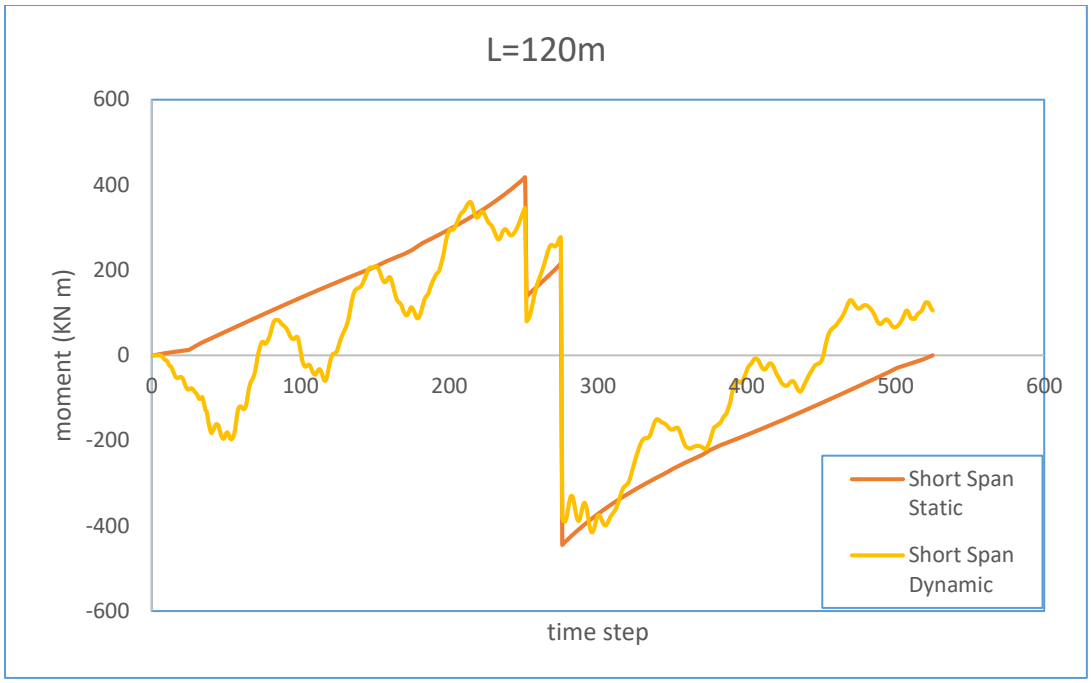

Figure 7-27 Mid-span shear force for 3-span bridge model L=120m

7.2.4 Vehicle travelling speeds comparison study

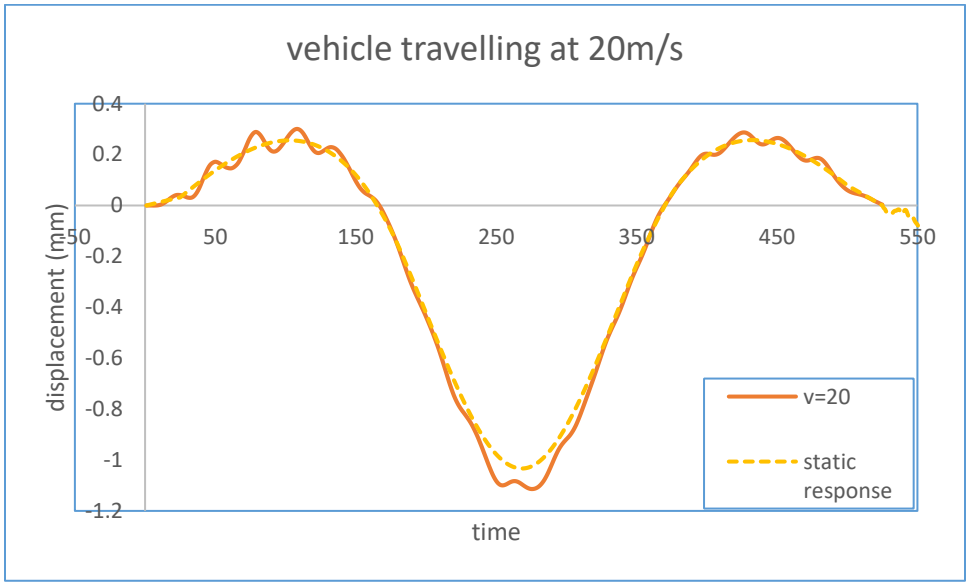

Figure 7-28 Mid-span displacement for 3-span bridge model v=20m/s

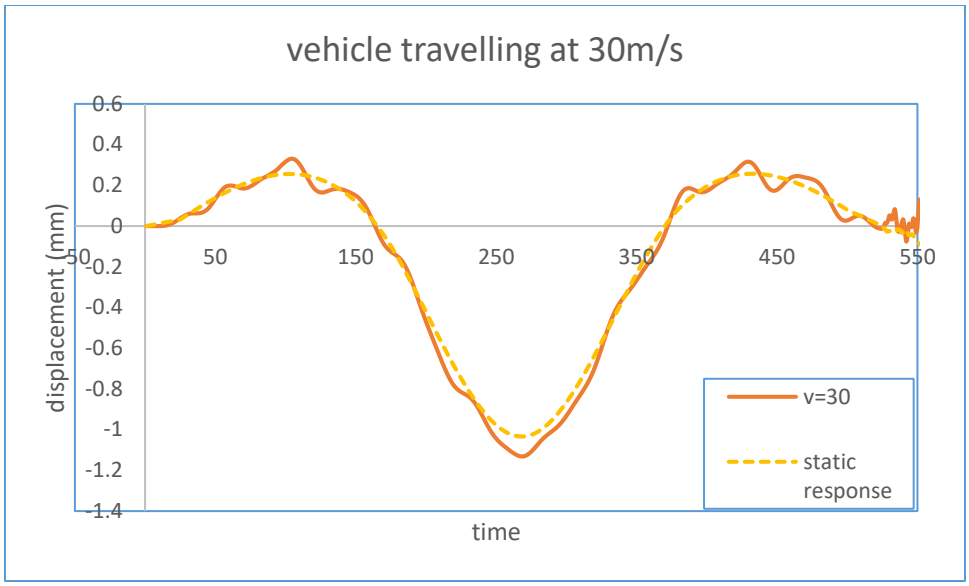

Figure 7-29 Mid-span displacement for 3-span bridge model v=30m/s

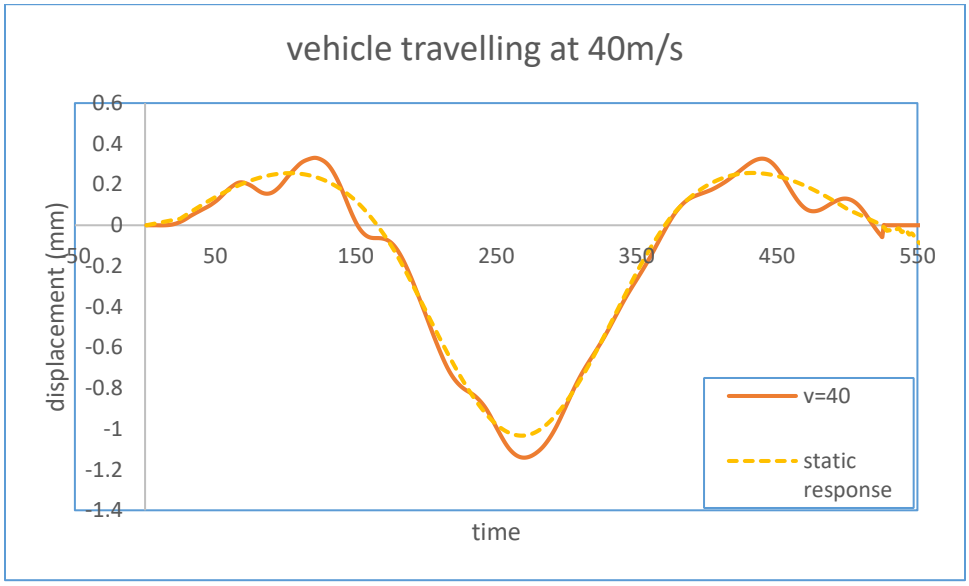

Figure 7-30 Mid-span displacement for 3-span bridge model v=40m/s

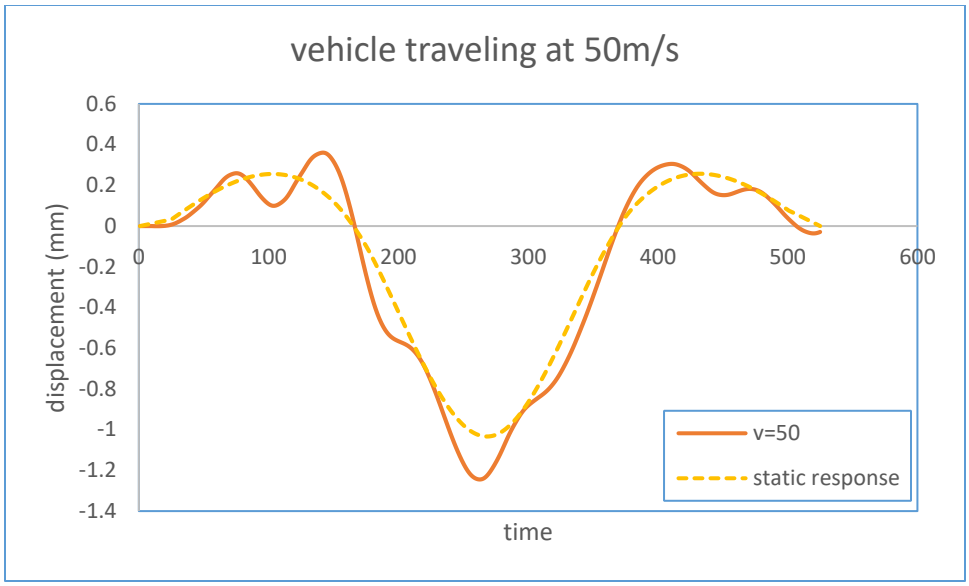

Figure 7-31 Mid-span displacement for 3-span bridge model v=50m/s

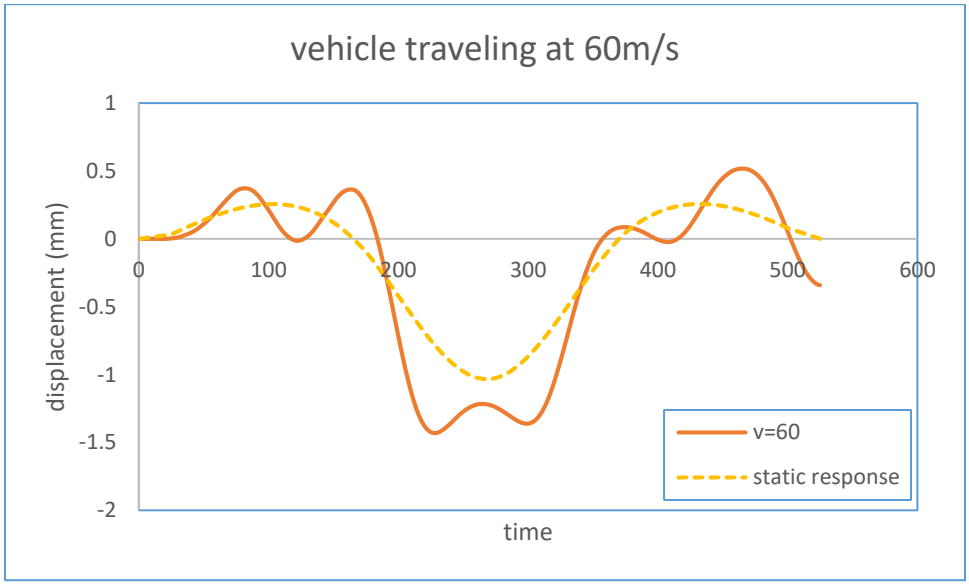

Figure 7-32 Mid-span displacement for 3-span bridge model v=60m/s

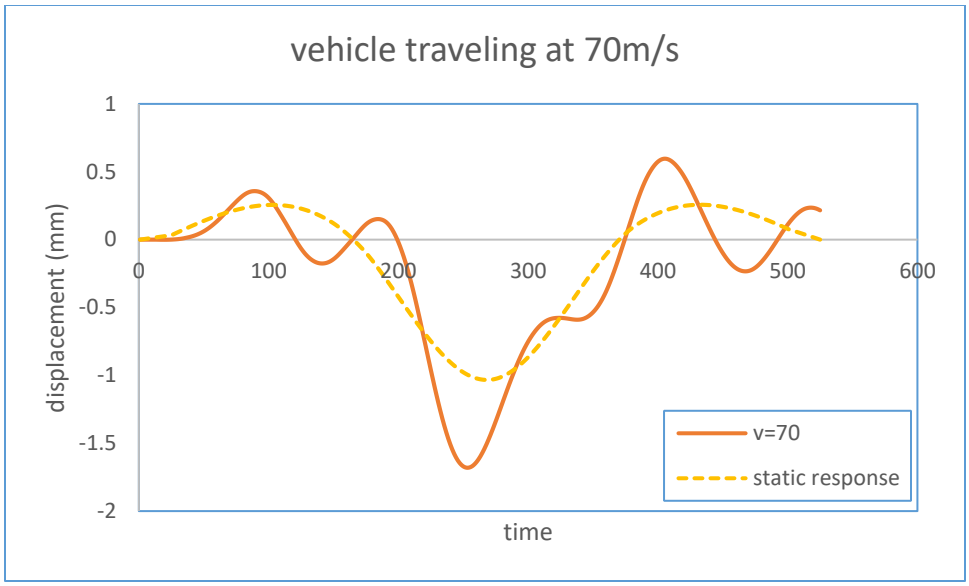

Figure 7-33 Mid-span displacement for 3-span bridge model v=70m/s

7.2.5 Deck roughness comparison study

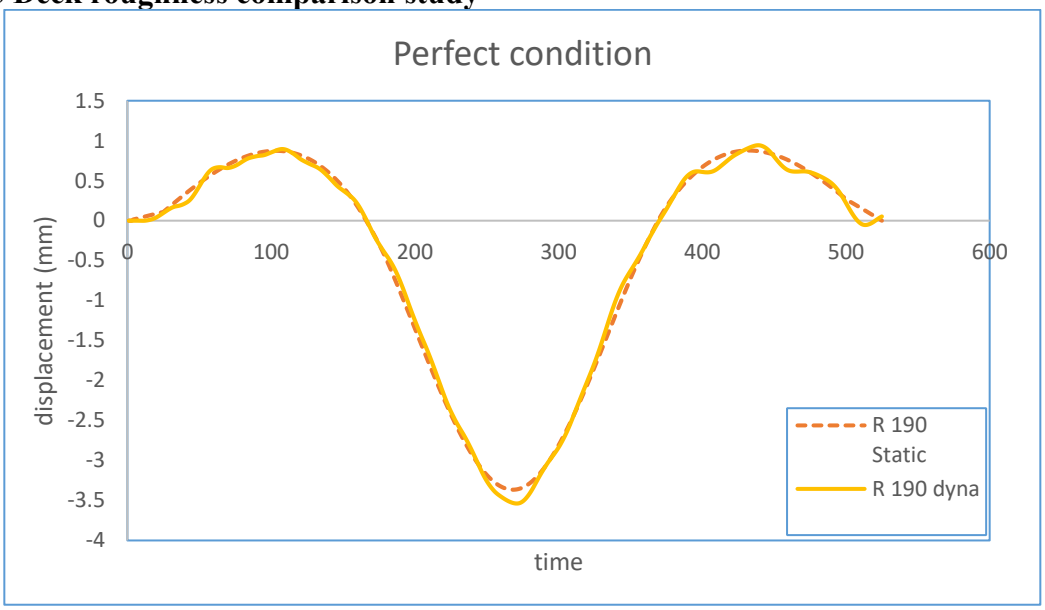

Figure 7-34 Mid-span displacement for 3-span bridge model v=30m/s L=235m perfect surface condition

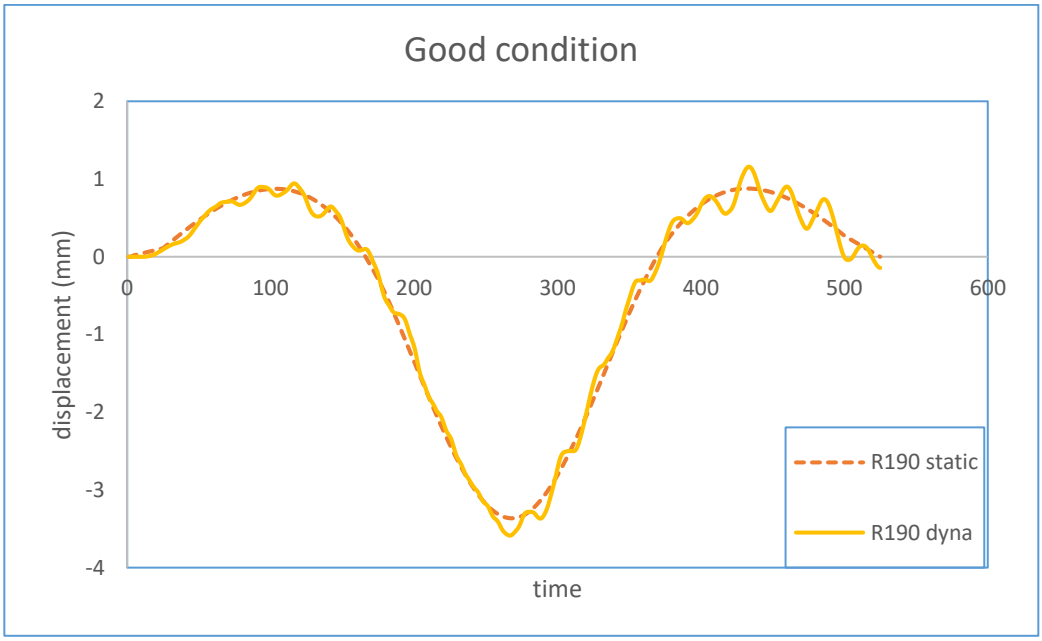

Figure 7-35 Mid-span displacement for 3-span bridge model v=30m/s L=235m good surface condition

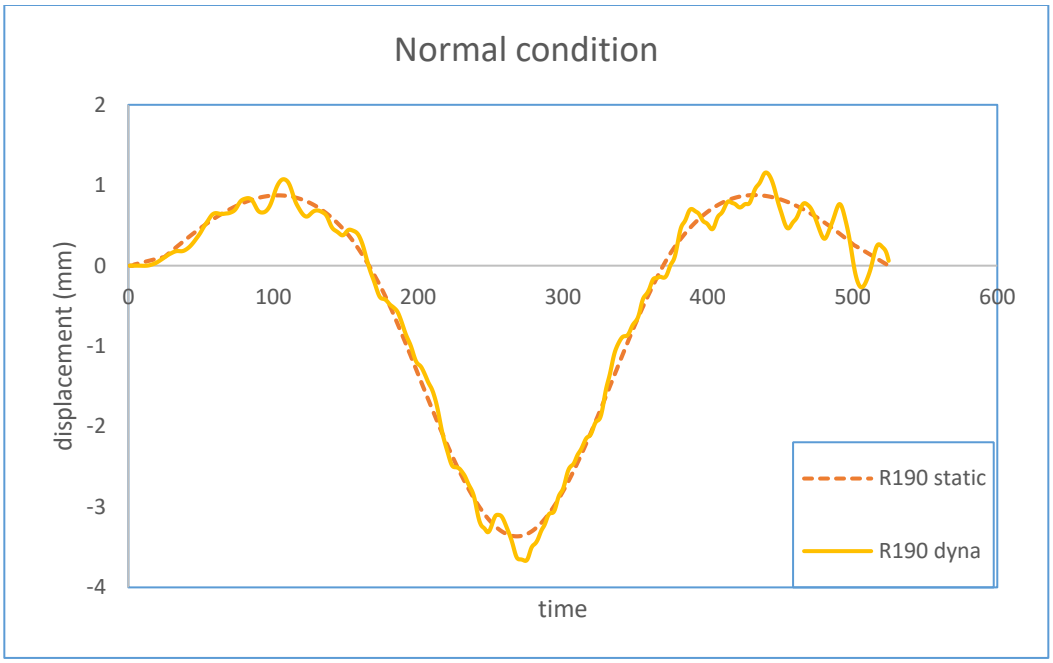

Figure 7-36 Mid-span displacement for 3-span bridge model v=30m/s L=235m normal surface condition

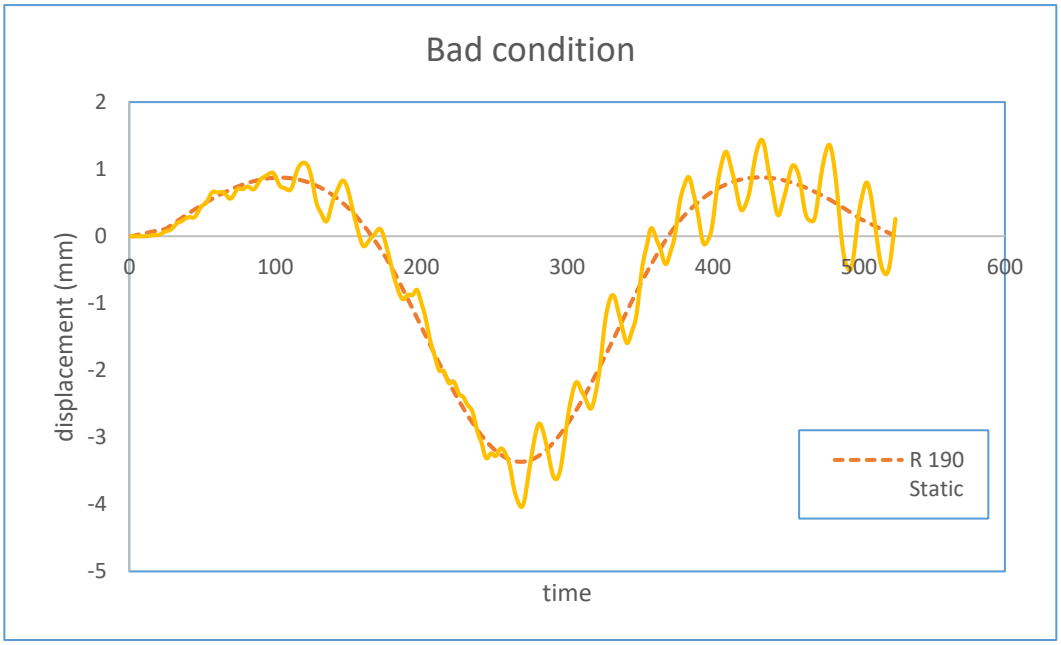

Figure 7-37 Mid-span displacement for 3-span bridge model v=30m/s L=235m bad surface condition

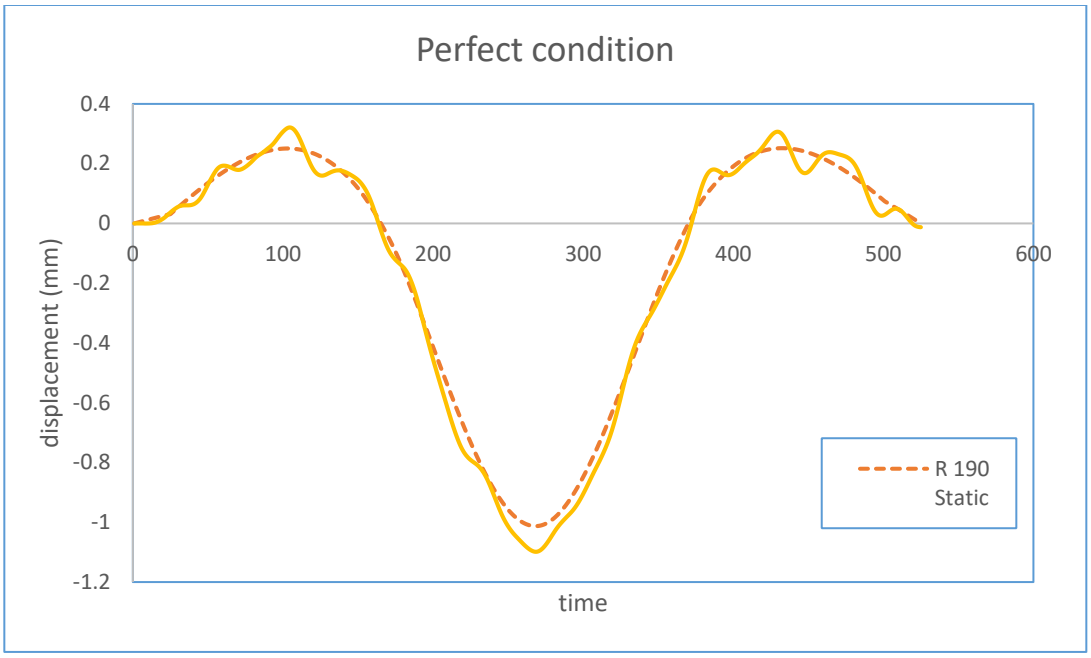

Figure 7-38 Mid-span displacement for 3-span bridge model v=30m/s L=175m perfect surface condition

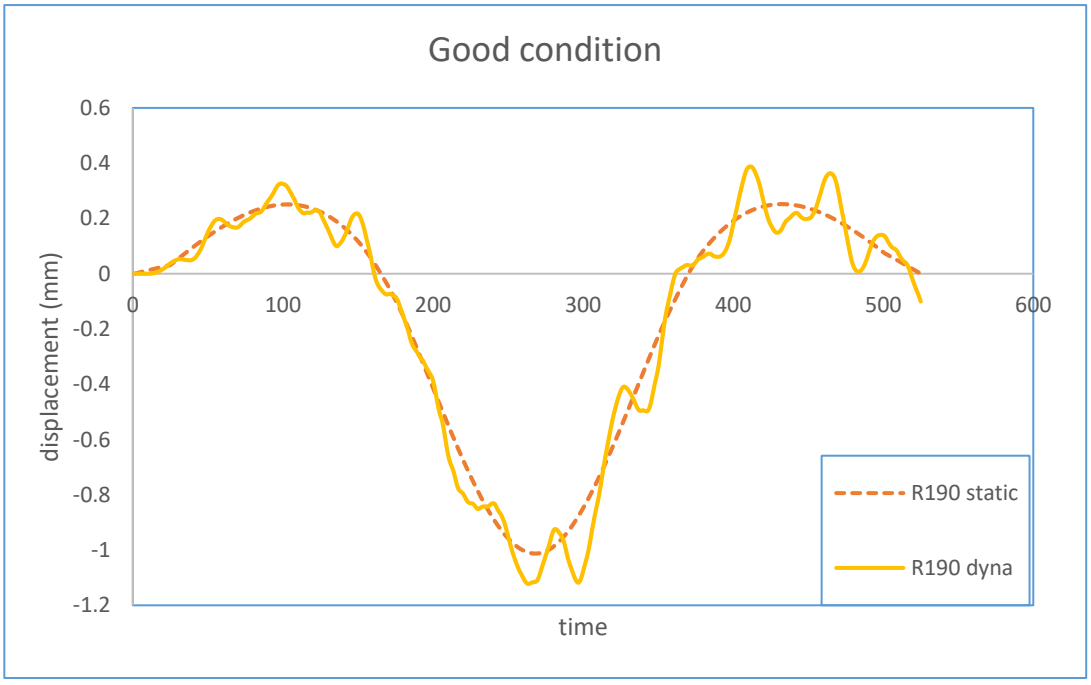

Figure 7-39 Mid-span displacement for 3-span bridge model v=30m/s L=175m good surface condition

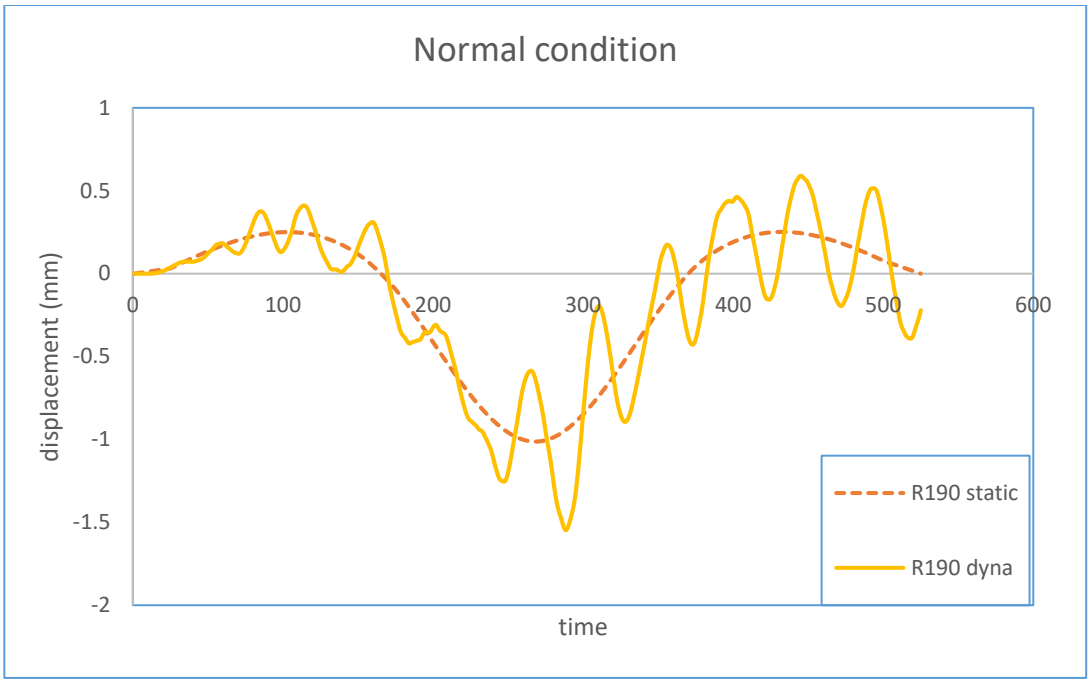

Figure 7-40 Mid-span displacement for 3-span bridge model v=30m/s L=175m normal surface condition

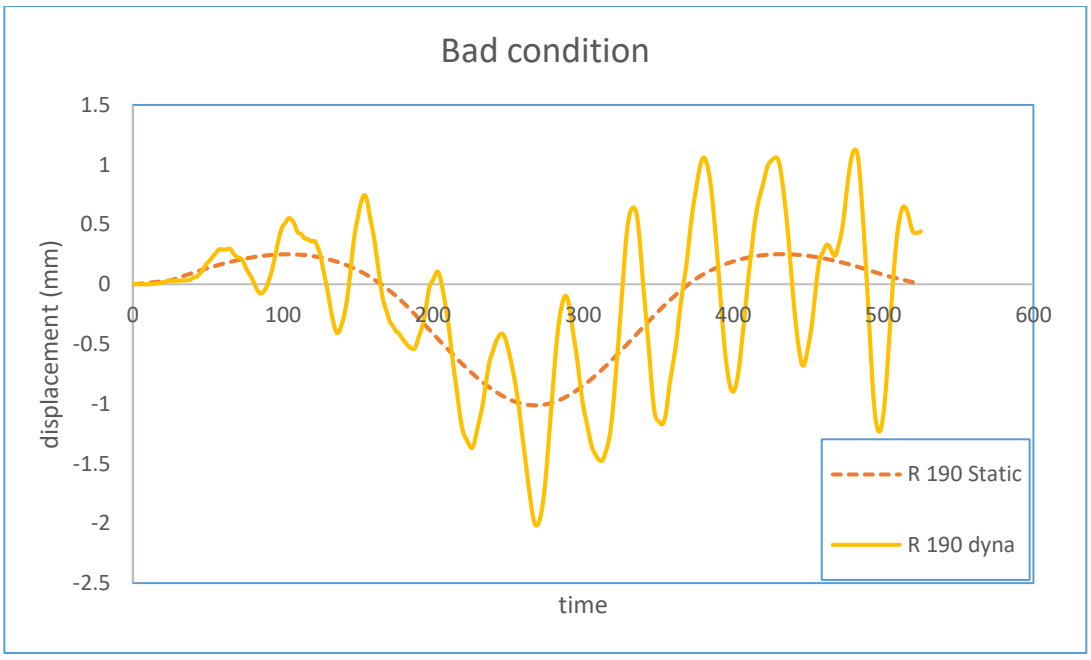

Figure 7-41 Mid-span displacement for 3-span bridge model v=30m/s L=175m bad surface condition

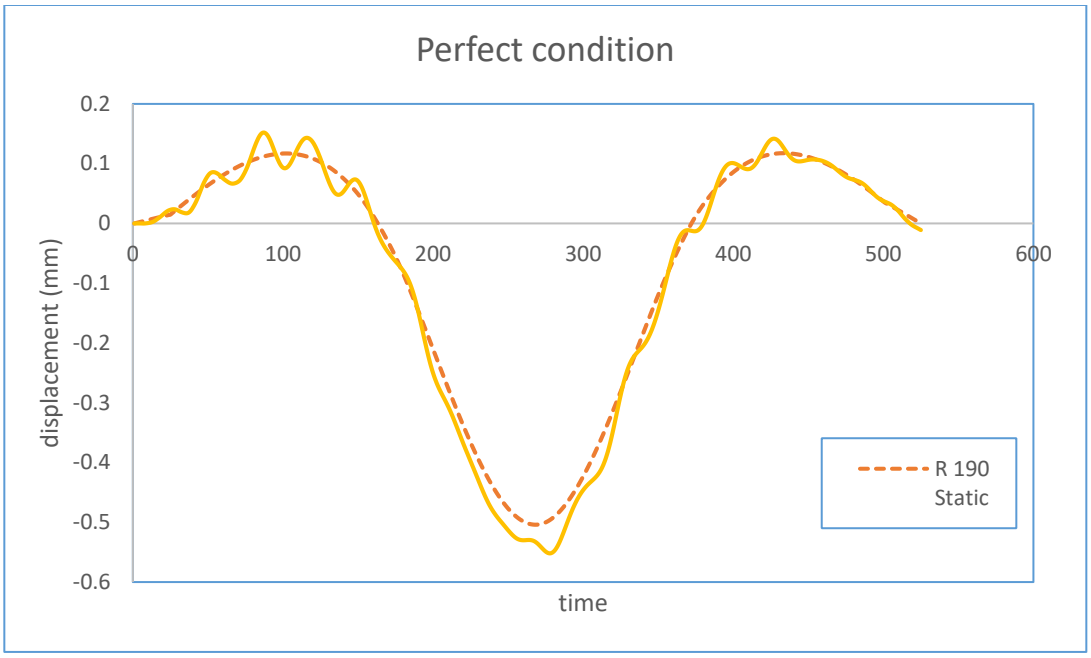

Figure 7-42 Mid-span displacement for 3-span bridge model v=30m/s L=120m perfect surface condition

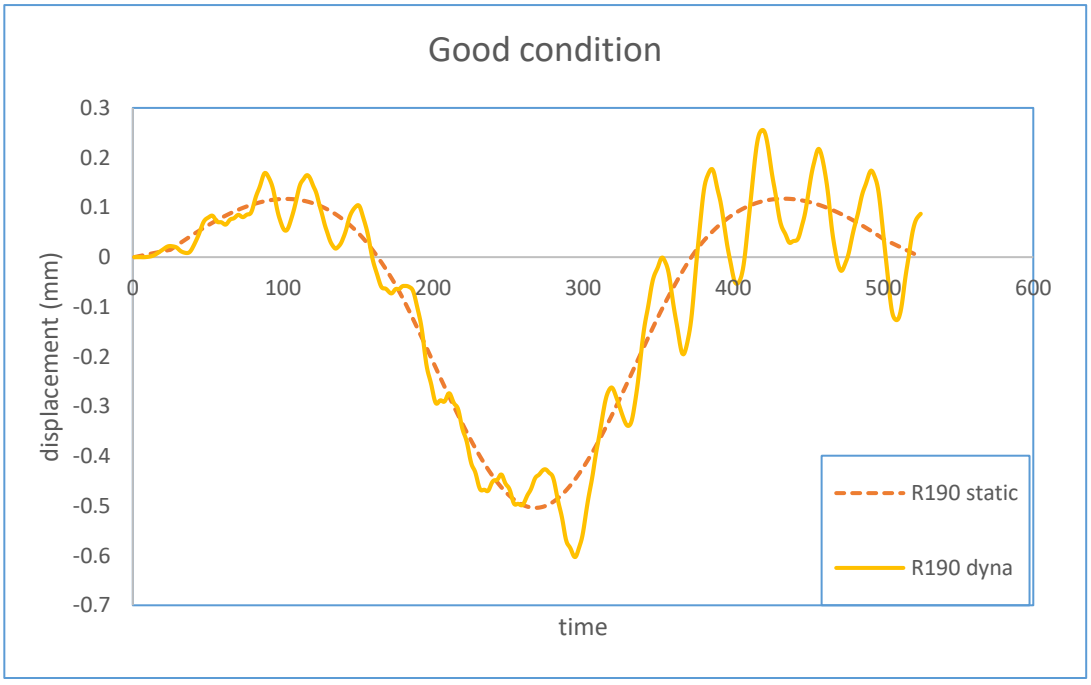

Figure 7-43 Mid-span displacement for 3-span bridge model v=30m/s L=120m good surface condition

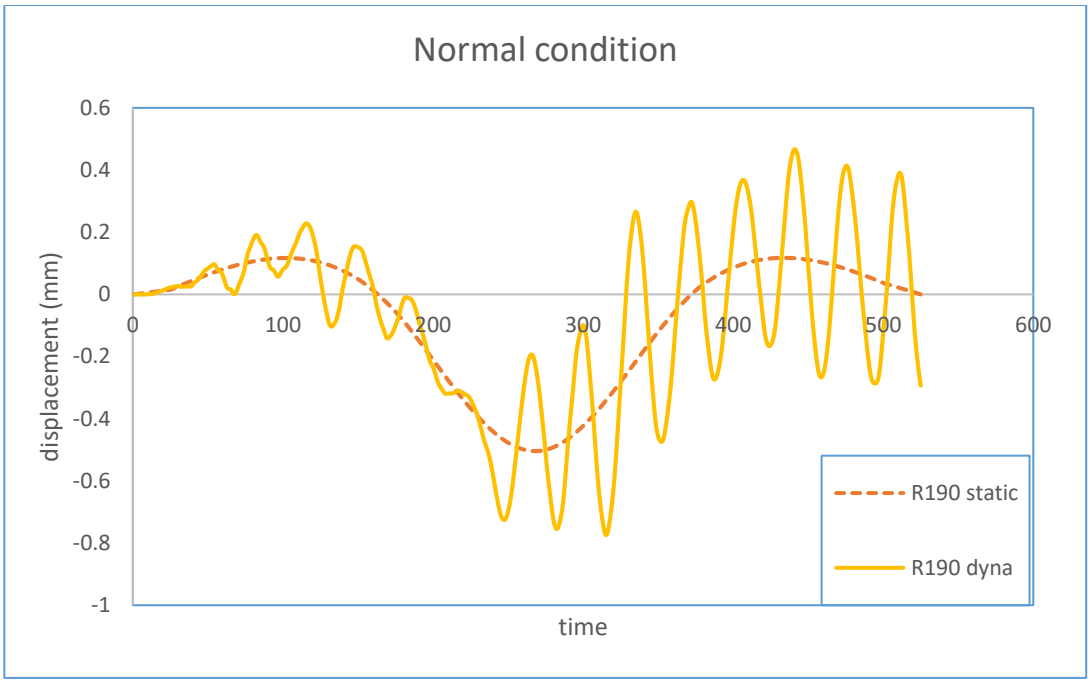

Figure 7-44 Mid-span displacement for 3-span bridge model v=30m/s L=120m normal surface condition

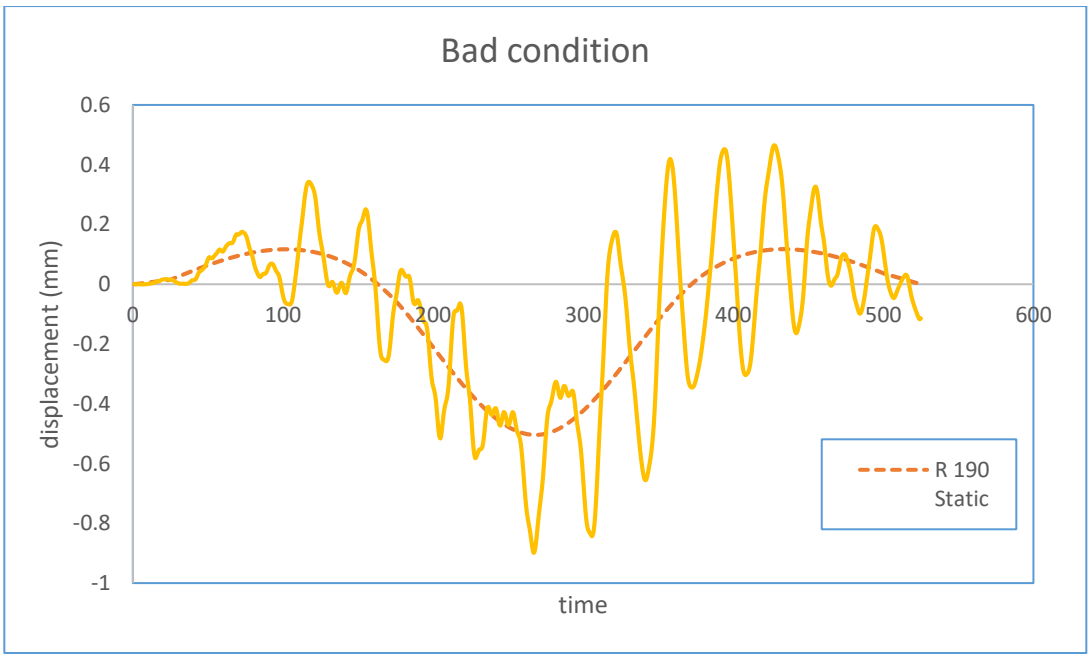

Figure 7-45 Mid-span displacement for 3-span bridge model v=30m/s L=120m normal surface condition

7.2.6 Eccentricity study

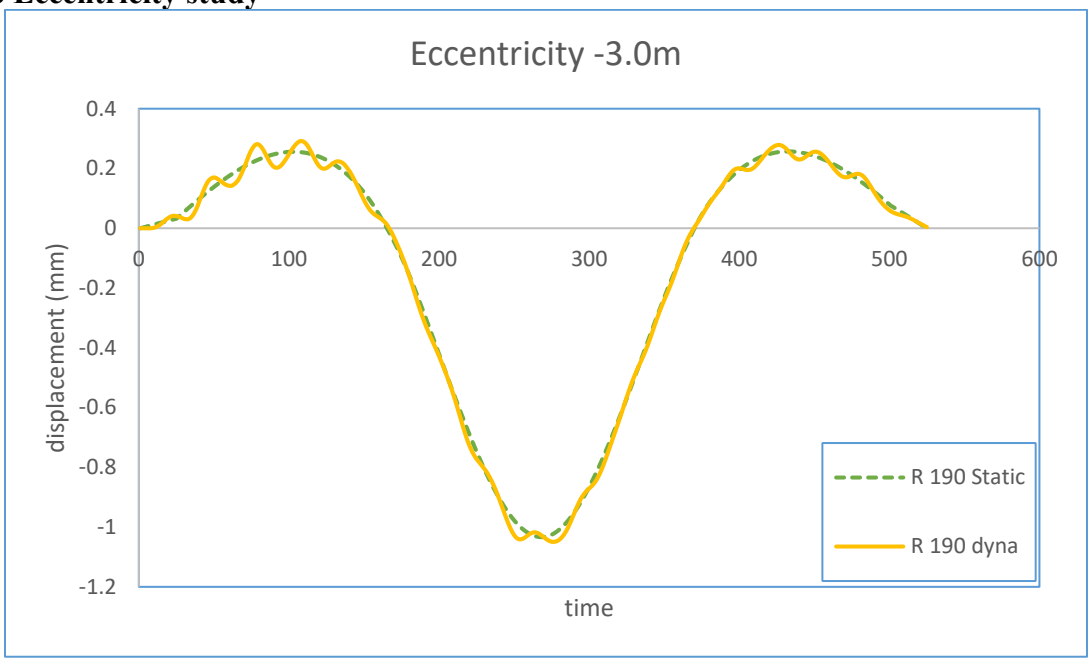

Figure 7-46 Mid-span displacement for 3-span bridge model with vehicle traveling through inner lane

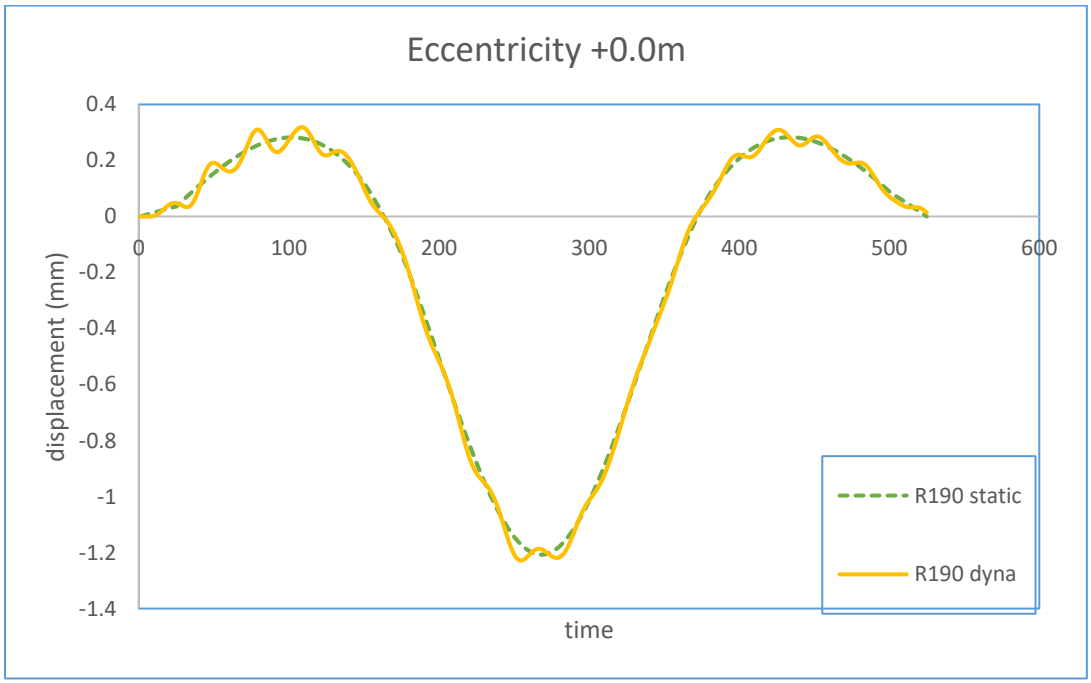

Figure 7-47 Mid-span displacement for 3-span bridge model with vehicle traveling through center lane

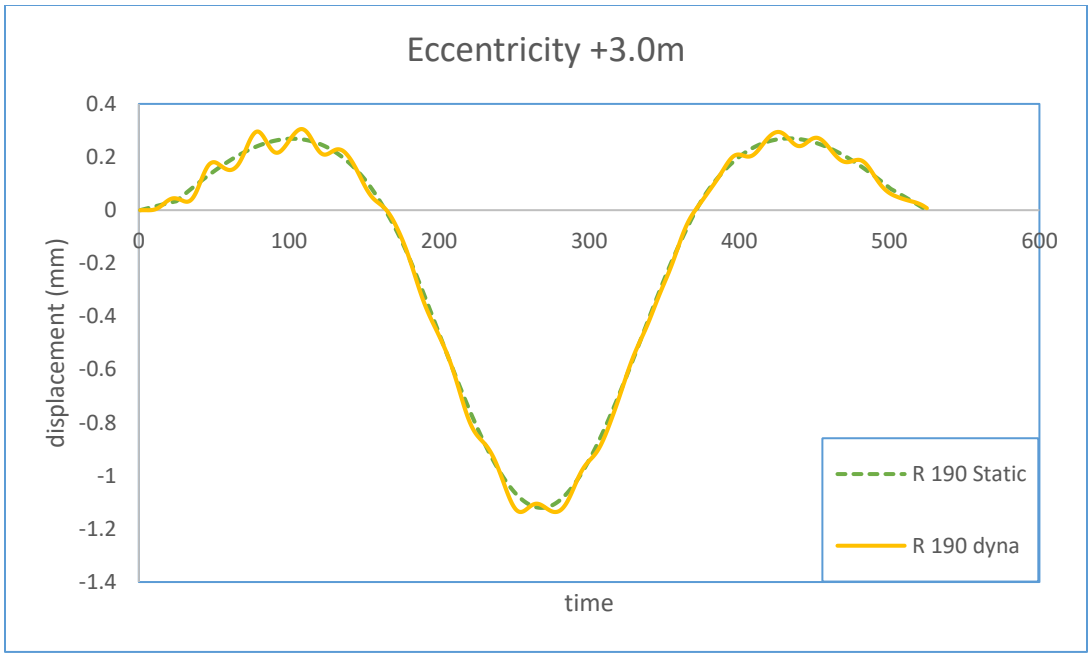

Figure 7-48 Mid-span displacement for 3-span bridge model with vehicle traveling through outer lane

7.2.7 For 2-span bridge configurations

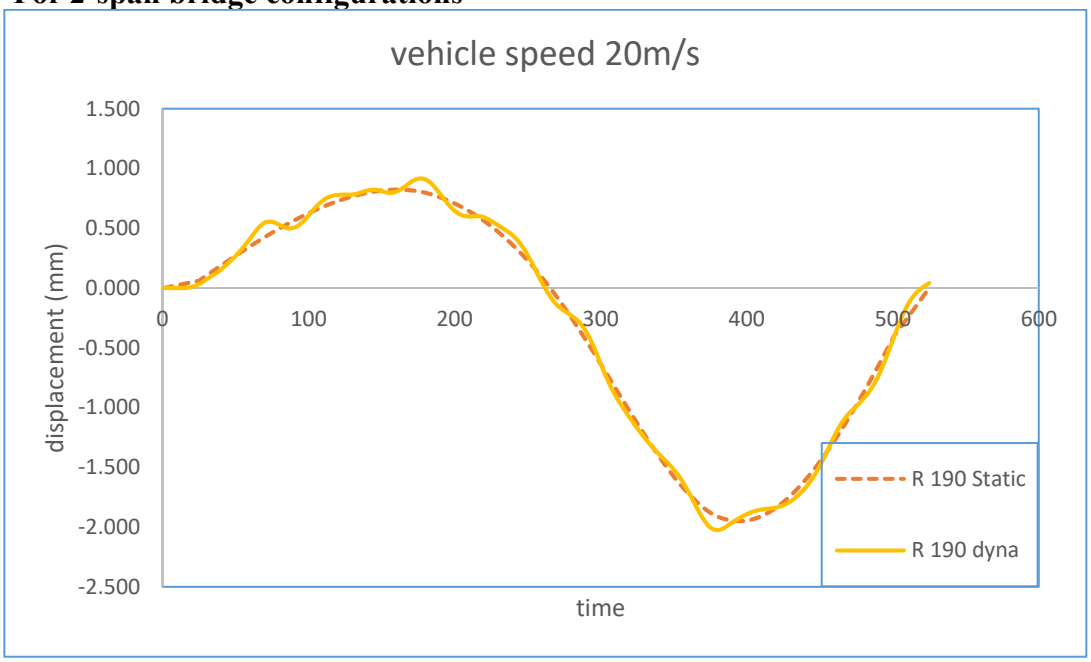

Figure 7-49 Mid-span displacement for 2-span bridge model v=20m/s

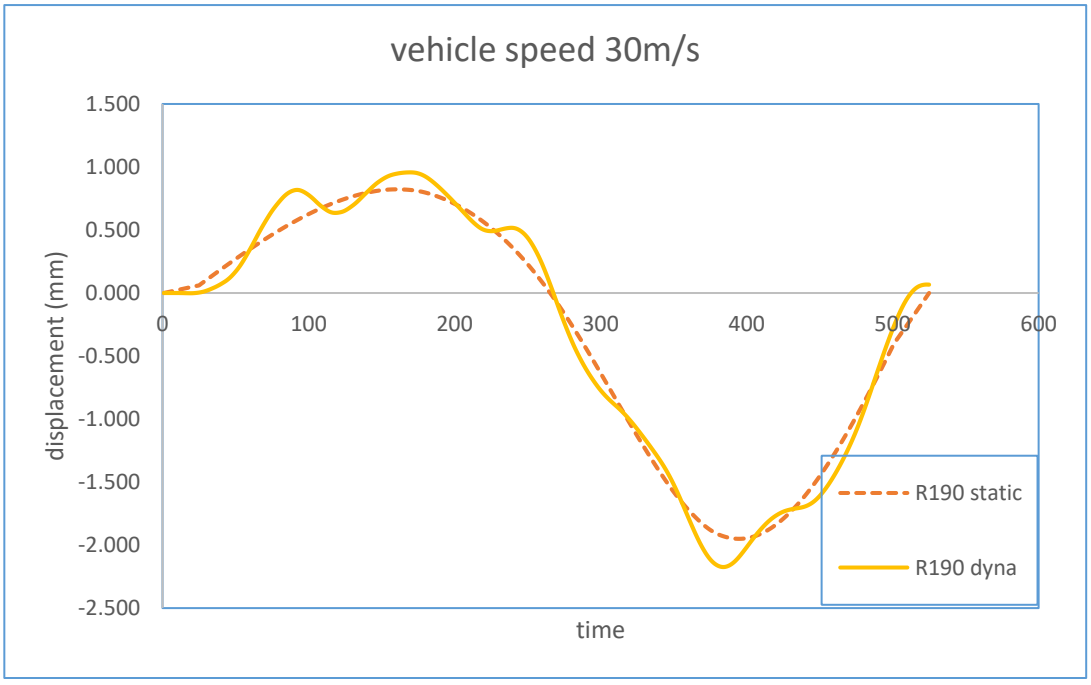

Figure 7-50 Mid-span displacement for 2-span bridge model v=30m/s

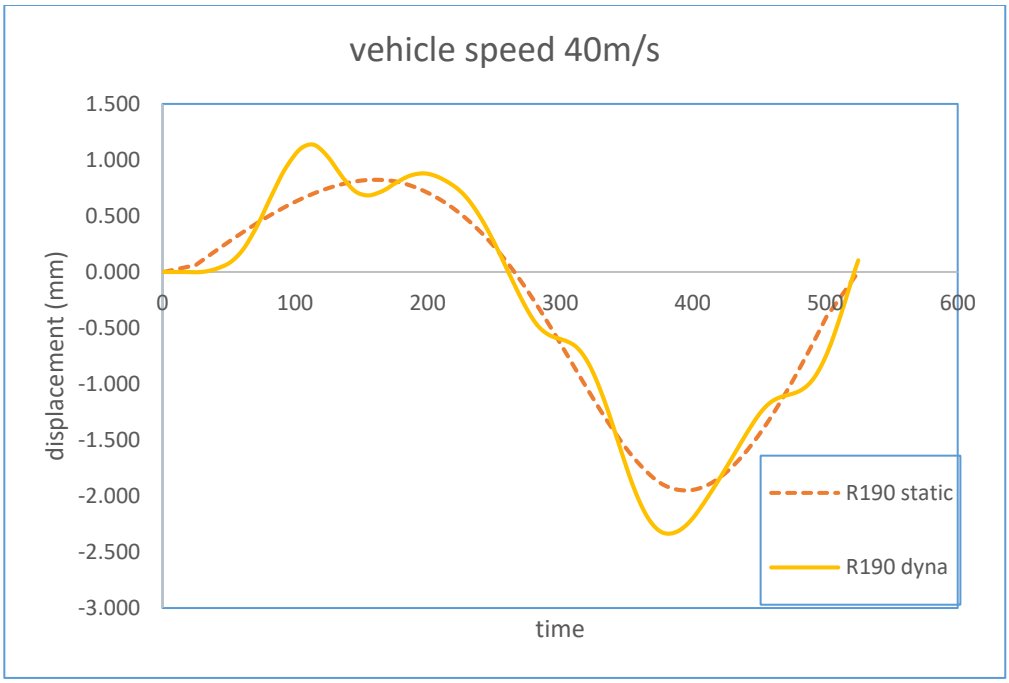

Figure 7-51 Mid-span displacement for 2-span bridge model v=40m/s

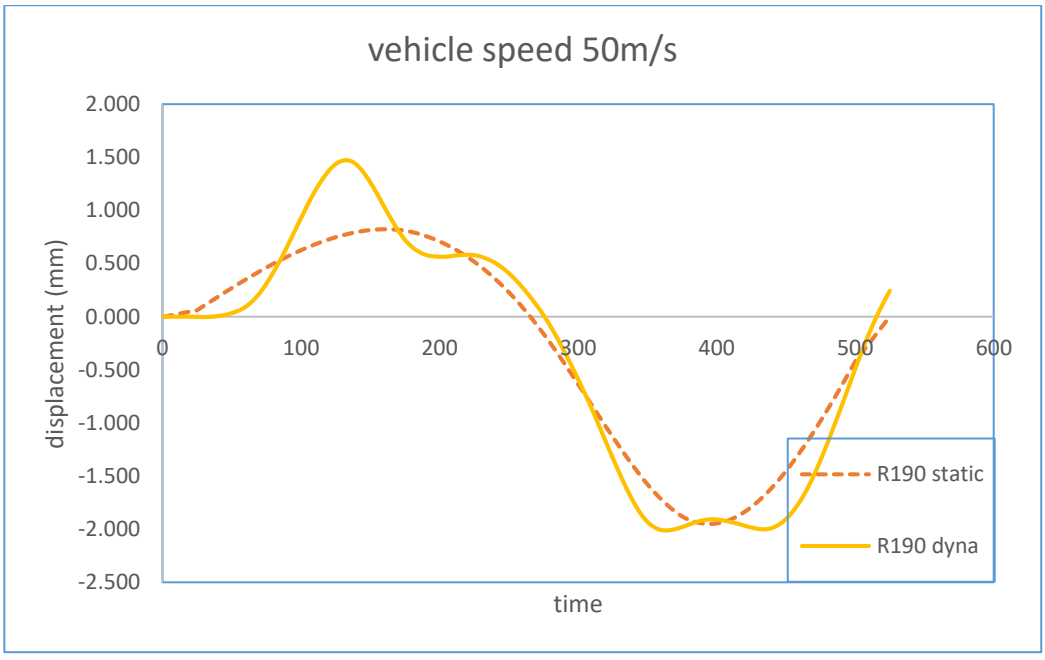

Figure 7-52 Mid-span displacement for 2-span bridge model v=50m/s

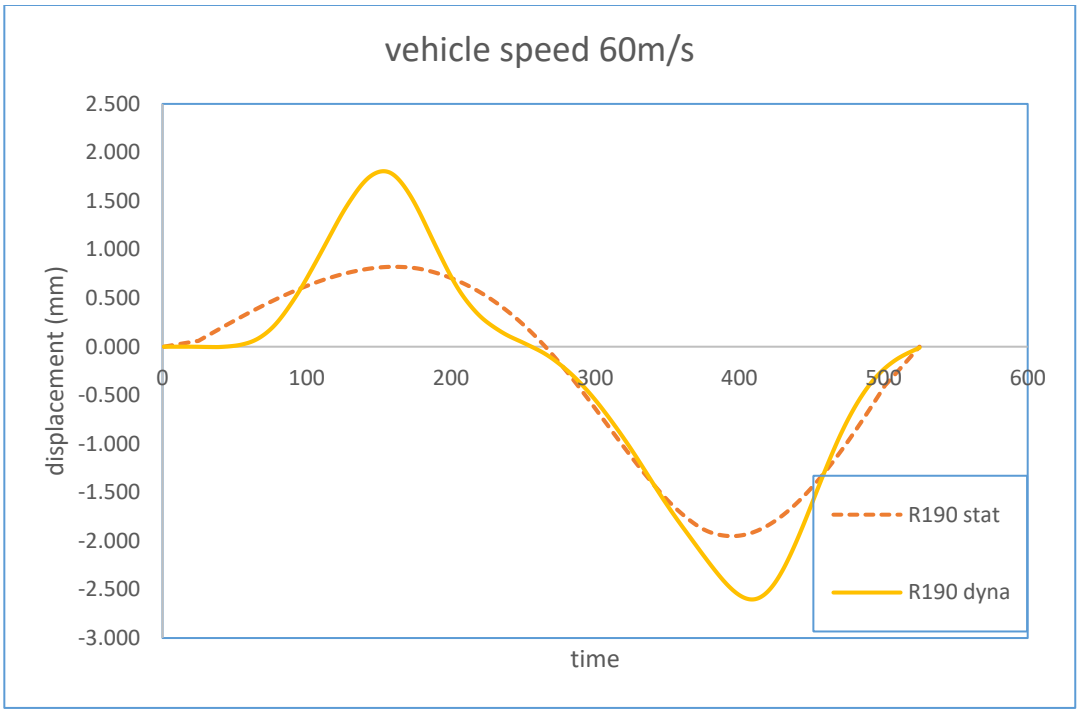

Figure 7-53 Mid-span displacement for 2-span bridge model v=60m/s

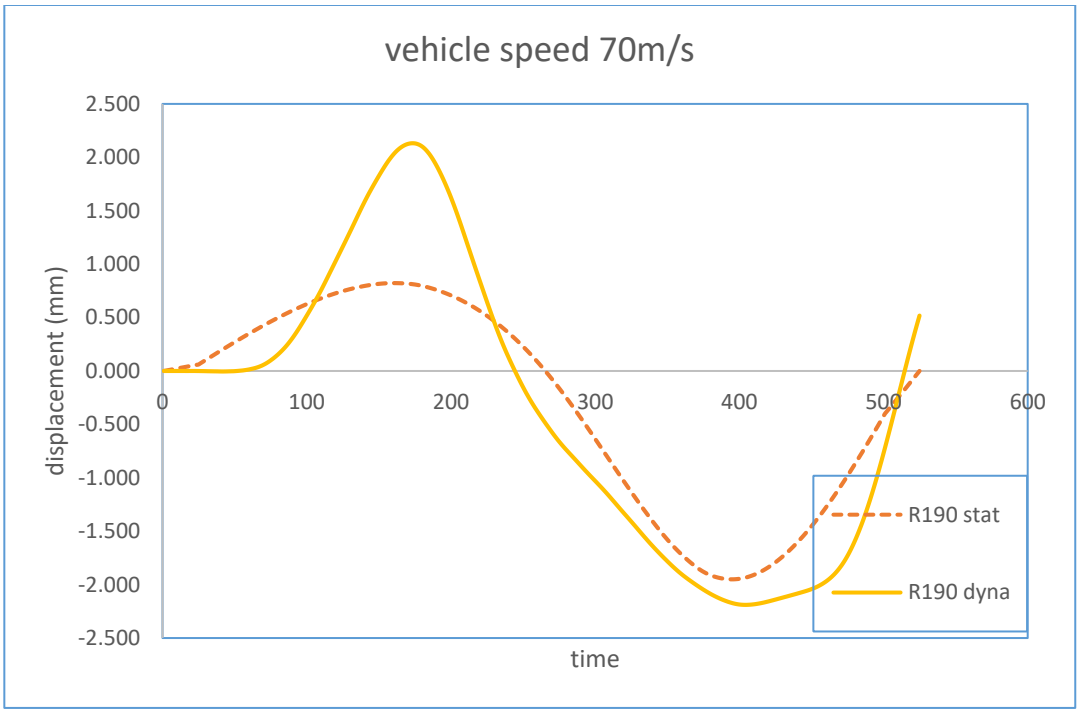

Figure 7-54 Mid-span displacement for 2-span bridge model v=70m/s

7.3 Discussion of Results

The results of the interaction analysis are evaluated by comparing the mid-span dynamic reactions with the static reactions. In the case of curvature radii study, it can be noted that as the radius increase, the bridge displacement, shear and moment reactions tend to become more stable. By evaluating the displacement reactions, it can be further noticed how the dynamic interaction is influenced by the curvature (as demonstrated in figure 7.55). As the radius increase, both static and dynamic displacement responses are lowered, while the differences of dynamic and static reactions also decline and start to stabilize after reaching R=150m (Figure 7.56). The difference (%) in the figure can be defined as:

$$Difference = \frac{d_D - d_S}{d_S} \times 100\% \quad (7.1)$$

Where d_D is the maximum absolute displacement for center span mid-point under dynamic vehicle load, and d_S is the corresponding displacement under the same vehicle static load. Such displacement difference percentage can be also considered as the dynamic amplified factor (impact factor) during vehicle bridge interaction. When radius is larger than 190m, the displacement impact factor stays around 7% to 9%. From curvature radii R=190m to R=50m, the maximum dynamic displacement reaction as well as the displacement dynamic impact factor increase rapidly. For the bridge configuration whose radius is 50m, the impact factor is 19.43%, 2.5 times of the impact factor (7.8%) from the original bridge configuration.

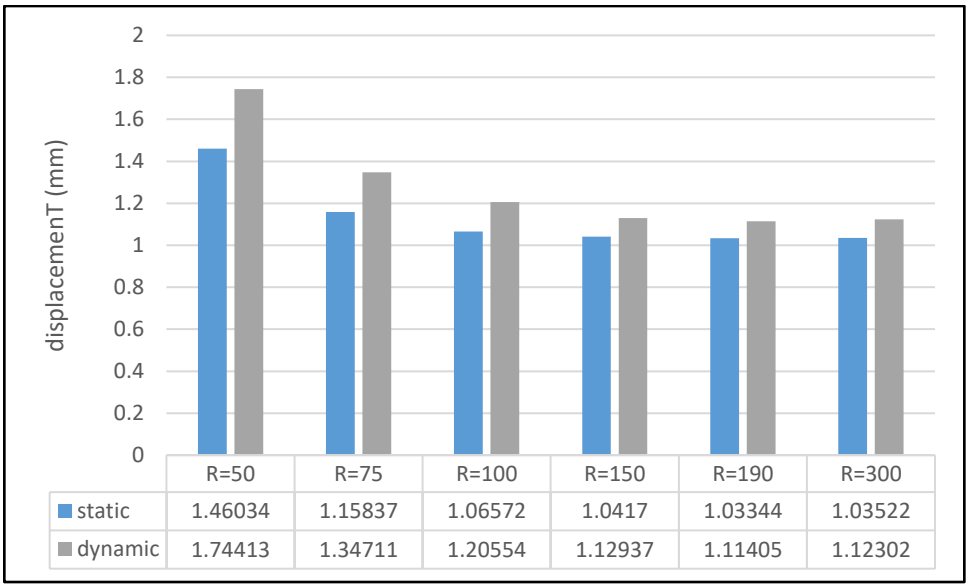

	R=50	R=75	R=100	R=150	R=190	R=300
static	1.46034	1.15837	1.06572	1.0417	1.03344	1.03522
dynamic	1.74413	1.34711	1.20554	1.12937	1.11405	1.12302

Figure 7-55 Displacement reactions with different radii

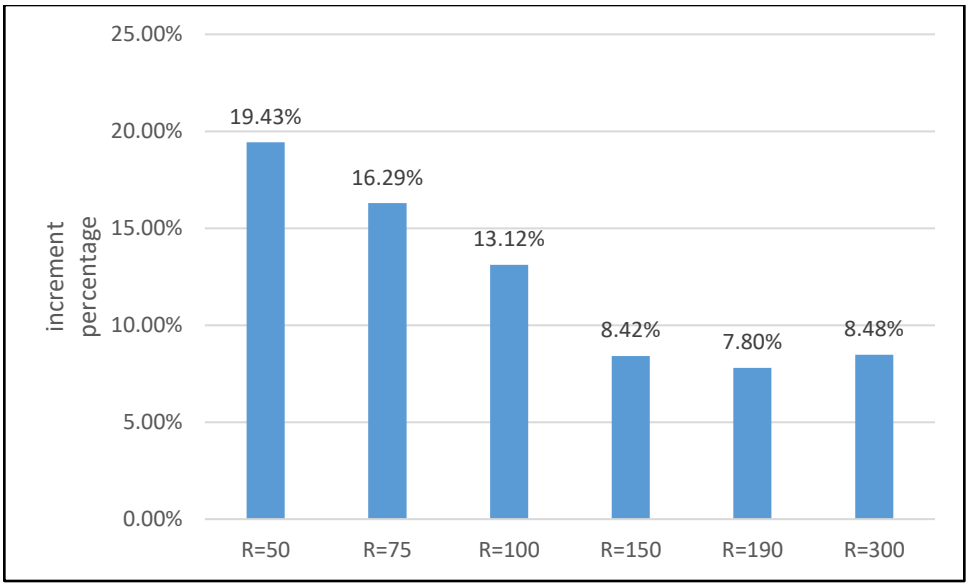

Figure 7-56 Differences of displacement increment

From figures 7.57 to 7.59, the bridge moment response, like the displacement response, has a relatively less influence in cases where the curvature radii is higher. When the radii drop below R=150m, both the positive and negative moment responses start to react dramatically, especially when the radius reach R=50m.

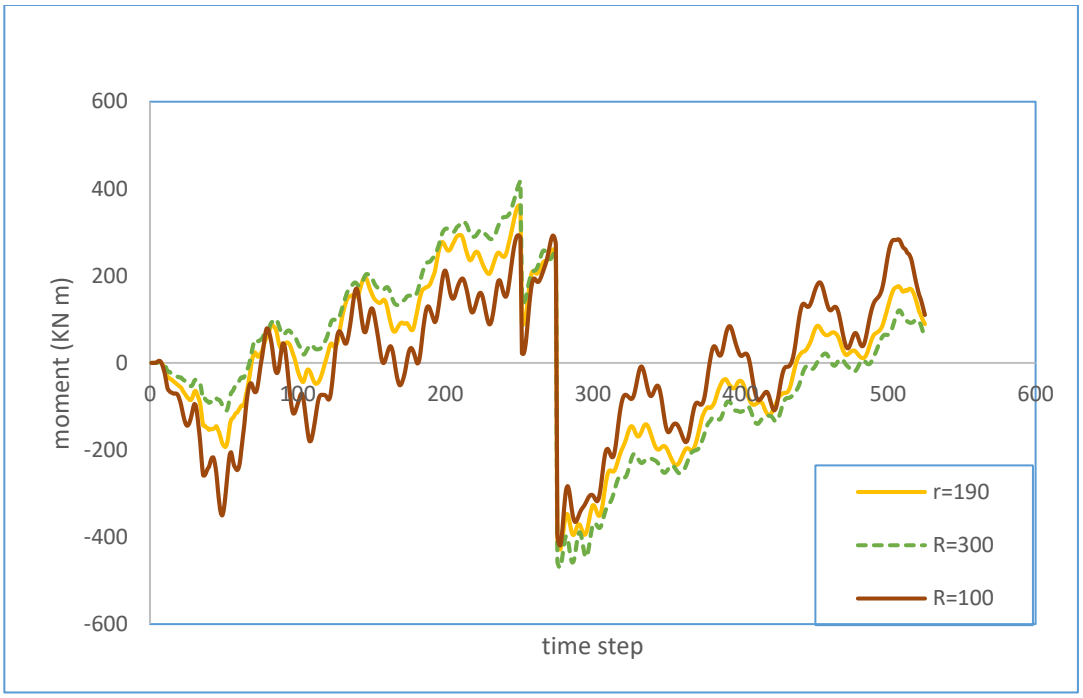

Figure 7-57 mid-span moment comparison under different radii configurations

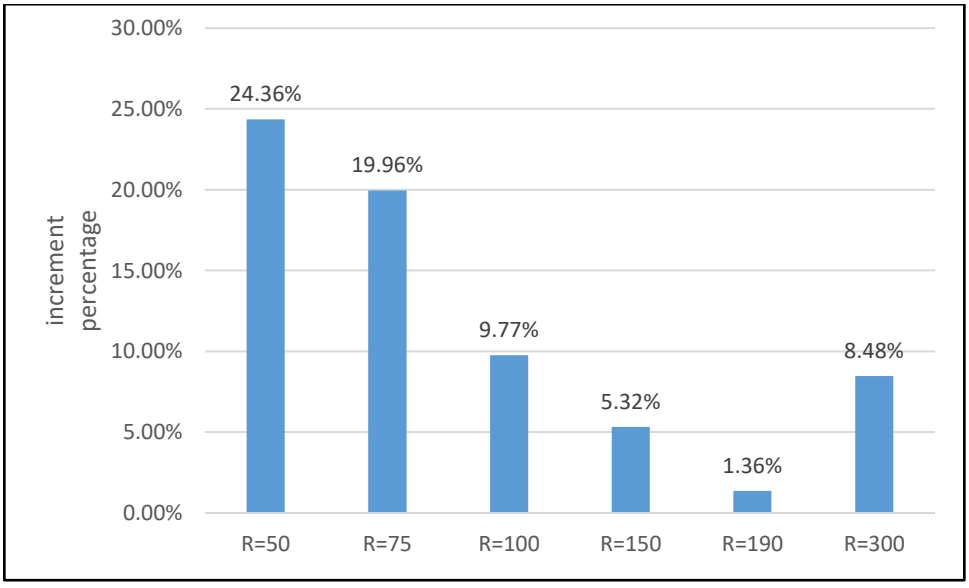

Figure 7-58 negative moment impact factors for different radii configurations

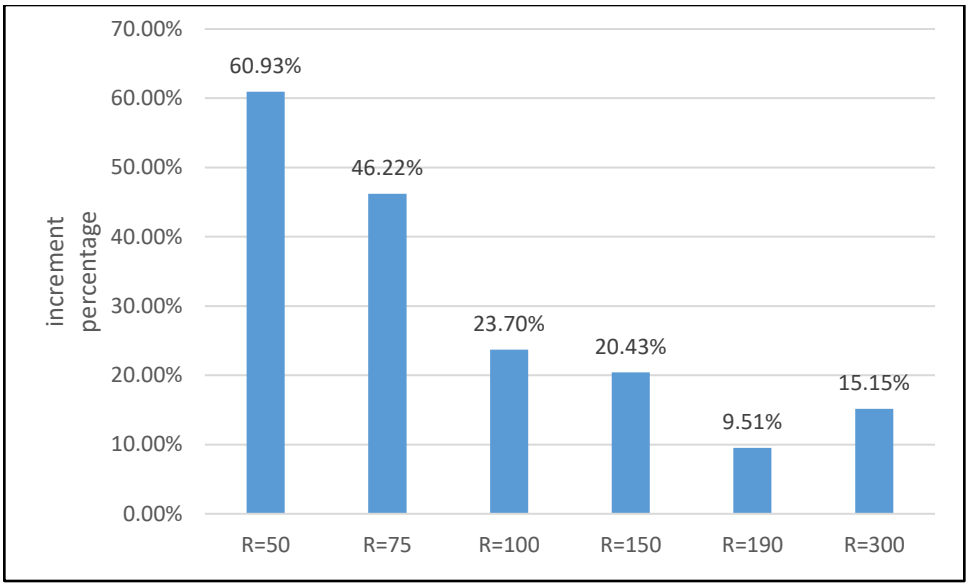

Figure 7-59 positive moment impact factors for different radii configurations

Bridge reactions from three different span length are gathered to study the influence of span length in vehicle bridge interaction. Figures 7.60 to 7.61 show summarize the maximum displacements and displacement impact factors of different configurations. Generally, with the increasing of span length, the bridge flexibility also increased. Bridge starts to increase the capability to absolve dynamic impact and reduce its effect on structure, thereafter has lowered the impact factors. In these parametric study cases, it can be observed that, though the maximum static displacements increase with the span length, dynamic displacements do not have a higher increment rate, which lead to lower impact factor.

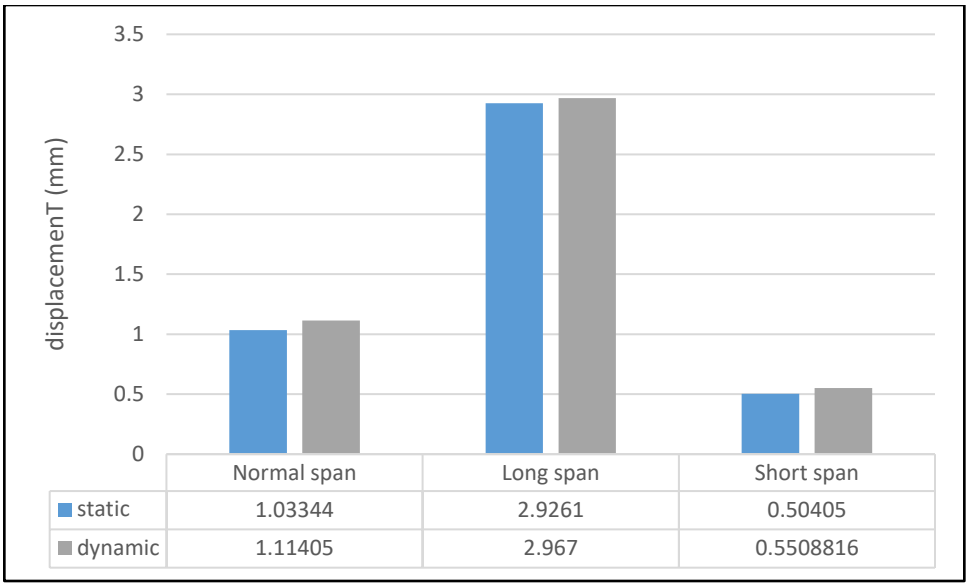

Figure 7-60 mid-span displacement comparison under different span length configurations

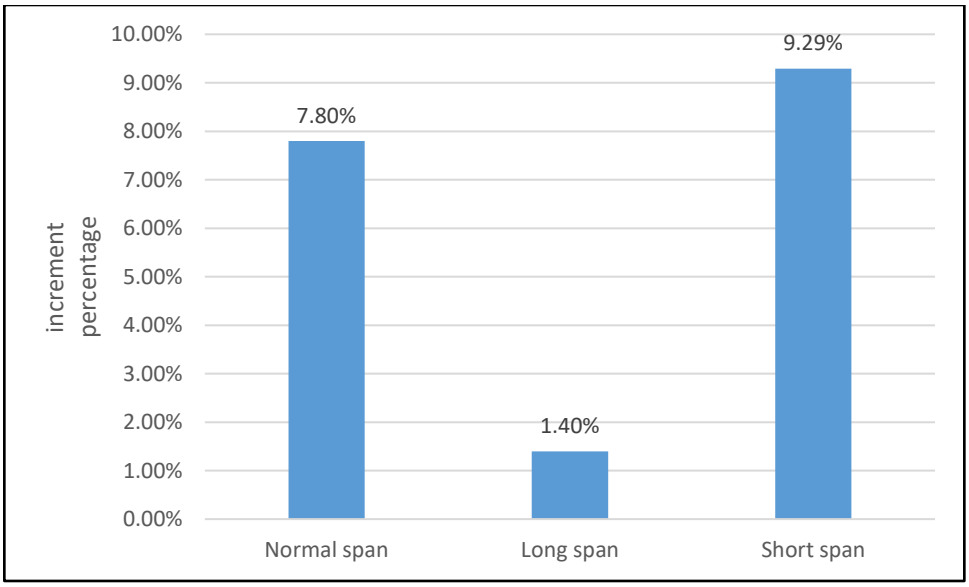

Figure 7-61 displacement increment comparison under different span length configurations

Figure 7.62 summarizes the displacement impact factors of bridge of different deck conditions and exciting vehicle traveling with various speed. Although the initial bridge reaction is rather small (less than 10% under different surfaces), the impact factors start to raise with an alarming speed after vehicle reaching certain travelling speed. When the vehicle speed reach the maximum in this analysis, the impact factor is over 0.6 in all cases, at this point the factor of vehicle travelling speed overshadows other factors such as bridge surface conditions.

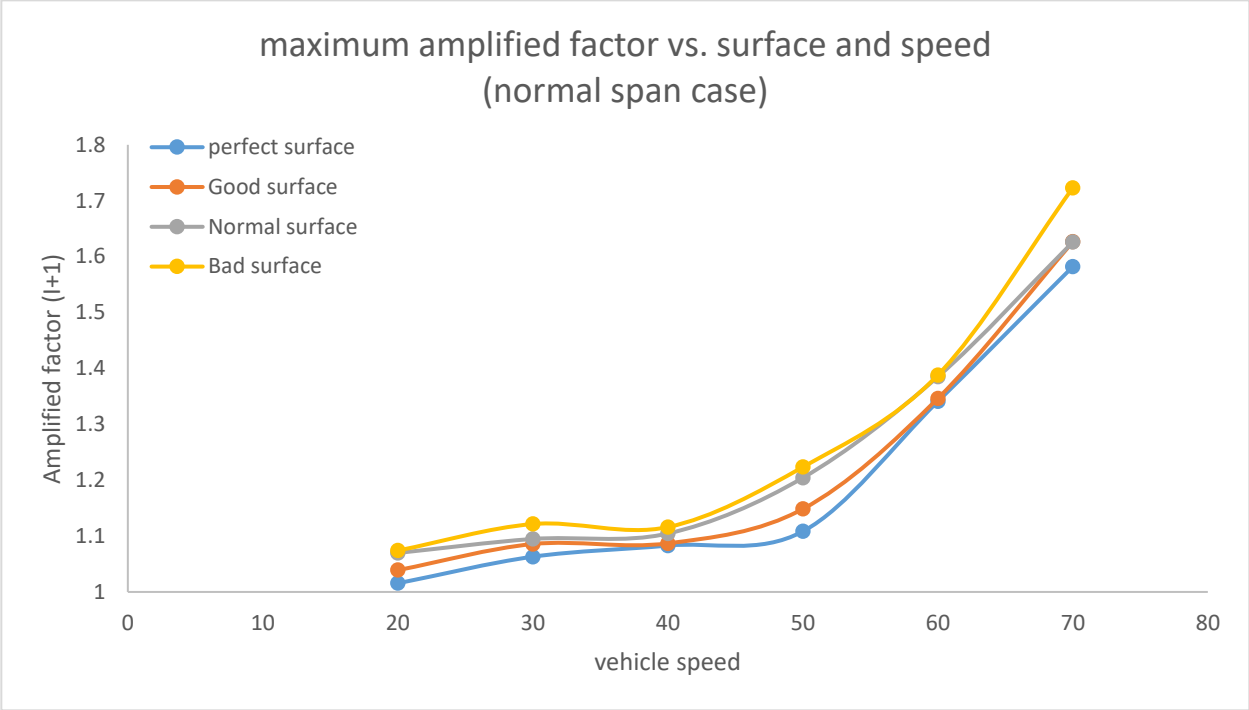

Figure 7-62 Amplified factors vs. surface condition vs. vehicle (Normal span case)

Following Table 7.1 and Figure 7.63 summarize the influence of bridge surface condition to the vehicle bridge interaction analysis. It can be easily observed that with "Perfect" and "Good" surface conditions, the impact factors are below 10% and 20% respectivily. With the deteriating of the bridge surface, the dynamic impact load increases dramatically. When the surface condition reaches "Bad", the impact factor could be as high as 99% even though the vehicle traveling speed is still low. At such case, a near-resonance vibration is probably to happen which leads to a unusually high response. The displacement reaction (Figure 7.12d) shows even after the vehicle pass through the observation point, the bridge vibration does not quickly die out like other cases. This is also an indication of near-resonance vibration occours.

Table 7-1 Impact factors (If) and Amplication factors (1+If) of different surfaces and span configurations

table of impact factor	surface condition			
	Perfect	Good	Normal	Bad
Long span bridge	1.014 1.40%	1.066 6.61%	1.090 9.05%	1.200 19.98%
Normal span bridge	1.078 7.80%	1.108 10.78%	1.525 52.53%	1.994 99.37%
Short span bridge	1.093 9.29%	1.195 19.54%	1.534 53.40%	1.783 78.28%

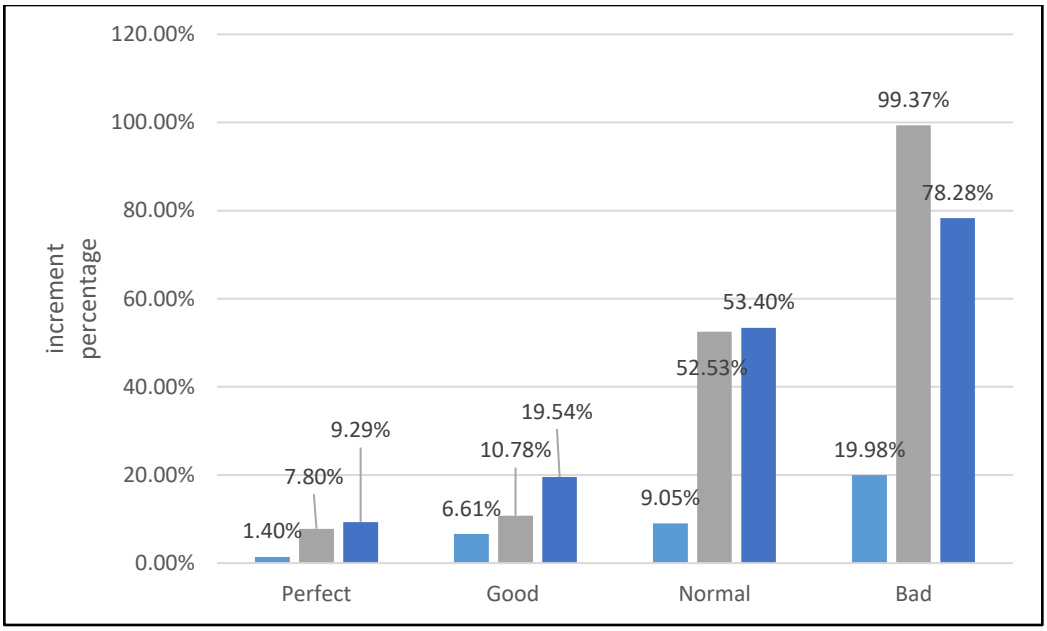

Figure 7-63 Impact factor of different surfaces and span configurations

Additional Figure 7.64 shows in the short span case (3 span total length =120m), the dynamic factor increases with surface conditions and vehicle traveling speed. Although both factors have positive impacts on the vehicle bridge interaction, the surface conditions have influences. As the surface condition deteriorates, the influence of vehicle speed in the dynamic interaction increases

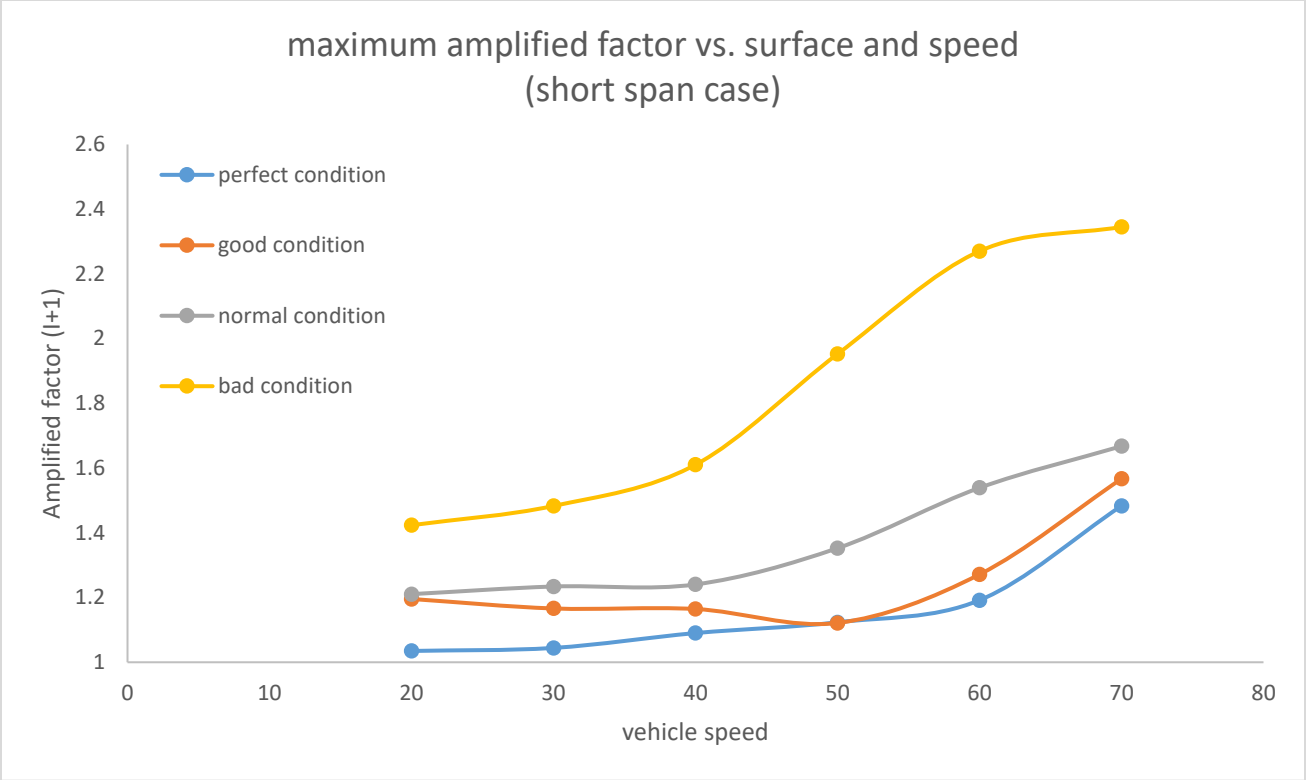

Figure 7-64 Amplified factors vs. surface condition vs. vehicle (Short span case)

A comparison is made in Figure 7.65 for eccentricity influence in vehicle bridge interaction. It can be observed that though generally the outer lane loading leads to higher impact factor. The difference in outer lane impact factor and inner lane impact factor is hardly noticeable compared to other factors such as speed and surface conditions.

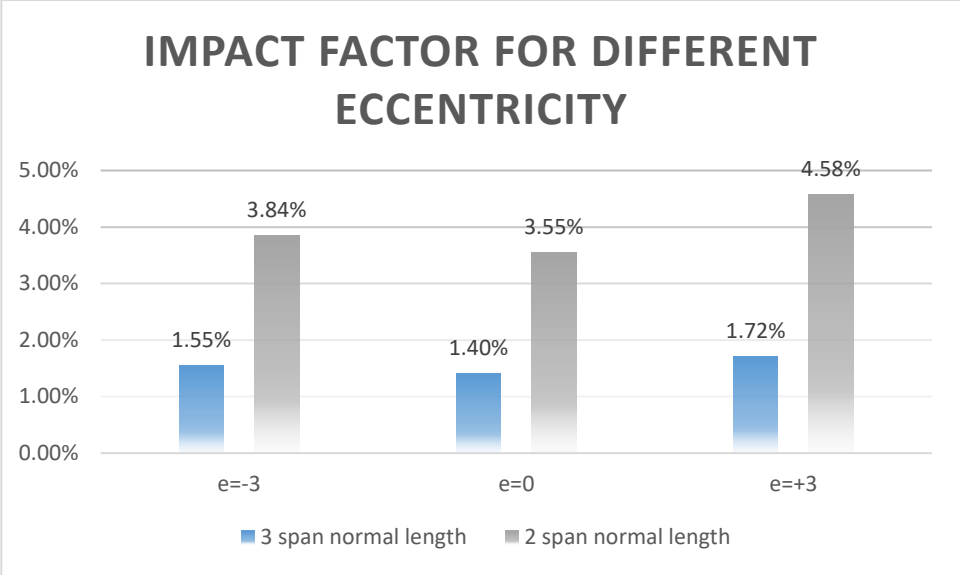

Figure 7-65 Impact factor for different eccentricity

8. Calculation of Impact Factor

8.1 Calculation based on bridge natural frequency

From previous parametric study, the dynamic interaction usually leads to higher dynamic load than static loading. Factors such as the surface conditions can have a decisive and random influence on the dynamic interaction analysis. The location of maximum dynamic reaction can occur at various points and different static reaction locations. Therefore, in this study, the maximum displacement during the interaction period is selected for the impact factor calculation. The empirical formula for impact factor is categorized by the bridge surface conditions and bridge speed limits. The bridge material and geometric property can be simplified as the bridge first flexural frequency in the empirical formula. The frequencies of the parametric study are summarized in Table 8.1.

Table 8-1 First flexural frequencies of parametric bridge cases.

bridge configuration		Radius R 300	R 250	R 190	R 150	R 100	R50
3 Span	120m length	3.614	3.603	3.5828	3.512	3.456	3.13466
	175m length	1.88	1.8644	1.8478	1.8037	1.741	1.39123
	235m length	0.8268	0.8251	0.825	0.8226	0.82	1.0047
2 Span	100m length	2.4889	2.454	2.369	2.253	2.198	2.04915
	150m length	1.8786	1.806	1.7038	1.621	1.5523	1.5047
	190m length	1.16835	1.1564	1.256	1.0062	1.0011	0.92867

Figures 8.1 to 8.12 collect the impact factors for different case scenarios and show the impact factor tendency line. To better cover the different demands for dynamic load allowance, three different categories are set in this study.

A. Design criteria (perfect surface) for low speed limit bridge (V=20m/s, 45mph),
B. Design criteria (perfect surface) for high speed limit bridge (V=30m/s, 65mph)
C. Service criteria (good surface condition) for low speed limit bridge (V=20m/s, 45mph).

The formula is based on the bridge configurations from the previous parametric study cases. The cases include two and three span bridges with total spans ranging from 120m to 235m, radii ranging from 50m to 300m. The impact factor in this formula describe the center span maximum displacement, moment, torsion and shear dynamic reactions.

The displacement impact factor (I) can be expressed by the bridge frequency (ν) as follows:

a. For low speed limit bridge design

$$I = \begin{cases} 0.05 + 0.113\nu & (0.5 \leq \nu \leq 1.5) \\ 0.22 & (1.5 < \nu \leq 4) \end{cases} \tag{8.1}$$

b. For high speed limit bridge design

$$I = \begin{cases} 0.05 + 0.12\nu & (0.5 \leq \nu \leq 1.5) \\ 0.23 & (1.5 < \nu \leq 4) \end{cases} \tag{8.2}$$

c. For low speed limit bridge service

$$I = \begin{cases} 0.05 + 0.133\nu & (0.5 \leq \nu \leq 1.5) \\ 0.25 & (1.5 < \nu \leq 4) \end{cases} \tag{8.3}$$

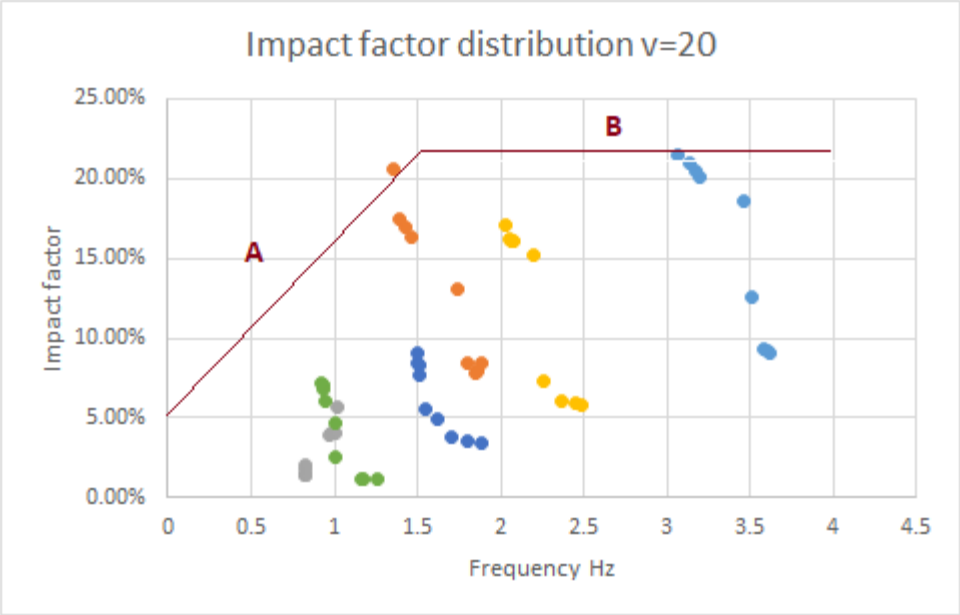

Figure 8-1 Displacement impact factor versus bridge frequency (v=20m/s) for perfect roughness

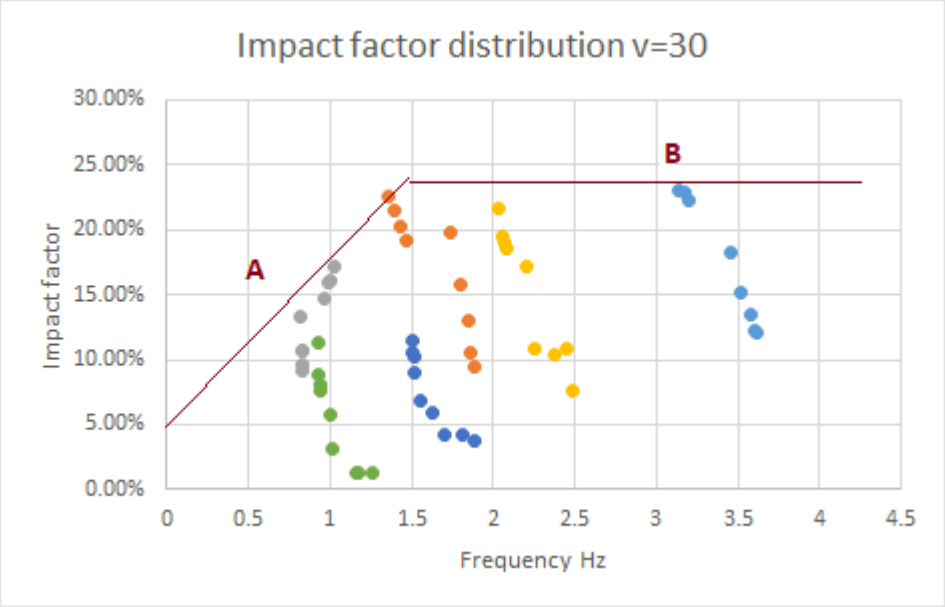

Figure 8-2 Displacement impact factor versus bridge frequency (v=30m/s) for perfect roughness

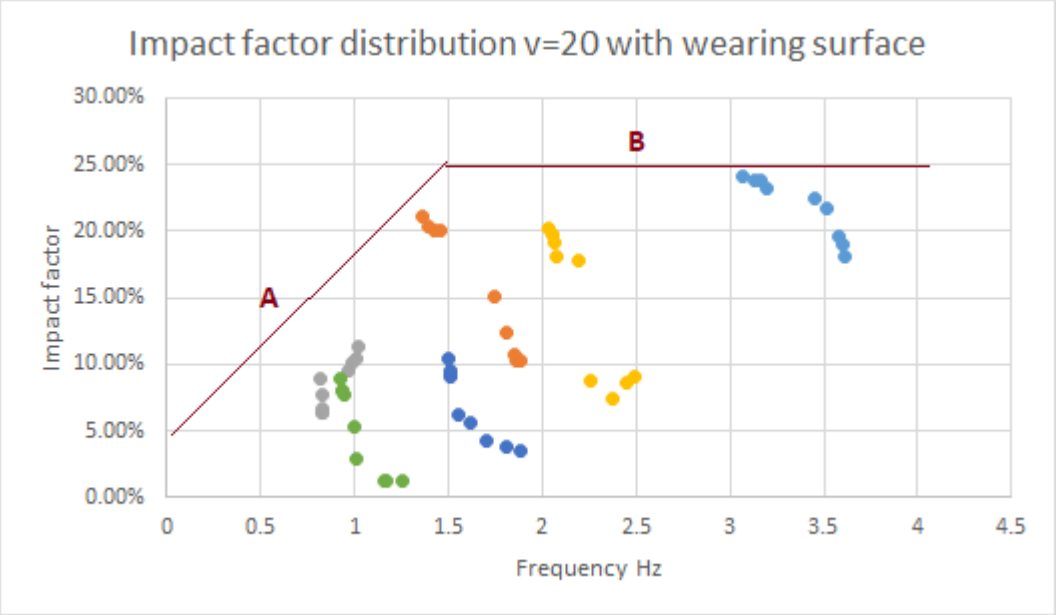

Figure 8-3 Displacement impact factor versus bridge frequency (v=20m/s) for wearing deck

The moment impact factor (I) can be expressed by the bridge frequency (ν) as follows:

a. For low speed limit bridge design

$$I = \begin{cases} 0.025 + 0.11\nu & (0.5 \le \nu \le 1.5) \\ 0.19 & (1.5 < \nu \le 4) \end{cases} \tag{8.4}$$

b. For high speed limit bridge design

$$I = \begin{cases} 0.05 + 0.123\nu & (0.5 \le \nu \le 1.5) \\ 0.21 & (1.5 < \nu \le 4) \end{cases} \tag{8.5}$$

c. For low speed limit bridge service

$$I = \begin{cases} 0.05 + 0.117\nu & (0.5 \le \nu \le 1.5) \\ 0.225 & (1.5 < \nu \le 4) \end{cases} \tag{8.6}$$

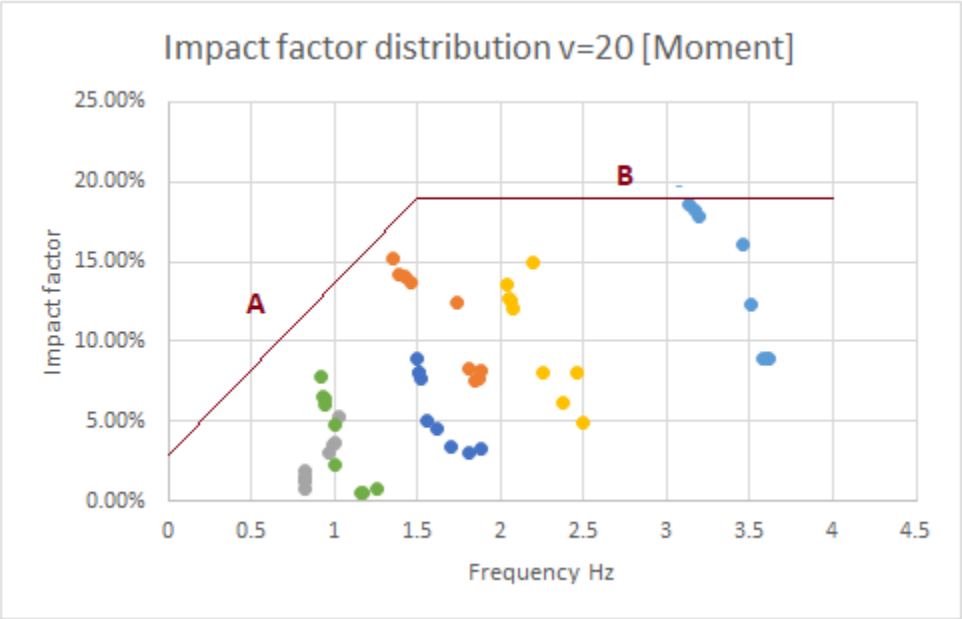

Figure 8-4 Moment impact factor versus frequency (v=20m/s) for perfect roughness

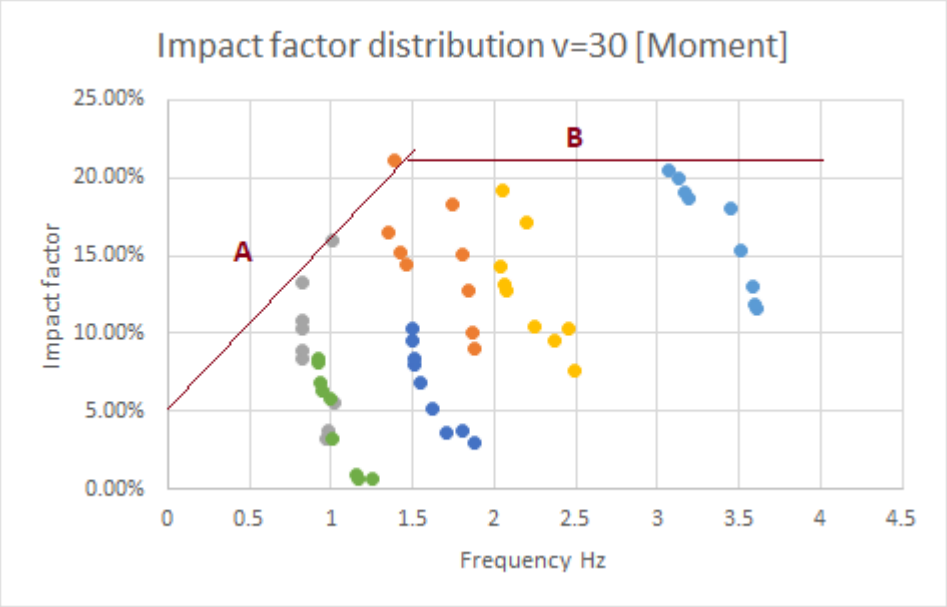

Figure 8-5 Moment Impact factor versus bridge frequency (v=30m/s) for perfect roughness

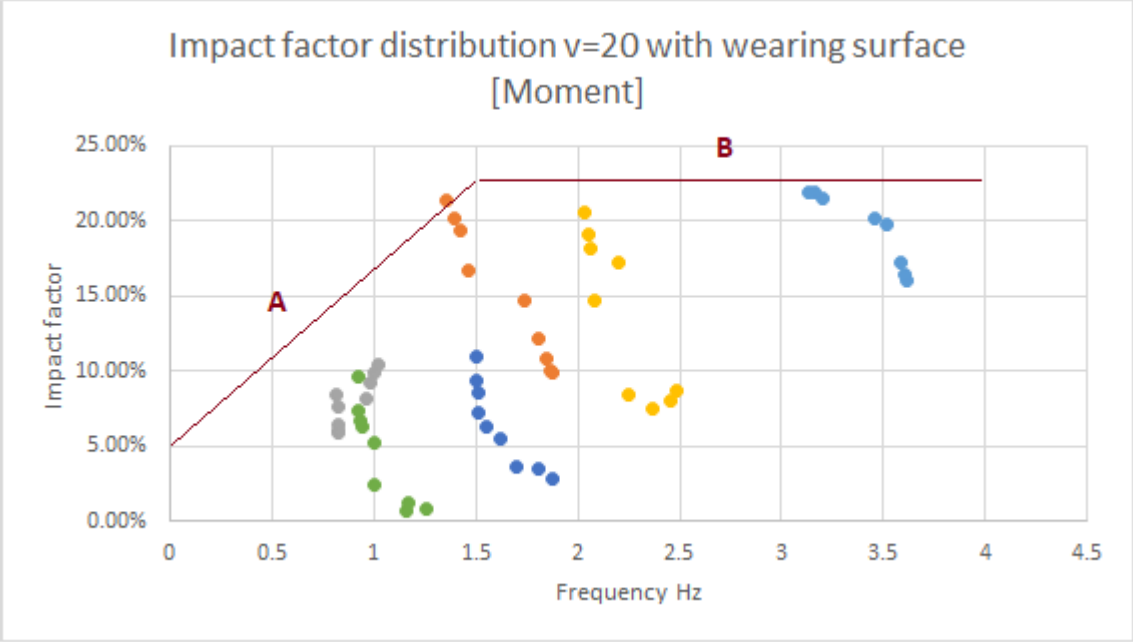

Figure 8-6 Impact factor versus bridge frequency (v=20m/s) for wearing deck

The torsional impact factor (I) can be expressed by the bridge frequency (ν) as follows:

a. For low speed limit bridge design

$$I = \begin{cases} 0.025 + 0.117\nu & (0.5 \le \nu \le 1.5) \\ 0.20 & (1.5 < \nu \le 4) \end{cases} \quad (8.7)$$

b. For high speed limit bridge design

$$I = \begin{cases} 0.025 + 0.147\nu & (0.5 \le \nu \le 1.5) \\ 0.245 & (1.5 < \nu \le 4) \end{cases} \quad (8.8)$$

c. For low speed limit bridge service

$$I = \begin{cases} 0.168\nu & (0.5 \leq \nu \leq 1.25) \\ 0.21 & (1.25 < \nu \leq 4) \end{cases} \tag{8.9}$$

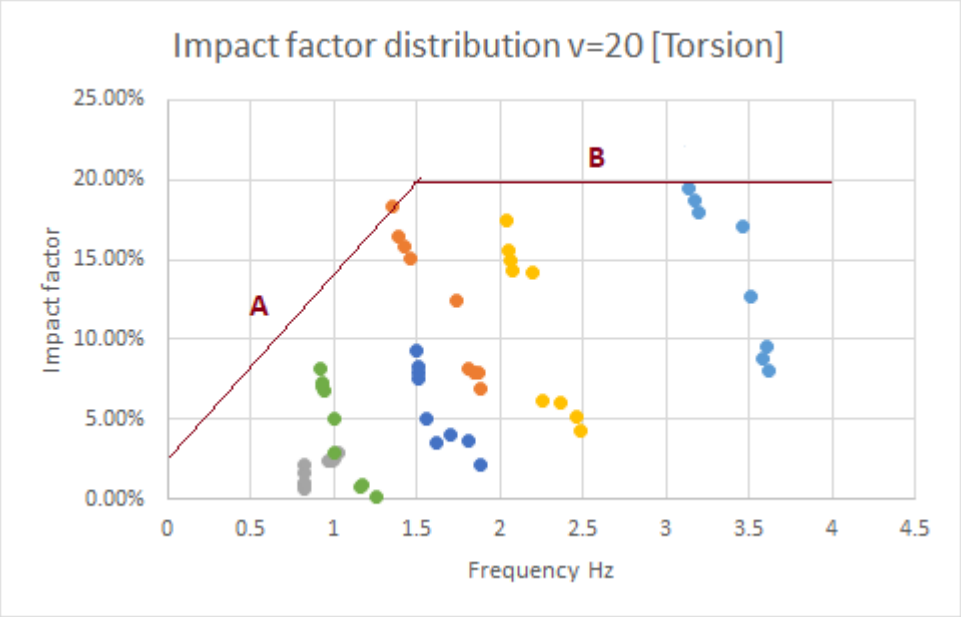

Figure 8-7 Torsional impact factor versus frequency (v=20m/s) for perfect roughness

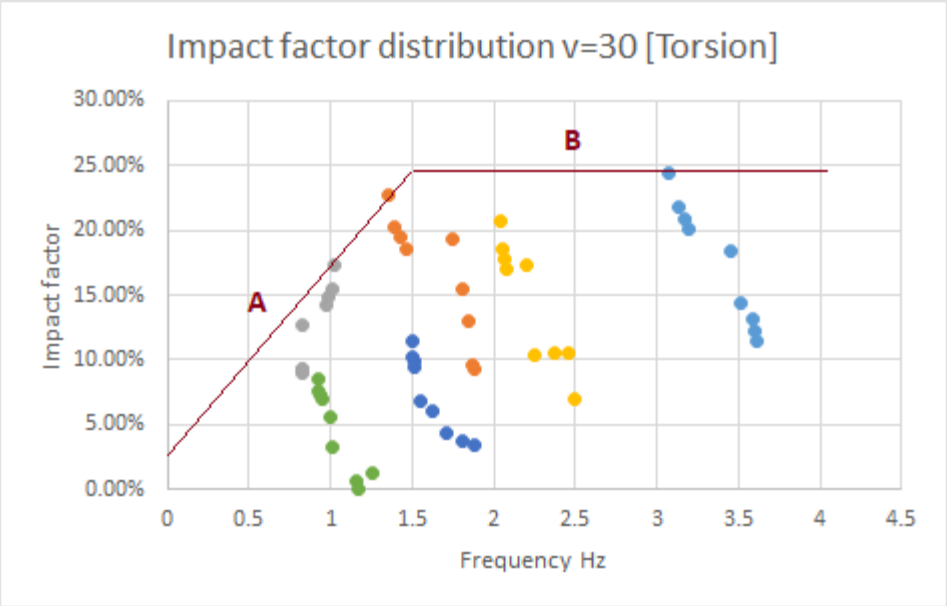

Figure 8-8 Torsional impact factor versus frequency (v=30m/s) for perfect roughness

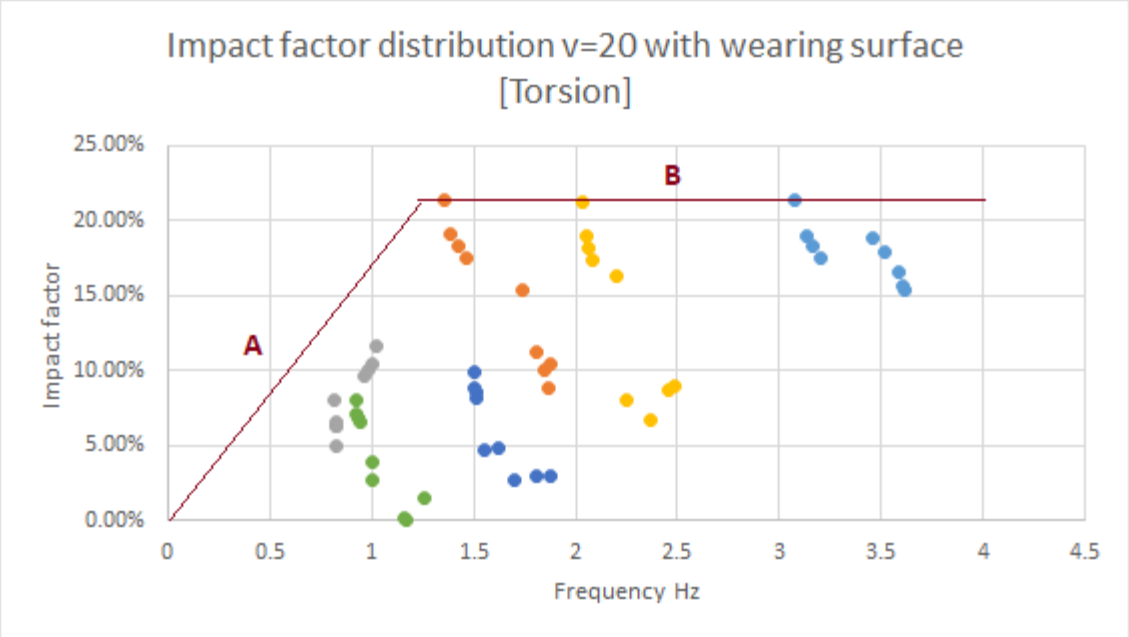

Figure 8-9 Torsional impact factor versus bridge frequency (v=20m/s) for wearing deck

The shear impact factor (I) can be expressed by the bridge frequency (ν) as follows:

d. For low speed limit bridge design

$$I = 0.155 \quad (0.5 \leq \nu \leq 4) \tag{8.10}$$

e. For high speed limit bridge design

$$I = 0.2 \quad (0.5 \leq \nu \leq 4) \tag{8.11}$$

f. For low speed limit bridge service

$$I = 0.22 \quad (0.5 \leq \nu \leq 4) \tag{8.12}$$

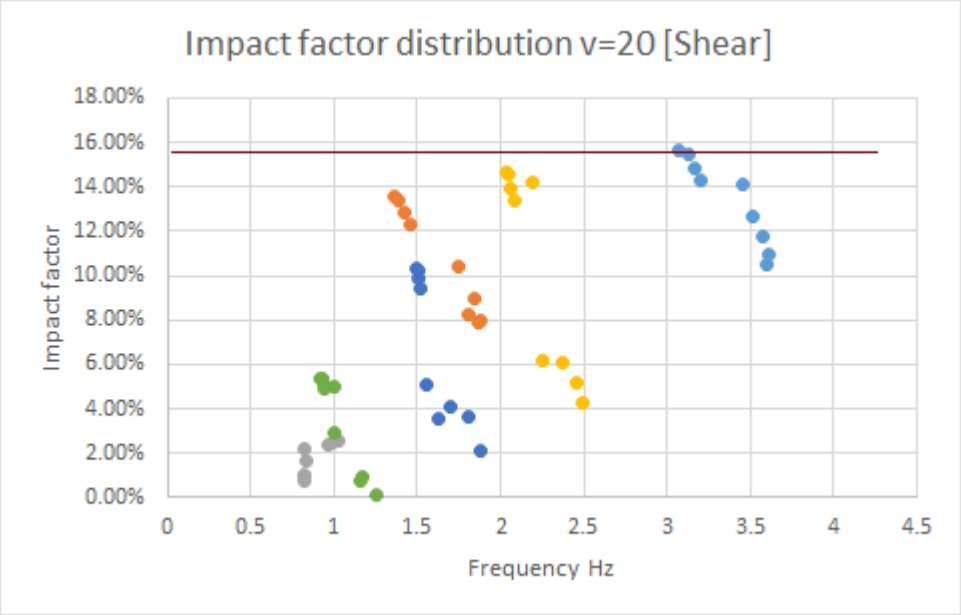

Figure 8-10 Shear impact factor versus frequency (v=20m/s) for perfect roughness

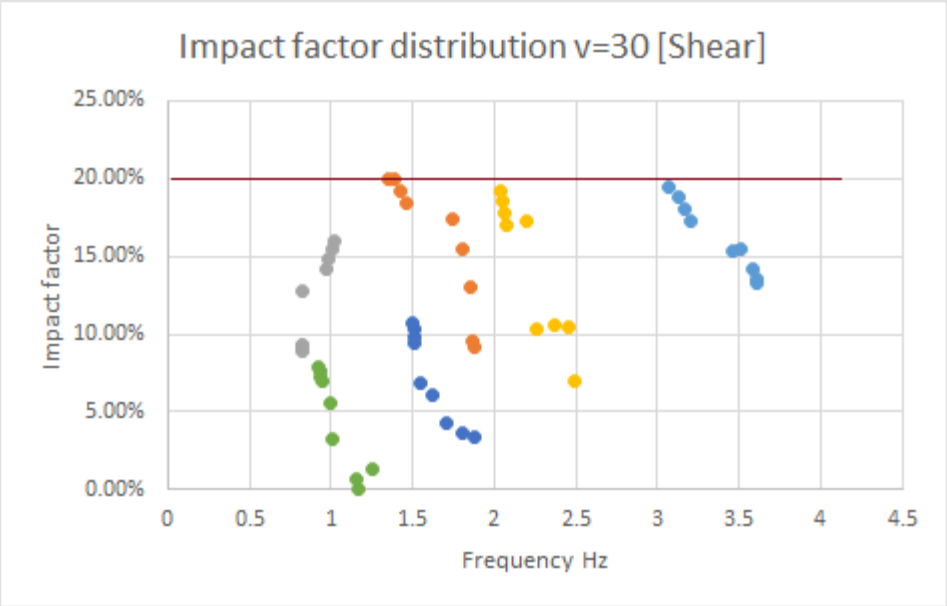

Figure 8-11 Shear impact factor versus frequency (v=30m/s) for perfect roughness

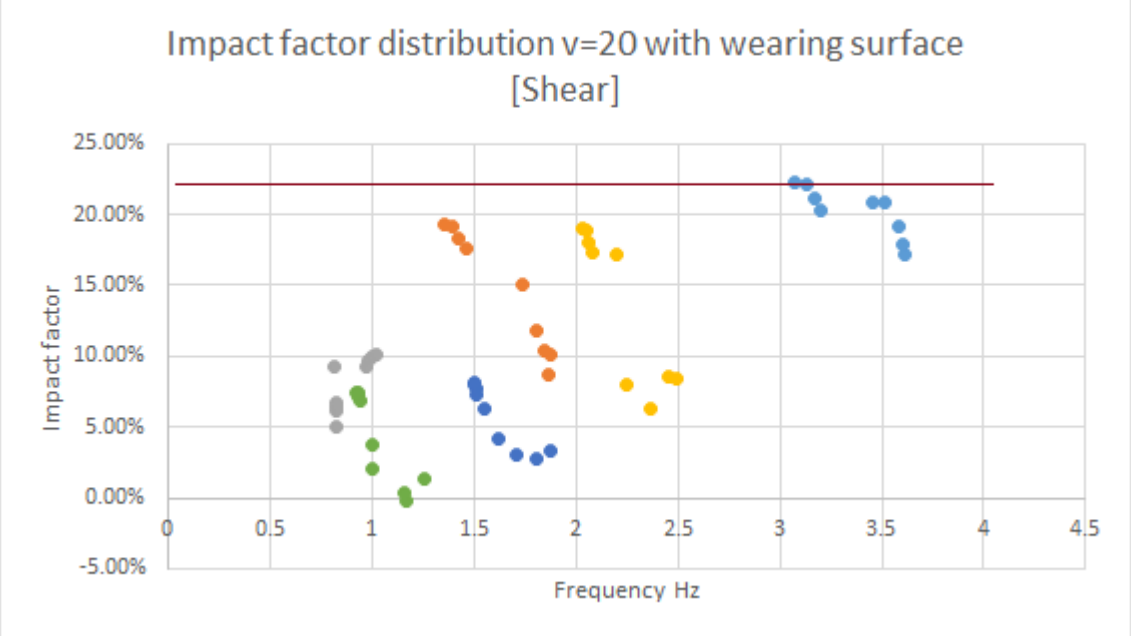

Figure 8-12 Shear impact factor versus bridge frequency (v=20m/s) for wearing deck

The empirical formulas generated above are a simplified method to calculate dynamic impact factors based on the bridge parametric study cases. Therefore, this formula should only apply to bridges with similar configurations and highway design parameters. Other empirical formulas are required for other types of bridges.

By comparing the different impact factor equations, it can be observed that displacement impact factor trend to be the highest among these dynamic factors. A comparison of different determining methods of displacement impact factor is summarized in Figure 8.13. The AASHTO LRFD Bridge Design specification 2017 consider most of the bridge components has a constant dynamic impact factor of 0.33 and 0.15 regardless of bridge configurations. While Canadian codes OHDBC 1982 and CHBDC 2000 both show similar impact factor develop trend as the current research, the impact factors increase as the bridge flexural frequency increase. All three impact factor determining methods have their fix maximum points for the impact factor. However, as the current study shows, the impact factor is heavily influenced by the bridge surface condition. As the bridge deck starts wearing off during the service period, the impact factor will rise rapidly and most likely grow beyond the limits set by AASHTO and OHDBC codes.

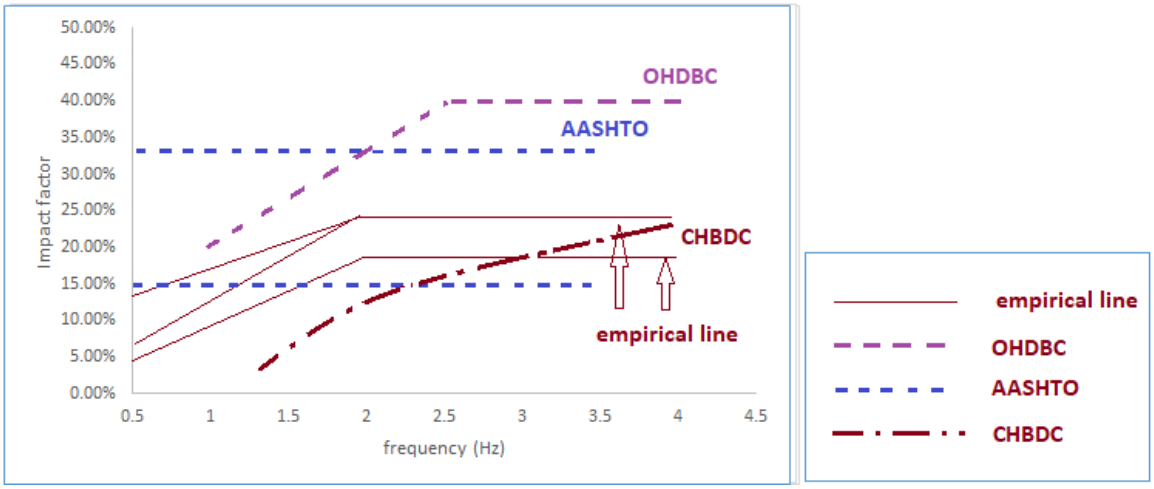

Figure 8-13 Comparison of different methods of determining impact factors

8.2 Calculation based on bridge central angle

There are multiple factors that affect the dynamic interaction in curved bridge. Another well accepted way to represent curved bridge property is to introduce curvature central angle (ϕ=L/R) in the formula. Similar to previous formula, this empirical formula for impact factor is categorized by bridge surface conditions and bridge speed limits. The bridge material and geometric property can be simplified as the bridge central angle in

the empirical formula. The central angles of the parametric study are summarized in the Table 8.2.

Table 8-2 Central angles of parametric bridge cases.

bridge configuration		Radius								
		R 300	R 250	R 190	R 150	R 100	R60	R55	R50	R40
3 Span	120m length	0.400	0.480	0.632	0.800	1.200	2.000	2.182	2.400	3.000
	175m length	0.583	0.700	0.921	1.167	1.750	2.917	3.182	3.500	4.375
	235m length	0.783	0.940	1.237	1.567	2.350	3.917	4.273	4.700	5.875
2 Span	100m length	0.333	0.400	0.526	0.667	1.000	1.667	1.818	2.000	2.500
	150m length	0.500	0.600	0.789	1.000	1.500	2.500	2.727	3.000	3.750
	190m length	0.633	0.760	1.000	1.267	1.900	3.167	3.455	3.800	4.750

Figures 8.14 to 8.25 collect the impact factors for different case scenarios and show the impact factor tendency lines. Same three different categories are set in study.

a. Design criteria (perfect surface) for low speed limit bridge (V=20m/s, 45mph),
b. Design criteria (perfect surface) for high speed limit bridge (V=30m/s, 65mph)
c. Service criteria (good surface condition) for low speed limit bridge (V=20m/s, 45mph).

The formula is based on bridge configurations from the previous parametric study cases. The cases include two and three span bridges with total spans ranging from 120m to 235m, radii ranging from 40m to 300m. The impact factors in this formula describe the center span maximum displacement dynamic reaction.

The displacement impact factor (I) can be expressed by the central angle (ϕ) as follows:

a. For low speed limit bridge design

$$I = \begin{cases} 0.05 + 0.136\phi & (0 \le \phi \le 1.25) \\ 0.22 & (1.25 < \phi \le 4.5) \end{cases} \quad (8.13)$$

b. For high speed limit bridge design

$$I = \begin{cases} 0.10 + 0.0867\phi & (0 \le \phi \le 1.5) \\ 0.23 & (1.5 < \phi \le 4.5) \end{cases} \quad (8.14)$$

c. For low speed limit bridge service

$$I = \begin{cases} 0.15 + 0.10\phi & (0 \le \phi \le 1.0) \\ 0.25 & (1.0 < \phi \le 4.5) \end{cases} \quad (8.15)$$

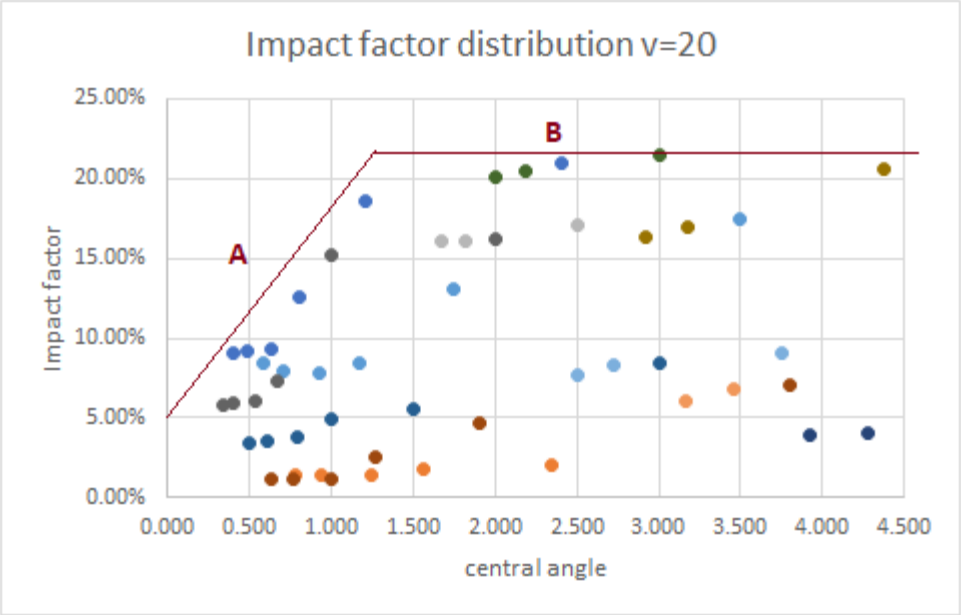

Figure 8-14 Displacement Impact factor versus bridge central angle (v=20m/s) for perfect roughness

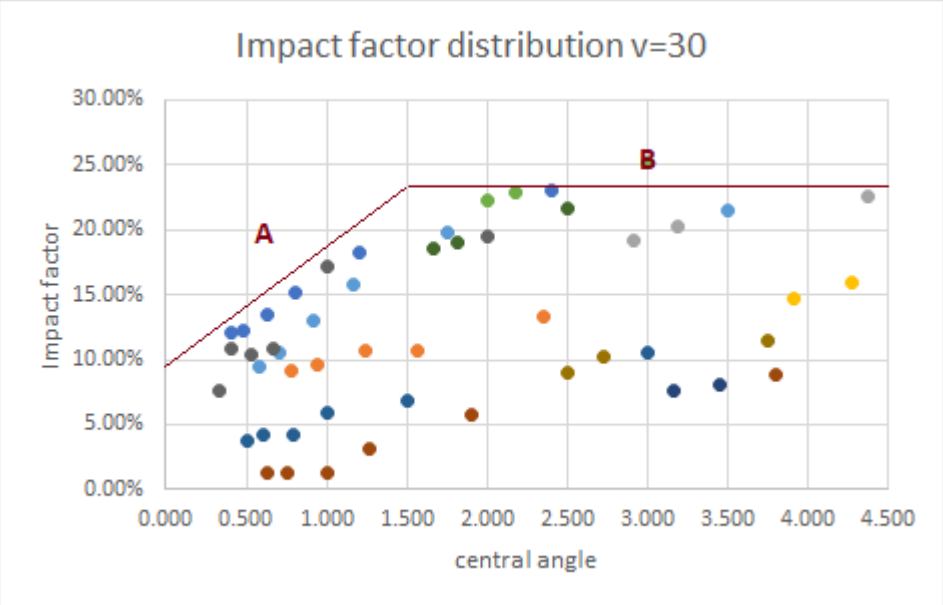

Figure 8-15 Displacement Impact factor versus bridge central angle (v=30m/s) for perfect roughness

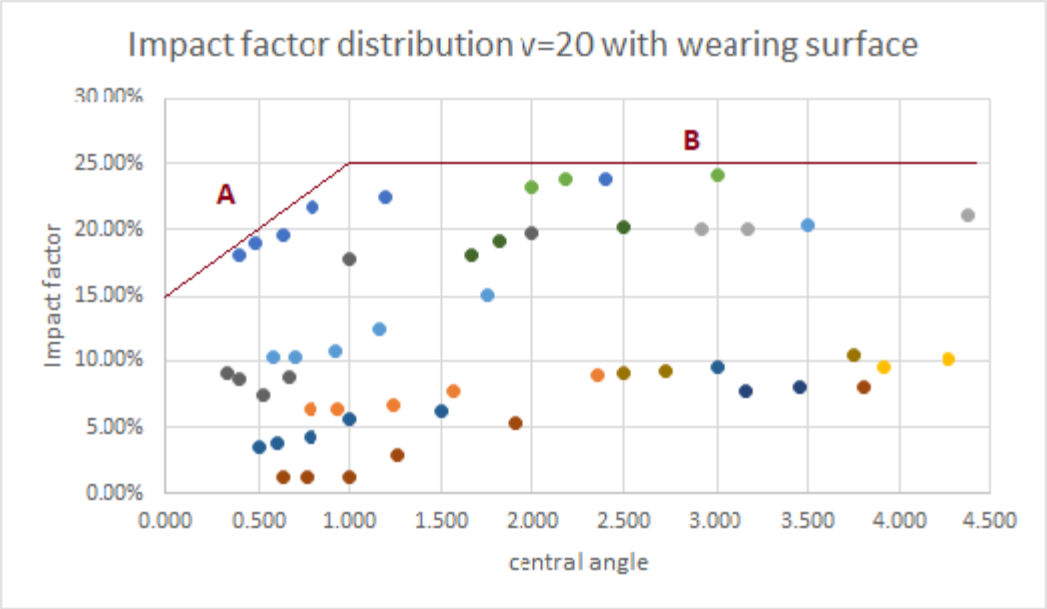

Figure 8-16 Displacement Impact factor versus bridge frequency (v=20m/s) for wearing deck

The moment impact factor (I) can be expressed by the central angle (ϕ) as follows:

a. For low speed limit bridge design

$$I = \begin{cases} 0.07 + 0.096\phi & (0 \le \phi \le 1.25) \\ 0.19 & (1.25 < \phi \le 4.5) \end{cases} \tag{8.16}$$

b. For high speed limit bridge design

$$I = \begin{cases} 0.09 + 0.08\phi & (0 \le \phi \le 1.5) \\ 0.21 & (1.5 < \phi \le 4.5) \end{cases} \tag{8.17}$$

c. For low speed limit bridge service

$$I = \begin{cases} 0.15 + 0.075\phi & (0 \le \phi \le 1.0) \\ 0.225 & (1.0 < \phi \le 4.5) \end{cases} \tag{8.18}$$

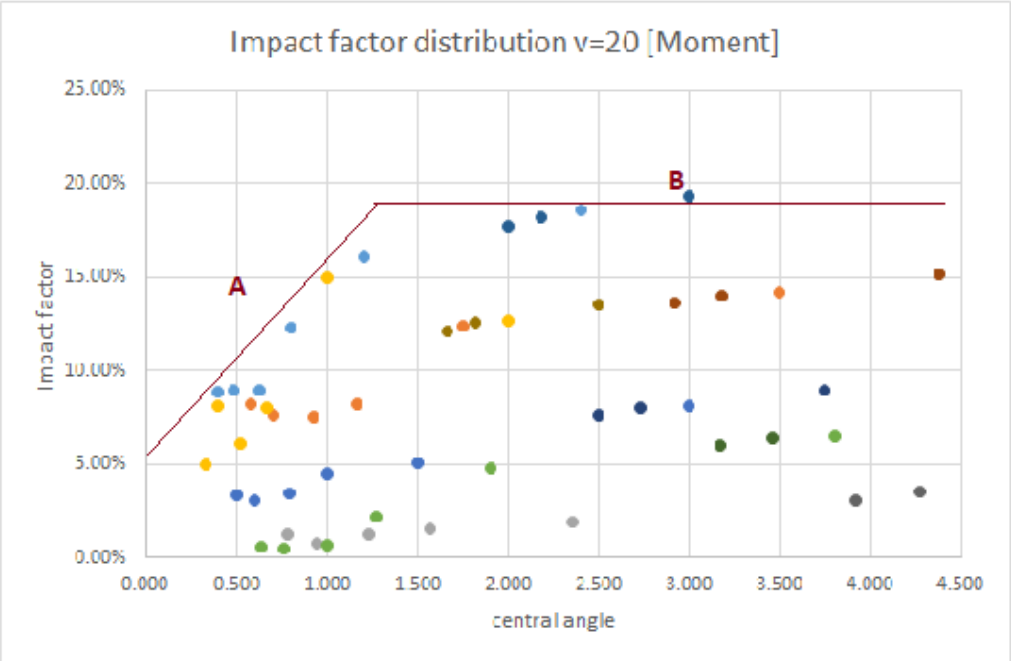

Figure 8-17 Moment impact factor versus bridge central angle (v=20m/s) for perfect roughness

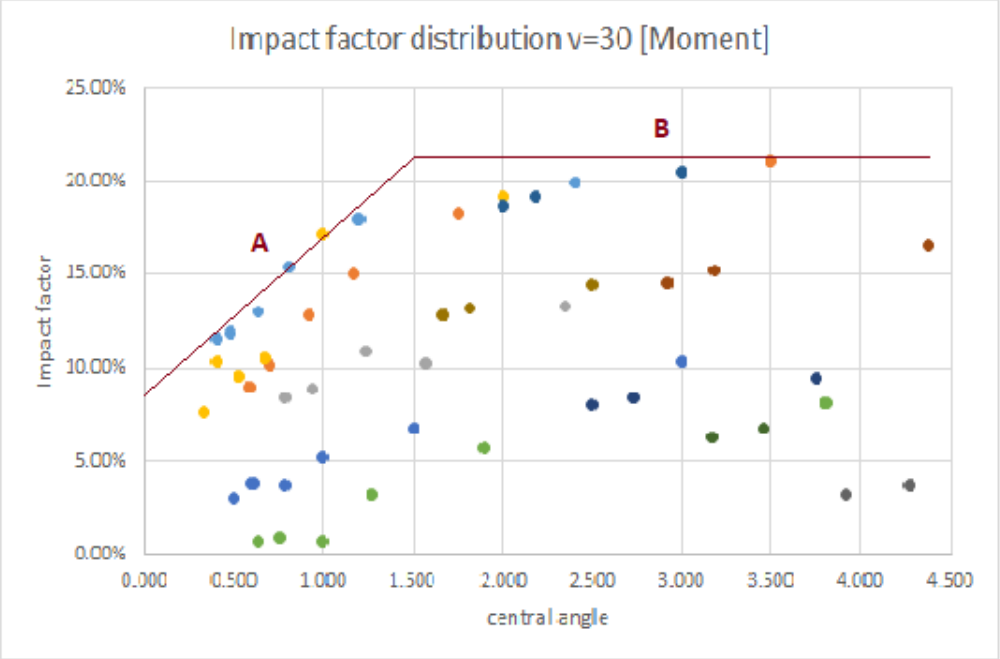

Figure 8-18 Moment impact factor versus bridge central angle (v=30m/s) for perfect roughness

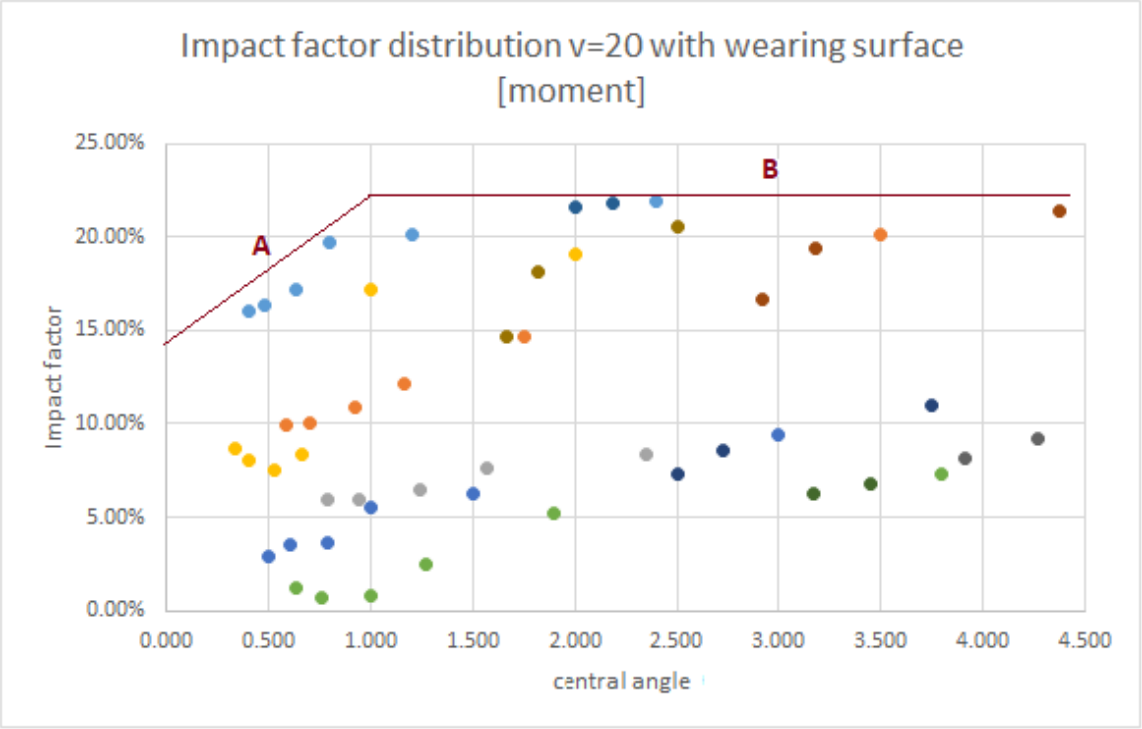

Figure 8-19 Moment impact factor versus bridge central angle (v=20m/s) for wearing deck

The torsional impact factor (I) can be expressed by the central angle (ϕ) as follows:

a. For low speed limit bridge design

$$I = \begin{cases} 0.05 + 0.12\phi & (0 \le \phi \le 1.25) \\ 0.20 & (1.25 < \phi \le 4.5) \end{cases} \tag{8.19}$$

b. For high speed limit bridge design

$$I = \begin{cases} 0.09 + 0.1033\phi & (0 \le \phi \le 1.5) \\ 0.245 & (1.5 < \phi \le 4.5) \end{cases} \tag{8.20}$$

c. For low speed limit bridge service

$$I = \begin{cases} 0.13 + 0.08\phi & (0 \le \phi \le 1.0) \\ 0.21 & (1.0 < \phi \le 4.5) \end{cases} \tag{8.21}$$

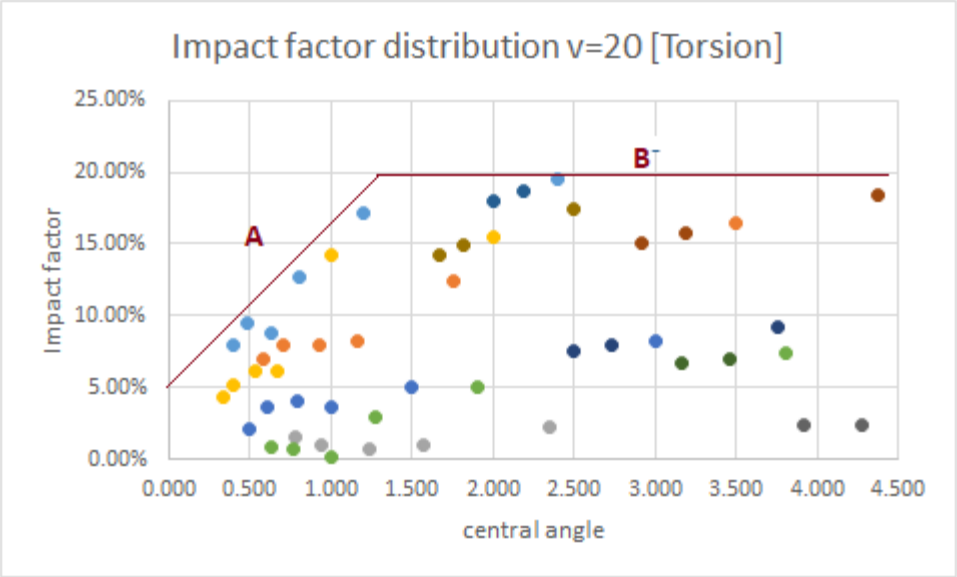

Figure 8-20 Torsional impact factor versus bridge central angle (v=20m/s) for perfect roughness

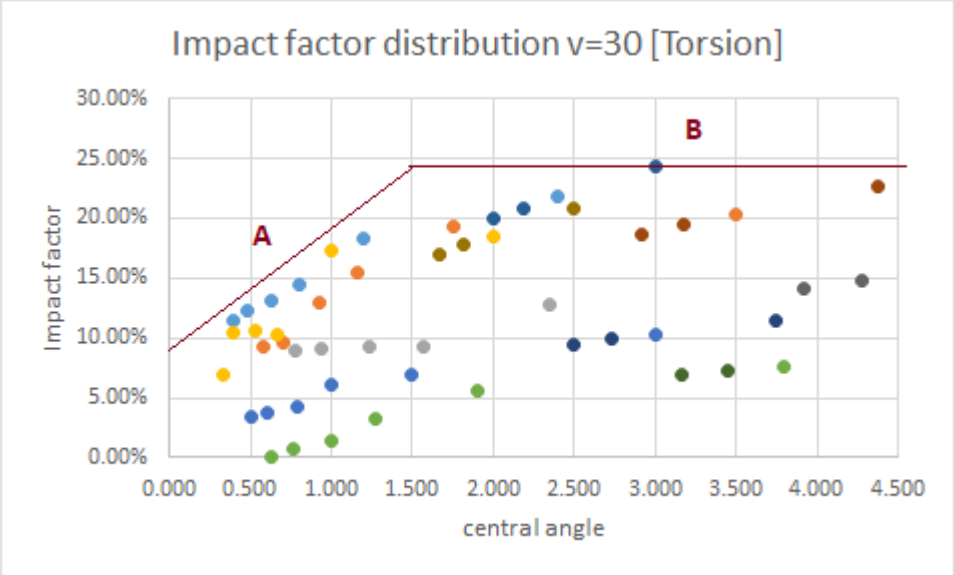

Figure 8-21 Torsional impact factor versus bridge central angle (v=30m/s) for perfect roughness

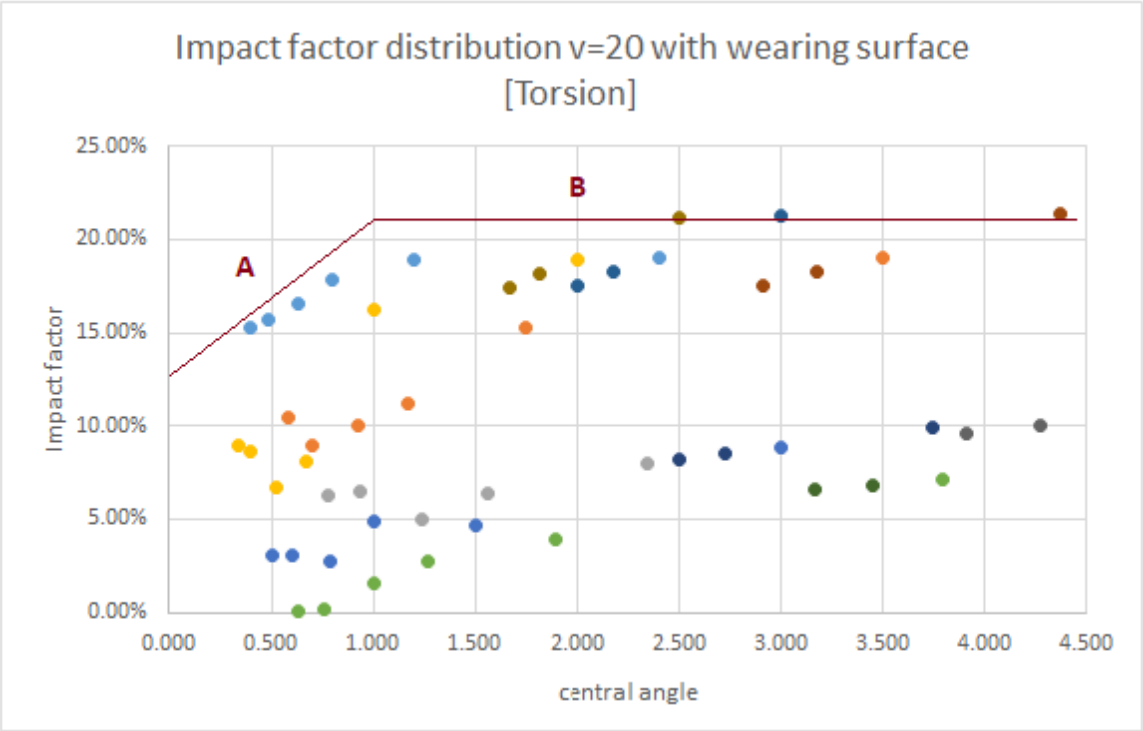

Figure 8-22 Torsional impact factor versus bridge central angle (v=20m/s) for wearing deck

The shear impact factor (I) can be expressed by the central angle (ϕ) as follows:

a. For low speed limit bridge design

$$I = 0.155 \quad (\phi \leq 4.5) \tag{8.22}$$

b. For high speed limit bridge design

$$I = 0.20 \quad (\phi \leq 4.5) \tag{8.23}$$

c. For low speed limit bridge service

$$I = 0.22 \quad (\phi \leq 4.5) \tag{8.24}$$

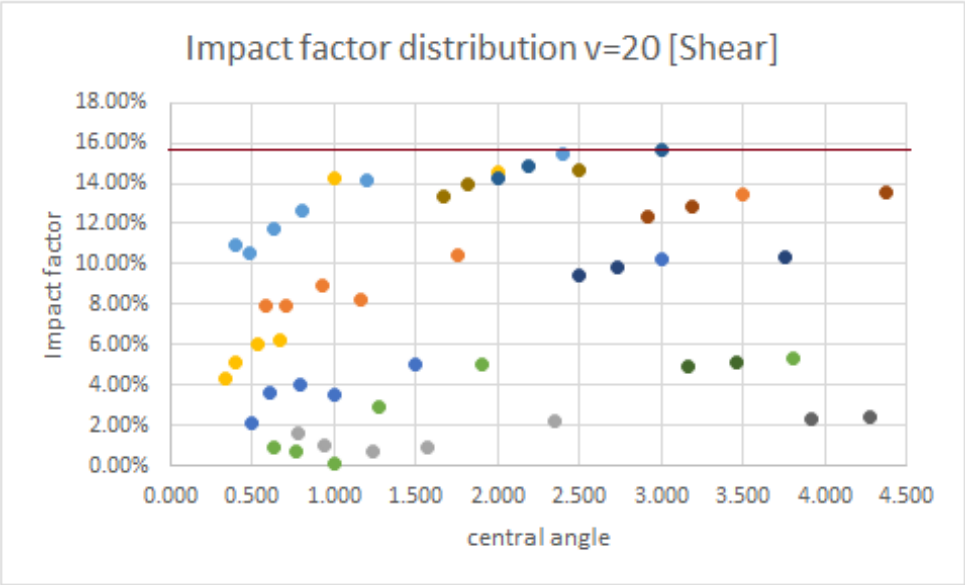

Figure 8-23 Shear impact factor versus bridge central angle (v=20m/s) for perfect roughness

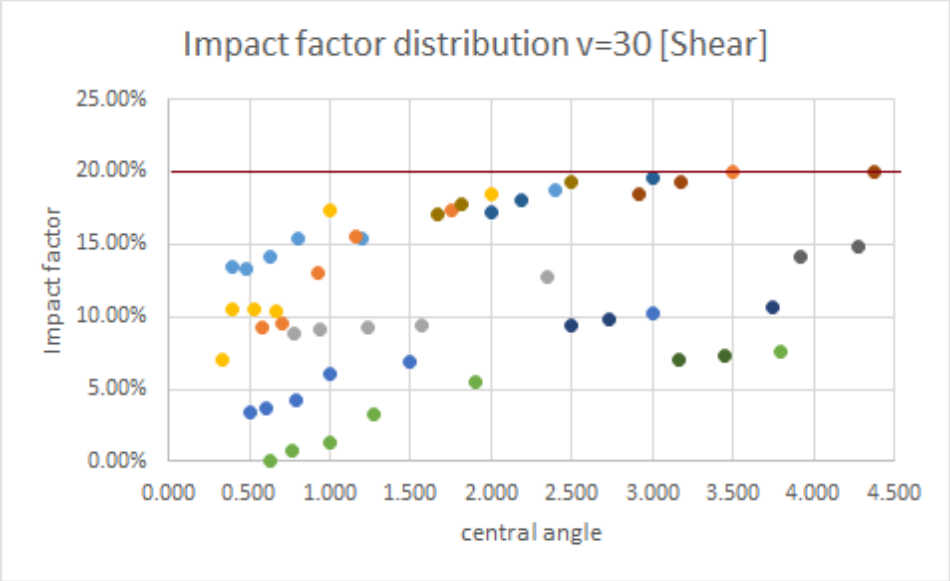

Figure 8-24 Shear impact factor versus bridge central angle (v=30m/s) for perfect roughness

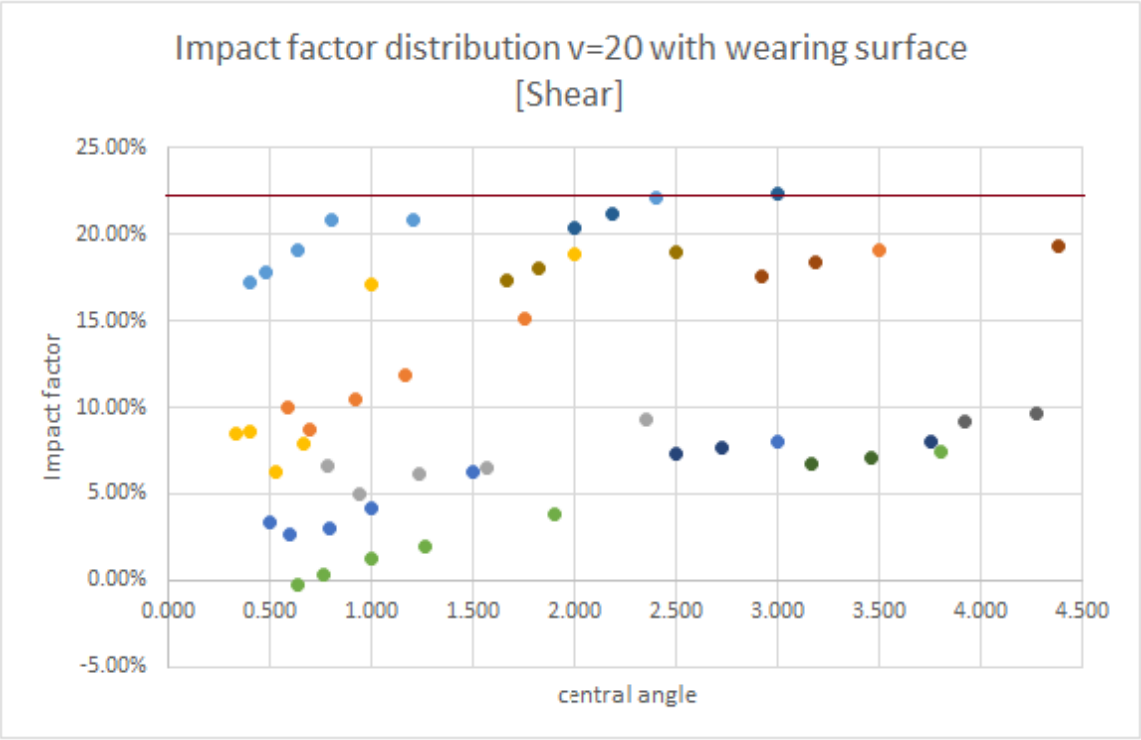

Figure 8-25 Torsional impact factor versus bridge central angle (v=20m/s) for wearing deck

The empirical formulas generated above are a simplified supplementary method in addition to the previous frequency depended method. In the cases of curved bridge problem, the central angle of the bridge can better account for the effect of bridge curvature property. From the parametric studies, it can be observed that for displacement, moment and torsional impact factors, these impact factors achieve their highest points when the bridge central angle reaches 1.0 (Slow traffic, wearing surface), 1.25 (Slow traffic, good surface) and 1.5 (Fast traffic, good surface). Combining the experience from parametric study, this indicates that when the ϕ is small, as the curvature radius decreases, the dynamic reaction increases dramatically.

9. Summary, Conclusions and Future Work

9.1 Summary and Conclusion

The objectives of this research are to study the vehicle-bridge interaction of curved bridges. Including the difference of static interaction and straight bridge dynamic interaction, the contribution of various factors in dynamic interaction are summarized. Besides, a set of simplified empirical equations for calculating curved bridge dynamic impact factor are finally developed.

Principles of vehicle-bridge interaction are presented along with the theoretical background of the topic. A review of available literature indicated that thought on the behavior of dynamic interaction is well recognized, however, there is no unified method to determine the impact factor among the current researches and design specifications. Besides, only few researches expanded the interaction topic to horizontally curved bridges.

Two existing curved bridges, one in concrete and another in steel, are presented to briefly demonstrate the behavior difference in vehicle-bridge interaction in horizontally curved bridge scenario. To observe how the different parameters affect the vehicle-bridge interaction, a detailed parametric study is conducted based on the existing steel curved bridge. The mid-span reactions are focused and utilized to generate the dynamic load

impact factor. Observations and conclusions obtained from the studies can be summarized as follows:

- Based on commercial software ANSYS Mechanical APDL command interface, the interaction system is modeled as a three-beam gird bridge model and a 24 degree-of-freedom 3-dimension truck model. These two subsystems are connected using simplified discrete iterative algorithm. The effects, such as bridge deck conditions and traffic speed, are introduced in the iterative algorithm and discussed extensively to study their influence in vehicle-bridge interaction problem.
- The curvature of the bridge horizontal layout has a noticeable effect on the vehicle-bridge interaction due to torsional effects and centrifugal forces. The parametric study shows a sharp turning bridge can be observed a considerable increment of impact factor. As the radius increases (e.g. less curved) the impact factor generally reduces, once the radius reaches certain threshold the impact factors convergence into the value of straight bridge impact factor.
- Bridge deck conditions and vehicle traveling speed are two major contributors in the dynamic interaction. Parametric study shows at the bad surface condition, the bridge could have a strong impact factor even the vehicle traveling at a relative low speed. As the vehicle reaches certain speed, the exciting frequency may resonance with the bridge, resulting a

much higher response behavior than the tendency shows. The occurrence of such resonance speed varies with the vehicle and bridge properties.

- Other factors' influences are also studied. The span length has a moderate impact on the dynamic interaction. When the radius of bridge is given, a longer span bridge leads to lower stiffness and more buffering space for dynamic load, the impact factor is generally in an inverse ratio to the bridge span length. Such observation agrees with the previous empirical function given by Koichi (1985). The traffic lane location has limited influence on the impact factor. For the case where traffic applies to the outer portion of the curve, both stress and dynamic impact factor are higher than that of inner portion of curve. However, such difference is marginal.
- The dynamic behaviors of torsion, shear and moment are also noticeable under different model parameters. However, the displacement impact factor of mid-span response is usually the most sensitive factor to the different parameters. Such factor is considered to be the primary indicator of dynamic interaction.
- To simplify the process of determining dynamic impact factor, the bridge first flexural frequency is chosen to represent the bridge material and geometric properties. Similar process is also adopted by Canadian code OHDBC.
- A second method based on the bridge central angle is developed in order to account for bridge curvature in determining dynamic impact factor. This

method is a supplementary method in addition to the frequency formula. Such method does not require engineers to acquire the bridge natural frequency when determining dynamic impact factor. Therefore, central angle method is more favored in US by the bridge community.

- By observing massive data of different bridge configurations, vehicle traveling pattern, the upper bound envelop curve of impact factor is summarized. Based on such curve, a set of simple empirical equations is made for the calculation of curved bridge impact factor. By comparing to the current design specifications, the empirical equations show certain degree of agreement in the lower bridge flexural frequency range. However, none of the current codes sufficiently consider the extra dynamic load introduced by a dilapidated surface condition. During the parametric study, it can be frequently observed that the displacement impact factor climbs beyond the 0.75, which is the highest allowance provided in current design codes. Also, the highway speed limit is ignored in current codes, for the highway where speed limit is lower than 20m/s (45mph), the current codes will yield a much conservative result.

9.1.1 Innovation in this study

The innovation and improvement provided in this study include:

- Improved the three-beam gird model based on shear-flexibility grillage analyzing method. The warping effect and torsional inertia are considered in the current model.

- Based on commercial software ANSYS Mechanical APDL command interface, the effects such as bridge deck conditions and traffic speeds are introduced in the vehicle-bridge-interaction system. A more detailed 24 degree-of-freedom, 3-dimension truck model is also integrated in the study.
- Based on the massive data from different bridge configurations and vehicle traveling pattern, the upper bound envelop curve of impact factor is summarized. A practical and simplified empirical equation for dynamic impact factor is summarized. Comments and suggestion are given by comparing the current specifications of dynamic allowance.

*9.2 Suggestions for f*uture Work

More future research is required to further investigate the dynamic interaction of curved bridge. These suggestions are listed below:

- One of the extensions for further work would be adding more vehicles simultaneously on the same lane and/or on multiple lanes at the same time. The extensive dynamic loading could expose a deeper insight into the dynamic interaction under heavy traffic loads.
- The different parameters may be assigned to further investigate the influence of empirical function of this study; for instance, the stiffness and damping of the vehicles, bridge bearing types.

- In the current study, the impact factor empirical function is based on the box steel girder bridge. Different bridge type should be introduced in further studies in order to expand the compatibility of this calculation method.
- Current impact factor function is expressed in terms of bridge first flexural frequency, similar to OHDBC specification. Some other researches conclude that the flexural frequency function has its limitation in terms of accuracy. In order to achieve a more comprehensive method, a better expression is required.

10. Appendix -A

Source code for vehicle bridge interaction

ANSYS Mechanical APDL

Program mainframe:

3-span bridge interaction model

!!!!!!!!!mainframe

fini

/clear,start

/config,NRES,300000

/prep7

**create,para_def,mac*

**dim,m_che,,4*

**dim,k_che,,4*

**dim,c_che,,4*

k_che(1)=12147760,1838752,4186428,1045356 !vehicle stiffness infomation

c_che(1)=3e4,1.2e4,1.4e5,1.7e5

```
m_che(1)=945,480,20433,8592          !unit:kg  vehicle weight

L=120                !The total span of bridge/m

dx=0.24              !element length corresponding to the sampling point

!delta_t=dx/v

E_num=L/dx           !Enum of the bridge

pi=3.14159

!rmid=280

phi=L/rmid*180/pi

dphi=phi/E_num

*dim,dz_che1,,E_num+100          ! vehicle wheel contract point (speed)

*dim,dz_che2,,E_num+100

*dim,z_che1,,E_num+25            !vehicle wheel contract point (location)

*dim,z_che2,,E_num+25

*dim,jiasudu,,E_num+100

*dim,sudu_front,,E_num+100,100

*dim,sudu_back,,E_num+100,100

*dim,weiyi_front,,E_num+1,100
```

**dim,weiyi_back,,E_num+1,100*

*!*dim,yb_mid,,E_num+25*

*!*dim,Mb_mid,,E_num+25*

*!*dim,ys,,E_num+25*

*!*dim,Ms,,E_num+25*

*!*dim,disp_mid,,E_num+25,12*

*!*dim,moment_mid,,E_num+25,12*

**dim,rx,,E_num+100 !surface condition information*

**dim,drx,,E_num+100*

**dim,disp_side,,550 !edge/center span displacement*

**dim,disp_mid,,550*

**dim,disp_side_L,,550*

**dim,disp_mid_L,,550*

**dim,disp_side_R,,550*

**dim,disp_mid_R,,550*

**dim,mx_side,,550 !edge span, moment torsion shear*

**dim,my_side,,550*

**dim,fz_side,,550*

**dim,mx_zhi,,550*

**dim,my_zhi,,550*

**dim,fz_zhi,,550*

**dim,mx_mid,,550 !center span, moment torsion etc.*

**dim,my_mid,,550*

**dim,fz_mid,,550*

**dim,mz_dun,,550*

**dim,fx_dun,,550*

!store the maximum value for each required section

**dim,disp_side_max,,15,15*

**dim,disp_mid_max,,15,15*

**dim,disp_side_L_max,,15,15*

**dim,disp_mid_L_max,,15,15*

**dim,disp_side_R_max,,15,15*

**dim,disp_mid_R_max,,15,15*

*dim,mx_side_max,,15,15

*dim,my_side_max,,15,15

*dim,fz_side_max,,15,15

*dim,mx_zhi_max,,15,15

*dim,my_zhi_max,,15,15

*dim,fz_zhi_max,,15,15

*dim,mx_mid_max,,15,15

*dim,my_mid_max,,15,15

*dim,fz_mid_max,,15,15

*dim,mz_dun_max,,15,15

*dim,fx_dun_max,,15,15

!store the min value for each required section

*dim,disp_side_min,,15,15

*dim,disp_mid_min,,15,15

*dim,disp_side_L_min,,15,15

*dim,disp_mid_L_min,,15,15

*dim,disp_side_R_min,,15,15

*dim,disp_mid_R_min,,15,15

*dim,mx_side_min,,15,15

*dim,my_side_min,,15,15

*dim,fz_side_min,,15,15

*dim,mx_zhi_min,,15,15

*dim,my_zhi_min,,15,15

*dim,fz_zhi_min,,15,15

*dim,mx_mid_min,,15,15

*dim,my_mid_min,,15,15

*dim,fz_mid_min,,15,15

*dim,mz_dun_min,,15,15

*dim,fx_dun_min,,15,15

!matrix for storing

*dim,uz_side,,550,15 !edge displacement

*dim,uz_side_L,,550,15

*dim,uz_side_R,,550,15

*dim,uz_mid,,550,15 !center displacement

*dim,uz_mid_L,,550,15

*dim,uz_mid_R,,550,15

*dim,fmx_side,,550,15 !edge moment torsion shear

*dim,fmy_side,,550,15

*dim,ffz_side,,550,15

*dim,fmx_zhi,,550,15 !support moment torsion shear

*dim,fmy_zhi,,550,15

*dim,ffz_zhi,,550,15

*dim,fmx_mid,,550,15 !center moment torsion shear

*dim,fmy_mid,,550,15

*dim,ffz_mid,,550,15

*dim,fmz_dun,,550,15

*dim,ffx_dun,,550,15

!dynamic amplified factors

*dim,DAF_min,,15,20

*dim,DAF_max,,15,20

```
*end



*create,vehicle_bridge,mac
/PREP7
/COM,create the vehicle model
ET,1,COMBIN14,,,2
ET,2,MASS21,,,4       ! TWO-DIMENSIONAL MASS
ET,3,BEAM3
*do,i,1,4
  R,i,k_che(i),c_che(i)
  R,i+4,m_che(i)
*enddo
R,9,1,1,1
MP,EX,9,2E14
MP,DENS,9,0
N,10001:10005:2,,0:1:0.5
```

N,10002:10006:2,3.6,0:1:0.5

type,1

real,1

E,10001,10003

TYPE,1

REAL,2

E,10002,10004

type,1

real,3

E,10003,10005

TYPE,1

REAL,4

E,10004,10006

**do,i,1,4*

type,2

real,i+4

E,10002+i

M,10002+i,UY ! MASTER DOF IN Y DIRECTION AT FREE END OF SPRING

**enddo*

TYPE,3

REAL,9

MAT,9

E,10005,10006

ALLS

D,10001,ALL,,,10002,1

D,10003,UX,,,10005,1

fini

/COM,create the bridge model

/prep7

et,15,beam4 !main girder

r,15,5.1478,74.326,3.4375 !steel

rmore,,3.4771,,,,3311

mp,ex,15,1.999e11 !steel

mp,dens,15,7500

et,16,beam4

r,16,2.4,0.288,0.800,2,1.2 !property of pier

RMORE,,0.721,,,,

mp,ex,16,3.45e10

mp,dens,16,2600

r,17,4.4647,65.8619,2.0522 !girder change section 1

rmore,,2.6034,,,,3311

r,18,4.4647,65.8619,2.0522 !girder change section 2

rmore,,2.6034,,,,3311

et,20,beam4 !rigid rod

mp,dens,20,0

mp,ex,20,3.45e14

mp,prxy,20,0.1667

R,20,1,1,1,1,1 !property of rigid rod

RMORE,,1,,,,

*afun,deg

*do,i,1,E_num+1 !create the load point

n,i,(rmid+ev)*cos((i-1)*dphi),(rmid+ev)*sin((i-1)*dphi),0.8

*enddo

*do,i,1001,E_num+1001 !create the beam element point

n,i,rmid*cos((i-1001)*dphi),rmid*sin((i-1001)*dphi)

*enddo

type,15

real,15

mat,15

*do,i,1001,E_num+1000 !main gird

e,i,i+1

*enddo

alls

*nsel,s,loc,y,rmid*sin(0*dphi),rmid*sin(8*dphi)*

*nsel,a,loc,y,rmid*sin(145*dphi),rmid*sin(157*dphi)*

*nsel,a,loc,y,rmid*sin(345*dphi),rmid*sin(357*dphi)*

*nsel,a,loc,y,rmid*sin(494*dphi),rmid*sin(501*dphi)*

nsel,r,loc,z,0

nsel,r,loc,x,50,300

esln,s,1,all

emodif,all,real,18

alls

n,3000,

type,16

real,16

mat,16

*n,600,rmid*cos((151-1)*dphi),rmid*sin((151-1)*dphi),-0.5*

*n,616,rmid*cos((151-1)*dphi),rmid*sin((151-1)*dphi),-8.5*

fill

*n,650,rmid*cos((351-1)*dphi),rmid*sin((351-1)*dphi),-0.5*

*n,666,rmid*cos((351-1)*dphi),rmid*sin((351-1)*dphi),-8.5*

fill

e,1151,600,3000

e,1351,650,3000

**do,i,1,16*

e,599+i,600+i,3000

e,649+i,650+i,3000

**enddo*

alls

n,700,rmid-2.5

n,701,rmid+2.5

*n,702,(rmid-2.5)*cos(phi),(rmid-2.5)*sin(phi)*

*n,703,(rmid+2.5)*cos(phi),(rmid+2.5)*sin(phi)*

*n,786,(rmid-2.5)*cos(85*dphi),(rmid-2.5)*sin(85*dphi)*

*n,787,(rmid+2.5)*cos(85*dphi),(rmid+2.5)*sin(85*dphi)*

*n,788,(rmid-2.5)*cos(250*dphi),(rmid-2.5)*sin(250*dphi)*

*n,789,(rmid+2.5)*cos(250*dphi),(rmid+2.5)*sin(250*dphi) !displacement observation points*

type,20

real,20

mat,20

e,1001,700

e,1001,701

e,1501,702

e,1501,703

e,1:501,1001:1501

e,1086,786

e,1086,787

e,1251,788

e,1251,789

csys,1

nsel,s,node,,1,2000

nrotat,all

csys,0

alls

d,700,uz,,,703,1

d,616,all,,,666,50

fini

**end*

!桥面不平度等级，共5 个等级，生成5 个宏文件

**create,addr0*

**VREAD,rx(1),rx0,txt,,JIK,1,E_num+100 !reading surface*

(F20.10)

**VREAD,drx(1),drx0,txt,,JIK,1,E_num+100 !*

(F20.10)

**end*

**create,addr1*

**VREAD,rx(1),rx1,txt,,JIK,1,E_num+100*

(F20.10)

**VREAD,drx(1),drx1,txt,,JIK,1,E_num+100 !*

(F20.10)

**end*

**create,addr2*

**VREAD,rx(1),rx2,txt,,JIK,1,E_num+100 !*

(F20.10)

**VREAD,drx(1),drx2,txt,,JIK,1,E_num+100 !*

(F20.10)

**end*

**create,addr3*

**VREAD,rx(1),rx3,txt,,JIK,1,E_num+100 !*

(F20.10)

**VREAD,drx(1),drx3,txt,,JIK,1,E_num+100 !*

(F20.10)

**end*

**create,addr4*

**VREAD,rx(1),rx4,txt,,JIK,1,E_num+100 !*

(F20.10)

**VREAD,drx(1),drx4,txt,,JIK,1,E_num+100 !*

(F20.10)

**end*

**create,addr5*

**VREAD,rx(1),rx5,txt,,JIK,1,E_num+100 !*

(F20.10)

**VREAD,drx(1),drx5,txt,,JIK,1,E_num+100 !*

(F20.10)

**end*

**create,vehicle_solu,mac*

/COM,

/solu

ANTYPE,TRANS

TRNOPT,FULL,,,,,1

OUTPR,basic,LAST

OUTRES,ALL,last

timint,on

kbc,1

nsubst,1

**do,i,1,E_num+25*

*time,i*delta_t*

alls

fdele,all,all

```
   f,10003,fy,k_che(1)*rx(i)+c_che(1)*v*drx(i)
   f,10004,fy,k_che(2)*rx(i+24)+c_che(2)*v*drx(i+24)
   solve
*enddo
fini


!!!!
/post26
nsol,2,10003,u,y,uy_10003
nsol,3,10004,u,y,uy_10004
deriv,4,2
deriv,5,3
vget,z_che1,2,delta_t
vget,z_che2,3,delta_t
vget,dz_che1,4,delta_t
vget,dz_che2,5,delta_t
fini
```

```
*end



*create,vehicle_solu2,mac
/COM,
/solu
ANTYPE,TRANS
TRNOPT,FULL,,,,,1
OUTPR,basic,LAST
OUTRES,all,last
timint,on
kbc,1
nsubst,1
*do,i,1,E_num+25
  *if,i,LE,24,then          !
    time,i*delta_t
    fdele,all,all
```

*f,10003,fy,k_che(1)*rx(i)+c_che(1)*v*drx(i)*

f,10004,fy,k_che(2)(rx(i+24)+weiyi_front(i,jj-1))+c_che(2)*(v*drx(i+24)+sudu_front(i,jj-1))*

solve

**elseif,i,GE,25,and,i,LE,E_num+1,then*

*time,i*delta_t*

fdele,all,all

f,10003,fy,k_che(1)(rx(i)+weiyi_back(i-24,jj-1))+c_che(1)*(v*drx(i)+sudu_back(i-24,jj-1))*

f,10004,fy,k_che(2)(rx(i+24)+weiyi_front(i,jj-1))+c_che(2)*(v*drx(i+24)+sudu_front(i,jj-1))*

solve

**else*

*time,i*delta_t*

fdele,all,all

f,10003,fy,k_che(1)(rx(i)+weiyi_back(i-24,jj-1))+c_che(1)*(v*drx(i)+sudu_back(i-24,jj-1))*

*f,10004,fy,k_che(2)*rx(i+24)+c_che(2)*v*drx(i+24)*

```
   solve
  *endif
*enddo
fini


!!!!
/post26
nsol,2,10003,u,y,uy_10003
nsol,3,10004,u,y,uy_10004
deriv,4,2
deriv,5,3
vget,z_che1,2,delta_t
vget,z_che2,3,delta_t
vget,dz_che1,4,delta_t
vget,dz_che2,5,delta_t
fini
*end
```

```
*create,bridge_solu,mac
/solu
ANTYPE,TRANS
TRNOPT,FULL,,,,,1
OUTPR,V,LAST
OUTRES,V,last
timint,on
alphad,0.06
betad,0.00015
kbc,1
nsubst,2
*do,i,1,E_num+25
  *if,i,LE,24,then
    time,i*delta_t
    fdele,all,all
```

*f,i,fx,(m_che(2)+m_che(4))*v**2/(rmid+ev)*

*f,i,fz,-(m_che(2)+m_che(4))*10-k_che(2)*(rx(i+24)+weiyi_front(i,jj)-z_che2(i))-c_che(2)*(v*drx(i+24)+sudu_front(i,jj)-dz_che2(i))*

solve

**elseif,i,GE,25,and,i,LE,E_num+1,then*

*time,i*delta_t*

fdele,all,all

*f,i,fx,(m_che(2)+m_che(4))*v**2/(rmid+ev)*

*f,i,fz,-(m_che(2)+m_che(4))*10-k_che(2)*(rx(i+24)+weiyi_front(i,jj)-z_che2(i))-c_che(2)*(v*drx(i+24)+sudu_front(i,jj)-dz_che2(i))*

*f,i-24,fx,(m_che(1)+m_che(3))*v**2/(rmid+ev)*

*f,i-24,fz,-(m_che(1)+m_che(3))*10-k_che(1)*(rx(i)+weiyi_back(i-24,jj)-z_che1(i))-c_che(1)*(v*drx(i)+sudu_back(i-24,jj)-dz_che1(i))*

solve

**else*

*time,i*delta_t*

fdele,all,all

*f,i-24,fx,(m_che(1)+m_che(3))*v**2/(rmid+ev)*

```
    f,i-24,fz,-(m_che(1)+m_che(3))*10-k_che(1)*(rx(i)+weiyi_back(i-24,jj)-
z_che1(i))-c_che(1)*(v*drx(i)+sudu_back(i-24,jj)-dz_che1(i))
    solve
   *endif
  *enddo
  fini

  /post1
  set,first
  *do,i,1,E_num+25
    set,near,1,,,i*delta_t
   *if,i,LE,24,then
    sudu_front(i,jj)=Vz(i)
    weiyi_front(i,jj)=uz(i)
   *elseif,i,GE,25,and,i,LE,E_num+1,then
    sudu_front(i,jj)=Vz(i)
    weiyi_front(i,jj)=uz(i)
    sudu_back(i-24,jj)=Vz(i-24)
```

```
   weiyi_back(i-24,jj)=uz(i-24)
  *else
   sudu_back(i-24,jj)=Vz(i-24)
   weiyi_back(i-24,jj)=uz(i-24)
  *endif
*enddo
fini
*end



*create,static_solu,mac
/solu
ANTYPE,TRANS
TRNOPT,FULL,,,,,1
OUTPR,V,LAST
OUTRES,V,last
timint,off
```

```
kbc,1
nsubst,1
*do,i,1,E_num+25
 *if,i,LE,24,then
  time,i
  fdele,all,all
  f,i,fz,-(m_che(2)+m_che(4))*10
  solve
 *elseif,i,GE,25,and,i,LE,E_num+1,then
  time,i
  fdele,all,all
  f,i,fz,-(m_che(2)+m_che(4))*10
  f,i-24,fz,-(m_che(1)+m_che(3))*10
  solve
 *else
  time,i
  fdele,all,all
```

```
   f,i-24,fz,-(m_che(1)+m_che(3))*10
   solve
  *endif
*enddo
fini
*end
```

2-span bridge interaction model:

```
!!!!!!!!!
fini
/clear,start
/config,NRES,300000
/prep7
```

```
*create,para_def,mac

*dim,m_che,,4

*dim,k_che,,4

*dim,c_che,,4

k_che(1)=12147760,1838752,4186428,1045356

c_che(1)=3e4,1.2e4,1.4e5,1.7e5

m_che(1)=945,480,20433,8592

L=150              !The total span of bridge/m

dx=0.30            !element length corresponding to the sampling point

!delta_t=dx/v

E_num=L/dx         !Enum of the bridge

pi=3.14159

!rmid=280

phi=L/rmid*180/pi

dphi=phi/E_num

*dim,dz_che1,,E_num+100

*dim,dz_che2,,E_num+100
```

*dim,z_che1,,E_num+25

*dim,z_che2,,E_num+25

*dim,jiasudu,,E_num+100

*dim,sudu_front,,E_num+100,100

*dim,sudu_back,,E_num+100,100

*dim,weiyi_front,,E_num+1,100

*dim,weiyi_back,,E_num+1,100

!*dim,yb_mid,,E_num+25

!*dim,Mb_mid,,E_num+25

!*dim,ys,,E_num+25

!*dim,Ms,,E_num+25

!*dim,disp_mid,,E_num+25,12

!*dim,moment_mid,,E_num+25,12

*dim,rx,,E_num+100

*dim,drx,,E_num+100

*dim,disp_side,,550

*dim,disp_mid,,550

*dim,disp_side_L,,550

*dim,disp_mid_L,,550

*dim,disp_side_R,,550

*dim,disp_mid_R,,550

*dim,mx_side,,550 !

*dim,my_side,,550

*dim,fz_side,,550

*dim,mx_zhi,,550

*dim,my_zhi,,550

*dim,fz_zhi,,550

*dim,mx_mid,,550

*dim,my_mid,,550

*dim,fz_mid,,550

*dim,mz_dun,,550

*dim,fx_dun,,550

*dim,disp_side_max,,15,15

*dim,disp_mid_max,,15,15

*dim,disp_side_L_max,,15,15

*dim,disp_mid_L_max,,15,15

*dim,disp_side_R_max,,15,15

*dim,disp_mid_R_max,,15,15

*dim,mx_side_max,,15,15

*dim,my_side_max,,15,15

*dim,fz_side_max,,15,15

*dim,mx_zhi_max,,15,15

*dim,my_zhi_max,,15,15

*dim,fz_zhi_max,,15,15

*dim,mx_mid_max,,15,15

*dim,my_mid_max,,15,15

*dim,fz_mid_max,,15,15

*dim,mz_dun_max,,15,15

*dim,fx_dun_max,,15,15

*dim,disp_side_min,,15,15

*dim,disp_mid_min,,15,15

*dim,disp_side_L_min,,15,15

*dim,disp_mid_L_min,,15,15

*dim,disp_side_R_min,,15,15

*dim,disp_mid_R_min,,15,15

*dim,mx_side_min,,15,15

*dim,my_side_min,,15,15

*dim,fz_side_min,,15,15

*dim,mx_zhi_min,,15,15

*dim,my_zhi_min,,15,15

*dim,fz_zhi_min,,15,15

*dim,mx_mid_min,,15,15

*dim,my_mid_min,,15,15

*dim,fz_mid_min,,15,15

*dim,mz_dun_min,,15,15

*dim,fx_dun_min,,15,15

*dim,uz_side,,550,15

*dim,uz_side_L,,550,15

*dim,uz_side_R,,550,15

*dim,uz_mid,,550,15 !

*dim,uz_mid_L,,550,15

*dim,uz_mid_R,,550,15

*dim,fmx_side,,550,15 !

*dim,fmy_side,,550,15

*dim,ffz_side,,550,15

*dim,fmx_zhi,,550,15 !

*dim,fmy_zhi,,550,15

*dim,ffz_zhi,,550,15

*dim,fmx_mid,,550,15 !

*dim,fmy_mid,,550,15

*dim,ffz_mid,,550,15

```
*dim,fmz_dun,,550,15        !

*dim,ffx_dun,,550,15

*dim,DAF_min,,15,20

*dim,DAF_max,,15,20

*end



*create,vehicle_bridge,mac

/PREP7

/COM,create the vehicle model

ET,1,COMBIN14,,,2     !

ET,2,MASS21,,,4       ! TWO-DIMENSIONAL MASS

ET,3,BEAM3

*do,i,1,4

  R,i,k_che(i),c_che(i)

  R,i+4,m_che(i)

*enddo
```

R,9,1,1,1

MP,EX,9,2E14

MP,DENS,9,0

N,10001:10005:2,,0:1:0.5

N,10002:10006:2,3.6,0:1:0.5

type,1

real,1

E,10001,10003

TYPE,1

REAL,2

E,10002,10004

type,1

real,3

E,10003,10005

TYPE,1

REAL,4

E,10004,10006

*do,i,1,4

type,2

real,i+4

E,10002+i

M,10002+i,UY ! MASTER DOF IN Y DIRECTION AT FREE END OF SPRING

*enddo

TYPE,3

REAL,9

MAT,9

E,10005,10006

ALLS

D,10001,ALL,,,10002,1

D,10003,UX,,,10005,1

fini

/COM,create the bridge model

/prep7

et,15,beam4

r,15,6.4601,89.4805,5.224 !steel 材料

rmore,,4.0677,,,,3311

mp,ex,15,1.999e11 !steel

mp,dens,15,7500

et,16,beam4 !

r,16,2.4,0.288,0.800,2,1.2 !property of pier

RMORE,,0.721,,,,

mp,ex,16,3.45e10

mp,dens,16,2600

r,17,4.7408,67.8761,2.8008 !

rmore,,3.3924,,,,3311

r,18,4.7408,67.8761,2.8008 !

rmore,,3.3924,,,,3311

et,20,beam4

mp,dens,20,0

mp,ex,20,3.45e14

mp,prxy,20,0.1667

R,20,1,1,1,1,1 !property of rigid rod

RMORE,,1,,,,

**afun,deg*

**do,i,1,E_num+1 !create the load point*

*n,i,(rmid+ev)*cos((i-1)*dphi),(rmid+ev)*sin((i-1)*dphi),0.8*

**enddo*

**do,i,1001,E_num+1001 !create the beam element point*

*n,i,rmid*cos((i-1001)*dphi),rmid*sin((i-1001)*dphi)*

**enddo*

type,15

real,15

mat,15

*do,i,1001,E_num+1000

e,i,i+1

*enddo

alls

nsel,s,loc,y,rmid*sin(0*dphi),rmid*sin(8*dphi)

nsel,a,loc,y,rmid*sin(145*dphi),rmid*sin(157*dphi)

nsel,a,loc,y,rmid*sin(345*dphi),rmid*sin(357*dphi)

nsel,a,loc,y,rmid*sin(494*dphi),rmid*sin(501*dphi)

nsel,r,loc,z,0

nsel,r,loc,x,50,300

esln,s,1,all

emodif,all,real,18

alls

n,3000,

type,16

real,16

mat,16

*n,600,rmid*cos((251-1)*dphi),rmid*sin((251-1)*dphi),-0.5 !2span configurations mid span pier*

*n,616,rmid*cos((251-1)*dphi),rmid*sin((251-1)*dphi),-8.5*

fill

*!n,650,rmid*cos((351-1)*dphi),rmid*sin((351-1)*dphi),-0.5*

*!n,666,rmid*cos((351-1)*dphi),rmid*sin((351-1)*dphi),-8.5*

!fill

e,1251,600,3000

!e,1351,650,3000

**do,i,1,16*

e,599+i,600+i,3000

!e,649+i,650+i,3000

**enddo*

alls

n,700,rmid-2.5

n,701,rmid+2.5

*n,702,(rmid-2.5)*cos(phi),(rmid-2.5)*sin(phi)*

*n,703,(rmid+2.5)*cos(phi),(rmid+2.5)*sin(phi)*

*n,786,(rmid-2.5)*cos(85*dphi),(rmid-2.5)*sin(85*dphi)*

*n,787,(rmid+2.5)*cos(85*dphi),(rmid+2.5)*sin(85*dphi) !edge span, useless in 2span case*

*n,788,(rmid-2.5)*cos(125*dphi),(rmid-2.5)*sin(125*dphi)*

*n,789,(rmid+2.5)*cos(125*dphi),(rmid+2.5)*sin(125*dphi) !displacement observation, points 2span ob-pt shift*

type,20

real,20

mat,20

e,1001,700

e,1001,701

e,1501,702

e,1501,703

e,1:501,1001:1501

e,1086,786

e,1086,787

e,1126,788

e,1126,789

csys,1

nsel,s,node,,1,2000

nrotat,all

csys,0

alls

d,700,uz,,,703,1

d,616,all,,,

fini

**end*

!Reading surface conditions,

**create,addr0*

**VREAD,rx(1),rx0,txt,,JIK,1,E_num+100*

(F20.10)

**VREAD,drx(1),drx0,txt,,JIK,1,E_num+100*

(F20.10)

**end*

**create,addr1*

**VREAD,rx(1),rx1,txt,,JIK,1,E_num+100*

(F20.10)

**VREAD,drx(1),drx1,txt,,JIK,1,E_num+100*

(F20.10)

**end*

**create,addr2*

**VREAD,rx(1),rx2,txt,,JIK,1,E_num+100*

(F20.10)

**VREAD,drx(1),drx2,txt,,JIK,1,E_num+100*

(F20.10)

**end*

**create,addr3*

**VREAD,rx(1),rx3,txt,,JIK,1,E_num+100*

(F20.10)

**VREAD,drx(1),drx3,txt,,JIK,1,E_num+100*

(F20.10)

**end*

**create,addr4*

**VREAD,rx(1),rx4,txt,,JIK,1,E_num+100*

(F20.10)

**VREAD,drx(1),drx4,txt,,JIK,1,E_num+100*

(F20.10)

**end*

**create,addr5*

**VREAD,rx(1),rx5,txt,,JIK,1,E_num+100*

(F20.10)

**VREAD,drx(1),drx5,txt,,JIK,1,E_num+100*

(F20.10)

**end*

**create,vehicle_solu,mac*

/COM，

/solu

ANTYPE,TRANS

TRNOPT,FULL,,,,,1

OUTPR,basic,LAST

OUTRES,ALL,last

timint,on

kbc,1

```
nsubst,1
*do,i,1,E_num+25
   time,i*delta_t
   alls
   fdele,all,all
   f,10003,fy,k_che(1)*rx(i)+c_che(1)*v*drx(i)
   f,10004,fy,k_che(2)*rx(i+24)+c_che(2)*v*drx(i+24)
   solve
*enddo
fini

/post26
nsol,2,10003,u,y,uy_10003
nsol,3,10004,u,y,uy_10004
deriv,4,2
deriv,5,3
vget,z_che1,2,delta_t
```

vget,z_che2,3,delta_t

vget,dz_che1,4,delta_t

vget,dz_che2,5,delta_t

fini

**end*

**create,vehicle_solu2,mac*

/COM,

/solu

ANTYPE,TRANS

TRNOPT,FULL,,,,,1

OUTPR,basic,LAST

OUTRES,all,last

timint,on

kbc,1

nsubst,1

```
*do,i,1,E_num+25
 *if,i,LE,24,then
  time,i*delta_t
  fdele,all,all
  f,10003,fy,k_che(1)*rx(i)+c_che(1)*v*drx(i)
  f,10004,fy,k_che(2)*(rx(i+24)+weiyi_front(i,jj-
1))+c_che(2)*(v*drx(i+24)+sudu_front(i,jj-1))
  solve
 *elseif,i,GE,25,and,i,LE,E_num+1,then
  time,i*delta_t
  fdele,all,all
  f,10003,fy,k_che(1)*(rx(i)+weiyi_back(i-24,jj-
1))+c_che(1)*(v*drx(i)+sudu_back(i-24,jj-1))
  f,10004,fy,k_che(2)*(rx(i+24)+weiyi_front(i,jj-
1))+c_che(2)*(v*drx(i+24)+sudu_front(i,jj-1))
  solve
 *else
  time,i*delta_t
```

```
        fdele,all,all
        f,10003,fy,k_che(1)*(rx(i)+weiyi_back(i-24,jj-
1))+c_che(1)*(v*drx(i)+sudu_back(i-24,jj-1))
        f,10004,fy,k_che(2)*rx(i+24)+c_che(2)*v*drx(i+24)
        solve
      *endif
    *enddo
    fini


    /post26
    nsol,2,10003,u,y,uy_10003
    nsol,3,10004,u,y,uy_10004
    deriv,4,2
    deriv,5,3
    vget,z_che1,2,delta_t
    vget,z_che2,3,delta_t
    vget,dz_che1,4,delta_t
    vget,dz_che2,5,delta_t
```

fini

**end*

**create,bridge_solu,mac*

/solu

ANTYPE,TRANS

TRNOPT,FULL,,,,,1

OUTPR,V,LAST

OUTRES,V,last

timint,on

alphad,0.06

betad,0.00015

kbc,1

nsubst,2

**do,i,1,E_num+25*

**if,i,LE,24,then*

*time,i*delta_t*

fdele,all,all

*f,i,fx,(m_che(2)+m_che(4))*v**2/(rmid+ev)*

*f,i,fz,-(m_che(2)+m_che(4))*10-k_che(2)*(rx(i+24)+weiyi_front(i,jj)-z_che2(i))-c_che(2)*(v*drx(i+24)+sudu_front(i,jj)-dz_che2(i))*

solve

**elseif,i,GE,25,and,i,LE,E_num+1,then*

*time,i*delta_t*

fdele,all,all

*f,i,fx,(m_che(2)+m_che(4))*v**2/(rmid+ev)*

*f,i,fz,-(m_che(2)+m_che(4))*10-k_che(2)*(rx(i+24)+weiyi_front(i,jj)-z_che2(i))-c_che(2)*(v*drx(i+24)+sudu_front(i,jj)-dz_che2(i))*

*f,i-24,fx,(m_che(1)+m_che(3))*v**2/(rmid+ev)*

*f,i-24,fz,-(m_che(1)+m_che(3))*10-k_che(1)*(rx(i)+weiyi_back(i-24,jj)-z_che1(i))-c_che(1)*(v*drx(i)+sudu_back(i-24,jj)-dz_che1(i))*

solve

**else*

*time,i*delta_t*

```
    fdele,all,all
    f,i-24,fx,(m_che(1)+m_che(3))*v**2/(rmid+ev)
    f,i-24,fz,-(m_che(1)+m_che(3))*10-k_che(1)*(rx(i)+weiyi_back(i-24,jj)-
z_che1(i))-c_che(1)*(v*drx(i)+sudu_back(i-24,jj)-dz_che1(i))
    solve
  *endif
*enddo
fini

/post1
set,first
*do,i,1,E_num+25
    set,near,1,,,i*delta_t
  *if,i,LE,24,then
    sudu_front(i,jj)=Vz(i)
    weiyi_front(i,jj)=uz(i)
  *elseif,i,GE,25,and,i,LE,E_num+1,then
    sudu_front(i,jj)=Vz(i)
```

```
   weiyi_front(i,jj)=uz(i)
   sudu_back(i-24,jj)=Vz(i-24)
   weiyi_back(i-24,jj)=uz(i-24)
  *else
   sudu_back(i-24,jj)=Vz(i-24)
   weiyi_back(i-24,jj)=uz(i-24)
  *endif
*enddo
fini
*end



*create,static_solu,mac
/solu
ANTYPE,TRANS
TRNOPT,FULL,,,,,1
OUTPR,V,LAST
```

```
OUTRES,V,last

timint,off

kbc,1

nsubst,1

*do,i,1,E_num+25

  *if,i,LE,24,then

    time,i

    fdele,all,all

    f,i,fz,-(m_che(2)+m_che(4))*10

    solve

  *elseif,i,GE,25,and,i,LE,E_num+1,then

    time,i

    fdele,all,all

    f,i,fz,-(m_che(2)+m_che(4))*10

    f,i-24,fz,-(m_che(1)+m_che(3))*10

    solve

  *else
```

```
    time,i
    fdele,all,all
    f,i-24,fz,-(m_che(1)+m_che(3))*10
    solve
  *endif
*enddo
fini
*end
```

Parameter preparation and program initiation

Static reaction:

```
fini

/clear,start

/config,NRES,300000

/prep7

!define the extreme value of static solu

*dim,static_max,,18        !input the extreme value of static analysis

*dim,static_min,,18

static_max(1)=0,1,1,1,1,1,1,1

static_max(9)=1,1,1,1,1,1

static_max(15)=1,1,1,1

static_min(1)=0,1,1,1,1,1,1,1

static_min(9)=1,1,1,1,1,1

static_min(15)=1,1,1,1

ev=-3.1

rmid=190.0
```

```
/input,para_def,mac

/input,vehicle_bridge,mac

*do,kk,1,1

  v=20+(kk-1)*2

  !v=v_che/3.6        !unit:m/s

  delta_t=dx/v

  /input,addr2

  /INPUT,static_solu,mac


 /post26

 NUMVAR,50

 nsol,2,1086,u,z

 nsol,3,1251,u,z

 esol,4,95,1086,M,x

 esol,5,95,1086,M,y

 esol,6,95,1086,F,z

 esol,7,159,1151,M,x
```

esol,8,159,1151,M,y

esol,9,159,1151,F,z

esol,10,260,1251,M,x

esol,11,260,1251,M,y

esol,12,260,1251,F,z

esol,13,510,1151,M,x

esol,14,510,1151,F,z

nsol,15,786,u,z

nsol,16,787,u,z

nsol,17,788,u,z

nsol,18,789,u,z

vget,disp_side,2,0

vget,disp_mid,3,0

vget,mx_side,4,0

vget,my_side,5,0

vget,fz_side,6,0

vget,mx_zhi,7,0

vget,my_zhi,8,0

vget,fz_zhi,9,0

vget,mx_mid,10,0

vget,my_mid,11,0

vget,fz_mid,12,0

vget,mz_dun,13,0

vget,fx_dun,14,0

vget,disp_side_L,15,0

vget,disp_side_R,16,0

vget,disp_mid_L,17,0

vget,disp_mid_R,18,0

**VSCFUN,a2_min,Min,disp_side*

**VSCFUN,a2_max,Max,disp_side*

*VSCFUN,a3_min,Min,disp_mid

*VSCFUN,a3_max,Max,disp_mid

*VSCFUN,a4_min,Min,mx_side

*VSCFUN,a4_max,Max,mx_side

*VSCFUN,a5_min,Min,my_side

*VSCFUN,a5_max,Max,my_side

*VSCFUN,a6_min,Min,fz_side

*VSCFUN,a6_max,Max,fz_side

*VSCFUN,a7_min,Min,mx_zhi

*VSCFUN,a7_max,Max,mx_zhi

*VSCFUN,a8_min,Min,my_zhi

*VSCFUN,a8_max,Max,my_zhi

*VSCFUN,a9_min,Min,fz_zhi

*VSCFUN,a9_max,Max,fz_zhi

*VSCFUN,a10_min,Min,mx_mid

*VSCFUN,a10_max,Max,mx_mid

*VSCFUN,a11_min,Min,my_mid

*VSCFUN,a11_max,Max,my_mid

*VSCFUN,a12_min,Min,fz_mid

*VSCFUN,a12_max,Max,fz_mid

*VSCFUN,a13_min,Min,mz_dun

*VSCFUN,a13_max,Max,mz_dun

*VSCFUN,a14_min,Min,fx_dun

*VSCFUN,a14_max,Max,fx_dun

*VSCFUN,a15_min,Min,disp_side_L

*VSCFUN,a15_max,Max,disp_side_L

*VSCFUN,a16_min,Min,disp_side_R

*VSCFUN,a16_max,Max,disp_side_R

*VSCFUN,a17_min,Min,disp_mid_L

*VSCFUN,a17_max,Max,disp_mid_L

*VSCFUN,a18_min,Min,disp_mid_R

*VSCFUN,a18_max,Max,disp_mid_R

!impact foctor computation

*DAF_min(kk,1)=a2_min*1000/static_min(2)*

*DAF_max(kk,1)=a2_max*1000/static_max(2)*

*DAF_min(kk,2)=a3_min*1000/static_min(3)*

*DAF_max(kk,2)=a3_max*1000/static_max(3)*

DAF_min(kk,3)=a4_min/1000/static_min(4)

DAF_max(kk,3)=a4_max/1000/static_max(4)

DAF_min(kk,4)=a5_min/1000/static_min(5)

DAF_max(kk,4)=a5_max/1000/static_max(5)

DAF_min(kk,5)=a6_min/1000/static_min(6)

DAF_max(kk,5)=a6_max/1000/static_max(6)

DAF_min(kk,6)=a7_min/1000/static_min(7)

DAF_max(kk,6)=a7_max/1000/static_max(7)

DAF_min(kk,7)=a8_min/1000/static_min(8)

DAF_max(kk,7)=a8_max/1000/static_max(8)

DAF_min(kk,8)=a9_min/1000/static_min(9)

DAF_max(kk,8)=a9_max/1000/static_max(9)

DAF_min(kk,9)=a10_min/1000/static_min(10)

DAF_max(kk,9)=a10_max/1000/static_max(10)

DAF_min(kk,10)=a11_min/1000/static_min(11)

DAF_max(kk,10)=a11_max/1000/static_max(11)

DAF_min(kk,11)=a12_min/1000/static_min(12)

DAF_max(kk,11)=a12_max/1000/static_max(12)

DAF_min(kk,12)=a13_min/1000/static_min(13)

DAF_max(kk,12)=a13_max/1000/static_max(13)

DAF_min(kk,13)=a14_min/1000/static_min(14)

DAF_max(kk,13)=a14_max/1000/static_max(14)

*DAF_min(kk,14)=a15_min*1000/static_min(15)*

*DAF_max(kk,14)=a15_max*1000/static_max(15)*

*DAF_min(kk,15)=a16_min*1000/static_min(16)*

*DAF_max(kk,15)=a16_max*1000/static_max(16)*

*DAF_min(kk,16)=a17_min*1000/static_min(17)*

*DAF_max(kk,16)=a17_max*1000/static_max(17)*

*DAF_min(kk,17)=a18_min*1000/static_min(18)*

*DAF_max(kk,17)=a18_max*1000/static_max(18)*

```
*do,i,1,E_num+25          !save the time history into array parameters
  uz_side(i,kk)=disp_side(i)*1000
  uz_side_L(i,kk)=disp_side_L(i)*1000
  uz_side_R(i,kk)=disp_side_R(i)*1000
  uz_mid(i,kk)=disp_mid(i)*1000
  uz_mid_L(i,kk)=disp_mid_L(i)*1000
  uz_mid_R(i,kk)=disp_mid_R(i)*1000
  fmx_side(i,kk)=mx_side(i)/1000
  fmy_side(i,kk)=my_side(i)/1000
  ffz_side(i,kk)=fz_side(i)/1000
  fmx_zhi(i,kk)=mx_zhi(i)/1000
  fmy_zhi(i,kk)=my_zhi(i)/1000
  ffz_zhi(i,kk)=fz_zhi(i)/1000
  fmx_mid(i,kk)=mx_mid(i)/1000
  fmy_mid(i,kk)=my_mid(i)/1000
```

```
    ffz_mid(i,kk)=fz_mid(i)/1000

    fmz_dun(i,kk)=mz_dun(i)/1000

    ffx_dun(i,kk)=fx_dun(i)/1000

  *enddo

*enddo



*mWRITE,uz_side(1,1),uz_sideev0,txt,,jik,15,525

(15F10.5)

*mWRITE,uz_side_L(1,1),uz_side_Lev0,txt,,jik,15,525

(15F10.5)

*mWRITE,uz_side_R(1,1),uz_side_Rev0,txt,,jik,15,525

(15F10.5)

*mWRITE,uz_mid(1,1),uz_midev0,txt,,jik,15,525

(15F10.5)

*mWRITE,uz_mid_L(1,1),uz_mid_Lev0,txt,,jik,15,525

(15F10.5)

*mWRITE,uz_mid_R(1,1),uz_mid_Rev0,txt,,jik,15,525
```

(15F10.5)

**mWRITE,fmx_side(1,1),fmx_sideev0,txt,,jik,15,525*

(15F15.3)

**mWRITE,fmy_side(1,1),fmy_sideev0,txt,,jik,15,525*

(15F15.3)

**mWRITE,ffz_side(1,1),ffz_sideev0,txt,,jik,15,525*

(15F15.3)

**mWRITE,fmx_zhi(1,1),fmx_zhiev0,txt,,jik,15,525*

(15F15.3)

**mWRITE,fmy_zhi(1,1),fmy_zhiev0,txt,,jik,15,525*

(15F15.3)

**mWRITE,ffz_zhi(1,1),ffz_zhiev0,txt,,jik,15,525*

(15F15.3)

**mWRITE,fmx_mid(1,1),fmx_midev0,txt,,jik,15,525*

(15F15.3)

**mWRITE,fmy_mid(1,1),fmy_midev0,txt,,jik,15,525*

(15F15.3)

**mWRITE,ffz_mid(1,1),ffz_midev0,txt,,jik,15,525*

(15F15.3)

**mWRITE,fmz_dun(1,1),fmz_dunev0,txt,,jik,15,525*

(15F15.3)

**mWRITE,ffx_dun(1,1),ffx_dunev0,txt,,jik,15,525*

(15F15.3)

**mWRITE,DAF_min(1,1),DAF_minev0,txt,,jik,18,15*

(18F10.4)

**mWRITE,DAF_max(1,1),DAF_maxev0,txt,,jik,18,15*

(18F10.4)

parsav,all,parameter_r2_ev0

Parameter preparation and program initiation

Dynamic reaction:

fini

/clear,start

/config,NRES,300000

/prep7

!define the extreme value of static solu

**dim,static_max,,18 !input the extreme value of static analysis*

**dim,static_min,,18*

static_max(1)=0,2.5444,2.3132,2442.8605,255.8959,171.2812,1844.2625,155.0776

static_max(9)=4.3855,2779.2288,379.6509,121.0748,929.5457,296.6038

static_max(15)=2.2836,2.8076,2.0310,2.5986

static_min(1)=0,-5.3162,-7.9336,-772.7560,-517.6901,-81.6588,-223.1713,-616.6158

static_min(9)=-281.9689,-321.4912,-427.5871,-137.1931,-600.1071,-30.5198

static_min(15)=-5.7943,-4.8449,-8.6182,-7.2535

ev=-3.1

rmid=190.0

/input,para_def,mac

/input,vehicle_bridge,mac

**do,kk,1,1*

*v=20+(kk-1)*2*

!v=v_che/3.6 !unit:m/s

delta_t=dx/v

```
/input,addr2

jj=1

/INPUT,vehicle_solu,mac

/INPUT,bridge_solu,mac

*do,jj,2,3

  /INPUT,vehicle_solu2,mac

  /INPUT,bridge_solu,mac

  fini

*enddo


/post26

NUMVAR,50

nsol,2,1086,u,z

nsol,3,1251,u,z

esol,4,95,1086,M,x

esol,5,95,1086,M,y

esol,6,95,1086,F,z
```

esol,7,159,1151,M,x

esol,8,159,1151,M,y

esol,9,159,1151,F,z

esol,10,260,1251,M,x

esol,11,260,1251,M,y

esol,12,260,1251,F,z

esol,13,510,1151,M,x

esol,14,510,1151,F,z

nsol,15,786,u,z

nsol,16,787,u,z

nsol,17,788,u,z

nsol,18,789,u,z

vget,disp_side,2,0

vget,disp_mid,3,0

vget,mx_side,4,0

vget,my_side,5,0

vget,fz_side,6,0

vget,mx_zhi,7,0

vget,my_zhi,8,0

vget,fz_zhi,9,0

vget,mx_mid,10,0

vget,my_mid,11,0

vget,fz_mid,12,0

vget,mz_dun,13,0

vget,fx_dun,14,0

vget,disp_side_L,15,0

vget,disp_side_R,16,0

vget,disp_mid_L,17,0

vget,disp_mid_R,18,0

**VSCFUN,a2_min,Min,disp_side*

**VSCFUN,a2_max,Max,disp_side*

*VSCFUN,a3_min,Min,disp_mid

*VSCFUN,a3_max,Max,disp_mid

*VSCFUN,a4_min,Min,mx_side

*VSCFUN,a4_max,Max,mx_side

*VSCFUN,a5_min,Min,my_side

*VSCFUN,a5_max,Max,my_side

*VSCFUN,a6_min,Min,fz_side

*VSCFUN,a6_max,Max,fz_side

*VSCFUN,a7_min,Min,mx_zhi

*VSCFUN,a7_max,Max,mx_zhi

*VSCFUN,a8_min,Min,my_zhi

*VSCFUN,a8_max,Max,my_zhi

*VSCFUN,a9_min,Min,fz_zhi

*VSCFUN,a9_max,Max,fz_zhi

*VSCFUN,a10_min,Min,mx_mid

*VSCFUN,a10_max,Max,mx_mid

*VSCFUN,a11_min,Min,my_mid

*VSCFUN,a11_max,Max,my_mid

*VSCFUN,a12_min,Min,fz_mid

*VSCFUN,a12_max,Max,fz_mid

*VSCFUN,a13_min,Min,mz_dun

*VSCFUN,a13_max,Max,mz_dun

*VSCFUN,a14_min,Min,fx_dun

*VSCFUN,a14_max,Max,fx_dun

*VSCFUN,a15_min,Min,disp_side_L

*VSCFUN,a15_max,Max,disp_side_L

*VSCFUN,a16_min,Min,disp_side_R

*VSCFUN,a16_max,Max,disp_side_R

*VSCFUN,a17_min,Min,disp_mid_L

*VSCFUN,a17_max,Max,disp_mid_L

*VSCFUN,a18_min,Min,disp_mid_R

*VSCFUN,a18_max,Max,disp_mid_R

!impact foctor computation

*DAF_min(kk,1)=a2_min*1000/static_min(2)*

*DAF_max(kk,1)=a2_max*1000/static_max(2)*

*DAF_min(kk,2)=a3_min*1000/static_min(3)*

*DAF_max(kk,2)=a3_max*1000/static_max(3)*

DAF_min(kk,3)=a4_min/1000/static_min(4)

DAF_max(kk,3)=a4_max/1000/static_max(4)

DAF_min(kk,4)=a5_min/1000/static_min(5)

DAF_max(kk,4)=a5_max/1000/static_max(5)

DAF_min(kk,5)=a6_min/1000/static_min(6)

DAF_max(kk,5)=a6_max/1000/static_max(6)

DAF_min(kk,6)=a7_min/1000/static_min(7)

DAF_max(kk,6)=a7_max/1000/static_max(7)

DAF_min(kk,7)=a8_min/1000/static_min(8)

DAF_max(kk,7)=a8_max/1000/static_max(8)

DAF_min(kk,8)=a9_min/1000/static_min(9)

DAF_max(kk,8)=a9_max/1000/static_max(9)

DAF_min(kk,9)=a10_min/1000/static_min(10)

DAF_max(kk,9)=a10_max/1000/static_max(10)

DAF_min(kk,10)=a11_min/1000/static_min(11)

DAF_max(kk,10)=a11_max/1000/static_max(11)

DAF_min(kk,11)=a12_min/1000/static_min(12)

DAF_max(kk,11)=a12_max/1000/static_max(12)

DAF_min(kk,12)=a13_min/1000/static_min(13)

DAF_max(kk,12)=a13_max/1000/static_max(13)

DAF_min(kk,13)=a14_min/1000/static_min(14)

DAF_max(kk,13)=a14_max/1000/static_max(14)

*DAF_min(kk,14)=a15_min*1000/static_min(15)*

*DAF_max(kk,14)=a15_max*1000/static_max(15)*

*DAF_min(kk,15)=a16_min*1000/static_min(16)*

*DAF_max(kk,15)=a16_max*1000/static_max(16)*

*DAF_min(kk,16)=a17_min*1000/static_min(17)*

*DAF_max(kk,16)=a17_max*1000/static_max(17)*

*DAF_min(kk,17)=a18_min*1000/static_min(18)*

*DAF_max(kk,17)=a18_max*1000/static_max(18)*

```
*do,i,1,E_num+25          !save the time history into array parameters
  uz_side(i,kk)=disp_side(i)*1000
  uz_side_L(i,kk)=disp_side_L(i)*1000
  uz_side_R(i,kk)=disp_side_R(i)*1000
  uz_mid(i,kk)=disp_mid(i)*1000
  uz_mid_L(i,kk)=disp_mid_L(i)*1000
  uz_mid_R(i,kk)=disp_mid_R(i)*1000
  fmx_side(i,kk)=mx_side(i)/1000
  fmy_side(i,kk)=my_side(i)/1000
  ffz_side(i,kk)=fz_side(i)/1000
  fmx_zhi(i,kk)=mx_zhi(i)/1000
  fmy_zhi(i,kk)=my_zhi(i)/1000
  ffz_zhi(i,kk)=fz_zhi(i)/1000
  fmx_mid(i,kk)=mx_mid(i)/1000
  fmy_mid(i,kk)=my_mid(i)/1000
```

```
    ffz_mid(i,kk)=fz_mid(i)/1000

    fmz_dun(i,kk)=mz_dun(i)/1000

    ffx_dun(i,kk)=fx_dun(i)/1000

  *enddo

*enddo


*mWRITE,uz_side(1,1),uz_sideev0,txt,,jik,15,525

(15F10.5)

*mWRITE,uz_side_L(1,1),uz_side_Lev0,txt,,jik,15,525

(15F10.5)

*mWRITE,uz_side_R(1,1),uz_side_Rev0,txt,,jik,15,525

(15F10.5)

*mWRITE,uz_mid(1,1),uz_midev0,txt,,jik,15,525

(15F10.5)

*mWRITE,uz_mid_L(1,1),uz_mid_Lev0,txt,,jik,15,525

(15F10.5)

*mWRITE,uz_mid_R(1,1),uz_mid_Rev0,txt,,jik,15,525
```

(15F10.5)

**mWRITE,fmx_side(1,1),fmx_sideev0,txt,,jik,15,525*

(15F15.3)

**mWRITE,fmy_side(1,1),fmy_sideev0,txt,,jik,15,525*

(15F15.3)

**mWRITE,ffz_side(1,1),ffz_sideev0,txt,,jik,15,525*

(15F15.3)

**mWRITE,fmx_zhi(1,1),fmx_zhiev0,txt,,jik,15,525*

(15F15.3)

**mWRITE,fmy_zhi(1,1),fmy_zhiev0,txt,,jik,15,525*

(15F15.3)

**mWRITE,ffz_zhi(1,1),ffz_zhiev0,txt,,jik,15,525*

(15F15.3)

**mWRITE,fmx_mid(1,1),fmx_midev0,txt,,jik,15,525*

(15F15.3)

**mWRITE,fmy_mid(1,1),fmy_midev0,txt,,jik,15,525*

(15F15.3)

**mWRITE,ffz_mid(1,1),ffz_midev0,txt,,jik,15,525*

(15F15.3)

**mWRITE,fmz_dun(1,1),fmz_dunev0,txt,,jik,15,525*

(15F15.3)

**mWRITE,ffx_dun(1,1),ffx_dunev0,txt,,jik,15,525*

(15F15.3)

**mWRITE,DAF_min(1,1),DAF_minev0,txt,,jik,18,15*

(18F10.4)

**mWRITE,DAF_max(1,1),DAF_maxev0,txt,,jik,18,15*

(18F10.4)

parsav,all,parameter_r2_ev0

11. Appendix – B

Code of Surface condition generator

Matlab

```
clear;

clc;

format short;

syms c k;

a=0.6;

b=0.5;

t=0.4;

v=0.3;

x=a./2.*c;

y=b./2.*k;

J=[a./2 0;0 b./2];

Y11=diff(y,k)./det(J);

Y12=-diff(y,c)./det(J);
```

```
Y21=-diff(x,k)./det(J);

Y22=diff(x,c)./det(J);

D=[Y11 Y12 0 0; 0 0 Y21 Y22; Y21 Y22 Y11 Y12];

N1=(1+c).*(1+k)./4;

N2=(1-c).*(1+k)./4;

N3=(1-c).*(1-k)./4;

N4=(1+c).*(1-k)./4;

N=[diff(N1,c) 0 diff(N2,c) 0 diff(N3,c) 0 diff(N3,c) 0; diff(N1,k) 0 diff(N2,k) 0
diff(N3,k) 0 diff(N3,k) 0; 0 diff(N1,c) 0 diff(N2,c) 0 diff(N3,c) 0 diff(N3,c); 0 diff(N1,k) 0
diff(N2,k) 0 diff(N3,k) 0 diff(N3,k)];

B=D*N;

C=(10.^7./(1-v.^2)).*[1 v 0; v 1 0; 0 0 (1-v)./2];

eK=B'*C*B.*t.*det(J);

k1=double(subs(eK,{c,k},{-1./sqrt(3),-1./sqrt(3)}));

k2=double(subs(eK,{c,k},{-1./sqrt(3),1./sqrt(3)}));

k3=double(subs(eK,{c,k},{1./sqrt(3),-1./sqrt(3)}));

k4=double(subs(eK,{c,k},{1./sqrt(3),1./sqrt(3)}));

eK=k1+k2+k3+k4;
```

```
Ty1=(1+c).*(1-(0.3.*c+5.7)./6);

Ty2=(1+c).*(1-(0.3.*c+5.1)./6);

Ty3=(1+c).*(1-(0.3.*c+4.5)./6);

Ty4=(1+c).*(1-(0.3.*c+3.9)./6);

Ty5=(1+c).*(1-(0.3.*c+3.3)./6);

Ty6=(1+c).*(1-(0.3.*c+2.7)./6);

Ty7=(1+c).*(1-(0.3.*c+2.1)./6);

Ty8=(1+c).*(1-(0.3.*c+1.5)./6);

Ty9=(1+c).*(1-(0.3.*c+0.9)./6);

Ty10=(1+c).*(1-(0.3.*c+0.3)./6);

C1=double(int(Ty1, c, -1, 1).*a.*t./4);

C2=double(int(Ty2, c, -1, 1).*a.*t./4);

C3=double(int(Ty3, c, -1, 1).*a.*t./4);

C4=double(int(Ty4, c, -1, 1).*a.*t./4);

C5=double(int(Ty5, c, -1, 1).*a.*t./4);

C6=double(int(Ty6, c, -1, 1).*a.*t./4);

C7=double(int(Ty7, c, -1, 1).*a.*t./4);
```

```
C8=double(int(Ty8, c, -1, 1).*a.*t./4);

C9=double(int(Ty9, c, -1, 1).*a.*t./4);

C10=double(int(Ty10, c, -1, 1).*a.*t./4);

T1=(1-c).*(1-(0.3.*c+5.7)./6);

T2=(1-c).*(1-(0.3.*c+5.1)./6);

T3=(1-c).*(1-(0.3.*c+4.5)./6);

T4=(1-c).*(1-(0.3.*c+3.9)./6);

T5=(1-c).*(1-(0.3.*c+3.3)./6);

T6=(1-c).*(1-(0.3.*c+2.7)./6);

T7=(1-c).*(1-(0.3.*c+2.1)./6);

T8=(1-c).*(1-(0.3.*c+1.5)./6);

T9=(1-c).*(1-(0.3.*c+0.9)./6);

T10=(1-c).*(1-(0.3.*c+0.3)./6);

D1=double(int(T1, c, -1, 1).*a.*t./4);

D2=double(int(T2, c, -1, 1).*a.*t./4);

D3=double(int(T3, c, -1, 1).*a.*t./4);

D4=double(int(T4, c, -1, 1).*a.*t./4);
```

```
D5=double(int(T5, c, -1, 1).*a.*t./4);

D6=double(int(T6, c, -1, 1).*a.*t./4);

D7=double(int(T7, c, -1, 1).*a.*t./4);

D8=double(int(T8, c, -1, 1).*a.*t./4);

D9=double(int(T9, c, -1, 1).*a.*t./4);

D10=double(int(T10, c, -1, 1).*a.*t./4);

F=[0; C1; 0; D1+C2; 0; D2+C3; 0; D3+C4; 0; D4+C5; 0; D5+C6; 0; D6+C7; 0; D7+C8; 0; D8+C9; 0; D9+C10; 0; D10; 0; 0; 0; 0; 0; 0; 0; 0; 0; 0; 0; 0; 0; 0; 0; 0; 0; 0; 0; 0; 0; 0; 0; 0; 0; 0; 0; 0; 0; 0; 0; 0; 0; 0; 0; 0; 0; 0; 0; 0; 0; 0; 0; 0];

gK=zeros(66,66);

for i=1:2:41;

gK(i:i+3,i:i+3)=gK(i:i+3,i:i+3)+eK(1:4,1:4);

end

for i=23:2:63;

gK(i:i+3,i:i+3)=gK(i:i+3,i:i+3)+eK(5:8,5:8);

end

for i=1:2:41;

gK(i:i+3,i+22:i+25)=gK(i:i+3,i+22:i+25)+eK(1:4,5:8);
```

```
end

for i=1:2:41;

gK(i+22:i+25,i:i+3)=gK(i+22:i+25,i:i+3)+eK(5:8,1:4);

end

gKBC=zeros(60,60);

gKBC(1:20,1:20)=gK(1:20,1:20);

gKBC(1:20,21:40)=gK(1:20,23:42);

gKBC(1:20,41:60)=gK(1:20,45:64);

gKBC(21:40,1:20)=gK(23:42,1:20);

gKBC(21:40,21:40)=gK(23:42,23:42);

gKBC(21:40,41:60)=gK(23:42,45:64);

gKBC(41:60,1:20)=gK(45:64,1:20);

gKBC(41:60,21:40)=gK(45:64,23:42);

gKBC(41:60,41:60)=gK(45:64,45:64);

gFBC=zeros(60,1);

gFBC(1:20,1)=F(1:20,1);

gFBC(21:40,1)=F(23:42,1);
```

```
gFBC(41:60,1)=F(45:64,1);

q=inv(gKBC)*gFBC;

for i=1:30;

Q(i,1)=q(2*i,1);

end

for i=1:10;

Y(i,1)=Q(i,1)+Q(i+10,1)+Q(i+20,1);

end

j=max(Y);

h=1/j;

Z=h.*Y;

clc

hw8tryout

%-- 4/24/2013 1:21 PM --%

%-- 5/13/2013 11:39 PM --%

clear;

clc;
```

```
format short;

syms c k;

a=0.6;

b=0.5;

t=0.4;

v=0.3;

x=a./2.*c;

y=b./2.*k;

J=[a./2 0;0 b./2];

Y11=diff(y,k)./det(J);

Y12=-diff(y,c)./det(J);

Y21=-diff(x,k)./det(J);

Y22=diff(x,c)./det(J);

D=[Y11 Y12 0 0; 0 0 Y21 Y22; Y21 Y22 Y11 Y12];

N1=(1+c).*(1+k)./4;

N2=(1-c).*(1+k)./4;

N3=(1-c).*(1-k)./4;
```

```
N4=(1+c).*(1-k)./4;

N=[diff(N1,c) 0 diff(N2,c) 0 diff(N3,c) 0 diff(N3,c) 0; diff(N1,k) 0 diff(N2,k) 0
diff(N3,k) 0 diff(N3,k) 0; 0 diff(N1,c) 0 diff(N2,c) 0 diff(N3,c) 0 diff(N3,c); 0 diff(N1,k) 0
diff(N2,k) 0 diff(N3,k) 0 diff(N3,k)];

B=D*N;

C=(10.^7./(1-v.^2)).*[1 v 0; v 1 0; 0 0 (1-v)./2];

eK=B'*C*B.*t.*det(J);

k1=double(subs(eK,{c,k},{-1./sqrt(3),-1./sqrt(3)}));

k2=double(subs(eK,{c,k},{-1./sqrt(3),1./sqrt(3)}));

k3=double(subs(eK,{c,k},{1./sqrt(3),-1./sqrt(3)}));

k4=double(subs(eK,{c,k},{1./sqrt(3),1./sqrt(3)}));

eK=k1+k2+k3+k4;

Ty1=(1+c).*(1-(0.3.*c+5.7)./6);

Ty2=(1+c).*(1-(0.3.*c+5.1)./6);

Ty3=(1+c).*(1-(0.3.*c+4.5)./6);

Ty4=(1+c).*(1-(0.3.*c+3.9)./6);

Ty5=(1+c).*(1-(0.3.*c+3.3)./6);

Ty6=(1+c).*(1-(0.3.*c+2.7)./6);
```

Ty7=(1+c).(1-(0.3.*c+2.1)./6);*

Ty8=(1+c).(1-(0.3.*c+1.5)./6);*

Ty9=(1+c).(1-(0.3.*c+0.9)./6);*

Ty10=(1+c).(1-(0.3.*c+0.3)./6);*

*C1=double(int(Ty1, c, -1, 1).*a.*t./4);*

*C2=double(int(Ty2, c, -1, 1).*a.*t./4);*

*C3=double(int(Ty3, c, -1, 1).*a.*t./4);*

*C4=double(int(Ty4, c, -1, 1).*a.*t./4);*

*C5=double(int(Ty5, c, -1, 1).*a.*t./4);*

*C6=double(int(Ty6, c, -1, 1).*a.*t./4);*

*C7=double(int(Ty7, c, -1, 1).*a.*t./4);*

*C8=double(int(Ty8, c, -1, 1).*a.*t./4);*

*C9=double(int(Ty9, c, -1, 1).*a.*t./4);*

*C10=double(int(Ty10, c, -1, 1).*a.*t./4);*

T1=(1-c).(1-(0.3.*c+5.7)./6);*

T2=(1-c).(1-(0.3.*c+5.1)./6);*

T3=(1-c).(1-(0.3.*c+4.5)./6);*

```
T4=(1-c).*(1-(0.3.*c+3.9)./6);

T5=(1-c).*(1-(0.3.*c+3.3)./6);

T6=(1-c).*(1-(0.3.*c+2.7)./6);

T7=(1-c).*(1-(0.3.*c+2.1)./6);

T8=(1-c).*(1-(0.3.*c+1.5)./6);

T9=(1-c).*(1-(0.3.*c+0.9)./6);

T10=(1-c).*(1-(0.3.*c+0.3)./6);

D1=double(int(T1, c, -1, 1).*a.*t./4);

D2=double(int(T2, c, -1, 1).*a.*t./4);

D3=double(int(T3, c, -1, 1).*a.*t./4);

D4=double(int(T4, c, -1, 1).*a.*t./4);

D5=double(int(T5, c, -1, 1).*a.*t./4);

D6=double(int(T6, c, -1, 1).*a.*t./4);

D7=double(int(T7, c, -1, 1).*a.*t./4);

D8=double(int(T8, c, -1, 1).*a.*t./4);

D9=double(int(T9, c, -1, 1).*a.*t./4);

D10=double(int(T10, c, -1, 1).*a.*t./4);
```

```
F=[0; C1; 0; D1+C2; 0; D2+C3; 0; D3+C4; 0; D4+C5; 0; D5+C6; 0; D6+C7; 0;
D7+C8; 0; D8+C9; 0; D9+C10; 0; D10; 0; 0; 0; 0; 0; 0; 0; 0; 0; 0; 0; 0; 0; 0; 0; 0;
0; 0; 0; 0; 0; 0; 0; 0; 0; 0; 0; 0; 0; 0; 0; 0; 0; 0; 0; 0; 0; 0; 0; 0; 0; 0; 0];

gK=zeros(66,66);

for i=1:2:41;

gK(i:i+3,i:i+3)=gK(i:i+3,i:i+3)+eK(1:4,1:4);

end

for i=23:2:63;

gK(i:i+3,i:i+3)=gK(i:i+3,i:i+3)+eK(5:8,5:8);

end

for i=1:2:41;

gK(i:i+3,i+22:i+25)=gK(i:i+3,i+22:i+25)+eK(1:4,5:8);

end

for i=1:2:41;

gK(i+22:i+25,i:i+3)=gK(i+22:i+25,i:i+3)+eK(5:8,1:4);

end

gKBC=zeros(60,60);

gKBC(1:20,1:20)=gK(1:20,1:20);
```

```
gKBC(1:20,21:40)=gK(1:20,23:42);

gKBC(1:20,41:60)=gK(1:20,45:64);

gKBC(21:40,1:20)=gK(23:42,1:20);

gKBC(21:40,21:40)=gK(23:42,23:42);

gKBC(21:40,41:60)=gK(23:42,45:64);

gKBC(41:60,1:20)=gK(45:64,1:20);

gKBC(41:60,21:40)=gK(45:64,23:42);

gKBC(41:60,41:60)=gK(45:64,45:64);

gFBC=zeros(60,1);

gFBC(1:20,1)=F(1:20,1);

gFBC(21:40,1)=F(23:42,1);

gFBC(41:60,1)=F(45:64,1);

q=inv(gKBC)*gFBC;

for i=1:30;

Q(i,1)=q(2*i,1);

end

for i=1:10;
```

```
Y(i,1)=Q(i,1)+Q(i+10,1)+Q(i+20,1);

end

j=max(Y);

h=1/j;

Z=h.*Y;

clc
```

12. Appendix -C

This appendix includes a sample of input files for analyzing and designing bridge configuration using DESCUS II.

```
0101VM bridge long version
0102DESCUS Project
0103
0103    1   0   10        3        2        20.00    1        2
0301
0301   1   1   0.684  1   3   1   2   0.886  1   3   1   3   0.430  1   3
0301   1   4   0.000  1   3   1   5   0.000  1   3
0301   2   1   0.300  1   3   2   2   0.950  1   3   2   3   0.750  1   3
0301   2   4   0.000  1   3   2   5   0.000  1   3
0301   3   1   0.000  1   3   3   2   0.750  1   3   3   3   0.950  1   3
0301   3   4   0.300  1   3   3   5   0.000  1   3
0301   4   1   0.000  1   3   4   2   0.430  1   3   4   3   0.886  1   3
0301   4   4   0.684  1   3   4   5   0.000  1   3
0401
```

```
0401     4   8.        0         0   0   0        0         0

0402

04020      0      43.67  2.    2.    1.    1.    24. 8.  4.     150.

0403

0403  HL 93    1      1

0501

0501  1  1   5014.  71.   0.56 10.   1.0  84.   0.75 0.075 4.874

0501  3    1

0501  4  1   5014.  71.   0.56 10.   2.25 84.   1.5  0.075 4.874

0501  5  1   5014.  71.   0.56 13.   4.4  84.   3.0  0.075 4.874

0502

0502  2                                        1000.    1000.

0503

0503  1250.     0       0

0601

0601  1    0.000  0.0000   1  98 232 320

0601  2    0.000 10.8370   2  96 227 317
```

0601 3 0.000 22.0000 3 93 218 311

0601 4 0.000 10.8400 4 91 213 305

0602

060216. 25. 16.

0701

0701 1 1 8 10.35564 3 -635.8370 8 12 10.35565 3 -635.8370

0701 1 12 16 10.35565 3 -635.8370 16 20 10.35565 3 -635.8370

0701 1 20 24 10.35565 3 -635.8370 24 28 10.35565 3 -635.8370

0701 1 28 32 10.35565 3 -635.8370 32 36 10.35565 3 -635.8370

0701 1 36 40 10.35565 3 -635.8370 40 44 10.35565 3 -635.8370

0701 1 44 48 10.35565 3 -635.8370 48 52 10.35565 3 -635.8370

0701 1 52 56 10.35565 3 -635.8370 56 61 10.35565 3 -635.8370

0701 1 61 65 10.35565 3 -635.8370 65 69 10.35565 3 -635.8370

0701 1 69 73 10.35565 3 -635.8370 73 77 10.35565 3 -635.8370

0701 1 77 82 10.35565 3 -635.8370 82 86 10.35565 3 -635.8370

0701 1 86 90 10.35565 3 -635.8370 90 94 10.35565 3 -635.8370

0701 1 94 98 10.35566 3 -635.8370 98 102 10.35564 3 -635.8370

0701 1 102 106 10.35565 3 -635.8370 106 110 10.35565 3 -635.8370

0701 1 110 114 10.35565 3 -635.8370 114 119 10.35565 3 -635.8370

0701 1 119 123 10.35565 3 -635.8370 123 127 10.35565 3 -635.8370

0701 1 127 131 10.35565 3 -635.8370 131 135 10.35565 3 -635.8370

0701 1 135 139 10.35565 3 -635.8370 139 143 10.35565 3 -635.8370

0701 1 143 147 10.35565 3 -635.8370 147 151 10.35565 3 -635.8370

0701 1 151 156 10.35565 3 -635.8370 156 160 10.35565 3 -635.8370

0701 1 160 164 10.35565 3 -635.8370 164 168 10.35565 3 -635.8370

0701 1 168 173 10.35565 3 -635.8370 173 177 10.35565 3 -635.8370

0701 1 177 181 10.35565 3 -635.8370 181 185 10.35565 3 -635.8370

0701 1 185 189 10.35565 3 -635.8370 189 193 10.35565 3 -635.8370

0701 1 193 197 10.35565 3 -635.8370 197 201 10.35565 3 -635.8370

0701 1 201 205 10.35565 3 -635.8370 205 209 10.35565 3 -635.8370

0701 1 209 214 10.35565 3 -635.8370 214 219 10.35565 3 -635.8370

0701 1 219 223 10.35565 3 -635.8370 223 228 10.35565 3 -635.8370

0701 1 228 232 1.03557 3 -635.8370 232 234 9.32008 3 -635.8370

0701 1 234 239 10.35565 3 -635.8370 239 243 10.35565 3 -635.8370

0701 1 243 248 10.35565 3 -635.8370 248 252 10.35565 3 -635.8370

0701 1 252 256 10.35565 3 -635.8370 256 260 10.35565 3 -635.8370

0701 1 260 264 10.35565 3 -635.8370 264 268 10.35565 3 -635.8370

0701 1 268 272 10.35565 3 -635.8370 272 276 10.35565 3 -635.8370

0701 1 276 280 10.35565 3 -635.8370 280 284 10.35565 3 -635.8370

0701 1 284 289 10.35565 3 -635.8370 289 293 10.35565 3 -635.8370

0701 1 293 297 10.35565 3 -635.8370 297 301 10.35565 3 -635.8370

0701 1 301 306 10.35565 3 -635.8370 306 309 10.35565 3 -635.8370

0701 1 309 313 10.35565 3 -635.8370 313 315 10.35565 3 -635.8370

0701 1 315 318 10.35565 3 -635.8370 318 319 10.35565 3 -635.8370

0701 1 319 320 1.03557 3 -635.8370

0701 2 2 7 10.17915 1 -625.0000 7 11 10.17915 1 -625.0000

0701 2 11 15 10.17915 1 -625.0000 15 19 10.17915 4 -625.0000

0701 2 19 23 10.17915 4 -625.0000 23 27 10.17915 4 -625.0000

0701 2 27 31 10.17915 4 -625.0000 31 35 10.17915 4 -625.0000

0701 2 35 39 10.17915 4 -625.0000 39 43 10.17915 4 -625.0000

0701 2 43 47 10.17915 4 -625.0000 47 51 10.17915 4 -625.0000

0701 2 51 55 10.17915 4 -625.0000 55 59 10.17915 4 -625.0000

0701 2 59 63 10.17915 4 -625.0000 63 67 10.17915 4 -625.0000

0701 2 67 71 10.17915 4 -625.0000 71 75 10.17915 4 -625.0000

0701 2 75 80 10.17915 5 -625.0000 80 84 10.17915 5 -625.0000

0701 2 84 88 10.17915 5 -625.0000 88 92 10.17915 5 -625.0000

0701 2 92 96 10.17916 5 -625.0000 96 100 10.17915 5 -625.0000

0701 2 100 104 10.17915 5 -625.0000 104 108 10.17915 5 -625.0000

0701 2 108 112 10.17915 5 -625.0000 112 117 10.17915 5 -625.0000

0701 2 117 121 10.17915 4 -625.0000 121 125 10.17915 4 -625.0000

0701 2 125 129 10.17915 4 -625.0000 129 133 10.17915 4 -625.0000

0701 2 133 137 10.17915 4 -625.0000 137 141 10.17915 4 -625.0000

0701 2 141 145 10.17915 4 -625.0000 145 149 10.17915 4 -625.0000

0701 2 149 154 10.17915 4 -625.0000 154 158 10.17915 4 -625.0000

0701 2 158 162 10.17915 4 -625.0000 162 166 10.17915 4 -625.0000

0701 2 166 170 10.17915 4 -625.0000 170 174 10.17915 4 -625.0000

0701 2 174 178 10.17915 5 -625.0000 178 182 10.17915 5 -625.0000

0701 2 182 186 10.17915 5 -625.0000 186 190 10.17915 5 -625.0000

0701 2 190 194 10.17915 5 -625.0000 194 198 10.17915 5 -625.0000

0701 2 198 202 10.17915 5 -625.0000 202 206 10.17915 5 -625.0000

0701 2 206 210 10.17915 5 -625.0000 210 215 10.17915 5 -625.0000

0701 2 215 220 10.17915 5 -625.0000 220 224 10.17915 5 -625.0000

0701 2 224 227 1.01792 5 -625.0000 227 231 9.16123 5 -625.0000

0701 2 231 236 10.17915 5 -625.0000 236 240 10.17915 5 -625.0000

0701 2 240 244 10.17915 5 -625.0000 244 247 10.17915 5 -625.0000

0701 2 247 251 10.17915 4 -625.0000 251 255 10.17915 4 -625.0000

0701 2 255 259 10.17915 4 -625.0000 259 263 10.17915 4 -625.0000

0701 2 263 267 10.17915 4 -625.0000 267 271 10.17915 4 -625.0000

0701 2 271 275 10.17915 4 -625.0000 275 279 10.17915 4 -625.0000

0701 2 279 283 10.17915 4 -625.0000 283 287 10.17915 4 -625.0000

0701 2 287 291 10.17915 4 -625.0000 291 295 10.17915 4 -625.0000

0701 2 295 299 10.17915 4 -625.0000 299 304 10.17915 4 -625.0000

0701 2 304 308 10.17915 4 -625.0000 308 312 10.17915 4 -625.0000

0701 2 312 314 10.17915 1 -625.0000 314 316 10.17915 1 -625.0000

0701 2 316 317 1.01792 1 -625.0000

0701 3 3 6 9.82085 1 -603.0000 6 10 9.82085 1 -603.0000

0701 3 10 14 9.82085 1 -603.0000 14 18 9.82085 4 -603.0000

0701 3 18 22 9.82085 4 -603.0000 22 26 9.82085 4 -603.0000

0701 3 26 30 9.82085 4 -603.0000 30 34 9.82085 4 -603.0000

0701 3 34 38 9.82085 4 -603.0000 38 42 9.82085 4 -603.0000

0701 3 42 46 9.82085 4 -603.0000 46 50 9.82085 4 -603.0000

0701 3 50 54 9.82085 4 -603.0000 54 58 9.82085 4 -603.0000

0701 3 58 62 9.82085 4 -603.0000 62 66 9.82085 4 -603.0000

0701 3 66 70 9.82085 4 -603.0000 70 74 9.82085 4 -603.0000

0701 3 74 78 9.82085 5 -603.0000 78 81 9.82085 5 -603.0000

0701 3 81 85 9.82085 5 -603.0000 85 89 9.82085 5 -603.0000

0701 3 89 93 9.82084 5 -603.0000 93 97 9.82085 5 -603.0000

0701 3 97 101 9.82085 5 -603.0000 101 105 9.82085 5 -603.0000

0701 3 105 109 9.82085 5 -603.0000 109 113 9.82085 5 -603.0000

0701 3 113 116 9.82085 5 -603.0000 116 120 9.82085 5 -603.0000

0701 3 120 124 9.82085 4 -603.0000 124 128 9.82085 4 -603.0000

0701 3 128 132 9.82085 4 -603.0000 132 136 9.82085 4 -603.0000

0701	3	136	140	9.82085	4	-603.0000	140	144	9.82085	4	-603.0000
0701	3	144	148	9.82085	4	-603.0000	148	152	9.82085	4	-603.0000
0701	3	152	155	9.82085	4	-603.0000	155	159	9.82085	4	-603.0000
0701	3	159	163	9.82085	4	-603.0000	163	167	9.82085	4	-603.0000
0701	3	167	171	9.82085	4	-603.0000	171	175	9.82085	4	-603.0000
0701	3	175	179	9.82085	5	-603.0000	179	183	9.82085	5	-603.0000
0701	3	183	187	9.82085	5	-603.0000	187	191	9.82085	5	-603.0000
0701	3	191	195	9.82085	5	-603.0000	195	199	9.82085	5	-603.0000
0701	3	199	203	9.82085	5	-603.0000	203	207	9.82085	5	-603.0000
0701	3	207	211	9.82085	5	-603.0000	211	216	9.82085	5	-603.0000
0701	3	216	218	0.98208	5	-603.0000	218	222	8.83877	5	-603.0000
0701	3	222	226	9.82085	5	-603.0000	226	230	9.82085	5	-603.0000
0701	3	230	235	9.82085	5	-603.0000	235	238	9.82085	4	-603.0000
0701	3	238	242	9.82085	4	-603.0000	242	246	9.82085	4	-603.0000
0701	3	246	250	9.82085	4	-603.0000	250	254	9.82085	4	-603.0000
0701	3	254	258	9.82085	4	-603.0000	258	262	9.82085	4	-603.0000
0701	3	262	266	9.82085	4	-603.0000	266	270	9.82085	4	-603.0000

0701 3 270 274 9.82085 4 -603.0000 274 278 9.82085 4 -603.0000

0701 3 278 282 9.82085 4 -603.0000 282 286 9.82085 4 -603.0000

0701 3 286 290 9.82085 4 -603.0000 290 294 9.82085 4 -603.0000

0701 3 294 298 9.82085 4 -603.0000 298 302 9.82085 4 -603.0000

0701 3 302 307 9.82085 1 -603.0000 307 310 9.82085 1 -603.0000

0701 3 310 311 0.98208 1 -603.0000

0701 4 4 5 9.64431 3 -592.1600 5 9 9.64430 3 -592.1600

0701 4 9 13 9.64430 3 -592.1600 13 17 9.64430 3 -592.1600

0701 4 17 21 9.64430 3 -592.1600 21 25 9.64430 3 -592.1600

0701 4 25 29 9.64430 3 -592.1600 29 33 9.64430 3 -592.1600

0701 4 33 37 9.64430 3 -592.1600 37 41 9.64430 3 -592.1600

0701 4 41 45 9.64430 3 -592.1600 45 49 9.64430 3 -592.1600

0701 4 49 53 9.64430 3 -592.1600 53 57 9.64430 3 -592.1600

0701 4 57 60 9.64430 3 -592.1600 60 64 9.64430 3 -592.1600

0701 4 64 68 9.64430 3 -592.1600 68 72 9.64430 3 -592.1600

0701 4 72 76 9.64430 3 -592.1600 76 79 9.64430 3 -592.1600

0701 4 79 83 9.64430 3 -592.1600 83 87 9.64430 3 -592.1600

0701 4 87 91 9.64429 3 -592.1600 91 95 9.64431 3 -592.1600

0701 4 95 99 9.64430 3 -592.1600 99 103 9.64430 3 -592.1600

0701 4 103 107 9.64430 3 -592.1600 107 111 9.64430 3 -592.1600

0701 4 111 115 9.64430 3 -592.1600 115 118 9.64430 3 -592.1600

0701 4 118 122 9.64430 3 -592.1600 122 126 9.64430 3 -592.1600

0701 4 126 130 9.64430 3 -592.1600 130 134 9.64430 3 -592.1600

0701 4 134 138 9.64430 3 -592.1600 138 142 9.64430 3 -592.1600

0701 4 142 146 9.64430 3 -592.1600 146 150 9.64430 3 -592.1600

0701 4 150 153 9.64430 3 -592.1600 153 157 9.64430 3 -592.1600

0701 4 157 161 9.64430 3 -592.1600 161 165 9.64430 3 -592.1600

0701 4 165 169 9.64430 3 -592.1600 169 172 9.64430 3 -592.1600

0701 4 172 176 9.64430 3 -592.1600 176 180 9.64430 3 -592.1600

0701 4 180 184 9.64430 3 -592.1600 184 188 9.64430 3 -592.1600

0701 4 188 192 9.64430 3 -592.1600 192 196 9.64430 3 -592.1600

0701 4 196 200 9.64430 3 -592.1600 200 204 9.64430 3 -592.1600

0701 4 204 208 9.64430 3 -592.1600 208 212 9.64430 3 -592.1600

0701 4 212 213 0.96442 3 -592.1600 213 217 8.67988 3 -592.1600

0701 4 217 221 9.64430 3 -592.1600 221 225 9.64430 3 -592.1600

0701 4 225 229 9.64430 3 -592.1600 229 233 9.64430 3 -592.1600

0701 4 233 237 9.64430 3 -592.1600 237 241 9.64430 3 -592.1600

0701 4 241 245 9.64430 3 -592.1600 245 249 9.64430 3 -592.1600

0701 4 249 253 9.64430 3 -592.1600 253 257 9.64430 3 -592.1600

0701 4 257 261 9.64430 3 -592.1600 261 265 9.64430 3 -592.1600

0701 4 265 269 9.64430 3 -592.1600 269 273 9.64430 3 -592.1600

0701 4 273 277 9.64430 3 -592.1600 277 281 9.64430 3 -592.1600

0701 4 281 285 9.64430 3 -592.1600 285 288 9.64430 3 -592.1600

0701 4 288 292 9.64430 3 -592.1600 292 296 9.64430 3 -592.1600

0701 4 296 300 9.64430 3 -592.1600 300 303 9.64430 3 -592.1600

0701 4 303 305 0.96442 3 -592.1600

0801

0801 1 1 2 2 2 2 3 2 3 3 4 2 4 8 7 2 5 7 6 2

0801 6 6 5 2 7 12 11 2 8 11 10 2 9 10 9 2 10 16 15 2

0801 11 15 14 2 12 14 13 2 13 20 19 2 14 19 18 2 15 18 17 2

0801 16 24 23 2 17 23 22 2 18 22 21 2 19 28 27 2 20 27 26 2

0801 21 26 25 2 22 32 31 2 23 31 30 2 24 30 29 2 25 36 35 2

0801 26 35 34 2 27 34 33 2 28 40 39 2 29 39 38 2 30 38 37 2

0801 31 44 43 2 32 43 42 2 33 42 41 2 34 48 47 2 35 47 46 2

0801 36 46 45 2 37 52 51 2 38 51 50 2 39 50 49 2 40 56 55 2

0801 41 55 54 2 42 54 53 2 43 61 59 2 44 59 58 2 45 58 57 2

0801 46 65 63 2 47 63 62 2 48 62 60 2 49 69 67 2 50 67 66 2

0801 51 66 64 2 52 73 71 2 53 71 70 2 54 70 68 2 55 77 75 2

0801 56 75 74 2 57 74 72 2 58 82 80 2 59 80 78 2 60 78 76 2

0801 61 86 84 2 62 84 81 2 63 81 79 2 64 90 88 2 65 88 85 2

0801 66 85 83 2 67 94 92 2 68 92 89 2 69 89 87 2 70 98 96 2

0801 71 96 93 2 72 93 91 2 73 102 100 2 74 100 97 2 75 97 95 2

0801 76 106 104 2 77 104 101 2 78 101 99 2 79 110 108 2 80 108 105 2

0801 81 105 103 2 82 114 112 2 83 112 109 2 84 109 107 2 85 119 117 2

0801 86 117 113 2 87 113 111 2 88 123 121 2 89 121 116 2 90 116 115 2

0801 91 127 125 2 92 125 120 2 93 120 118 2 94 131 129 2 95 129 124 2

0801 96 124 122 2 97 135 133 2 98 133 128 2 99 128 126 2 100 139 137 2

0801 101 137 132 2 102 132 130 2 103 143 141 2 104 141 136 2 105 136 134 2

0801 106 147 145 2 107 145 140 2 108 140 138 2 109 151 149 2 110 149 144 2

0801 111 144 142 2 112 156 154 2 113 154 148 2 114 148 146 2 115 160 158 2

0801 116 158 152 2 117 152 150 2 118 164 162 2 119 162 155 2 120 155 153 2

0801 121 168 166 2 122 166 159 2 123 159 157 2 124 173 170 2 125 170 163 2

0801 126 163 161 2 127 177 174 2 128 174 167 2 129 167 165 2 130 181 178 2

0801 131 178 171 2 132 171 169 2 133 185 182 2 134 182 175 2 135 175 172 2

0801 136 189 186 2 137 186 179 2 138 179 176 2 139 193 190 2 140 190 183 2

0801 141 183 180 2 142 197 194 2 143 194 187 2 144 187 184 2 145 201 198 2

0801 146 198 191 2 147 191 188 2 148 205 202 2 149 202 195 2 150 195 192 2

0801 151 209 206 2 152 206 199 2 153 199 196 2 154 214 210 2 155 210 203 2

0801 156 203 200 2 157 219 215 2 158 215 207 2 159 207 204 2 160 223 220 2

0801 161 220 211 2 162 211 208 2 163 228 224 2 164 224 216 2 165 216 212 2

0801 166 234 231 2 167 231 222 2 168 222 217 2 169 239 236 2 170 236 226 2

0801 171 226 221 2 172 243 240 2 173 240 230 2 174 230 225 2 175 248 244 2

0801 176 244 235 2 177 235 229 2 178 252 247 2 179 247 238 2 180 238 233 2

0801 181 256 251 2 182 251 242 2 183 242 237 2 184 260 255 2 185 255 246 2

0801 186 246 241 2 187 264 259 2 188 259 250 2 189 250 245 2 190 268 263 2

0801 191 263 254 2 192 254 249 2 193 272 267 2 194 267 258 2 195 258 253 2

0801 196 276 271 2 197 271 262 2 198 262 257 2 199 280 275 2 200 275 266 2

0801 201 266 261 2 202 284 279 2 203 279 270 2 204 270 265 2 205 289 283 2

0801 206 283 274 2 207 274 269 2 208 293 287 2 209 287 278 2 210 278 273 2

0801 211 297 291 2 212 291 282 2 213 282 277 2 214 301 295 2 215 295 286 2

0801 216 286 281 2 217 306 299 2 218 299 290 2 219 290 285 2 220 309 304 2

0801 221 304 294 2 222 294 288 2 223 313 308 2 224 308 298 2 225 298 292 2

0801 226 315 312 2 227 312 302 2 228 302 296 2 229 318 314 2 230 314 307 2

0801 231 307 300 2 232 319 316 2 233 316 310 2 234 310 303 2

13. Reference

AASHTO (2014). Load Resistance and Factor Design: Bridge Design Specifications, Seventh Edition, American Association of State Highway and Transportation Officials, Washington D.C.

AASHTO (2017). Load Resistance and Factor Design: Bridge Design Specifications, Eighth Edition, American Association of State Highway and Transportation Officials, Washington D.C.

Y.B. Yang, J.D. Yau, Y.S. Wu (2004), "Vehicle-Bridge Interaction Dynamics With Applications to High-Speed Railways", World Scientific Publishing Co.

Hu Ding, Kang Li Shi, Li Qun Chen and Shao Pu Yang (2013), "Dynamic response of an infinite Timoshenko beam on a nonlinear viscoelastic foundation to a moving load", Nonlinear Dynamic 2013, 73: 285-298

L. Ma, W. Zhang, W.S. Han and J.X.Liu (2019) "Determining the dynamic amplification factor of multi-span continuous box girder bridges in highways using vehicle-bridge interaction analyses", Engineering Structure, vol.181: 47-59

Cai C.B, He Q.L. and Zhu S.Y (2018), "Dynamic interaction of suspension-type monorail vehicle and bridge: Numerical simulation and experiment", Mechanical Systems and Signal Processing, vol.118: 388-407

Zeng Q., Yang Y.B. and Elias G. (2016), "Dynamic response of high speed vehicles and sustaining curved bridges under conditions of resonance", Engineering Structure, vol. 114: 61-74

Zhou S.H., Song G.Q., Wang R.P., Wen B.C. and Ren Z.H (2017), "Nonlinear dynamic analysis for coupled vehicle-bridge vibration system on nonlinear foundation", Mechanical Systems and Signal Processing, vol. 87: 259-278

Arshad Mehmood, Ahmad Ali Khan et (2014), "Vibration Analysis of Beam Subjected to Moving Loads Using Finite Element Method", IOSR Journal of Engineering 2014 Vol 04 issue 5

M.Ichikawa, Y.Miyakawa, A.Matsuda (2000), "Vibration Analysis of the continuous Beam Subjected to a Moving Mass", Journal of Sound and Vibration 2000 vol. 230 issue 3:493-506

S,Eftekhar Azam, M.Mofid, R.Afghani Khorasknai (2012),"Dyanamic response of Timoshenko beam under moving mass", Scientia Iranica 2013 vol.20 issue 1

AV Pesterev, LA Bergman (2000), "Am improved series expansion of the solution to the moving oscillator problem", Journal of Vibration and Acoustics, Transactions of the ASME 2000 Jan 1:54-61

AV Pesterev, LA Bergman (2001), "Response of elastic continuum carrying multiple moving oscillators", Journal of engineering mechanics 127 issue 3:260-265

Mario Fafard, Mallikarjuna Bennur (1996), "A general multi-axle vehicle model to study the bridge-vehicle interaction" Engineering Computations 14 issue 5:491-508

Gupta R.K. (1980),"Dynamic loading of highway bridges", Journal of Engineering Mechanics 106 issue 2: 377-397

Ton-Lo Wang, Dongzhou Huang et al. (1996),"Dynamic Behavior of Continuous and Cantilever Thin-walled Box Girder Bridges", Journal of Bridge Engineering 1996 Vol.1 issue 2

Wu J.S. and Dai C.W. (1987), "Dynamic responses of multispan nonuniform beam due to moving loads", Journal of Structural Engineering ASCE 113 issue 3:458-474

Marchesiello S, Fasana A, Garibaldi L and Piombo, (1999) "Dynamics of multi-span continuous straight bridges subject to multi-degrees of freedom moving vehicle excitation" Journal of Sound and Vibration 224 issue 3: 541-561

Yang Y.B., Liao S.S. and Lin B.H. (1995) "Impact formulas for vehicles moving over simple and continuous beams", Journal of Structural Engineering ASCE 121 issue 11: 1644-1650

Paultre P., Chaallal O. and Proulx J. (1992), "Bridge dynamics and dynamic amplification factors – A review of analytical experimental findings" Canadian Journal Civil Engineering vol.19: 260-278

Huang E.S. and Nowak A.S. (1991), "Simulation of dynamic load for bridges", Journal of Structural Engineering ASCE, vol.117 issue 5: 1413-1434

Chang D. and Lee H. (1994), "Impact factors for simple-span highway girder bridges", Journal of Structure Engineering ASCE vol.120 issue 3: 704-715

Dodds C.J. and Robson J.D. (1973), "The description of road surface roughness", Journal of Sound and Vibration vol.31 issue 2: 175-183

Marcondes J, Burgess G.J., Harichandran R. and Snyder M.B. (1991),"Spectral analysis of highway pavement roughness", Journal of Transportation Engineering ASCE, vol.117 issue 5: 540-549

Tan C.P. and Shore S. (1968), "Dynamic response of a horizontally curved bridge", Journal of Structural Division ASCE, vol. 94 issue 3: 761-781

Tan C.P. and Shore S. (1968), "Response of horizontally curved bridges to moving load", Journal of Structural Division ASCE, vol. 94 issue 9: 2135-2151

Yang Y.B., Wu C.M. AND Yau J.D. (2001), "Dynamic response of a horizontally curved beam subjected to vertical and horizontal moving loads", Journal of Sound and Vibration vol.243 issue 3: 519-537

Song Y.F. and He S.H. (2001), "Study on Key Response Factors for Impact Force Withstood by Highway Bridge", Journal of Xi'an Highway University, vol.21 issue 2: 47-49

M. Maijka and Michael Hartnett (2008), " Effects of speed, load and damping on the dynamic response of railway bridges and vehicles", Computers & Structures vol. 86, issue 6: 556-572

Chunhua Liu, Dongzhou Huang, Ton-Lo Wang (2002), "Analytical dynamic impact study based on correlated road roughness", Computers and Structures 2002 vol.80: 1639–1650

Ton-Lo Wang and Dongzhou Huang (1992), Cable-Stayed Bridge Vibration Due To Road Surface Roughness, Journal of Structural Engineering, Vol. 118

Mohammad Al-Emrani (2005),"Fatigue Performance of Stringer-to-Floor-Beam Connections in Riveted Railway Bridges", ASCE_1084-0702_2005_10:2_179

Khaled M. Sennah, Xuesheng Zhang, and John B. Kennedy (2004) "Impact Factors for Horizontally Curved Composite Box Girder Bridges", ASCE_1084-0702_2004_9:6_512

Dongzhou Huang (2005), "Dynamic Analysis of Steel Curved Box Girder Bridges", Journal of Bridge Engineering 2005.

Ton-Lo Wang, Dongzhou Huang, Mohsen Shahawy and Kaizan Huang (1995),"Dynamic response of Highway Girder Bridges", Computers & Structures Vol 60: 1021-1027

Hid N. Grouni, Andrze S. Nowak (1984), "Calibration of the Ontario Bridge Design Code 1983 edition", Canadian journal of civil engineering 1984. 11: 760-770.

Hid N. Grouni, Andrze S. Nowak (1993), "Calibration of the Ontario Highway Bridge Design Code 1991 edition", Canadian journal of civil engineering 1994.21: 25-35.

Dongzhou Huang, Ton-Lo Wang and Mohsen Shahawy (1993), "Impact Analysis of Continuous Multi-girder Bridges due to Moving Vehicles" Journal of Structural Engineering, vol.118: 2953

Dongzhou Huang, Ton-Lo Wang, M. Shahawy (1997), "Vibration of horizontally curved box girder bridges due to vehicles", Computers & Structures, vol 68: 513-528

Hongyi Li (2005), "Dynamic Response Of Highway Bridge Subjected To Heavy Vehicles", The Florida State University, FAMU-FSU College of Engineering.

CSI. CSiBridge 2017. Berkeley, CA: Computers and Structures, Inc.

Kalny, O., (2015). CSI Knowledge Base, Internet:

https://wiki.csiamerica.com/display/kb/Home.

Fu, C. C. (2009). DESCUS II. Win-DESCUS User's manual for Design and Analysis of Curved BOX-Girder Bridge Systems, 12. College Park, MD: The BEST Center, University of Maryland.